GeoFocus volume 36

Daniela Kati KÖNIG

Roman metallurgical ceramics: an archaeometrical approach

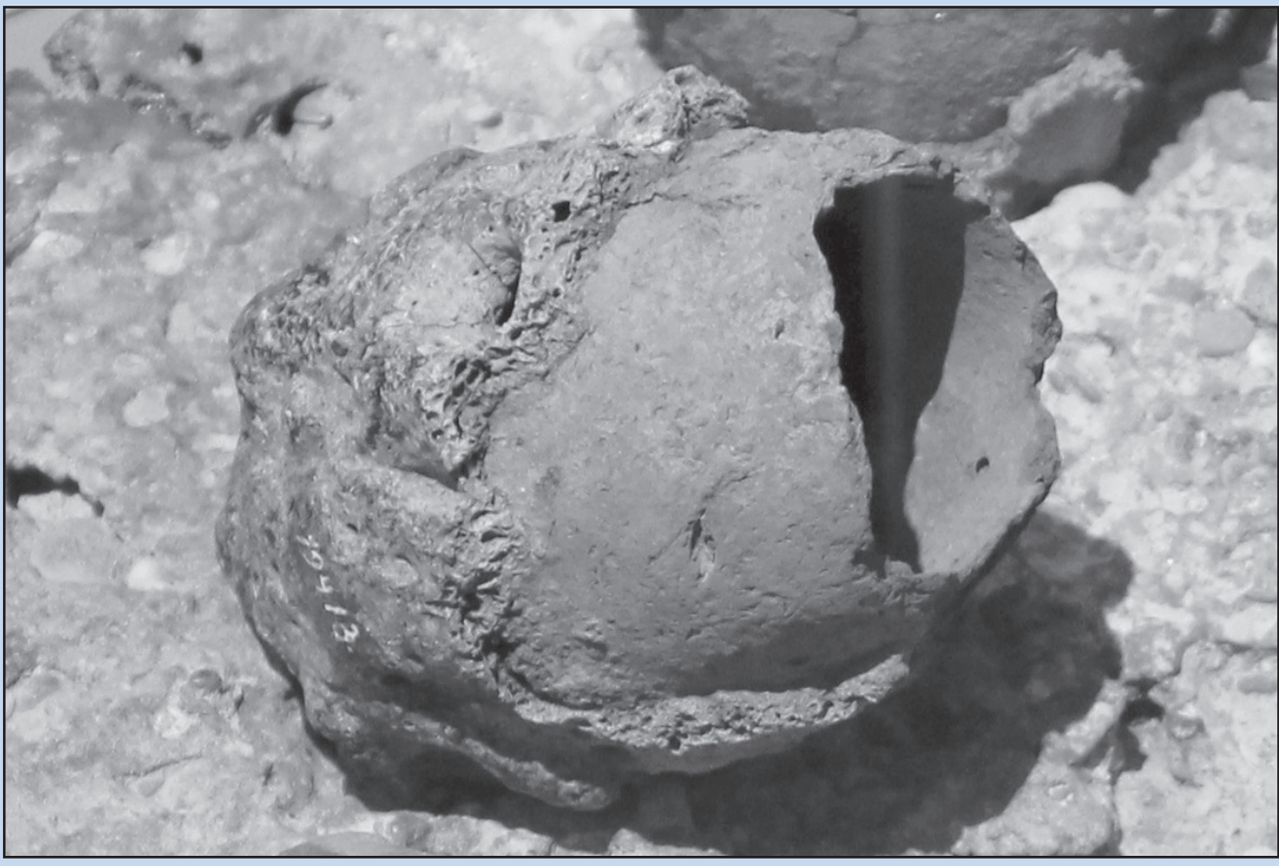

Département de Géosciences, Sciences de la Terre, Université de Fribourg (Suisse)

Daniela Kati KÖNIG (2014)
GeoFocus volume 36

Already published:

Vol. 11 **FREUDIGER-BONZON, Jeanne** (2005) Archaeometrical study (petrography, mineralogy and chemistry) of Neolithic Ceramics from Arbon Bleiche 3 (Canton of Thurgau, Switzerland) (187 pp.).

Vol. 12 **STOFFEL, Markus** (2005) Spatio-temporal variations of rockfall activity into forests - results from tree-ring and tree analysis (188 pp.).

Vol. 13 **RAMEIL, Niels** (2005) Carbonate sedimentology, sequence stratigraphy, and cyclostratigraphy of the Tithonian in the Swiss and French Jura Mountains - a high-resolution record of changes in sea level and climate (246 pp.).

Vol. 14 **BRAILLARD, Luc** (2006) Morphogenèse des vallées sèches du Jura tabulaire d'Ajoie (Suisse): rôle de la fracturation et étude des remplissages quaternaires (224 pp.).

Vol. 15 **GOYETTE-PERNOT, Joëlle** (2006) L'Ambroisie: analyse statistique et modélisation numérique de sa trajectoire aérobiologique (274 pp.).

Vol. 16 **TRESCH, Jonas** (2007) History of a Middle Berriasian transgression (Switzerland, France, and southern England) (271 pp.).

Vol. 17 **BONNET, Cécile** (2007) Interactions between tectonics and surface processes in the Alpine foreland: Insights from analogue model and analysis of recent faulting (189 pp.).

Vol. 18 **VONLANTHEN, Pierre** (2007) EBSD-based investigations of upper mantle xenoliths, snowball garnets and advanced ceramics (114 pp.).

Vol. 19 **VÉDRINE, Stéphanie** (2007) High-frequency palaeoenvironmental changes in mixed carbonate-siliciclastic sedimentary systems (Late Oxfordian, Switzerland, France, and southern Germany) (216 pp.).

Vol. 20 **BOLLSCHWEILER, Michelle** (2008) Spatial and temporal occurrence of past debris flows in the Valais Alps - results from tree-ring analysis (182 pp.).

Vol. 21 **MARTY, Daniel** (2008) Sedimentology, taphonomy, and ichnology of Late Jurassic dinosaur tracks from the Jura carbonate platform (Chevenez-Combe Ronde tracksite, NW Switzerland): insights into the tidal-flat palaeoenvironment and dinosaur diversity, locomotion, and palaeoecology (278 pp.).

Vol. 22 **STIENNE, Noémie** (2010) Paléoécologie et taphonomie comparative en milieux carbonatés peu profonds (Oxfordien du Jura Suisse et Holocène du Belize) (248 pp.).

Vol. 23 **WAITE, Richard** (2010) The palaeoecology of high-spired gastropods and the lost palaeosols: depositional reconstructions on a shallow carbonate platform (Late Kimmeridgian, Swiss Jura Mountains) (149 pp.).

Vol. 24 **MARGRET, Stephan** (2010) Benthic foraminifera associated to cold-water coral ecosystems (248 pp.).

Vol. 25 **VON ALLMEN, Katja** (2010) Variations of calcium and barium isotopes and elemental contents in biogenic and abiogenic geological archives (97 pp.).

Vol. 26 **VOUILLAMOZ, Naomi / SAUDAN, Corinne / MOSAR, Jon** (2010) Microzonage sismique du canton de Fribourg - Cartographie au 1:25'000 des sols de fondation selon la norme SIA 261 (57 pp.).

Vol. 27 **IBELE, Tobias,** (2011) Tectonics of the Western Swiss Molasse Basin during Cenozoic Time (166 pp.).

Vol. 28 **GENNARI, Giordana, (2011)** The Mediterranean - Black Sea connections: The fundamental role of foraminifera as a multifaceted tool for the geological reconstruction of the last 10 ky (171 pp.).

Vol. 29 **MORARD, Sébastien, (2011)** Effets de la circulation d'air par effet de cheminée dans l'évolution du régime thermique des éboulis froids de basse et moyenne altitude (220 pp.).

Vol. 30 **BOCHUD, Martin, (2011)** Tectonics of the Eastern Greater Caucasus in Azerbaijan (201 pp.).

Vol. 31 **MATZENAUER, Eva, (2012)** Tectonics of the Préalpes Klippen and the Subalpine Molasse (Canton Fribourg, Switzerland) (207 pp.).

Vol. 32 **MENNECART, Bastien, (2012)** The Ruminantia (Mammalia, Cetartiodactyla) from the Oligocene to the Early Miocene of Western Europe: systematics, palaeoecology and palaeobiogeography (263 pp.).

Vol. 33 **JARAMILLO-VOGEL, David, (2013)** Shallow-marine sedimentary records of the Eocene–Oligocene greenhouse–icehouse transition (Italy, Switzerland and France) (182 pp.).

Vol. 34 **TRITTSCHACK, Roy, (2013)** Dehydroxylation kinetics of the serpentine group minerals (132 pp.).

Vol. 35 **LAVOYER, Thibault, (2013)** Paléontologie et stratigraphie de la partie nord du fossé rhénan supérieur moyen au cours du Paléogène : relations entre le système du rift, les transgressions marines et le paléoclimat (204 pp.).

GeoFocus volume 36

Daniela Kati KÖNIG (2014)

ISSN 1424 - 1463

GeoFocus is the publication series of the Department of Geosciences, University of Fribourg, Switzerland, and can be ordered at:
Department of Geosciences - Earth Sciences - University of Fribourg - 1700 Fribourg, Switzerland - http://www.unifr.ch/geoscience/geology

Already published:

Vol. 1 **HILLGÄRTNER, Heiko** (1999) The evolution of the French Jura platform during the Late Berriasian to Early Valanginian: controlling factors and timing (203 pp.).

Vol. 2 **DUPRAZ, Christophe** (1999) Paléontologie, paléoécologie et évolution des faciès récifaux de l'Oxfordien Moyen-Supérieur (Jura suisse et français) (247 pp.).

Vol. 3 **BASSANT, Philip** (1999) The high-resolution stratigraphic architecture and evolution of the Burdigalian carbonate-siliciclastic sedimentary systems of the Mut Basin, Turkey (278 pp.).

Vol. 4 **COLOMBIÉ, Claude** (2002) Sédimentologie, stratigraphie séquentielle et cyclostratigraphie du Kimméridgien du Jura suisse et du Bassin vocontien (France): relations plate-forme - bassin et facteurs déterminants (198 pp.).

Vol. 5 **PICOT, Laurent** (2002) Le Paléogène des synclinaux du Jura et de la bordure sud-rhénane: paléontologie (Ostracodes), paléoécologie, biostratigraphie et paléogéographie (240 pp.).

Vol. 6 **DAPPLES, Florence** (2002) Instabilités de terrain dans les Préalpes fribourgeoises (Suisse) au cours du Tardiglaciaire et de l'Holocène: influence des changements climatiques, des fluctuations de la végétation et de l'activité humaine (158 pp.).

Vol. 7 **HUG, Wolfgang Alexander** (2003) Sequenzielle Faziesentwicklung der Karbonatplattform des Schweizer Jura im Späten Oxford und frühesten Kimmeridge (156 pp.).

Vol. 8 **OSWALD, Daniel** (2003) Analyse de l'activité de glissements de terrain et relation avec les conditions climatiques: Exemples dans les Préalpes fribourgeoises (Suisse) (147 pp.).

Vol. 9 **BECKER, Damien** (2003) Paléoécologie et paléoclimats de la Molasse du Jura (Oligo-Miocène): apport des Rhinocerotoidea (Mammalia) et des minéraux argileux (327 pp.).

Vol. 10 **DELALOYE, Reynald** (2005) Contribution à l'étude du pergélisol de montagne en zone marginale (240 pp.).

GeoFocus is the publication series of the Department of Geosciences, University of Fribourg, Switzerland, and can be ordered at:
Department of Geosciences - Earth Sciences - University of Fribourg - 1700 Fribourg, Switzerland - http://www.unifr.ch/geoscience/geology

Aus dem Departement für Geowissenschaften

Universität Freiburg (Schweiz)

Roman metallurgical ceramics: an archaeometrical approach

INAUGURAL-DISSERTATION

zur Erlangung der Würde eines *Doctor rerum naturalium*

der Mathematisch-Naturwissenschaftlichen Fakultät

der Universität Freiburg in der Schweiz

vorgelegt von

Daniela Kati König

aus

Markkleeberg, Deutschland

These N° 1832

2014

Multiprint SA, Fribourg, 2014

Von der Mathematisch-Naturwissenschaftlichen Fakultät der Universität Freiburg in der Schweiz angenommen, auf Antrag von

Hr. Prof. Dr. Vincent Serneels	Universität Freiburg/Schweiz	Dissertationsleiter
Hr. Prof. Dr. Thilo Rehren	UCL/Katar	Gutachter
Hr. Dr. Alex R. Furger	Augusta Raurica/Schweiz	Gutachter
Fr. Prof. Dr. Anneleen Foubert	Universität Freiburg/Schweiz	Präsidentin der Prüfungskommission

Freiburg i. Ü., den 28. März 2014

Dissertationsleiter

.....
Prof. Dr. Vincent Serneels

Dekan der Fakultät

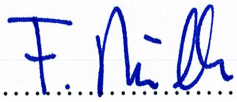

.....
Prof. Dr. Fritz Müller

CONTENTS

ABSTRACT

This Ph.D. thesis focuses on technical ceramics, i.e., copper-alloy related metal-melting crucibles, brass-making crucibles and lost-wax moulds from five different excavation sites in Central and Western Europe dating to the Roman period. An archaeometrical approach using analytical techniques from the field of Earth Sciences was used in order to gain information about the production routine, i.e., used materials like clay, temper and non-plastic inclusions, firing temperature, number of use etc. as well as information on trading relations and exchange of technological knowledge. For this, 18 metal-melting crucibles, eight brass-making crucibles and 16 mould fragments from Autun/France were studied by using petrographical (optical microscopy), elemental (SEM-EDS, EMPA, XRF-WDS) and mineralogical (XRD) techniques. Additionally, 15 metal-melting crucible fragments from Augst/Switzerland and ten metal-melting vessels from Avenches/Switzerland were compared concerning their macroscopic attributes (shape, size etc.), geochemical and mineralogical properties. Trading relations between both Roman towns were assayed based on the crucibles characteristics. Moreover, eight metal-melting crucible fragments from Xanten/ Germany were investigated in a similar manner and compared with the ones from the aforementioned excavation.

A single set of technical ceramics composed of five metal-melting crucibles, three fragments of oven-walls, one “Bouchon” used for preparation of sculptures and nine ceramic samples with unclear relation to its origin coming from an excavation in Marsens En Barras/Switzerland was also analysed based on mineralogical criteria. But, they have not been compared with fragments of other localities due their own characteristics.

This thesis consists of six stand-alone articles which are either published, accepted for publication, under review or ready for submission.

The first paper (Chapter 3) deals with Roman metal-melting crucibles from Autun/France. The 18 vessel fragments show a double-layered structure, i.e., a non-vitrified ceramic inner layer and most often a strongly vitrified outer layer. In addition to these layers there is an innermost vitrified engobe observable in almost all fragments studied. These crucibles are relatively large in size with a maximum capacity of around 19 kg of metal charge. Estimated (maximum) firing temperatures of single fragments point to a maximum of 1400 °C.

The second article (Chapter 4) describes eight fragments of brass-making crucibles from the Rue Bouteiller (Autun/France) and sixteen lost-wax moulds fragments from the Lycee Militaire (Autun/France) concerning their structure (number of layers) and geochemical/ mineralogical composition. Whereas brass-making crucibles are building up of a main non-vitrified ceramic body with an occurring vitrified engobe and an additional non-vitrified outer layer for fixing the lid, moulds consist of one main ceramic body with a very fine ceramic cover, which formerly was in direct contact to the metal artefact itself. All acquired data indicate common clay and temper material used for brass-making crucibles and moulds from Autun/France. The clay and temper material used for this kind of

technical ceramic is the same used for the metal-melting crucibles in Autun/France.

The third paper (Chapter 5) delineates eight metal-melting crucible fragments from Xanten/Germany concerning their overall structure and geochemical/mineralogical composition. These vessels are also double-layered with a non-vitrified inner layer, a vitrified outer layer and an occurring vitrified engobe in some cases. These crucibles are much smaller than the ones from Autun/France. They show a volumetric capacity of a maximum of 1.5 kg. Estimated firing temperatures reach a maximum of 1100 °C.

Paper four (Chapter 6) focuses on Roman metal-melting crucibles from two Swiss excavation sites within the former Roman settlements Augusta Raurica (15 samples) and Aventicum (ten samples). The investigated set of samples were analysed in the same way as those of Autun/France and Xanten/Germany and additionally characterised by portable-XRF analyses. The data serve as a base for a comparison with other metal-melting crucibles examined in this Ph.D. thesis. This article describes not only the structure and mineralogical properties of these vessels which are similar to the ones from Autun/France and Xanten/Germany, but tries to gain information about clay sources and possible trading activities regarding the crucibles between both Roman settlements only or an unknown locality in addition.

Appendix 1 (in German) is connected to the aforementioned chapter as it is a more detailed description of metal-melting crucibles from Augst/Switzerland and Avenches/Switzerland. This article discusses in detail the clay composition, estimated firing temperatures as well as indications for trading of crucibles between former Roman settlements in Switzerland. This article contains clearly displayed contributions of Alex R. Furger .

The fifth publication (Chapter 7) was done to assemble differences and communalities in terms of surface and shape properties, petrographical and mineralogical properties and their interpretation between the individual sets of Roman metal-melting crucibles discussed in chapters 3, 5 and 6. This work tries to verify the hypothesis of a common recipe to produce metal-melting crucibles within the Roman Empire, at least valid for the sites studied within Central and Western Europe.

The last chapter (Chapter 8) is only a part of an archaeological excavation report which is made on different ceramic samples (five metal-melting crucibles, three fragments of oven-walls, one “Bouchon” and nine ceramic samples with unclear relation to its origin) from Marsens En Barras/Switzerland. The samples derive from a very small-scaled copper-alloy manufacturing site within a small Roman settlement with a specialisation in iron manufacturing. The metal-melting crucibles are made of a single layer with a ceramic inside and a vitrified outside. They are thus not compatible with other Roman crucibles investigated within this Ph.D. thesis. The ceramic is made of non-refractory clay coming from the Molasse sediments and partially contain organic temper.

ZUSAMMENFASSUNG

Die vorliegende Doktorarbeit beschäftigt sich mit technischen Keramiken aus fünf verschiedenen archäologischen Ausgrabungen in West- und Zentraleuropa. Diese technischen Keramiken umfassen Schmelztiegel für Kupferlegierungen, Zementationstiegel für die Herstellung von Messing und Abgussformen. Wesentliche Fragen beziehen sich auf: (1) den Herstellungsprozess bezogen auf verwendetes Material, Brenntemperaturen, Anzahl der Nutzung einzelner Tiegel, usw.; (2) den Wissensaustausch zwischen unterschiedlichen römischen Siedlungen und Städten; (3) den möglichen Handel von Schmelztiegeln zwischen unterschiedlichen Städten beziehungsweise Fabrikationsorten und den Städten.

Die 18 Schmelztiegel, acht Zementations-tiegel und 16 Fragmente von Abgussformen aus Autun/Frankreich wurden bezüglich ihrer petrographischen (Mikroskopie), geochemischen (REM-EDS, EMS, RFA-WDS) und mineralogischen (RPD) Eigenschaften hin untersucht. Zusätzlich wurden 15 Schmelztiegelfragmente aus Augst/Schweiz und zehn Schmelztiegelbruchstücke aus Avenches/ Schweiz hinsichtlich optischer Eigenschaften (z.B. Form, Größe, etc.), geochemischer und mineralogischer Eigenschaften, sowie dem Handel von Schmelztiegeln verglichen. Außerdem wurden acht Schmelztiegel-bruchstücke aus Xanten/Deutschland in der gleichen Weise analysiert und den anderen Schmelztiegeln gegenübergestellt. Zudem wurden fünf Schmelztiegelfragmente, drei Bruchstücke von Ofenwandungen, ein „Bouchon“, welcher für die Herstellung von Plastiken verwendet wurde, und neun nicht eindeutig zugeordnete keramische Probenstücke aus Marsens En Barras/Schweiz untersucht. Diese wurden jedoch nicht mit den anderen analysierten technischen Keramiken verglichen.

Diese Arbeit besteht aus sieben einzelnen Artikeln, welche entweder bereits publiziert oder für die Publikation akzeptiert wurden, beziehungsweise sich gerade unter Begutachtung bei Fachzeitschriften befinden oder für die Eingabe bei einer Zeitschrift bereit sind.

Der erste Artikel (Kapitel 3) beschäftigt sich mit Schmelztiegeln aus Autun/Frankreich. Die 18 Tiegelbruchstücke zeigen einen zwei-lagigen Aufbau mit einer nicht verglasten inneren Lage und einer mehr oder minder gut verglasten äußeren Lage. Zusätzlich ist eine verglaste Engobe in den meisten Fragmenten zu finden. Die Schmelztiegel sind mit einer Metallkapazität von 19 kg relativ groß. Ermittelte Brenntemperaturen erreichen ein Maximum von 1400 °C.

Die zweite Publikation (Kapitel 4) beschreibt Zementationstiegel und Abgussformen aus Autun/Frankreich hinsichtlich ihrer Struktur (z.B. Anzahl der keramischen Lagen) und geochemischen/ mineralogischen Zusammen-setzung. Die Zementationstiegel bestehen aus einer nicht verglasten keramischen Lage mit einer Engobe und einer im oberen Drittel auftretenden äußeren nicht verglasten Lage, die zur Abdichtung von Tiegel und Deckel verwendet wurde. Hingegen bestehen die Abgussformen aus einem nicht verglasten keramischen Körper der im direkten Kontakt mit dem Metall einen feinen Tonüberzug aufweist. Der Ausgangston und die zugegebene Magerung in diesen beiden Keramiken ist der gleiche wie der, der für die Schmelztiegel

von Autun/Frankreich Verwendung fand. Die drei Typen von technischen Keramiken aus Autun/ Frankreich werden hinsichtlich ihrer nachgewiesenen Eigenschaften miteinander verglichen.

Artikel drei (Kapitel 5) befasst sich mit Schmelztiegeln aus Xanten/Deutschland bezogen auf deren Struktur und geochemisch-mineralogische Zusammensetzung. Alle Tiegel sind zweilagig aufgebaut, wobei die innere Lage nicht verglast und die äußere Lage vollständig verglast ist. Allen Proben gemein ist eine innere Engobe. Die Schmelztiegel sind mit einer Metallkapazität von 1,5 kg deutlich kleiner als die aus Autun/ Frankreich stammenden. Die mineralogischen Befunde deuten auf geringere maximale Brenn-temperaturen (rund 1100 °C) hin.

Mit römischen Schmelztiegeln aus zwei Ausgrabungen in der Schweiz (Augusta Raurica und Aventicum) beschäftigt sich der vierte Bericht (Kapitel 6). Bruchstücke beider Ausgrabungen wurden hinsichtlich ihrer Vergleichbarkeit der Analyseergebnisse sowohl untereinander, als auch mit den zuvor beschriebenen Schmelztiegeln untersucht. Chemische Daten die mittels portabler RFA Analyse erhoben wurden, ergänzen die geochemischen Labor-untersuchungen. Dieser Bericht befasst sich nicht ausschließlich mit der Struktur der Tiegel, welche mit denen aus Autun/Frankreich und Xanten/Deutschland vergleichbar ist, sondern auch mit der Tonherkunft und möglichem Handel von Schmelztiegeln zwischen beiden römischen Städten respektive möglichem Handel zwischen einem unbekannten Produktionsort und den beiden römischen Städten.

Im Appendix I findet sich ein weiterer in deutscher Sprache verfasster Aufsatz über die Proben aus Augst und Avenches (beide: Schweiz). Der Bericht befasst sich ausschließlich mit den gefundenen Schmelztiegeln in Bezug auf deren Tonzusammensetzung, Aufbau, Form und Brenntemperaturen als auch mit dem Handel der Tiegel.

Der Vergleich zwischen den in Artikel eins bis vier untersuchten Schmelztiegeln wird in der fünften Publikation (Kapitel 7) bezüglich ihrer Form, Aufbau, petrographischen und geochemischen Zusammensetzung hin betrachtet. Diese Arbeit versucht ein allgemeingültiges Rezept für römische Schmelztiegel zumindest für die untersuchten Standorte in Zentraleuropa aufzuzeigen und zu erörtern.

Bei dem letzten Kapitel (Kapitel 8) handelt es sich um einen Teilbericht für eine archäologische Publikation im Rahmen der Ausgrabung Marsens En Barras/Schweiz. Die Proben stammen aus einer kleinmaßstäblichen Kupfer verarbeitenden Werkstatt, in deren Umfeld in großem Maßstab Eisen verarbeitet wurde. Die untersuchten Schmelztiegel sind verglichen mit den anderen nicht eindeutig zweilagig. Sie zeigen zwar unterschiedliche Eigenschaften bezüglicher der Verglasung (innen - nicht verglast, außen - verglast), jedoch sind diese beiden Bereiche in keinem der untersuchten Fragmente voneinander trennbar. Der verwendete Ton entstammt den lokalen Molassevorkommen und weist eine geringe thermische Stabilität auf. Zusätzlich treten organische Magerungsbestandteile auf, welche in keiner sonstigen, der im Rahmen dieser Dissertation untersuchten, technischen Keramiken auftreten.

ACKNOWLEDGEMENTS

I would like to thank all the people who helped me during the last four years of my Ph.D. thesis.

First of all, I would like to express my deep gratitude to Prof. Vincent Serneels, my research supervisor, for his patient guidance, enthusiastic encouragement and useful critiques of this research work.

Special thanks go to Prof. Bernard Grobéty and Prof. Marino Maggetti (both University of Fribourg/Switzerland) for their helpful suggestions and discussions. I thank Mr. Christoph Neururer (University of Fribourg/Switzerland) for his technical support, Mr. Jean-Paul Bourqui and Mr. Patrick Dietsché for the sample preparation. My grateful thanks are also extended to Dr. Martin Robyr (University of Bern/Switzerland) for the EMPA support and Dr. Eric Reusser (ETH Zurich/Switzerland) for the Raman support.

I also express gratitude to Mr. Alex R. Furger (Augusta Raurica/Switzerland) and Dr. Markus Helfert (University Frankfurt a. M./Germany) for their fruitful discussions about metal-melting crucibles and with the portable XRF analyses of the samples from Augst/Switzerland. And many thanks Alex for providing the sample material from Augusta Raurica and Mrs. Marie-France Meylan-Krause (Avenches/Switzerland) to provide the samples from Aventicum.

Many thanks go to Dr. Bernd Liesen (LVR-Archaeological Park Xanten/Germany) who makes the samples from Colonia Ulpia Traiana available for my studies.

I furthermore thank Dr. Yannick Labaune (Autun/France) for providing the ceramic samples from Augustodunum.

Thanks to all my friends and colleagues at the Department of Geosciences in Fribourg, you made the last four years to a delightful and pleasant experience: André, Andres, Anna, Anneleen, Bastien, Cédric, Claudio, Claudius, Daniel, David, Eva, Flavius, Florent, Giordana, Gisela, Ildiko, Jean-Pierre, Juanita, Jon, Luc, Maëlle, Mario, Marius, Martin, Martinus, Monica, Naomi, Raphaëlle, Silvia, Thibault, Tobias. I would like to thank Nicole Brugger for her pleasant way to help me in administrative issues.

I would also like to thank my mother for the support she provided me through my entire life and in particular, I must acknowledge my little son Leonard Richard and my husband and best friend, Roy, without whose love, encouragement and editing assistance, I would not have finished this thesis.

ABBREVIATION LIST

°C	degree Celsius
A.D.	Anno Domini
BSE	backscattered electron(s)
B.C.	Before Christ
ca.	circa
cm	centimetre(s)
cm^{-1}	wavenumber units
e.g.	exempli gratia/ for example
EDS	energy dispersive X-Ray spectroscopy
EMPA	Electron microprobe analysis
et al.	et alii/ and others
etc.	et cetera/ and more
FEG	field emission gun
g	Gramm/gramme
Gew.%	Gewichtsprozent
in prep.	in preparation
i.e.	id est/ that means
kg	kilograms
km	kilometre(s)
kV	kilovolt
L	litre(s)
LVR	Landschaftsverband Rheinland
m	metre(s)
M.	Massstab
mA	milliampere
mg	milligram(s)
min	minute(s)
ml	millilitre(s)
mm	millimetre(s)
ms	millisecond(s)
mW	milliwatt
µl	microlitre(s)
µm	micrometre(s)
nA	nanoampere
n. Chr.	nach Christus
nm	nanometre(s)
Ph.D.	Doctor of Philosophy
ppm	part per million
p-XRF	portable X-ray fluorescence analysis
REM	Rasterelektronenmikroskop(ie)
RPD	Röntgenpulverdiffraktometrie
SE	secondary electron(s)
s	second(s)
SEM	scanning electron microscop(e/y)
vol.%	volume percent
vs.	versus
XRD	X-ray diffraction analysis
XRF	X-ray fluorescence analysis
XRPD	X-ray powder diffraction analysis
WDS	wavelength dispersive X-ray spectroscopy
wt.%	weight percent

Further/ special characters and abbreviations are indicated in the respective chapters of this Ph.D. thesis.

1 - INTRODUCTION

1.1 RESEARCH BACKGROUND

In general, technical ceramics are defined as ceramics which exhibits a high degree of industrial efficiency due to their carefully designed microstructure. Technical ceramics including principally ceramics with superior mechanical properties such as great strength, a high level of elasticity, enhanced hardness, hest resistance and abrasion resistance (Somiya 1989). The term technical ceramic is a designation for ceramics used in 'industrial' applications like, e.g. crucibles or moulds, which are discussed in more detail below.

Crucibles, in general, and moulds are important artefacts to receive detailed technological and metallurgical knowledge about specific metalworking areas (Tite *et al.* 1985, Nielen 2006). Thus, there exists a specific interest to study such artefacts by a series of modern analytical techniques usually used in Material Sciences in order to obtain a comprehensive knowledge about the artefacts and to compare artefacts coming from different excavation sites with each other.

In archeometry, it is usual to differentiate functional categories of crucibles which are considered to be main processes, i.e., melting and cementation (Bayley and Rehren 2007). The nature of these processes determines fundamentally the vessel form and the ceramic fabric (Rehren 2003). Metal-melting vessels are the most frequent type (Bayley and Rehren 2007). It was essential to design them small but strong in order to guarantee easy handling of such crucibles. Furthermore, such a handling requires a fabric which ensures mechanical stability at temperatures well above 1000 °C (Bayley 1992, Bayley and Rehren 2007). Correspondingly, the volume was frequently limited to a maximum of one litre of liquid metal, but often much less prior to the Industrial Revolution (Bayley 1992, Bayley and Rehren 2007). Nevertheless, there are exceptions of these limitations as reported from the excavation of Autun/France (König and Serneels 2013).

Cementation crucibles were considered for the reaction of solids (e.g., metal, ore etc.) with a vapour phase, which requires carefully controlled temperatures and atmospheres to guarantee that the vapour phase stays in contact with the other ingredients (Bayley and Rehren 2007). Brass-making crucibles are a certain kind of cementation crucibles with explicit and diagnostic features like poorly refractory fabrics, particular during the Roman period, and the high level of zinc detectable in all of them (Martinon-Torres and Rehren 2002). These kinds of crucibles are usually small in size (Bayley 1984, Rehren 1999) as this was favourable for the energy balance of the process (Bayley and Rehren 2007). The crucibles have to be a kind of closed vessel. As the fabric is not sufficiently porous, a small opening is essential to relieve any build-up of pressure (Bayley and Rehren 2007). In order to maximise the ratio of surface area (heat input) to volume (heat use), these crucibles are usually small and/or tubular rather than spherical in shape (Bayley and Rehren 2007). In general, an increased production caused a higher number of vessels used, rather than increasing the size of individual vessels (Rehren 1999). Again, there are some exceptions of such a general rule as demonstrated in a Roman excavation near Lyon/France and Autun/France (Picon *et al.* 1995, Chardron-Picault and Picon 1997).

Cast objects like fibulae were made by melting metal in a crucible and pouring it into a mould, where it became solid. For the Roman period, two types of moulds are known, i.e., investment and piece moulds. Investment moulds were prepared by the lost-wax technique and destroyed after use. These kinds of moulds were made of clay (Bayley and Butcher 2004), i.e., without any specific constraints regarding temperature stability. Piece moulds consist of two or more individual pieces and were either made of stone but clay also. Such moulds can usually be reused. But, piece moulds of clay are as much destroyed as investment moulds. For Roman finds in Britain, Bayley and Butcher (2004) describe mainly piece moulds for casting single fibulae or brooches. They also describe continental finds, e.g., from Autun/France (Chardron-Picault and Pernot 1999) and Nandin/France (Marquart 1935), for which they imply a simultaneous casting of two or more fibulae within one mould. This suggests assembling of individual clay moulds to multiples before casting (Beck *et al.* 1982/3).

1.2 GOALS

The goal of this Ph.D. thesis is the result of open questions concerning Roman technical ceramics especially Roman metal-melting crucibles and exceptionally large brass-making crucibles from Autun/France. Most descriptions of Roman crucibles in literature focus on archaeological important properties only, i.e., shape, size, decoration patterns, colours etc. Thus, only less is known about (distinct) material properties, i.e., number of individual layers distinguishable by their mineralogical characteristics, composition of temper and non-plastic inclusions allowing among others to reconstruct certain preparation techniques, element content present within individual layers helpful for the determination of a clay source, occurrence of temperature specific mineral phases useful for reconstructing ancient firing temperatures, composition of metal remnants etc. It is clear that not all open questions can be answered during the timeframe of a single thesis, but this study shall serve to create a basis for material properties of Roman metal-melting crucibles by answering questions related to the aforementioned set of issues, i.e., collecting information about used raw materials, the production routine and the recipes for making metal-melting crucibles. Therefore, the thesis is subdivided into six single papers and/or contributions of publications, respectively, which discuss mainly following issues:

- The characterisation of Roman metal-melting crucibles, brass-making crucibles and moulds concerning their overall structure, their geochemical and mineralogical communalities and differences as well as their firing temperatures.

- The acquired data should be used to evaluate the possible existence of a common Roman recipe for making such vessels, i.e., a similar or even identical technological routine using similar raw materials in order to produce vessels with common structural and functional characteristics.

- Trading of crucibles between individual Roman settlements.

These questions should be solved by the application of a series of invasive analytical techniques, i.e., SEM-EDX, EMPA, XRD, XRF, Raman spectroscopy and one minimal invasive technique, i.e., portable XRF. All results are evaluated concerning their conclusiveness.

2 - EXPERIMENTAL METHODS

A complete summary about all samples studied and the analytical techniques applied to them is given in Appendix 2. It is clear that not all samples were analysed with all methods available due to following reasons. Sometimes single methods were not appropriate or it was not necessary to analyse each single sample of a given set with exactly the same method. This chosen approach was thus a compromise between time efficiency, questions necessary to answer with and potential success of solving question by increasing the number of samples studied only.

Portable XRF were only used for samples from Augusta Raurica because it was project collaboration between Alex Furger, Markus Helfert and myself, whereas Markus Helfert performed the portable XRF measurements and provided the data for comparison with my own dataset.

It is important to mention that each investigation method is limited with respect to their informativeness. It was thus necessary to combine a certain extend of analytical techniques available. During the thesis I tried to perform the analyses reliable and reproducible but due to different sample material and amounts as well as different temper grains, non-plastic inclusions and sizes, it was not possible to perform the analyses strictly identical in all cases. Especially for XRF analyses this was occasionally impossible caused by the small amount of sample material (less than two grams) to produce the pressed pills and, therefore, to perform the analyses.

Electron microprobe investigations were chosen to a limited extends in order to quantify metal remnants in a much better way than possible by means of SEM-EDS analysis only. However, due to the properties of the glassy materials (engobe and outer layer) it was difficult to assess quantitative data of good quality because of evaporation and high diffusion rates of some light elements within the glass during the measurement. It was thus decided to give up the idea of further measurements.

2.1 SCANNING ELECTRON MICROSCOPY (SEM)

Fabric studies were made on polished thin-sections by using a “FEI SIRION XL 30S FEG” scanning electron microscope (SEM). Secondary electron (SE) and back-scattered images (BSE) were recorded with an acceleration potential of 20 to 25 kV, a beam current of 1.2 nA, a working distance of 8 mm and a measuring time of 50 seconds per point. Semi-quantitative chemical analyses were obtained by energy dispersive spectrometry (EDS) with an “EDAX NEW-XL30” detector. Cross-section scans were used to generate X-ray maps of the elements Al, Na, Mg, Si, P, K, Sn, Ca, Ti, V, Mn, Fe, Cu and Zn (25 kV - 1.2 nA, dwell time 50 ms per pixel).

2.2 ELECTRON MICROPROBE

Metal droplets and the innermost thin layer (engobe) were quantitatively analysed with a "JEOL JXA-8200" microprobe at the University of Bern/Switzerland (15 kV - 20 nA, 5 µm spot size).

Element calibrations for metal droplets were carried out with a $CuZn_3$ alloy (Cu, Zn), natural crocoite (Pb), natural cassiterite (Sn), synthetic bunsenite (Ni) and synthetic ilmenite (Fe).

According to this, the calibration for the engobe were done with natural wollastonite (Ca), natural orthoclase (K, Si), synthetic anorthite (Al), natural albite (Na), synthetic ilmenite (Fe, Ti), synthetic forsterite (Mg), natural cassiterite (Sn), $CuZn_3$ alloy (Cu, Zn), synthetic tephroite (Mn) and natural monazite (P).

2.3 X-RAY POWDER DIFFRACTION

XRD analyses were obtained by using a "PHILIPS PW1800" diffractometer with CuKα radiation at 40 kV - 40 mA (0.02 °2Θ/step, 5 s/step, 5 - 90 °2Θ) and a conventional Bragg-Brentano geometry. The system was run with a variable divergence slit and a receiving slit size of 0.1 mm. A silicon standard was measured alongside the investigated samples in order to calibrate the peak position which allowed us to estimate firing temperatures from temperature sensitive cristobalite peaks.

2.4 PORTABLE ENERGY-DISPERSIVE X-RAY FLUORESCENCE ANALYSIS (CONTRIBUTION: M. HELFERT)

A total of 188 crucible fragments from Augusta Raurica were selected for portable energy-dispersive X-Ray fluorescence analysis (p-XRF) and 485 measurements were taken. Since the procedure has been discussed in detail elsewhere, only the main features shall be outlined here (Helfert and Böhme 2010, Daszkiewicz and Schneider 2011, Goren *et al.* 2011, Helfert *et al.* 2011, Helfert 2013). P-XRF has been used for a number of years as a qualitative and quantitative method of identifying multiple chemical elements in inorganic materials using a wide range of applications (cf. Potts and West 2008, Helfert and Ramminger 2012, Shackley 2012, Shugar and Mass 2012). The portable instruments allow to quickly carrying out the measurements on site in museum storerooms and excavations in a non-destructive or minimally-invasive manner on object surfaces or prepared areas and outcrops. The crucibles were measured using the analyser owned by the Institute of Archaeological Sciences at the Goethe University in Frankfurt am Main/Germany. It is an X-Ray fluorescence spectrometer XL3t 900SHe GOLDD (Geometrical Optimized Large Area Drift Detector) made by Thermo Fischer Scientific Niton which uses the latest detector technology and software.

While measurements can be carried out using the industrial calibration based on an international set of standards, an additional empiric fine calibration is recommended. This is necessary because measurements are not usually carried out on homogenous, plane powder samples but, as in the case of archaeological ceramics, on fresh breaks, resulting in more pronounced matrix effects. Therefore, the spectrometer was calibrated in the "mining Cu/Zn" mode prior to its use by measuring 140 samples of various types of fine and coarse pottery (from different places of production), where were previously measured by XRF-WDS and by comparing the reference and actual values. This process allowed us to correct the systematic discrepancies in the measurements between the different types of analysis. Without this fine calibration, the

measurements generated would not have been sufficiently comparable to other sample series that were created using other methods. As it stands, the configuration of the spectrometer allows us to precisely identify nine main and thirteen trace elements which can be used in the study (Helfert 2013).

The analyses were carried out in a confined space at a room temperature of between 18 and 25 °C and a relative humidity of approximately 50 %. Prior to being measured, the crucible fragments had been air-dried and stored in plastic bags. All ceramic measurements were carried out on fresh breaks. This was done to avoid measuring contaminants from the deposition in the ground or from the use of the crucibles. It was sometimes difficult to find a suitable location to measure used crucibles because they often bore lutum on the outside as well as casting and slag residue on the inside. Because the ceramic fragments were sometimes only a few millimetres thick, it was not always possible to exclude the presence of residual contamination on the samples in the measurement areas, which had diameters of 8 mm.

The measurements within the metal remnants on the crucibles were all carried out on the interior surfaces and in some cases also on the exterior surfaces. Because the metal residues were very small in some cases, the quantitative results cannot be viewed as representative of the alloys melted in the Roman-period crucibles, so that the study explored this particular question only from a qualitative point of view. Each artefact took 360 seconds to measure. The fragments were generally measured once. In cases where a fresh break was long enough, several measurements were carried out. It was hoped that more precise results could be obtained by creating average values, particularly for crucible clays tempered with coarse grains of quartz.

2.5 X-RAY FLUORESCENCE SPECTROSCOPY

Bulk chemical analyses (XRF-WDS) were carried out using a “PHILIPS PW2400”. All analyses were performed on pressed powder discs, which were prepared with 1.5 - 8 g of sample material and evaluated using “uniquant” (www.uniquant.com). The disc diameter was constant (32 mm), only the thicknesses varied as a function of the sample weight. Very thin discs (1.5 - 4 g) were pressed twice, i.e. with boric acid for the second time, to guarantee stability during the measuring procedure.

Some of the investigated samples were also prepared as glass pills in order to compare assessed data. Therefore, 0.7 g of the calcined sample as well as 0.35 g of Li fluoride and 6.65 g of Li tetraborate were mixed and melted in a Pt crucible at a temperature of 1150 °C. These pills were also analysed using the “PHILIPS PW2400” XRF-WDS and assessed using the software “basalt”.

2.6 THERMOGRAVIMETRIC ANALYSES (TGA)

The loss on ignition (LOI) was estimated with the help of a “Mettler-Toledo TGA/ SDTA 851e” thermogravimetry device (TGA) including a 801RO sample robot and a Mettler-Toledo TSO800GC1 gas controller at the College of Engineering and Architecture in Fribourg/Switzerland.All samples have been deposited in 70 µl sized Al_2O_3 crucibles and were measured under a constant flux of 100 ml/min N_2 respectively He.

2.7 RAMAN-SPECTROSCOPY

Raman spectroscopy was carried out on an DILOR Labram Raman spectroscope equipped with an “Olympus BX40” microscope at the Swiss Federal Institute of Technology Zurich/ Switzerland. All Raman spectra were acquired by using an argon laser (green laser) with λ = 514.5 nm at a power of 370 mW and 25 A. The measurement were done on polished thin-sections or surfaces of samples with a 100x magnification. The wave number calibration was done with silicon on the 520.5 cm^{-1} Raman band.

3 - ROMAN DOUBLE-LAYERED CRUCIBLES FROM AUTUN/FRANCE: A PETROLOGICAL AND GEOCHEMICAL APPROACH

D. König, V. Serneels

*Published in Journal of Archaeological Sciences **40**(1), 156–165 (2013)*

ABSTRACT

Eighteen double-layered crucible fragments found in an archaeological excavation site of the Lycée militaire (Autun/France), which dates to the Gallo-Roman period, were analysed with a series of classical mineralogical techniques in order to obtain knowledge about the raw materials of the individual layers. This work focuses on the usage of the crucibles as well as technical aspects of their production. The crucible fragments were studied by using petrographical (optical microscopy), elemental (SEM-EDS, EMPA, XRF-WDS) and mineralogical (XRD) techniques.

The two main layers of the crucibles are made of high refractory, kaolinite-based ceramic with granite-related temper grains. The analytical and petrographical results show remarkable differences between these two layers. The outer one is dominated by a high content of vitrified mullite-bearing matrix and contains analcime which was formed during the burial stage. In contrast, the inner layer is characterised by a non-vitrified matrix with a high content of orthorhombic mullite, β-cristobalite and α-quartz. An engobe is detectable in the majority of the fragments. The mineral composition allows an estimation of the firing temperatures, which have reached approximately 1200 up to 1400 °C.

3.1 INTRODUCTION

Crucibles and moulds from archaeological excavations are tools indicating specific metalworking practices of a certain period and bearing a large amount of information concerning the local metalworking, i.e., metal composition, production routine etc. (e.g., Nielen 2006, Tite *et al.* 1985).

Former studies generally distinguish between three functional groups of metalworking crucibles, namely cementation, assaying and melting crucibles (e.g., Bayley and Rehren 2007). Melting crucibles are the most common type and are known since the Late Neolithic (Bayley and Rehren 2007). It was necessary to construct them small but strong in order to guarantee easy handling of such metal charged vessels. Accordingly, the volume was commonly limited to a maximum of one litre of liquid metal, but often much less, prior to the Industrial Revolution. Such an usage also requires a fabric which ensures mechanical stability at temperatures well above 1000 °C (Bayley 1992, Bayley and Rehren 2007).

Individual crucibles show different fabric and material characteristics according to their special function. Bayley and Rehren (2007) classify crucibles using three main attributes: firstly, features related to the crucible design (e.g., shape

and size), secondly, the ceramic fabric including mineralogical and structural features and thirdly, the technical function. One milestone in the development of crucibles is the usage of refractory materials, mainly white-firing kaolinitic clays. These materials first arose in the Late Iron Age, became a major component of crucibles during the Roman period, but their complete technical potential was only developed during the medieval period (Freestone 1989, Rehren 2003, Bayley and Rehren 2007, Martinón-Torres *et al.* 2008, Thornton and Rehren 2009). A common type of Roman crucible is characterised by a double-layered wall structure. Some authors suggest an insulation function of the outer layer which can give off heat more equally, thus reducing the probability of a thermal shock (e.g., Bayley and Rehren 2007).

This article is a petrological and geochemical approach to identify and classify the metalworking crucibles from Autun/France. Individual aims are: (1) the detailed understanding of the ceramic structure and the investigation of the mineralogical/geochemical composition of the two main layers; (2) the characterisation of a potential engobe with regard to function and characteristics; (3) the identification of multiple usages; (4) the calculation of mineral-related firing temperatures; (5) the understanding of the production processes of the crucibles.

3.2 DOUBLE-LAYERED CRUCIBLES FROM AUTUN

The modern town of Autun/France (Fig. 3-1) developed from the Roman town of Augustodunum, one of the most important settlements in Gaul. Excavations at the site of the Lycée militaire have brought to light a craftsman district dominated by copper-based metalworking. More than 50 workshops were producing between the 1st and 3rd century A.D. (Chardron-Picault and Pernot 1999).

Figure 3-1. *Map of France with Autun in.*

Large quantities of crucible fragments (650 kg) and lids, and in few cases completely preserved crucibles (Fig. 3-2), were found in the area of the Lycée militaire. Preserved and reconstructed crucibles occur in slightly different shapes and at least three sizes with a volumetric capacity between 0.3 and 2.2 litres, i.e., 2.5 to 19 kilograms metallic charge. The crucible shapes are mainly cylindrical with a hemispherical base and some of them show a tapering shape to the top. Main types are recloseable with a separate lid and without any spout. This design is almost identical throughout the different crucibles sizes.

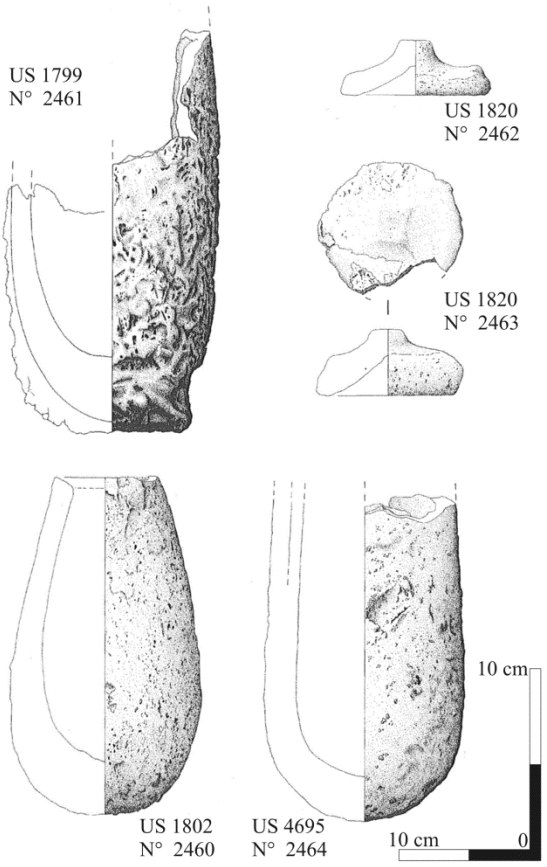

Figure 3-2. *Drawings of three representative crucible shapes from Autun; US 1799, N° 2461 – inner diameter: 11.5 cm, metal load: 21 cm; US 1802, N° 2460 – inner diameter: 9.5 cm, metal load: 18 cm; US 4695, N° 2464 – inner diameter: 10.3 cm, metal load: 18 cm. (modified after Chardron-Picault and Pernot 1999).*

3.3 RESULTS AND DISCUSSION

In general, all studied crucibles from Autun show a double-layered wall structure as exemplarily shown in Fig. 3-3. Individual layers possess their own thicknesses and fabric characteristics. The thickness of the outer layer increases from top to bottom, while the inner one remains nearly constant (Table 3-1; Fig. 3-3). Outer and inner layers can optically be distinguished by their different colours and the vitrified/ non-vitrified appearance. These optical features indicate mineralogical heterogeneities between single layers and individual fragments. The inner layer is covered by an added engobe (see Section 3.3.2) as already reported from other excavations like Neuss and Eberdingen-Hochdorf (Modarressi-Tehrani 2004, Nielen 2006). The outer, highly vitrified surface shows charcoal imprints implying heating from below. Copper-related colours (red and green) on the outer surface of the outer layer result from varying redox conditions during the metal-melting process in the furnace.

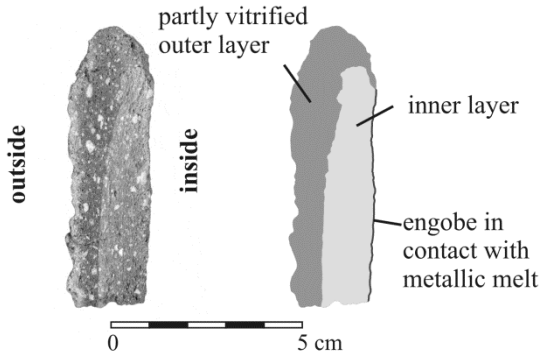

Figure 3-3. *Photograph of sample ATM 005 (left) and a sketch (right) of its main structural units.*

Sample	Thickness (mm) bulk (in; out)	Presence of an engobe	d_{101} Crs (nm)	Mineral content - inner layer	Mineral content - outer layer
ATM 001	19 (12; 7)	x	0.4062	Qtz+Crs+Mul+Or	Qtz+Crs+Mul+Anl
ATM 002	16 (12; 4)	x	0.4060	Qtz+Crs+Mul+Or	Qtz+Crs+Mul+Anl
ATM 003	16 (6-12; 10-4)	(x)	-	Qtz+Mul+Lct	Qtz+Mul
ATM 004	20 (10; 10)	x	0.4065	Qtz+Mul+Or	Qtz+Crs+Mul
ATM 005	21 (8-12; 13-9)	(x)	0.4062	Qtz+Crs+Mul	Qtz+Crs+Mul+Anl+Spl
ATM 006	17 (10; 7)	x	0.4059	Qtz+Crs+Mul+An	Qtz+Crs+Mul+Anl+An
ATM 007	15 (9-12; 6-3)	(x)	0.4063	Qtz+Crs+Mul+Lct+Anl	
ATM 008	26-35 (20-23; 15-3)	x	0.4058	Qtz+Crs+Mul+Or	Qtz+Crs+Mul+Anl
ATM 009	37-69 (22; 15-47)	x	0.4061	Qtz+Crs+Mul+Or	Qtz+Crs+Mul
ATM 010	40 (21; 19)		0.4059	Qtz+Crs+Mul	Qtz+Crs+Mul+Anl+Or
ATM 011	45 (20; 25)		0.4060	Qtz+Crs+Mul+Or	Qtz+Crs+Mul+Anl+Or
ATM 012	16-20 (11-12; 9-4)	x	0.4059	Qtz+Crs+Mul+Anl	
ATM 013	23 (15; 8)	x	0.4058	Qtz+Crs+Mul	Qtz+Crs+Mul+Anl
ATM 014	22 (18; 5)	x	0.4058	Qtz+Crs+Mul	Qtz+Crs+Mul+Anl
ATM 015	21-25 (11-15; 10)	x	-	Qtz+Crs+Mul+Anl	
ATM 016	18 (12-15; 6-3)	x	0.4059	Qtz+Crs+Mul+Or	
ATM 017	20-24 (15-17; 5-7)	x	0.4061	Qtz+Crs+Mul	Qtz+Crs+Mul+Anl+An
ATM 018	42 (22; 20)		-	Qtz+Mul+Or	Qtz+Crs+Mul+Anl

Mineral abbreviations: quartz (Qtz); cristobalite (Crs); mullite (Mul); analcime (Anl); orthoclase (Or); spinel (Spl); anorthite (An); leucite (Lct)

Table 3-1. *Crucible thickness and qualitative mineral content of both layers (i – inner layer; o – outer layer) determined by XRD; some specimens could not mechanically be separated.*

3.3.1 Geochemical and mineralogical characterisation of the two main layers

Macroscopically as well as microscopically it is possible to separate the layers with respect to their porosity, colour, grade of vitrification and the number and size of temper as well as non plastic inclusions (Fig. 3-4, Fig. 3-5). Observable matrix variations between both layers are linked to chemical and mineralogical variations. Temper grains consisting of quartz, feldspar and minor amounts of mica. Their proportions differ between the main layers of the investigated fragments. The outer layer consists of 60 - 70% temper grains dominated by potassium feldspar over quartz. In contrast, the inner layer possesses a total of 40 - 50% temper grains with nearly equal amounts of potassium feldspar and quartz. Generally, temper grains are sharp edged and vary in size between tens of micrometres and some millimetres.

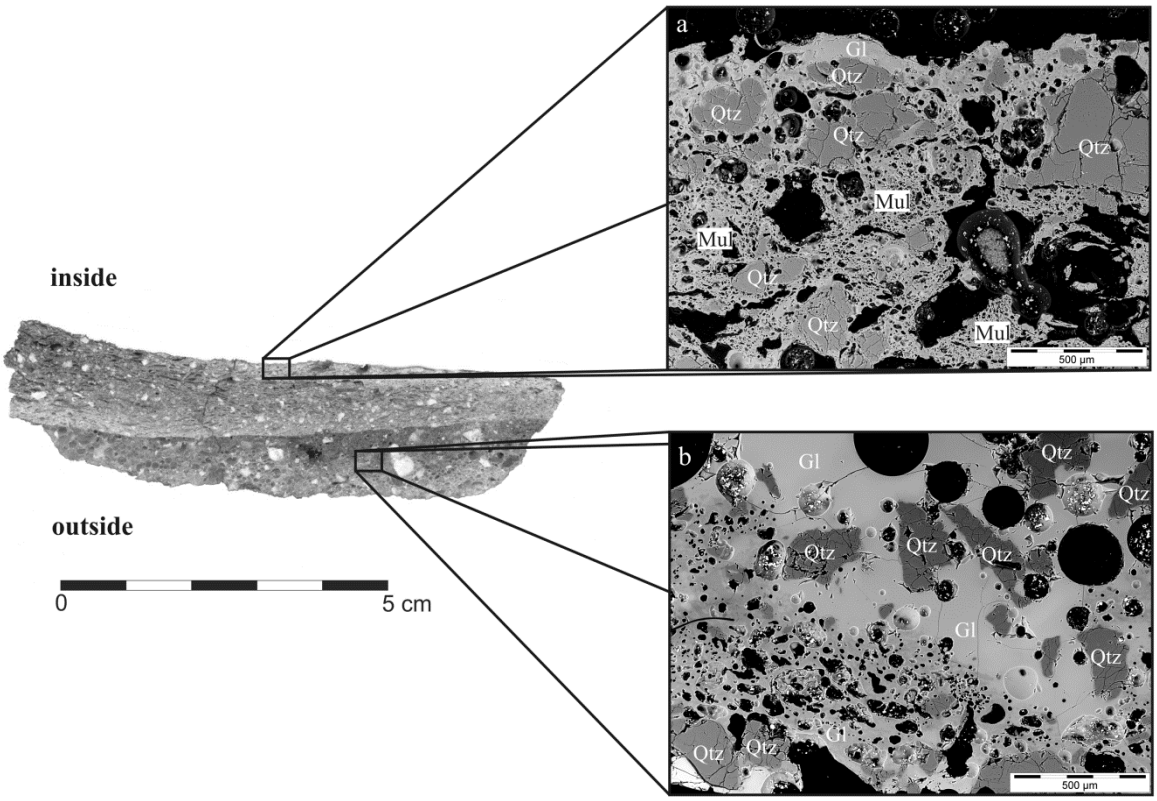

Figure 3-4. left: *representative section through the crucible fragment ATM 004, which illustrates both main layers with different colour and fabric characteristics;* ***right:*** *SEM-BSE images representing the differing fabric characteristics of the inner (a) and outer (b) layer; Qtz - quartz; Mul - mullite; Gl - glass.*

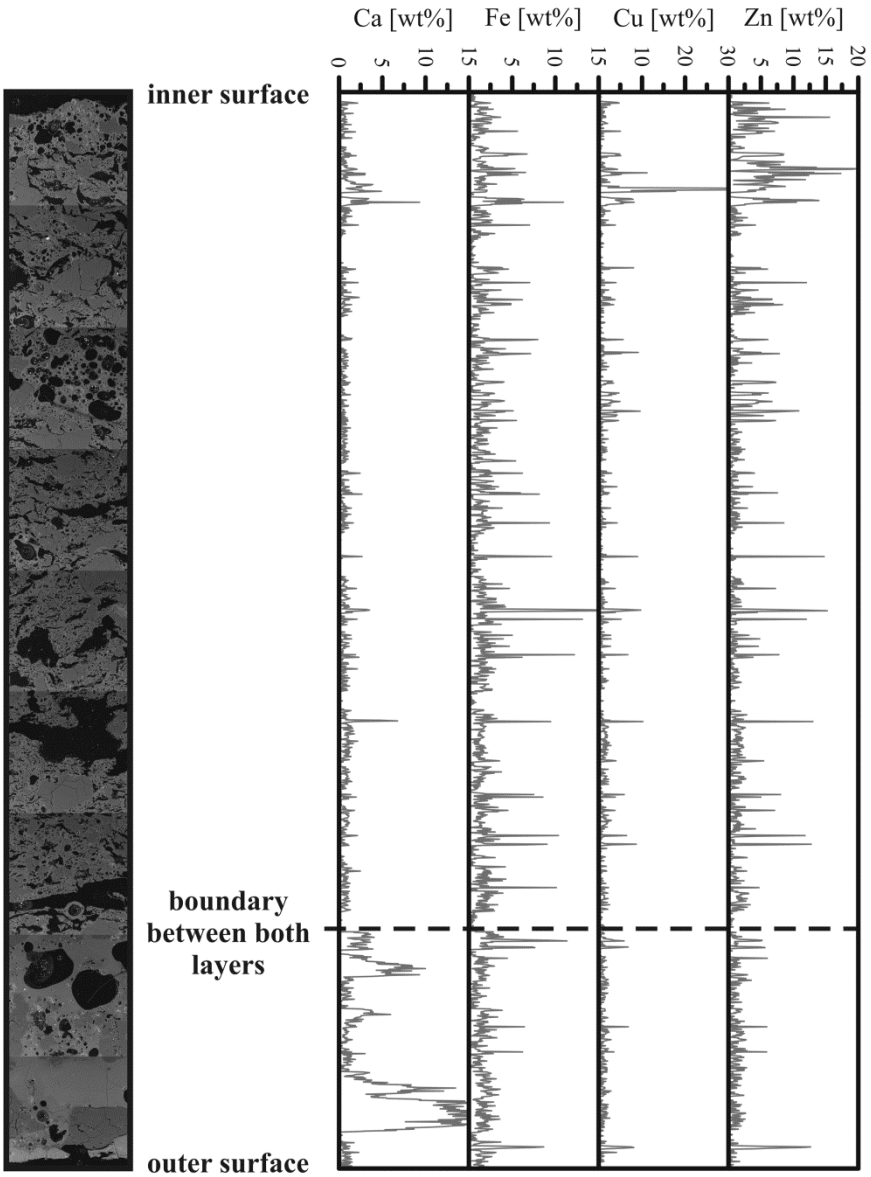

Figure 3-5. (a-d) *SEM-BSE images showing different types of temper grains within the inner layer; Qtz - quartz; Mul - mullite; Or - orthoclase; Bt - biotite.*

The low amount of detectable mica flakes has no influence on thermal stability. The outer layer shows a much higher porosity than the inner one, which is a direct consequence of its high degree of vitrification. During the firing process pore volume and size steadily increase until a maximum porosity is reached at a temperature around 950 °C to 1050 °C (May and Butterworth 1962, Maggetti and Kahr 1980). A closed porosity within the glassy matrix is a common feature observed in all fragments of the outer layer. In contrast, the inner layer shows a semi-open porosity. These pores are a result of a thermally induced dehydroxylation and subsequent phase transformation of kaolinite to

mullite during firing in the furnace and are not related to an addition of fibrous organic material.

SEM investigations show remarkable differences within the two main layers and the engobe, namely in texture (vitrified/non-vitrified). Moreover, calcium element maps and line measurements are suited to show major differences in bulk chemistry along the wall section. The border between the main layers as well as the engobe is marked by a significant change in the calcium content (Fig. 3-6). Moreover, the engobe is characterised by an appearance of metal droplets consisting of copper-tin or copper-zinc alloys (Appendix 3). Additionally, element migration (Zn) related to the metal-melting process is observable along the inner layer. SEM-BSE investigations are also suited to distinguish between primary mullite within the vitrified matrix and micrometre sized acicular secondary mullite in direct contact to potassium feldspar grains (Fig. 3-7) (Lee and Iqbal 2001).

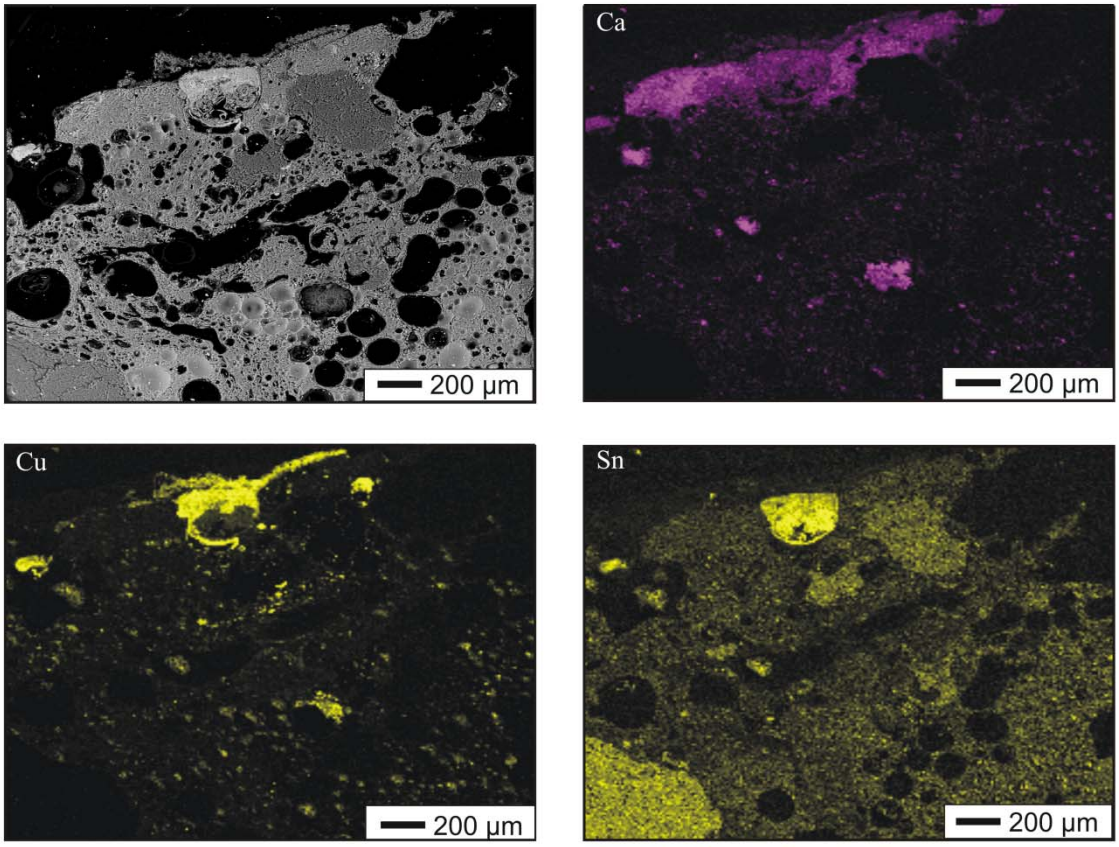

Figure 3-6. *SEM-BSE image and element maps showing the engobe with high calcium content compared to the inner layer; copper and tin maps showing the metal droplets within the engobe; the bright area in the left corner of the tin map corresponds to a measurement artifact (overlap of SEM-EDS Si line and Sn line).*

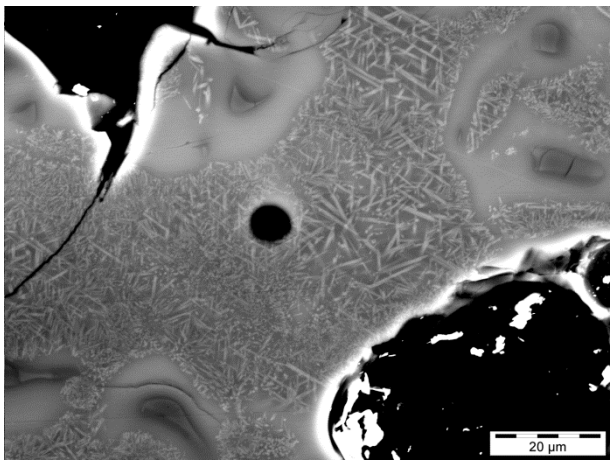

Figure 3-7. *SE image of acicular secondary mullite surrounded by a matrix of primary mullite.*

Based on XRD analyses (Table 3-1) quartz, mullite, potassium feldspar and cristobalite have been identified as the main constituents of both layers, accompanied by minor amounts of analcime in the outer layer. The amplitudes and the broadness of cristobalite peaks as well as a high background in the 40 to 55 °2Theta region indicate weak crystallinity and a high amount of glassy material within the outer layer of the ceramics. XRD detectable analcime is a typical alteration product of the vitrified phase developed in ceramics fired at high temperature (Pradell *et al.* 2010).

XRF bulk data verifies the chemical heterogeneities between both main layers. Table 3-2 summarises semi-quantitative data of the major components of the crucibles and indicates a dominance of SiO_2 and Al_2O_3, followed by K_2O in the inner and CaO in the outer layer, respectively. The content of alkali earth elements is mainly attributed to the matrix and the feldspar remnants therein. TG analyses yield a LOI of less than 0.2 wt.% within the ceramics, which is a direct consequence of the high firing temperature. However, LOI does not wholly account for the deviation of the total sum of the elements, which is in fact due to the utilisation of pressed powder discs, instead of more accurately measurable glass discs (Table 3-2). Thus, all XRF data have been declared as "semi-quantitative".

The compositional variations of the main layers are also visible in diagrams of Al_2O_3-SiO_2, MgO-SiO_2, CaO-SiO_2 and K_2O-SiO_2, which allow a clear distinction (Fig. 3-8). The outer layer contains a higher amount of CaO, MgO, K_2O and Fe_2O_{3tot} than the inner one. The content of Al_2O_3 behaves contrariwise. The binary plots of SiO_2/Al_2O_3-CaO, SiO_2/Al_2O_3-MgO, Fe_2O_{3tot}/Al_2O_3-CaO and Fe_2O_{3tot}/Al_2O_3-MgO point towards two distinguishable clay types and sources, respectively (Fig. 3-9).

	ATM 009_1 in	ATM 009_1 out	ATM 010_1 in	ATM 010_1 out	ATM 011_1 in	ATM 011_1 out	ATM 012_2	ATM 013_2 in	ATM 013_2 out	ATM 014_1 in	ATM 014_1 out	ATM 015_2	ATM 016_1	ATM 017_1 in	ATM 017_1 out	ATM 018_1 in	ATM 018_1 out
SiO_2 (wt.%)	64.5	71.4	67.8	65.7	68.6	74.7	71.6	70.4	69.6	68.1	69.5	72.5	66.9	71.3	69.4	71.1	72.6
TiO_2 (wt.%)	0.7	0.7	0.7	0.6	0.7	0.6	0.6	0.6	0.3	0.8	0.6	0.6	0.8	0.8	0.4	0.6	0.8
Al_2O_3 (wt.%)	28.5	16.8	24.6	15.6	23.6	10.3	18.9	19.9	17.9	23.2	13.3	19.2	23.4	20.4	17.5	19.8	12.9
Fe_2O_3 (wt.%)	1.7	3.0	2.0	4.1	1.8	2.7	1.7	2.0	1.8	2.0	3.9	1.8	2.1	2.1	1.8	1.8	2.5
MnO (wt.%)	0.01	0.05	0.03	0.46	0.03	0.39	0.06	0.06	0.11	0.02	0.45	0.03	0.02	0.04	0.25	0.05	0.15
MgO (wt.%)	0.6	0.8	0.5	0.5	0.6	0.7	0.5	0.7	0.7	0.6	0.7	0.7	0.6	0.5	0.8	0.6	0.8
CaO (wt.%)	0.2	1.7	0.3	3.0	0.3	4.0	1.6	1.1	3.1	0.4	3.8	0.5	1.4	0.5	4.4	1.0	3.5
Na_2O (wt.%)	0.3	0.9	0.3	2.7	0.4	0.8	0.7	0.5	0.8	0.5	0.9	0.5	0.4	0.5	0.6	0.4	0.7
K_2O (wt.%)	3.2	4.4	3.4	5.1	3.7	5.1	3.9	4.5	5.3	4.1	6.3	3.9	4.1	3.6	4.6	4.2	5.7
P_2O_5 (wt.%)	0.2	0.2	0.3	2.3	0.3	0.8	0.3	0.3	0.3	0.2	0.5	0.3	0.3	0.3	0.4	0.3	0.3
Sum before norm. (wt.%)	99.4	93.5	92.4	91.6	97.9	91.4	89.5	91.8	96.0	90.4	94.6	88.8	89.6	91.4	93.5	92.8	91.0
Sum norm. (wt.%)	100	100	100	100	100	100	100	100	100	100	100	100	100	100	100	100	100
Ba (ppm)	1070	1020	930	2810	1070	3800	1800	2040	1640	1160	1870	1350	1190	1130	1710	2190	1520
Cr (ppm)	<100	<100	<100	<100	<100	<100	<100	<100	<100	<100	<100	<100	<100	<100	<100	<100	<100
Cu (ppm)	150	390	4150	1520	1000	1830	880	450	5040	680	1810	140	770	200	330	300	710
Nb (ppm)	<100	<100	<100	<100	<100	<100	<100	<100	<100	<100	<100	<100	<100	<100	<100	<100	<100
Ni (ppm)	<100	<100	-	<100	<100	-	<100	-	-	-	-	-	-	<100	-	-	<100
Pb (ppm)	<100	<100	<100	<100	100	<100	<100	<100	<100	<100	<100	<100	<100	<100	<100	<100	<100
Rb (ppm)	210	270	220	630	240	320	310	230	450	260	410	240	270	230	400	200	440
Sn (ppm)	<100	<100	<100	<100	204	<100	<100	<100	165	<100	<100	<100	100	<100	<100	-	-
Sr (ppm)	100	120	<100	250	110	110	120	110	130	120	150	<100	130	100	210	100	170
V (ppm)	<100	<100	<100	<100	<100	<100	<100	<100	<100	<100	<100	<100	<100	<100	<100	<100	<100
Y (ppm)	<100	<100	<100	<100	<100	<100	<100	<100	<100	<100	<100	<100	<100	<100	<100	<100	<100
Zn (ppm)	6900	1060	7370	930	1000	450	8170	7670	4620	10900	470	7980	18300	12400	3180	7350	570
Zr (ppm)	240	330	250	280	250	400	240	230	140	280	370	230	300	280	170	220	510

	ATM 009_1 in	ATM 009_1 out	ATM 010_1 in	ATM 010_1 out	ATM 011_1 in	ATM 011_1 out	ATM 012_2	ATM 013_2 in	ATM 013_2 out	ATM 014_1 in	ATM 014_1 out	ATM 015_2	ATM 016_1	ATM 017_1 in	ATM 017_1 out	ATM 018_1 in	ATM 018_1 out
SiO_2 (wt.%)	64.5	71.4	67.8	65.7	68.6	74.7	71.6	70.4	69.6	68.1	69.5	72.5	66.9	71.3	69.4	71.1	72.6
TiO_2 (wt.%)	0.7	0.7	0.7	0.6	0.7	0.6	0.6	0.6	0.3	0.8	0.6	0.6	0.8	0.8	0.4	0.6	0.8
Al_2O_3 (wt.%)	28.5	16.8	24.6	15.6	23.6	10.3	18.9	19.9	17.9	23.2	13.3	19.2	23.4	20.4	17.5	19.8	12.9
Fe_2O_3 (wt.%)	1.7	3.0	2.0	4.1	1.8	2.7	1.7	2.0	1.8	2.0	3.9	1.8	2.1	2.1	1.8	1.8	2.5
MnO (wt.%)	0.01	0.05	0.03	0.46	0.03	0.39	0.06	0.06	0.11	0.02	0.45	0.03	0.02	0.04	0.25	0.05	0.15
MgO (wt.%)	0.6	0.8	0.5	0.5	0.6	0.7	0.5	0.7	0.7	0.6	0.7	0.7	0.6	0.5	0.8	0.6	0.8
CaO (wt.%)	0.2	1.7	0.3	3.0	0.3	4.0	1.6	1.1	3.1	0.4	3.8	0.5	1.4	0.5	4.4	1.0	3.5
Na_2O (wt.%)	0.3	0.9	0.3	2.7	0.4	0.8	0.7	0.5	0.8	0.5	0.9	0.5	0.4	0.5	0.6	0.4	0.7
K_2O (wt.%)	3.2	4.4	3.4	5.1	3.7	5.1	3.9	4.5	5.3	4.1	6.3	3.9	4.1	3.6	4.6	4.2	5.7
P_2O_5 (wt.%)	0.2	0.2	0.3	2.3	0.3	0.8	0.3	0.3	0.3	0.2	0.5	0.3	0.3	0.3	0.4	0.3	0.3
Sum before norm. (wt.%)	99.4	93.5	92.4	91.6	97.9	91.4	89.5	91.8	96.0	90.4	94.6	88.8	89.6	91.4	93.5	92.8	91.0
Sum norm. (wt.%)	100	100	100	100	100	100	100	100	100	100	100	100	100	100	100	100	100
Ba (ppm)	1070	1020	930	2810	1070	3800	1800	2040	1640	1160	1870	1350	1190	1130	1710	2190	1520
Cr (ppm)	<100	<100	<100	<100	<100	<100	<100	<100	<100	<100	<100	<100	<100	<100	<100	<100	<100
Cu (ppm)	150	390	4150	1520	1000	1830	880	450	5040	680	1810	140	770	200	330	300	710
Nb (ppm)	<100	<100	<100	<100	<100	<100	<100	<100	<100	<100	<100	<100	<100	<100	<100	<100	<100
Ni (ppm)	<100	<100	-	<100	<100	-	<100	-	-	-	-	-	-	<100	-	-	<100
Pb (ppm)	<100	<100	<100	<100	100	<100	<100	<100	<100	<100	<100	<100	<100	<100	<100	<100	<100
Rb (ppm)	210	270	220	630	240	320	310	230	450	260	410	240	270	230	400	200	440
Sn (ppm)	<100	<100	<100	<100	204	<100	<100	<100	165	<100	<100	<100	100	<100	<100	-	-
Sr (ppm)	100	120	<100	250	110	110	120	110	130	120	150	<100	130	100	210	100	170
V (ppm)	<100	<100	<100	<100	<100	<100	<100	<100	<100	<100	<100	<100	<100	<100	<100	<100	<100
Y (ppm)	<100	<100	<100	<100	<100	<100	<100	<100	<100	<100	<100	<100	<100	<100	<100	<100	<100
Zn (ppm)	6900	1060	7370	930	1000	450	8170	7670	4620	10900	470	7980	18300	12400	3180	7350	570
Zr (ppm)	240	330	250	280	250	400	240	230	140	280	370	230	300	280	170	220	510

Table 3-2. *Semi-quantitative bulk chemical data of the crucibles separated by layer (XRF-WDS); shaded - main metallic charge material.*

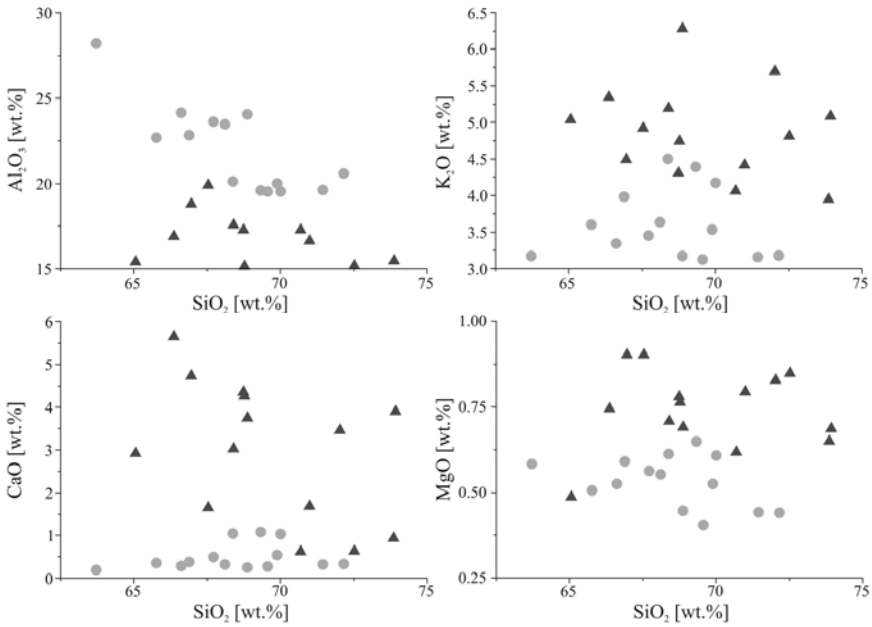

Figure 3-8. *Diagrams of selected XRF data points allowing a distinct separation related to Al_2O_3, MgO, CaO and K_2O in the main layers (inner layer - dots; outer layer - triangles).*

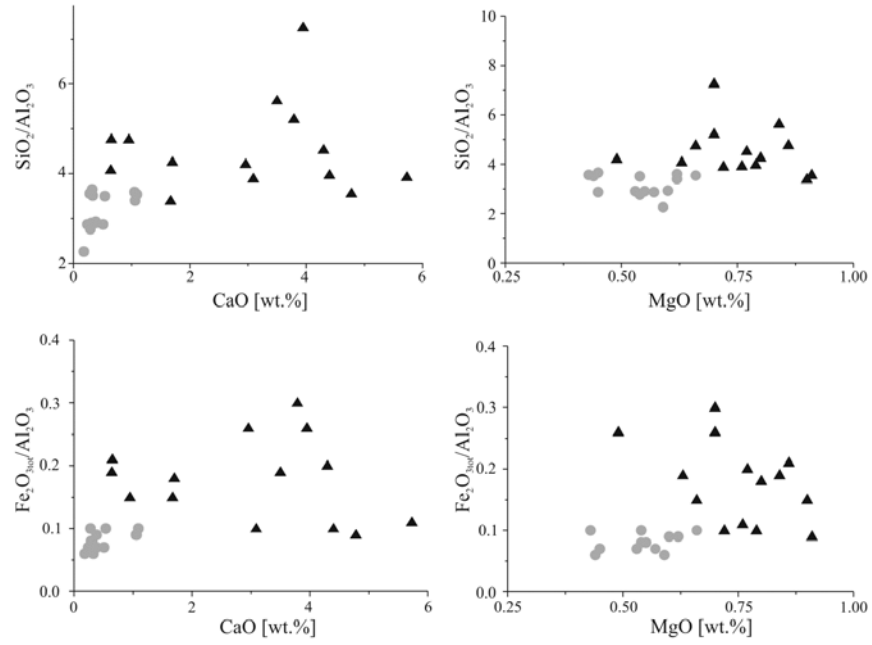

Figure 3-9. *Binary diagrams of SiO_2/Al_2O_3 and Fe_2O_{3tot}/Al_2O_3 ratios plotted against CaO and MgO indicating no linear dependence between the inner and the outer layer (inner layer - dots; outer layer - triangles).*

The above-mentioned results lead to a similar outcome and interpretation, namely that the inner and outer layers are different. In general, it is possible to argue with two reasons for the present ceramic properties. Firstly, the differences in porosity and the total amount of vitrified matrix directly correspond to the chosen production routine. A second, but not less important cause is related to the kind of usage, i.e., the way the crucibles were used for the melt production, which had a direct impact on the observed zinc migration within the wall sections. The inner layer is made up of 50 % non-vitrified matrix (mainly mullite), and 50 % temper grains, which are composed of even amounts of quartz and feldspar, which are often intergrown (Fig. 3-5). In contrast, the outer layer is made up of 40 % vitrified matrix containing mullite and analcime, and 60 - 70 % temper grains consisting of more feldspar than quartz. Thus, the ceramics are predominantly composed of granite-related temper grains hosting in an orthorhombic mullite bearing matrix which was formed by the dehydroxylation of kaolinite as well as the stepwise phase transformation to mullite, primarily initiated by the firing process. The outer layer has a slightly different chemical composition related to a marly limestone, marl or ash additive. A more detailed specification of the calcium additive was not yet possible due to missing sediment grains or locally enriched phosphate traces. However, anyone of these additives would have been used to increase the calcium and magnesium content in order to obtain a glassy layer. A primary calcium enriched kaolinitic clay can be excluded, cause of a general rareness of such clays in nature. The use of two different kaolinitic clays implies detailed knowledge of the chemical composition of different clay types, which can be excluded for Roman times. In general, the complete mineral composition of the investigated crucibles allows conclusions about firing and collapse temperatures, which will be discussed in Section 3.3.4.

An outer layer resulting from a reaction with fuel ash components can be excluded, because of a missing reaction rim. Calcium and magnesium are evenly distributed in the outer layer, i.e., there is no detectable diffusion front observable. Furthermore, the measured magnesium content is too low for a mid-European fuel ash mainly produced from hardwood with quite higher magnesium contents. In addition, there is a sharp boarder between both layers resulting from chemical and compositional differences (Fig. 3-3). Moreover, the binary plots in Fig. 3-9 reflecting the clay composition point towards two different clay sources.

3.3.2 The engobe as a kind of inner protecting layer

The engobe is preserved in the majority of investigated fragments and has an average thickness of 100 µm (Table 3-1; Fig. 3-10). Almost all preserved metal droplets of the investigated crucibles are distributed on top of remnants of this protecting layer and not within the semi-open porosity of the inner layer except of crack related porosity.

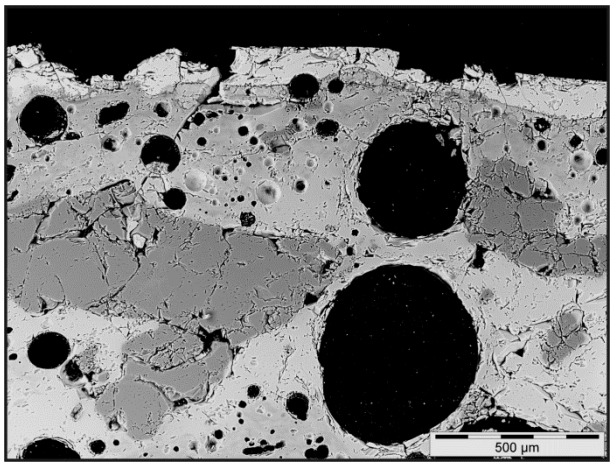

Figure 3-10. *BSE image of the vitrified engobe and the ceramic inner layer of the crucible ATM 002.*

Besides SEM-EDS and EMPA, the engobe was analysed by Raman spectroscopy to gather additional data. XRD and XRF-WDS analysis were not performed owing to low sample amounts. However, Raman data yield no evidence for a charcoal based layer or fuel ash migration within the inner layer. Both, SEM-EDS and EMPA (Table 3-3) deliver enriched amounts of calcium and potassium with respect to the inner layer. In general, the results indicate a similar composition like the outer layer except of non plastic inclusions, which are missing in the engobe. The instability under the electron beam also indicates a predominantly vitrified character of this layer. Generally, these results favour a similar raw material like the matrix material of the outer layer. Therefore we assume that this engobe is neither the result of migration processes nor formed during use. This layer is rather an added layer with protecting function than a layer formed by chance. One important indication for this theory is the consistent existents of this engobe from the bottom to the top of the crucibles with almost the same composition in several investigated fragments.

Sample	SiO_2 (wt.%)	TiO_2 (wt.%)	Al_2O_3 (wt.%)	Fe_2O_{3tot} (wt.%)	MnO (wt.%)	MgO (wt.%)	CaO (wt.%)	Na_2O (wt.%)	K_2O (wt.%)	P_2O_5 (wt.%)	CuO_{tot} (wt.%)	SnO_{tot} (wt.%)	ZnO (wt.%)	Total
ATM 002	52.78	0.77	23.40	1.87	0.23	0.95	7.81	1.16	8.04	0.16	-	0.02	3.76	100.94
ATM 002	53.15	0.72	22.51	1.73	0.32	0.99	8.19	1.07	8.51	0.45	-	0.02	3.31	100.98
ATM 002	54.58	0.69	22.09	1.26	0.32	0.96	8.03	1.12	9.04	-	0.08	-	2.44	100.61
ATM 002	52.68	0.74	23.27	1.71	0.32	0.94	8.51	1.11	8.43	0.44	-	-	2.79	100.94
ATM 002	53.80	0.57	20.84	2.76	0.22	1.21	7.19	1.06	8.04	0.74	-	-	3.63	100.05
ATM 002	55.40	0.54	19.68	2.82	0.27	1.25	6.77	1.07	8.23	0.54	-	-	4.11	100.68
ATM 002	55.94	0.45	16.33	1.93	0.28	1.12	11.52	0.90	5.95	0.74	-	0.01	5.04	100.19
ATM 004	48.12	0.17	31.92	0.52	0.03	0.17	15.22	1.36	1.22	0.40	0.54	0.03	1.18	100.87
ATM 004	45.55	0.43	34.19	1.29	0.08	0.81	1.00	1.98	5.94	0.18	-	0.02	9.15	100.62
ATM 004	48.90	0.77	11.86	3.35	0.83	2.17	16.94	1.27	3.30	-	0.20	0.04	10.59	100.22
ATM 012	57.11	0.61	16.43	0.63	0.45	2.02	15.24	2.12	4.68	-	0.01	-	1.02	100.33
ATM 012	54.39	0.65	15.34	0.38	0.54	2.30	20.91	1.00	3.36	0.28	0.72	-	0.60	100.48
ATM 012	55.42	0.60	16.22	0.19	0.53	2.28	20.31	1.04	3.39	0.13	0.32	-	0.25	100.68
ATM 012	57.34	0.77	17.85	0.71	0.39	1.80	12.61	2.08	5.51	0.43	0.20	0.01	1.01	100.72

Table 3-3. *EMPA data of the engobe of three different crucibles.*

3.3.3 Multiple usages

An indicator for multiple usages is given by the ceramic material itself. Clearly visible repairing marks on the outer layer are present in some of the investigated crucible sherds. These are characterised by a duplication of the outer layer, which is marked by the multiplication of the reddish coloured surfaces. The internal composition, structure and main element chemistry of these both layers is almost identical. Thus, we assume an identical raw material used for the primary outer layer and the added one. The overall implication is that the crucible itself was used at least two times.

Preliminary microprobe analyses on preserved metal particles give a hint for multiple usages, too. In general, there are two kinds of alloys found in single crucibles, Cu-Zn and Cu-Sn, with minor traces of iron and lead (Appendix 3).

3.3.4 Estimation of firing temperatures

For a discrimination of a certain firing temperature interval, a combination of different methods had to be used. XRD analyses which represent the coexistence of various mineral phases serve as an indicator for reached temperature ranges. According to Lee *et al.* (1999), elongated mullite needles develop between 1100 and 1200 °C and diminish the amount of previously formed spinel. The crystallisation of cristobalite from an amorphous silicate-rich phase starts at temperatures above 1300 °C. This minimum temperature can also favour the coexistence of orthorhombic mullite ($Al_6Si_2O_{13}$) and cristobalite (Gualtieri *et al.* 1995, Lee *et al.* 1999).

The sum of SiO_2, Al_2O_3 and K_2O yields between 90 and 96 %, which allows us to use the ternary SiO_2-K_2O-Al_2O_3 phase diagram to estimate the maximum stability temperatures of the investigated ceramics. The residual 4 to 10 % are mainly attributed to CaO containing additives, which were used to lower the breakdown temperature of the outer layer. In general, the inner layer is characterised by a significant higher amount of Al_2O_3 compared to the outer layer, which corresponds to a higher amount of kaolinitic clay and therefore a high amount of mullite in the ceramic (Fig. 3-11).

Cristobalite and tridymite are high temperature – low pressure silica polymorphs. It is generally accepted that pure silica systems do not generate tridymite as a stable phase (Hill and Roy 1958, Holmquist 1961, Stevens *et al.* 1997). The SiO_2 transformation is thus not only a function of pressure and temperature, but composition also. Stevens *et al.* (1997) argued that sodium or potassium carbonate additives can favour the formation of tridymite in SiO_2 rich ceramics. However, despite traces of potassium and sodium, tridymite is missing at all in all investigated samples. Recent works of Artioli *et al.* (2008) and Pradell *et al.* (2010) have demonstrated that tridymite formation is related to the existence of stabilising alkali ions, but the differences in the reached temperatures and pressures are in fact also important. The phase transition of α-quartz to β-cristobalite in pure silica systems occurs above temperatures of 1400 °C with an intermediate amorphous phase (Stevens *et al.* 1997). Multi-element/-mineral ceramics as presented here tend to influence such reaction temperatures and probably resulting in lower temperatures of such phase transitions.

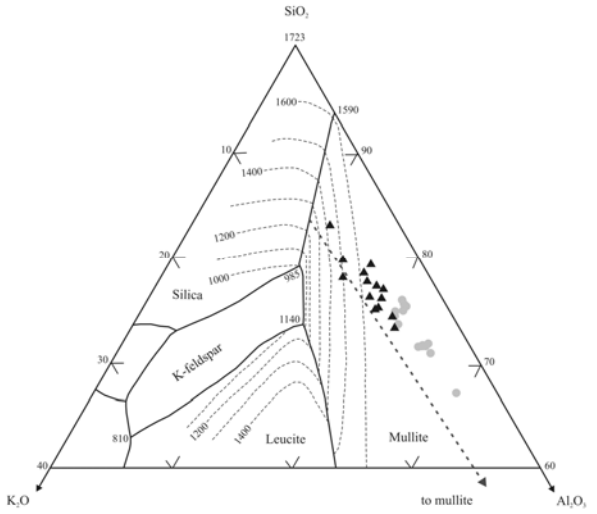

Figure 3-11. *High-silica part of the SiO_2-K_2O-Al_2O_3 phase diagram (modified after Osborn 1977, Maggetti et al. 2010). Isotherms are shown every hundred degrees; temperatures in °C. The fat dotted line is the projection toward the mullite-silica cotectic line. The grey dots correspond to the inner layer and the black triangles to the outer layer.*

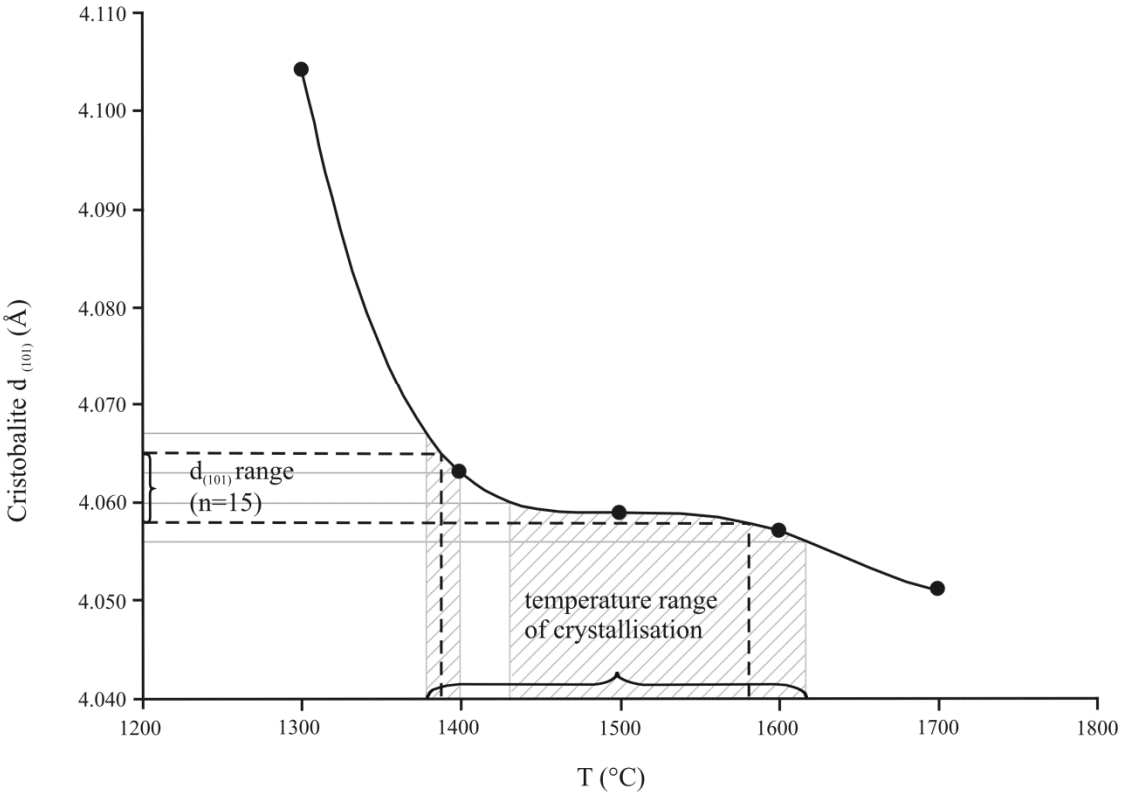

Figure 3-12. *Variation curve of the cristobalite $d_{(101)}$ peak as a function of temperature (after Eramo, 2005). The dotted lines show the $d_{(101)}$ range of the crucibles in 15 samples as well as the corresponding range of formation temperature. The grey shaded area displays the error of the peak position.*

Due to the fact that the crystalline order of cristobalite is increasing with temperature (Verduch 1958, Sosman 1965, Eramo 2005), it is possible to use the $d_{(101)}$ peak range as a temperature indicator, which shifts to lower d-values as the formation temperatures increase (Verduch 1958, Eramo 2005). The $d_{(101)}$ cristobalite peak positions of 15 crucibles (Fig. 3-12) lie in the range of 0.4058 to 0.4065 nm (±0.0002 nm), which correspond to firing temperatures above 1380 °C.

In addition, the amount of analcime, which is a secondary devitrification product of potassium- and sodium-rich glassy phases under humid and acidic environmental conditions in the burial stage, can be used as indicator for firing temperatures higher than 1200 °C. In general, the amount of analcime increases with increasing firing temperature (Buxeda *et al.* 2002, Schwedt *et al.* 2006, Pradell *et al.* 2010).

All these data indicate firing temperatures higher than necessary for the production of α-brass with melting point of around 1000 to 1050 °C. Nevertheless, the mineral assemblage indicates firing temperatures between 1200 and 1400 °C, i.e., much higher than the necessary melting temperature. Such an overheating might be necessary to melt the load in large crucibles as shown in Fig. 3-2 in a moderate period of time. Moreover, it enables a longer handling of the molten content to produce a higher number of small artefacts like fibulae. Indications for such a

high overheating are present in all investigated crucible fragments. This fact demonstrates the skills of Roman craftsmen which enabled them to produce in an »industrial« way, i.e., consistent production of a high quantity of crucibles and metal artefacts during decades.

3.4 CONCLUSION

Summing up, the results of this work demonstrate that all investigated crucibles are double-layered with clear mineralogical and structural differences in individual layers. Owing to differences in the feldspar-quartz proportions of the temper grains, it is possible to propose a granitic source for the raw material. The matrix of both layers consists of kaolinitic clay with high refractory characteristics. Only the outer layer has an additive which reduces the refractory performance of the matrix material, thus increasing the insulation function of the layer. The detected engobe consists of a material nearly identical to the matrix of the outer layer. It delays the migration of a liquid metal charge, giving it a protecting function and avoiding metal losses.

Clear evidence for a multiple usage were presented based on partial duplication of the outer layer as well as varying metal compositions of the metal droplets in single crucibles. The applied cristobalite peak method and temperature estimation derived from the mineral assemblage suggest relatively high firing temperatures (≥1380 °C). This range is generally higher than temperatures described for Roman metal-melting crucibles in literature (Tylecote 1982, Freestone 1989, Rehren 2003, Hein *et al.* 2007). However, such high pre-firing temperatures are already reported from a $15^{th}/16^{th}$ century excavation in Hesse/Germany (Martinón-Torres *et al.* 2008) and from the 17^{th} century glass-melting crucibles from Derrière Sairoche/Switzerland (Eramo 2006).

Overall, the crucibles were produced using a certain routine, which seems to be identical for all analysed fragments. At first the inner layer was built up of kaolinitic clay and a granite-related temper. This layer has been dried or fired at low temperatures. Afterwards, the outer layer consisting of a different kind of clay with a higher calcium content and granitic temper was added. The engobe was probably produced simultaneously by elutriate the clay of the outer layer and dispersing this suspension along the inner layer of the crucible which initially led to a millimetre thin layer covering the whole inside. Subsequent firing created a glassy engobe and outer layer with a ceramic inner layer in-between. Thus, the used production routine seems to be an appropriate method to produce crucibles stable under high temperature and suited for a multiple use.

4 - A PETROLOGICAL AND GEOCHEMICAL CHARACTERISATION OF ROMAN MOULDS AND BRASS-MAKING CRUCIBLES FROM AUTUN/FRANCE

Daniela König

Reviewed by Journal of Archaeological and Anthropological Sciences - not yet ready for publication

ABSTRACT

A multi-analytical approach using petrographical (optical microscopy), elemental (SEM-EDS, XRF-WDS) and mineralogical (XRD) techniques has been applied in order to characterise ceramic properties of Roman brass-making crucibles and lost-wax fibulae moulds. The outcome of this study will be compared with an earlier study dealing with Roman metal-melting crucibles from the same excavation site in Autun/France.

All investigated refractory ceramics are most likely composed of kaolinitic clay and a certain amount of interstratified kaolinite-smectite clay plus artificial temper grains comprised of quartz, feldspar and minor amounts of muscovite. The primary mineral composition is, thus, independent of the latter use. Notably differences arise from varying firing temperatures as inferred from a variable mineralogy with respect to the modification of primary minerals within the matrix. Thus, metal-melting crucibles are characterised by a coexistence of primary and secondary mullite as well as cristobalite which point towards firing temperatures between 1200 °C and 1400 °C. Slightly lower firing temperatures are expected for brass-making crucibles due to the cementation process (up to 1100 °C). Most of the investigated moulds are free of mullite, but meta-kaolinite bearing, which indicate maximum temperatures between 500 °C and 700 °C. However, some of them are also characterised by the occurrence of mullite within the matrix. This fact suggests firing temperatures which have probably reached around 950 °C. The most probable reason for this exception might be caused by massive pre-heating in a charcoal bed before use. The presence of secondary formed minerals, i.e. gahnite ($ZnAl_2O_4$) and willemite (Zn_2SiO_4) in brass-making crucibles, is in contrast to their absence in metal-melting crucibles and moulds.

4.1 INTRODUCTION

Crucibles and moulds are important artefacts to receive knowledge about specific metalworking practices (Nielen 2006, Tite *et al.* 1985). Thus, there is a specific interest to study such artefacts by a series of modern analytical techniques usually used in Material Sciences in order to obtain a detailed knowledge about used raw materials, their handling and the produced metal-alloys itself.

In general, it is possible to distinguish functional categories of crucibles which are considered to be main processes, i.e. melting and cementation (Bayley and Rehren 2007). The nature of these processes determines fundamentally the vessel form and the ceramic fabric (Rehren 2003). Metal-melting crucibles are the most common type (Bayley and Rehren 2007). It was important to design them small but strong in order to guarantee easy handling of such vessels. Furthermore, such

an usage requires a fabric which ensures mechanical stability at temperatures well above 1000 °C (Bayley 1992, Bayley and Rehren 2007). Correspondingly, the volume was commonly limited to a maximum of one litre of liquid metal, but often much less, prior to the Industrial Revolution (Bayley 1992, Bayley and Rehren 2007). Nevertheless, there are exceptions of these limitations as reported from excavation in Autun/ France (König and Serneels 2013 - Chapter 3).

Cementation crucibles are designed for the reaction of solids (e.g. metal, ore, etc.) with a vapour phase, which require carefully controlled temperatures and atmospheres to guarantee that the vapour phase stays in contact with the other ingredients (Bayley and Rehren 2007). Brass-making crucibles are a certain kind of cementation crucibles with specific and diagnostic features like poorly refractory fabrics, particular during the Roman period, and the high level of zinc detectable in all of them (Martinon-Torres and Rehren 2002). These kinds of crucibles are usually small in size (Bayley 1984, Rehren 1999) as this was beneficial for the energy balance of the process (Bayley and Rehren 2007). The crucibles have to be a kind of closed vessel. As the fabric is not sufficiently porous, a small opening is essential to relieve any build-up of pressure (Bayley and Rehren 2007). In order to maximise the ratio of surface area (heat input) to volume (heat use), these vessels are usually small and/or tubular rather than spherical in shape (Bayley and Rehren 2007). So far only a few case studies about brass-making crucibles of Roman age are published in literature and pointing to a diversified set of technologies. Findings are ranging from small-scaled vessels in Xanten/Germany (Rehren 1999) to large-scaled vessels from Lyon/France and Autun/France (Picon *et al.* 1995, Chardron-Picault and Picon 1997).

Cast objects like fibulae or brooches were made by melting metal in a crucible and pouring it into a mould, where it became solid. For the Roman period, two types of moulds are known, i.e. investment and piece moulds (Bayley and Butcher 2004). Investment moulds are such which were made by the lost-wax technique and destroyed after use. These kinds of moulds were most often made of fine clay in order to reproduce very detailed ornamentation (Bayley and Butcher 2004). There was no specific requirement regarding long lasting high temperature stability. Only necessities were dimensional stability and resistance against bursting which was guaranteed by pre-firing in order to release the wax (Davey 2009). Piece moulds consist of two or more pieces and made of stone or even clay. Such a mould can usually be reused. For Roman finds in Britain, Bayley and Butcher (2004) describe mainly piece moulds for casting single fibulae or brooches. They also describe continental finds, e.g. from Autun/France (Chardron-Picault and Pernot 1999) and Nandin/France (Marquart 1935), for which they suggest a simultaneous casting of two or more fibulae within one mould. This implies assembling of individual clay moulds to multiples before casting (Beck *et al.* 1982/3).

This study focuses on brass-making crucibles and lost-wax moulds from Autun/France in comparison to metal-melting crucibles from the same excavation. The aims of the study of technical ceramics from Autun/France are: (1) identification of the ceramic material regarding to clay and temper and their presence within different types of technical ceramics, i.e. metal-melting crucibles, brass-making crucibles and moulds; (2) to define the effect of use and the subsequently occurring differences, i.e. colour, ceramic thickness, number of layers, function of layers, etc.

4.2 Brass-making crucibles and moulds from Autun/France

The sample material derives from excavations at two different sites, of the Lycée militaire and Rue Bouteiller, inside one of the most important urban settlements in Gaul, the Roman town Augustodunum/Autun (Fig. 4-1 and 4-2).

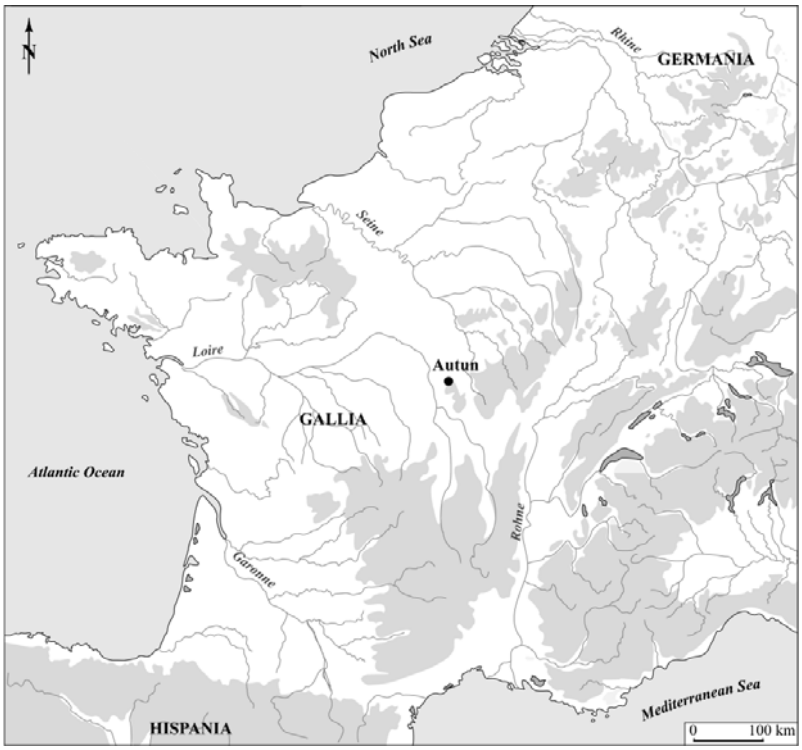

Figure 4-1. *Map of a part of Roman Gaul with Autun in.*

The urban craftsmen district was dominated by copper-based metalworking, with more than 50 proved workshops which have been in production between the 1st and 3rd century A.D. (Chardron-Picault and Pernot 1999).

The brass-making crucibles are easily distinguishable from metal-melting crucibles owing to their colour, specific shape and a lid joint with the ceramic by a secondary layer in the upper part. The shape of the brass-making crucibles mirrors a reverse water droplet with a flat bottom, while next to it the crucible reaches its largest diameter (Chardron-Picault and Picon 1997). Seventy-five kilos of these fragments were found during excavations in the Rue Bouteiller in Autun/France (Fig. 4-2) and indicating, therefore, a large-scaled brass production within the former Roman settlement Augustodunum. Almost all of the crucible fragments are characterised by single wall-structures (Fig. 4-3).

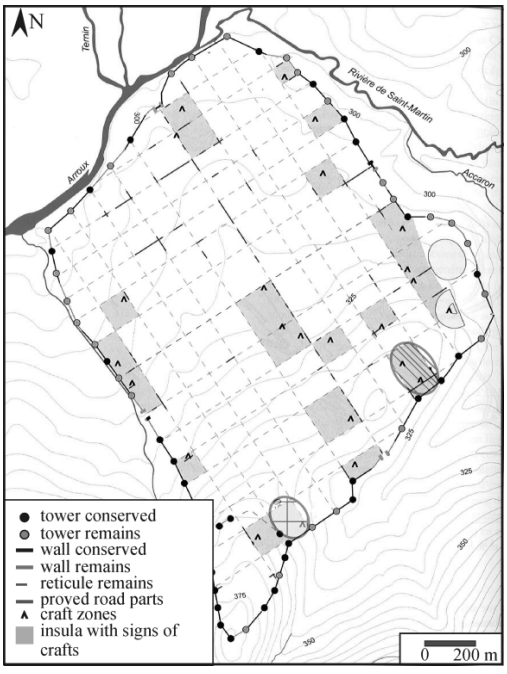

Figure 4-2. *Map of the Roman town Augustodunum with the localisation of craftswork; hatched - Lycée militaire; gridded - Rue Bouteiller (after Chardron-Picault et al. 2010).*

Only a few of them contain an in parts preserved second layer, which is already detectable by the naked eye and added to join the lid with the main ceramic body. All studied fragments representing the upper part of the crucibles and contain some decorative elements such as incised wavy lines. This type of brass-making crucible has comprehensively been described and drawn in a set of artefacts deriving from excavations of Roman settlements in Lyon (Picon *et al.* 1995) and Autun (Chardron-Picault and Picon 1997).

The amount of excavated and stored lost-wax mould fragments reaches around 280 kg and can mainly be attributed to five different types of two-part fibulae (Chardron-Picault and Pernot 1999) (Fig. 4-4). The latter mainly derive from the area of the Lycée militaire in the former Roman town Augustodunum (Fig. 4-2). Following Chardron-Picault and Pernot (1999), two different types of moulds used for the production of fibulae can be distinguished, i.e. single and multiple ones. In addition to specific moulds made for fibulae production, there are some minor finds of moulds used for bell production, small casting moulds and further ones which cannot be assigned to a certain artefact.

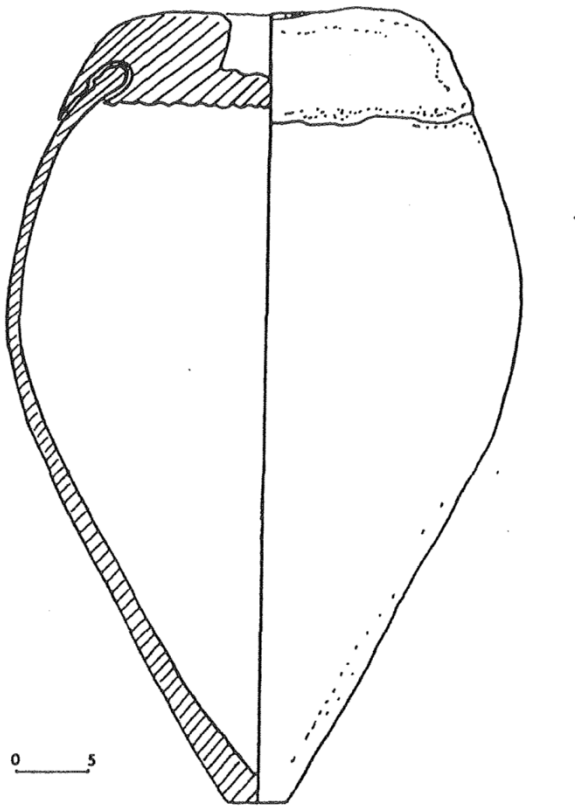

Figure 4-3. *Reconstruction of a brass-making crucible including a lid (drawn by A. Desbat and published in Picon et al. 1995).*

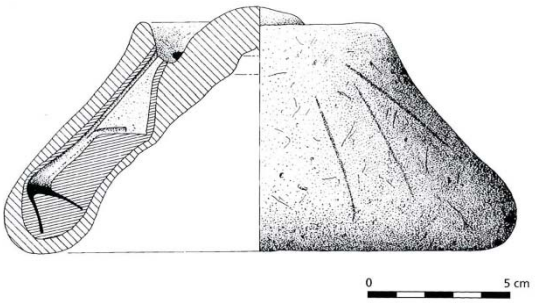

Figure 4-4. *Schematic sketch of a multiple Roman fibulae mould from Augustodunum (Chardron-Picault and Pernot 1999).*

4.3 BRASS-MAKING CRUCIBLES

There is an ongoing debate on brass-making crucibles and the technological processes they were designed for. Whereas Rehren and Martinón-Torres (2008) favour the argument that the Roman brass-making crucibles were used for cementation processes at 950 °C to 1050 °C, Craddock and Eckstein (2003) opine, based on a carefully selected literature review, that brass production is not strictly speaking a process without the presence of liquid brass formed by the reaction of solid copper and gaseous zinc at temperatures between 1000°C and 1100°C. Craddock and Eckstein (2003) support their arguments by the presence of high amounts of copper, lead and zinc, but without metal prills, within one completely recovered crucible examined by Bayley (1990). Based on the opinion of Craddock and Eckstein (2003), these elements are mandatory within the walls of brass-making crucibles due to melting of the brass during production. Latter also mention that it is doubtful to associate so called brass-making crucibles from Xanten/Germany (Rehren 1999) and Lyon/France (Picon *et al.* 1995) with brass production due to the absence of remnants of copper and lead ("metallic salts" sensu Craddock and Eckstein 2003) along the inner walls. However, whether Craddock and Eckstein (2003) nor Bayley (1990) clearly state if the Cu, Zn and Pb enrichments are present within in discrete metal droplets, some kind of slag or simply as mineral phases within the ceramic. It is, thus, impossible to judge by their arguments only if a crucible was made and used for brass production or not. However, the high amount of zinc as represented by discrete zinc minerals within the studied ceramics of Autun is a main evidence for a cementation process as there is no other metallurgical process known from Antiquity to generate such high amounts of Zn within the body of a ceramic vessel. The cementation process is characterised by a reaction of a solid phase with a vapour phase, i.e. solid copper and gaseous zinc for the production of brass (Rehren and Martinón-Torres 2008). But, it cannot be excluded that the melting point of the generated brass is reached during such a process. Such a brass melting during the cementation process evoked some researchers (Craddock and Lambert 1985, Jackson and Craddock 1995) to suggest a direct casting of objects from such brass-making crucibles without any further refining or melting of the generated brass (Craddock and Eckstein 2003). But, such arguments are in conflict with the occurrence of two different types of vessels namely brass-making and metal-melting crucibles, or more generally speaking, archaeologically, mineralogically and geochemically distinguishable crucibles from different Roman settlements in France and Germany (Picon *et al.* 1995, Chardron-Picault and Picon 1997, Rehren 1999, König and Serneels 2013 - Chapter 3).

All examined brass-making crucibles are characterised and distinguishable from metal-melting crucibles from Autun/France (König and Serneels 2013 - Chapter 3) by their remarkable purple blue colour (7.5 PB 7/4 - 6/6 – Munsell color chart) and the occurrence of a fixed lid. Macro- as well as microscopically it is possible to differentiate the wall sections of brass-making crucibles into three functional layers, namely an inner layer, the joining layer between the lid and the crucible itself (Fig. 4-5 and Table 4-1) as well as an occurring internal engobe. The ceramic of the inner layer has an average amount of 40 to 50 % of temper grains, which mainly consists of equal amounts of quartz and feldspar as well as less than five percent muscovite. The joining layer is a two to five millimetre thick layer of fired clay with an amount of temper grains between 50 and 60 %. The temper grains consist mainly of quartz and feldspar with equal amounts of both. Generally, temper grains are sharp edged and vary in size between tens of micrometers and some centimetres. Artificially added temper material present in all three types of ceramics most likely derives from a granitic source as there are plenty intergrowths of quartz, feldspar and in some cases mica. Such a source is not unlikely as there are

local occurrences of granitic rocks as well as their erosional products in the area around Autun/France. Imprints of charcoal or tools have not been recognised in any of the investigated brass-making crucibles.

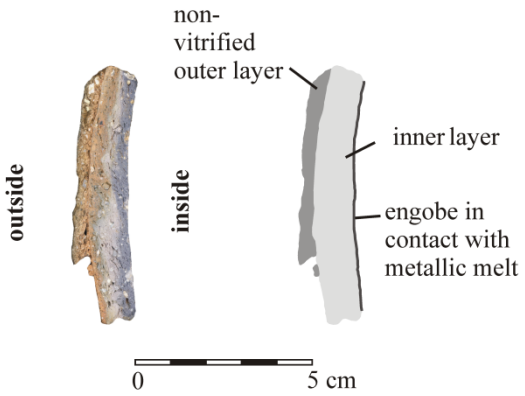

Figure 4-5. *Section through a brass-making crucible showing the three characteristic layers.*

SEM investigations reveal significant differences in the two layers and the engobe. The occurring engobe (Fig. 4-6), in general, is characterised by an enrichment of calcium compared to the inner ceramic layer. The engobe of one sample is additionally enriched in potassium compared to the overall enrichment in calcium. Furthermore, copper enriched areas are visible within the engobe (Fig. 4-6). The ceramic body shows a significant zinc gradient detectable with high concentrations along the inner part and diminishing outwards. These chemical findings correspond with the macroscopically visible change of the purple colour within the investigated fragments, i.e., there is a transition from dark purple (inside) to light purple (outside).

Temper grains like feldspar and mica show evidence for vitrification and dehydroxylation, respectively, in SEM micrographs (Fig. 4-7). Difficulties arising from this behaviour are lacking mica peaks and sometimes also badly resolved feldspar peaks in XRD data. Organic temper was not detected by optical microscopy and SEM analyses. The matrix of the ceramic shows a semi-open porosity due to a thermally induced dehydroxylation and the subsequent phase transformation of kaolinite to mullite during firing. There is no evidence for elongated mullite needles (secondary mullite) in direct contact to potassium feldspar.

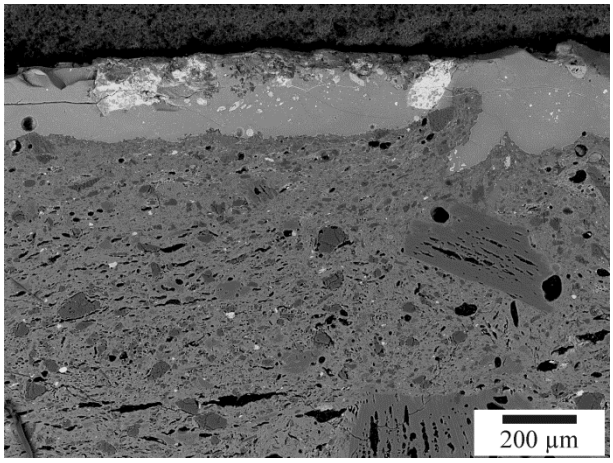

Figure 4-6. *SEM-BSE image of the vitrified engobe and the ceramic inner layer of the brass-making crucible ATM 037, bright whitish areas within the engobe are enriched in copper.*

Qualitative phase analyses by XRD confirmed the presence of quartz and feldspar as well as mullite, which build up the ceramic itself. XRD investigations yield two matches for zinc minerals, i.e. willemite (Zn_2SiO_4) and gahnite ($ZnAl_2O_4$). The presence of these minerals is also confirmed by optical SEM analyses in which they show crystals with a needle-like habit surrounded by the mullite-rich matrix. As these minerals are finely dispersed and relatively small, they are causal for the purple colour of the ceramics. The investigated joining layer show similar to the inner layer quartz and feldspar as temper grains and mullite as matrix material. In contrast, only gahnite is detectable within the joining layer.

	Thickness (mm)	Presence of an engobe	Mineral content
moulds			
ATM 019	16	-	Qtz+Pl+k-Fsp
ATM 020	19	-	Qtz+Pl+k-Fsp+Ms
ATM 021	16	-	Qtz+Pl+k-Fsp+Ms
ATM 022	08	-	Qtz+Pl+k-Fsp+(Mul+Spl)
ATM 023	18	-	Qtz+Pl+k-Fsp+Ms
ATM 024	17	-	Qtz+Pl+k-Fsp+(Mul)
ATM 025	06	-	Qtz+k-Fsp+Mul+Spl
ATM 026	05	-	Qtz+Pl+k-Fsp+Ms
ATM 027	14	-	Qtz+Pl+k-Fsp
ATM 028	18	-	Qtz+k-Fsp+(Mul+Spl)
ATM 029	07	-	Qtz+Pl+k-Fsp+Ms
ATM 030	09	-	Qtz+Pl+k-Fsp+Ms
ATM 031	10	-	Qtz+Pl+k-Fsp+Ms
ATM 032	09	-	Qtz+Pl+k-Fsp+Ms
ATM 033	07	-	Qtz+Pl+k-Fsp+Ms+(Mul+Spl)
ATM 034	06	-	Qtz+Pl+k-Fsp+(Mul)
brass-making crucibles			
ATM 035	22	x	Qtz+k-Fsp+Gah+Wil+Mul
ATM 036	09	x	Qtz+Wil
ATM 037 in	14	(x)	Qtz+k-Fsp+Gah+Wil+Mul
ATM 037 out			Qtz+k-Fsp+Gah+(Mul)
ATM 038	11	x	Qtz+k-Fsp+Gah+Wil+Mul
ATM 039	10	x	Qtz+k-Fsp+Gah+Wil
ATM 040	17	x	Qtz+Gah+Wil+Mul+Crs
ATM 041 in	12	x	Qtz+k-Fsp+Gah+Wil+Mul
ATM 041 out			Qtz+k-Fsp+Gah+(Mul)
ATM 042	09	x	Qtz+k-Fsp+Gah+Wil+Mul

Mineral abbreviations: cristobalite (Crs); gahnite (Gah); mullite (Mul); muscovite (Ms); plagioclas (Pl); potassium feldspar (k-Fsp); quartz (Qtz); spinel (Spl); willemite (Wil)

Table 4-1. *Total thickness of moulds and brass-making crucibles, presence (x) or absence (-) of an engobe and qualitative mineral content determined by XRD.*

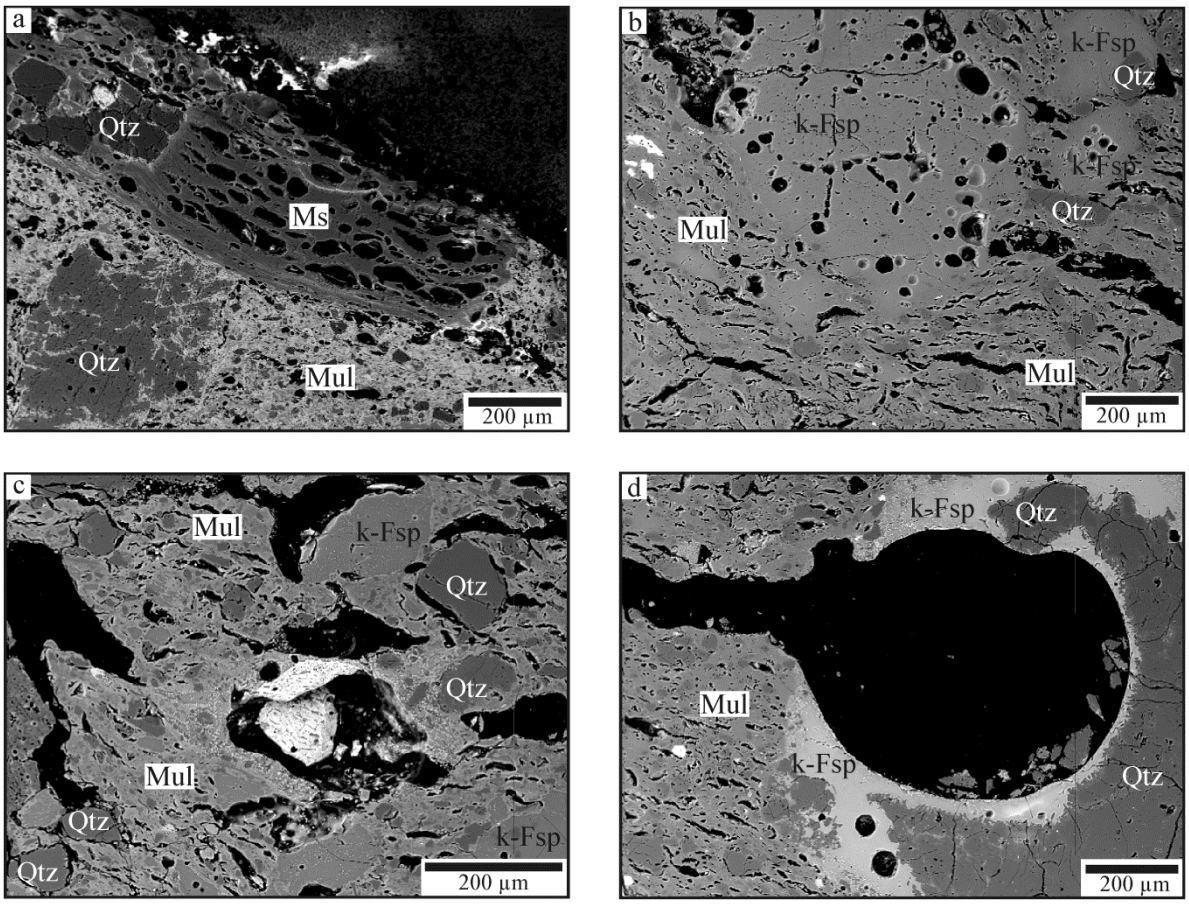

Figure 4-7. (a-d) *SEM-BSE images of the inner layer showing different types of, in parts thermally altered, temper grains in a mullite rich matrix; Qtz - quartz; Mul - mullite; k-Fsp - potassium feldspar; Ms – muscovite.*

Especially for the inner layer, semi-quantitative XRF analyses (Table 4-2) illustrate a relatively high amount of zinc compared to all other technical ceramics from the Roman period excavated in Autun. This zinc enrichment is a direct result of the utilisation of the crucible and, therefore, a clear evidence for brass production. XRF data of the two investigated joining layers are comparable with those of the inner ones in case zinc is excluded when summing up the chemical data.

4.4. LOST-WAX MOULDS

All moulds studied have single layered wall-structures with a fine clay coating in direct contact to the metal load (Fig. 4-8). The ceramic matrix appears (light to dark) grey. 30 up to 40 % of sharp edged temper grains are already visible with the naked eye (maximum grain size 5 mm) and are dominated by quartz over feldspar. Minor amounts of muscovite temper have additionally been identified by polarised light and SE microscopy (Fig. 4-9). Aforementioned characteristics are only valid for the main ceramic body, the thin internal layer shows no artificially added temper and non-

plastic inclusions. This coating seems to be a layer which was originally applied on the wax model to create a perfect negative imprint without interfering coarse temper grains as already described in literature (e.g. Kearns *et al.* 2010). This layer also helps to minimise the contamination of the alloy and decrease the surface exposed to reaction (Kearns *et al.* 2010).

Some of the studied moulds preserve the primary mineral content to a certain extent and show no evidence for mica dehydroxylation, but kaolinite breakdown. These observations arise in parts from XRD studies as there are well resolved mica peaks present, but no kaolinite peaks at all. Feldspars are optically in good order, too. As a result of these ceramic properties, the highest temperatures reached must have been much lower than for the crucibles studied. SEM investigations depict a homogenous matrix and a uniform distribution of temper grains. Some of them can clearly be attributed to rock-fragments, i.e. mica-quartz-feldspar, in addition to monomineralic grains (Fig. 4-9). All investigated moulds are free of residual metal droplets.

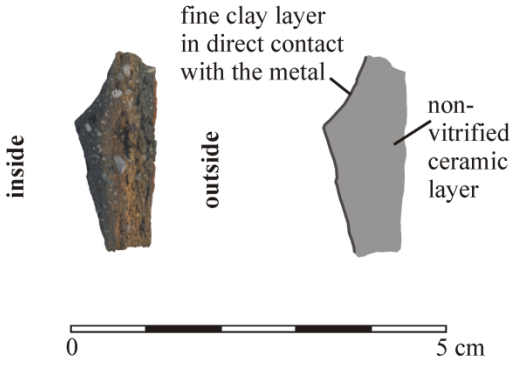

Figure 4-8. *Section through a mould fragment with the main ceramic body and a fine clay layer in direct contact with the metal load.*

Interestingly, there are a few samples showing the presence of mullite and/or spinel-like phase within the matrix material (Table 4-1), i.e. the heat-induced transformation products of kaolinite and meta-kaolinite. Those samples without any mullite are probably built up of meta-kaolinite, a X-ray amorphous and therefore not detectable phase in XRD spectra, but in SEM data. Moreover, there are no detectable zinc or copper minerals present within these ceramics.

4.5 COMPARISON BETWEEN THE THREE MAIN TYPES OF COPPER-ALLOY RELATED CERAMICS FROM AUTUN

4.5.1 Structure of the investigated ceramic types

Three main types of copper-alloy related ceramics were recognised during the excavations in Autun/France, i.e. metal-melting crucibles, brass-making crucibles and moulds (Chardron-Picault and Pernot 1999). The properties of the wall structures of all three types are summarised in Table 4-3. Whereas metal-melting and brass-making crucibles consist of more than one ceramic layer, all investigated moulds are made up of a single ceramic body. The joining layer of metal-melting crucibles has an insulation function and helps to keep the heat within the metallic charge (e.g. Bayley and Rehren 2007). The inner layer is important for the stability of the crucible and, therefore, composed of a high-temperature resistant material, i.e. a mullite bearing ceramic. Brass-making crucibles, unlike metal-making ones, are not vitrified on the outer surface. The joining layer of this crucible type is not comparable with the outer layer of the metal-melting crucibles. This is caused by different purposes the layer was added for.

.

	ATM 019	ATM 020 in	ATM 020 out	ATM 021	ATM 022	ATM 023	ATM 024	ATM 025	ATM 026	ATM 027	ATM 028	ATM 029	ATM 030	ATM 031	ATM 032	ATM 033	ATM 034
SiO_2 (wt.%)	67.1	72.1	68.3	67.2	66.5	71.1	70.4	68.3	70.9	68.5	70.5	70.4	70.7	70.1	66.9	69.9	70.2
TiO_2 (wt.%)	0.7	0.3	0.7	0.7	0.5	0.4	0.5	0.5	0.5	0.6	0.5	0.4	0.6	0.6	0.5	0.6	0.5
Al_2O_3 (wt.%)	19.8	19.1	19.6	20.3	21.3	20.5	19.1	20.3	19.1	19.6	19.6	19.7	17.8	18.5	21.3	19.4	20.2
Fe_2O_3 (wt.%)	4.8	2.0	4.6	4.8	4.2	2.4	3.3	3.7	3.6	4.4	3.6	2.9	3.5	3.3	3.5	3.7	3.0
MnO (wt.%)	0.04	0.03	0.04	0.04	0.04	0.02	0.05	0.03	0.04	0.03	0.04	0.02	0.04	0.04	0.04	0.03	0.02
MgO (wt.%)	1.6	0.7	1.5	1.6	1.4	0.9	1.0	1.1	0.8	1.3	0.8	1.1	1.0	1.0	1.3	1.1	1.0
CaO (wt.%)	0.8	0.9	0.4	0.6	0.5	0.4	0.3	0.4	0.4	0.6	0.4	0.5	0.6	1.0	0.8	0.6	0.4
Na_2O (wt.%)	1.0	0.2	0.9	0.8	1.0	0.4	0.9	0.9	0.4	0.8	0.4	0.8	1.1	0.7	0.7	0.6	0.6
K_2O (wt.%)	3.6	3.6	3.6	3.6	4.3	3.6	4.2	4.6	3.8	3.8	4.0	4.0	4.2	3.9	4.2	3.7	3.9
P_2O_5 (wt.%)	0.6	1.1	0.3	0.4	0.4	0.4	0.1	0.2	0.3	0.4	0.3	0.2	0.3	0.9	0.8	0.4	0.2
Sum before norm.(wt.%)	97.0	100.0	98.7	98.2	96.3	99.7	97.4	96.8	98.1	97.4	96.0	98.1	96.2	94.9	99.2	97.0	98.7
Sum norm. (wt.%)	100	100	100	100	100	100	100	100	100	100	100	100	100	100	100	100	100
Ba (ppm)	2150	2210	2430	1870	1260	1220	1500	1650	1190	1740	1130	1900	1900	1250	1700	1630	1190
Cr (ppm)	<100	<100	<100	<100	<100	<100	<100	<100	<100	<100	<100	<100	<100	<100	<100	<100	<100
Cu (ppm)	180	370	100	270	350	270	<100	280	120	500	140	140	370	1300	280	230	<100
Nb (ppm)	<100	<100	<100	<100	<100	<100	<100	<100	<100	<100	<100	<100	<100	<100	<100	<100	<100
Ni (ppm)	-	-	-	-	-	-	-	-	-	-	-	-	-	-	-	-	-
Pb (ppm)	120	110	120	130	110	110	110	110	110	120	120	130	210	120	150	140	110
Rb (ppm)	340	380	350	330	390	370	370	400	320	340	350	390	320	310	380	360	390
Sn (ppm)	-	-	-	-	<100	-	-	-	<100	-	-	-	<100	<100	-	<100	-
Sr (ppm)	120	110	110	110	110	100	100	100	<100	100	85	100	120	120	120	100	<100
V (ppm)	<100	<100	<100	<100	<100	<100	<100	<100	<100	<100	<100	<100	<100	<100	<100	<100	<100
Y (ppm)	<100	<100	<100	<100	<100	<100	<100	<100	<100	<100	<100	<100	<100	<100	<100	<100	<100
Zn (ppm)	460	400	250	340	900	1030	290	540	760	910	660	1370	900	1270	1690	1030	1750
Zr (ppm)	320	150	330	310	260	190	300	270	310	290	330	220	390	360	240	290	230

Table 4-2-1. *Semi-quantitative bulk chemical data of brass-making crucibles partly separated by layer (XRF-WDS); shaded - main metallic charge material.*

	ATM 035	ATM 036	ATM 037 in	ATM 037 out	ATM 038	ATM 039	ATM 040	ATM 041 in	ATM 041 out
SiO_2 (wt.%)	69.8	69.3	68.0	66.4	72.5	72.5	65.5	71.2	70.1
TiO_2 (wt.%)	0.7	0.8	0.9	0.6	0.5	0.4	0.5	0.4	0.4
Al_2O_3 (wt.%)	22.1	22.8	23.0	23.4	19.3	20.5	23.1	21.5	21.5
Fe_2O_3 (wt.%)	2.6	2.5	3.1	3.7	2.2	2.3	4.8	2.9	2.6
MnO (wt.%)	0.02	0.03	0.02	0.05	0.01	0.03	0.12	0.05	0.02
MgO (wt.%)	0.6	0.6	0.7	0.6	0.6	0.5	1.0	0.5	0.4
CaO (wt.%)	0.3	0.3	0.5	0.6	0.3	0.3	1.1	0.4	0.2
Na_2O (wt.%)	0.5	0.1	0.5	0.3	0.7	0.3	0.6	0.0	0.4
K_2O (wt.%)	3.2	3.5	3.2	3.5	3.7	3.0	2.7	2.9	4.3
P_2O_5 (wt.%)	0.2	0.1	0.2	0.7	0.1	0.1	0.6	0.1	0.1
Sum before norm.(wt.%)	95.9	104.2	94.5	96.7	91.1	97.5	94.5	96.4	88.1
Sum norm. (wt.%)	100	100	100	100	100	100	100	100	100
Ba (ppm)	960	830	900	1770	1330	890	1090	580	1020
Cr (ppm)	<100	<100	<100	<100	<100	<100	<100	<100	<100
Cu (ppm)	<100	150	1040	360	<100	<100	490	100	<100
Nb (ppm)	<100	<100	<100	<100	<100	<100	<100	<100	<100
Ni (ppm)	-	-	-	-	-	-	-	-	-
Pb (ppm)	160	<100	320	180	350	<100	190	<100	<100
Rb (ppm)	290	250	320	270	260	190	210	150	310
Sn (ppm)	<100	-	-	-	-	-	-	<100	-
Sr (ppm)	<100	<100	110	130	100	<100	100	<100	110
V (ppm)	<100	<100	<100	<100	<100	<100	<100	<100	<100
Y (ppm)	<100	<100	<100	<100	<100	<100	<100	<100	<100
Zn (ppm)	102500	208200	60700	19000	99600	133900	87100	213800	39900
Zr (ppm)	320	150	330	310	260	190	300	270	310

Table 4-2-2. *Semi-quantitative bulk chemical data of moulds partly separated by layer (XRF-WDS); shaded - main metallic charge material.*

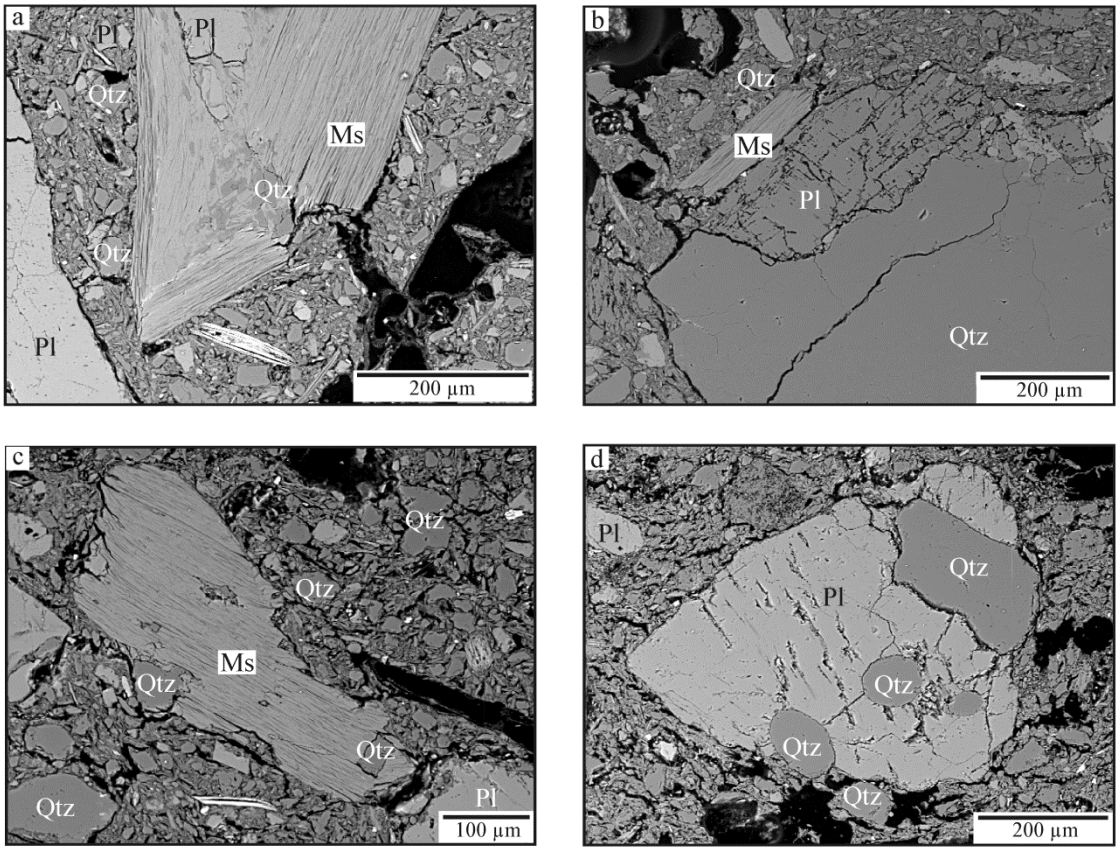

Figure 4-9. (a-d) *SEM-BSE images showing different types of temper grains within the moulds; Qtz - quartz; Pl - plagioclas; Ms – muscovite.*

It is evident from the upper parts of the brass-making crucibles, that the joining layer was added to stick the lid and the crucible itself together. Accordingly, this layer is only present along the upper part of the crucibles as already described by Chardron-Picault and Picon (1997).

The engobe of both crucible types probably possess also a specific function, i.e. this sub-millimetre thin layer had guaranteed to pull out the metallic charge almost completely. This hypothesis rests on the fact that only very few metal remnants have been found in any of the brass-making crucibles studied and only some tiny remnants in the metal-making ones.

In contrast to the analysed crucibles, the moulds are predominantly composed of a single layered ceramic without any kind of vitrification. The very thin layer which is in direct contact with the metal load is not comparable with the engobe, but this layer provided the possibility to produce objects with a very smooth surface due to the absence of artificial added temper.

4.5.2 Chemical composition of the investigated ceramic types

The chemical composition of the inner layer of metal-melting crucibles, brass-making crucibles and moulds is almost the same, except for the

variable amount of MgO (Figs. 4-10 and 4-11). This difference could either be attributed to the presence of Mg bearing mica added as temper or a slight variation of the clay composition, i.e. a higher amount of Mg-rich clays, e.g. smectite, within the moulds. The outer layer of metal-melting crucibles is characterised by calcium and potassium enrichments in comparison to the inner layer. This is probably resulting from an additive which reduces the refractory performance of the matrix material (König and Serneels 2013 - Chapter 3). Adding a Ca rich material to commonly used clay for both ceramic layers seems more feasible than trying to find another clay source possessing the requested properties to vitrify extensively during use. Such a technique is quite common and comprehensively discussed in literature (*Lutum sapientiae* – Furger forthcoming). In addition, selecting clay with the requested properties from a clay pit would require a very high knowledge about the chemistry and the behavior at high temperatures of different natural clay materials already at Roman times. This seems rather unlikely.

The almost homogeneous chemical composition (Table 4-2 and Table 3-2) point towards a similar or even identical raw material for all three types of ceramics investigated (Fig. 4-11). Minor differences are caused by chemical variations in temper and/or additives and the added amount of the latter itself. Metal-melting crucibles and moulds are 100-times poorer in zinc but equally enriched in copper compared to brass-making crucibles. These differences are related to different production steps the ceramics were used for, i.e. brass-making versus metal-melting and casting. Such enrichments of zinc in brass-making crucibles, metal-melting crucibles and moulds are in agreement with literature data on this topic (e.g. Bayley 1990, Picon *et al.* 1995, Rehren 1999) and favour a subdivision into brass-making and metal-melting crucibles. Kearns *et al.* (2010) comprehensively document and discuss the effect of copper alloy composition on final metal enrichments within the ceramic body of moulds.

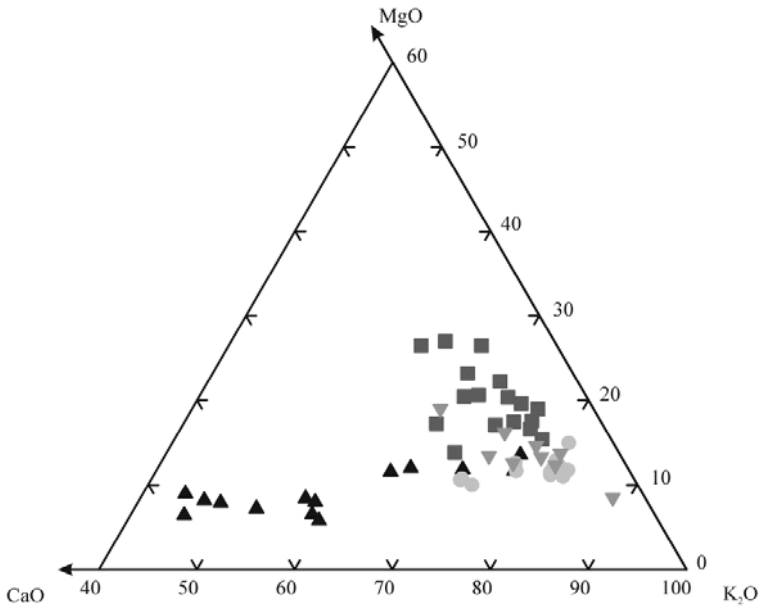

Figure 4-10. *Ternary diagrams of XRF analyses allowing a distinct separation of the outer layer of metal-melting crucibles with a lower refractory performance from the rest of the investigated ceramics; grey dots - metal-melting crucibles (inner layer); black triangle - metal-melting crucibles (outer layer); square - moulds; triangle upside down - brass-making crucibles.*

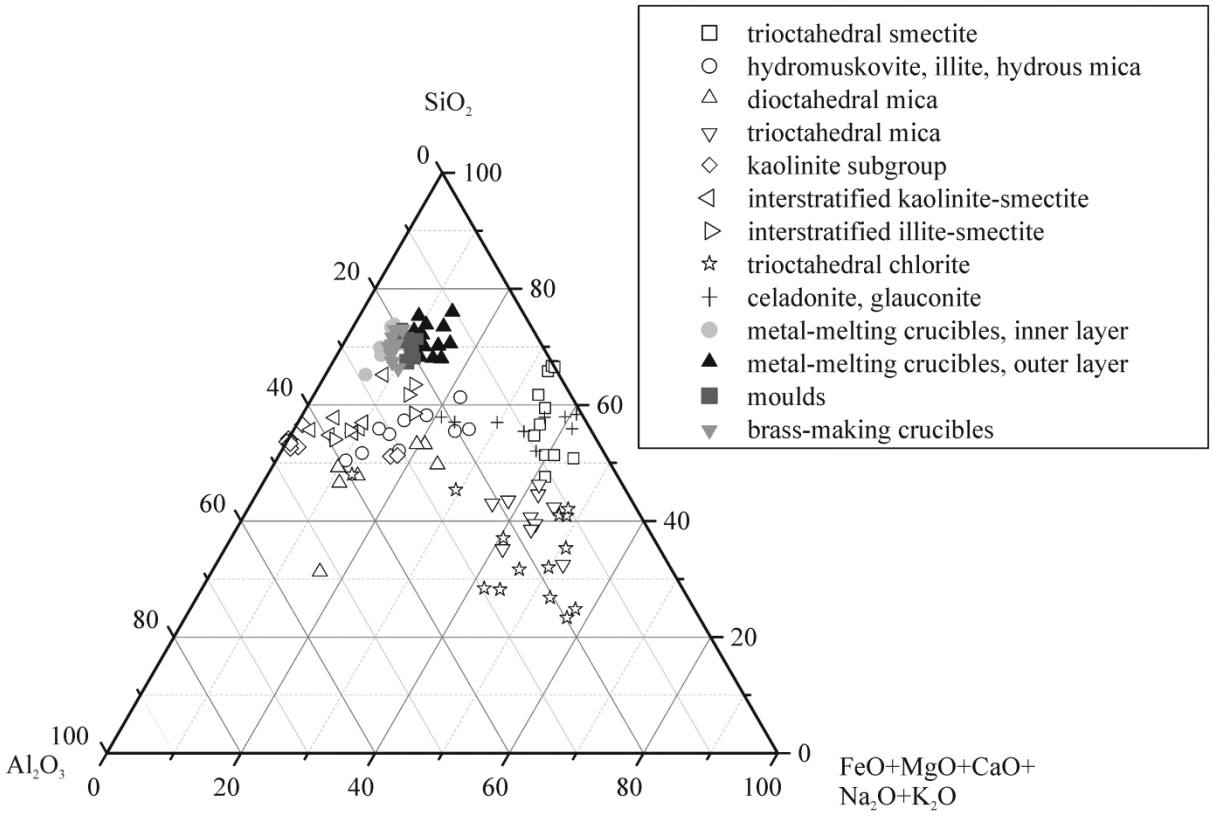

Figure 4-11. *Ternary diagram illustrating the chemical composition of major clay groups (Newman 1987) and those of the ceramics studied; data used after omitting Zn and renormalizing to 100%.*

A comparison of the acquired chemical data with literature data of typical groups of clay minerals (Newman 1987), i.e. kaolinite, illite, smectite etc., allows to determine possible clays used as raw materials for the analysed Roman ceramics (Fig. 4-11). The inner layer of metal-melting crucibles as well as the other investigated two types of ceramics are always characterised by a raw material bearing a certain amount of kaolinite group minerals as interpreted from the abundant occurrence of mullite, meta-kaolinite and a kaolinite breakdown related spinel-like phase. The chemical composition is much closer to a raw clay rich in kaolinite, but also containing kaolinite-smectite clays (Fig. 4-11, Table 4-3). The occupied area of the investigated samples compared with the field of pure kaolinite and kaolinite-smectite, respectively, (Fig. 4-11) is a direct consequence of the presence of quartz and feldspar within the ceramic.

Differences in matrix minerals are related to varying firing temperatures, which had been much lower for the investigated moulds compared to the metal-melting crucibles and brass-making ones as well. The latter show a mullite-bearing matrix with only two exceptions (ATM 036 and ATM 039). ATM 040 is additionally characterised by cristobalite in the matrix. As the latter is not present in all other brass-making crucibles studied, firing temperatures had to be a little bit lower than for the metal-melting crucibles (Lee *et al.* 2008). Brass-making crucibles are the only ceramics studied with a presence of gahnite and willemite. They are related to the high amount of zinc present and indicate, therefore, an outward directed diffusion of this element. The diffusion gradient

itself is optically represented by the gradient in purple colour within the inner layer.

The estimated firing temperatures of the metal-melting crucibles ascertained by mineralogical techniques are between 1200 °C and 1400 °C (König and Serneels 2013 - Chapter 3). In a similar way firing temperatures of brass-making crucibles can be estimated. Due to the presence of primary mullite in six of eight brass-making crucibles it is also possible to postulate firing temperatures of around 1100 °C (Lee *et al.* 1999). The two crucibles without mullite are either fired at lower temperatures or fired for a shorter period of time. Both possibilities prevent a formation of mullite, but induce a kaolinite dehydroxylation causing X-ray amorphous meta-kaolinite.

As moulds are characterised by remnants of muscovite, as inferred from badly resolved XRD peaks, the presence of mullite and in four cases spinel also, firing temperatures had to be lower than for the crucibles studied. Mullite and spinel peaks are nicely resolved only in sample ATM 025. XRD data of all other moulds show badly resolved XRD peaks at the positions of mullite and spinel due to a broad full width at half maximum and indicating, therefore, only very small and tiny amounts crystallized from a X-ray amorphous phase. Their presence is thus indicated in parenthesis (Table 1). This behaviour suggests an initial stage of growth for mullite and a spinel-like phase and, thus, either minimum temperatures necessary for a formation of both mineral phases or a much shorter dwell time compared to that of moulds showing clearly resolved XRD peaks. Muscovite usually dehydroxylates between 550 °C and 800 °C with a maximum dehydroxylation peak at around 700 °C (Guggenheim *et al.* 1987). As SEM micrographs indicate an apparently well preserved structure of muscovite, the maximum firing temperature in these samples should have reached temperatures below the muscovite dehydroxylation peak maximum. Most of the samples showing a coexistence of mullite and a spinel-like phase are barren in muscovite (Table 4-1). In addition, there is only one sample (ATM 033) with coexisting mullite, spinel and muscovite remnants. Thus, there is a close relationship between the muscovite breakdown and the mullite and spinel growth, which allows us to determine the maximum temperature the moulds were affected by. Moreover, missing kaolinite peaks in XRD data, but a ceramic matrix chemically similar to kaolinite favours the presence of meta-kaolinite. This fact can also be used to define a minimum firing temperature the ceramics were subjected to. Following Lee *et al.* (2008), kaolinite breakdown and subsequent formation of meta-kaolinite happens at 500 °C to 600 °C, whereas mullite and a spinel-like phase are formed from around 950 °C onwards. Therefore, all muscovite barren, but mullite and spinel containing moulds must have reached a temperature of 700 °C to at least 950 °C. Those free of mullite and spinel, but still muscovite containing might have reached 500 °C to 700 °C only. Such high firing temperatures reached in the mullite containing mould samples cannot be explained by a production routine using the lost-wax method. There, temperatures usually reach a maximum of around 600 °C (Davey 2009). The high temperatures necessary for the formation of mullite might be caused by massive and probably unintended overheating during use. For instance, during the process the moulds were pre-heated prior to the casting process in a big open furnace within a charcoal bed. Some of the excavated furnaces for pre-heating of moulds in the metal workshops of Autun/France show a high heat impact in several areas (Chardron-Picault and Pernot 1999). Another possibility sometimes discussed in literature to reach such extensive phase transformation reactions (e.g. meta-kaolinite to mullite and a spinel-like phase) is a heat transfer during casting. However, such a scenario is rather unlikely due to the small metal amount in comparison to the volume of a mould shown in Fig. 4 and the rapid cooling rate of the metal load itself. It is more likely for moulds bearing a high content of liquid charge, e.g. moulds used for the production of bells and statues.

Summing up, all obtained results of this multi-analytical approach point to an almost homogeneous raw material used for the production of metal-melting crucibles, brass-making crucibles and moulds. Mineralogical differences (mineral content) and ceramic properties (textural properties) are thus caused by differences in firing temperatures and use. These findings do not correspond with earlier interpretations of Martinón-Torres and Rehren (2002) and Bayley and Rehren (2007). For most of their analysed crucible fragments, they suggest that a diagnostic feature of brass-making crucibles is their less refractory fabric when compared with metal-melting ones. The latter also stress differences in the refractory character between metal-melting crucibles and brass-making crucibles in the same workshop. However, the case study of Martinón-Torres and Rehren (2002) deals with ceramics of the 15th century A.D. only.

Caused by the end of brass production in Western Europe well before the collapse of the Roman Empire, there seems to be no knowledge transfer possible between the Roman period and the Middle Ages (Rehren and Martinón-Torres 2008). Based on the findings discussed in this paper, it seems that Roman brassmakers from Autun/France had a broad knowledge and technological skills to produce specialised vessels with functional properties out of carefully selected and processed source materials in order to withstand high pressures and temperatures. The use of one specific clay source, i.e. the usage of kaolinite rich clay, for the production of different kinds of ceramics studied, implies a detailed knowledge about the refractory properties of such a clay material. Their well-suited refractory character for any kind of application studied herein made it to the favoured material of choice for the Roman manufacturers in Augustodunum. The studied ceramics are from two excavation sites of the the Roman town Augustodunum (Fig. 4-2). That implies two possibilities for manufacturing technical ceramics there. One possibility is a specialised workshop in one part of the city, which was not yet identified. The other and more common possibility is: presence of various, but small workshops which have used the same clay/raw material and the same technological skills and techniques to produce different technical ceramics independently from each other. There are evidences for ceramic workshops within the Roman town Augustodunum which produced ceramics with identical shapes like those investigated herein (Chardron-Picault and Pernot 1999).

The fact that the technology also including the shape, size, structure and composition of brass-making crucibles from the Middle Ages and the Renaissance differ considerably in comparison to the investigated Roman ones is consistent with a gap in brass production between the late Roman Empire and the cultural epochs mentioned before in Central Europe (Moesta 1986, Dungworth 1995, Martinón-Torres and Rehren 2002, Rehren and Martinón-Torres 2008). Rehren and Martinón-Torres (2008) argue that the practical of brass-making were not in the public domain and thus also not technically portrayed by Pliny which finally led to a loss of know-how, i.e. there was simply no written source for a “brass recipe”. Thus, it was necessary to reinvent and improve the brass-making during latter days.

4.6 Conclusions

A detailed mineralogical analysis of three different types of technical ceramics excavated and stored in Autun/France allows identifying potential clay sources, to estimate firing temperatures and reconstruct certain production steps of the ceramic manufacturing and alloy production. All collected data point towards a single clay source used for all types of ceramics. Mineralogical and chemical differences between individual layers are resulting from various amounts of calcium-containing additives which are responsible for a decrease in the refractory character and, thus, the vitrification.

Mineralogical heterogeneities are caused by different firing temperatures and a high diffusivity of zinc in brass-making ceramics as a consequence of the utilisation. Estimated firing temperatures for metal-melting crucibles are between 1200 °C and 1400 °C, for brass-making crucibles around 1100 °C and for the majority of the investigated mould samples between 500 °C and 700 °C. Some mould specimens have presumably reached 950 °C as inferred from the presence of mullite and a kaolinite breakdown-related spinel-like phase. These above mentioned differences in firing temperatures are also the result of use. As the studied ceramic artefacts are similar but derive from two different excavation sites in former Augustodunum, there are two thinkable possibilities for local craftsmen's work. First, all technical ceramics have been produced in one area of the city and sold individually to the metal-workers. But, there is no evidence for a high scale production of technical ceramics in former Augustodunum. Thus, it is much more likely that smaller pottery workshops produced crucibles and moulds with an access to the same pottery clay or at least the same components for the pottery's clay recipe.

	metal-melting crucibles*	brass-making crucibles	moulds
surface and shape properties			
shape and size	• mainly cylindrical with a hemi-spherical base and some of them show a tapering shape to the top • three sizes with a volumetric capacity between 0.3 and 2.2 L, i.e., 2.5 - 19 kg metallic charge	• the shape mirrors a reverse water droplet with a flat bottom, while next to the crucible reaches its largest diameter • maximum high reaches 55 centimetre, the maximum diameter 35 centimetre and a capacity up to 35 litres	• single and multiple moulds • multiple ones are rounded shaped and contain up to 12 fibulae in one mould
lids	x	x	-
number of layers (scale 1:1)	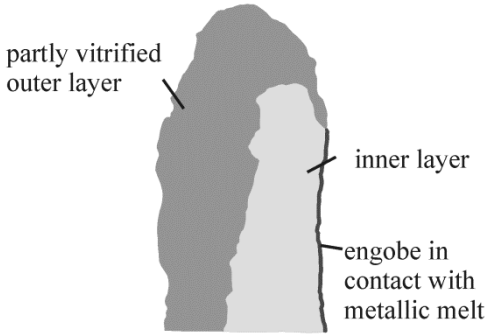	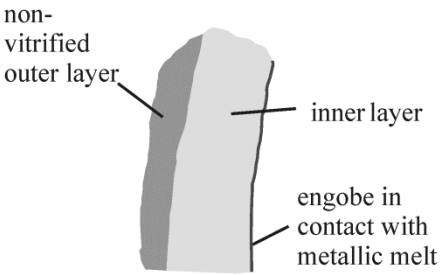	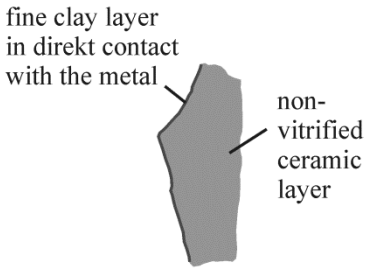
existence of an engobe	x	x	x
repairing traces	x	-	-
petrographical and mineralogical properties			
vitrification	engobe and outer layer	-	-
porosity	**i.l.** semi-open porosity **o.l.** mainly closed porosity with rounded shaped pores	**i.l.** semi-open porosity **o.l.** semi-open porosity	semi-open porosity
temper			

	composition	**i.l.** quartz + feldspar + mica	**o.l.** quartz + feldspar	**i.l.** quartz + feldspar + mica	**o.l.** quartz + feldspar	quartz + feldspar + mica
	shape	**i.l.** angular; feldspar totally molten; micas completely dehydrated	**o.l.** angular; feldspar totally molten	**i.l.** angular; feldspar totally molten; micas completely dehydrated	**o.l.** angular; quartz and feldspar in good order	angular; quartz, feldspar and mica in good order
matrix						
	composition	**i.l.** primary mullite and secondary mullite needles + cristoballite + (spinel)	**o.l.** primary mullite + cristobalite + analcime	**i.l.** mainly mullite; in some cases meta-kaolinite	**o.l.** transition phase between meta-kaolinite and mullite	meta-kaolinite; only one sample with clear mullite presence
additional mineral phases		-		willemite + gahnite		-
interpretation						
used clay material		**i.l.** kaolinitic clay	**o.l.** kaolinitic clay + marly limestone, marl or ash additive	**i.l.** kaolinitic clay	**o.l.** kaolinitic clay	kaolinitic clay
used temper		**i.l. + o.l.** granitic material or something related to that		**i.l. + o.l.** granitic material or something related to that		granitic material or something related to that
firing temperature		1200 °C up to 1400 °C		at least 1100 °C		500 °C up to 700 °C; in one case clearly up to 950 °C

i.l. - inner layer; **o.l.** - outer layer

* König and Serneels (2013)

Table 4-3. *Comparison between different technical ceramics from Autun/France.*

5 - AN ANALYTICAL STUDY OF ROMAN CRUCIBLES FROM XANTEN/GERMANY

D. König

ABSTRACT

This paper deals with Roman metal-melting crucibles from Xanten/Germany in relation to geochemical composition, overall structure and use. The investigated crucibles originate from a small scaled copper-alloy processing and always show a two layer structure with an additionally occurring internal engobe. The composition of clay and temper of the different layers is approximately similar, except of a Ca-rich glass forming material within the outer layer and the engobe. The ceramic matrix is predominantly composed of primary mullite which in some samples occurs together with a spinel-like phase. The outer layers are additionally characterised by analcime which was formed during the burial stage. Assessed firing temperatures are around 1100 °C.

5.1 INTRODUCTION

Crucibles are important ceramic vessels in metal processing. They have to provide special refractory characteristics (high softening point) and a high mechanical strength (thermal shock resistance) (Bayley and Rehren 2007). Different types of crucibles are known of which metal-melting and metal-making (e.g., brass-making ones) form essential technological groups. Different uses basically determine the selection of raw materials (e.g., type of clay and temper used), the vessel form and the final ceramic fabric (Rehren 2003). Metal-melting crucibles are usually designed small but strong enough in order to guarantee an easy handling of such vessels. Metal-melting of copper alloys requires a strong temperature stability of the ceramic fabric well above 1000 °C (Bayley 1992, Bayley and Rehren 2007). Instead of metal-melting ones, brass-making crucibles are a kind of cementation vessel which offer unique ceramic features like poorly refractory fabrics, particular during the Roman period and with a high level of zinc within the ceramic (Martinon-Torres and Rehren 2002). To reach a maximum ratio between surface area (heat input) and volume (heat use), these vessels are commonly small and tubular in shape (Bayley and Rehren 2007). Thus, an increased production requires a higher number of vessels used instead of an increased size of individual vessels (Rehren 1999). Nevertheless, exceptions are known from Roman excavations in Lyon/France and Autun/France (Picon *et al.* 1995, Chardron-Picault and Picon 1997, König in prep. - Chapter 4).

This paper deals chiefly with the petrographical and geochemical composition of crucibles from Xanten/Germany. By doing so, following questions have to be answered. (1) Is a two layer structure and an occurring engobe recognizable in all crucibles examined? (2) Has the engobe formed by chance or is it a wittingly added layer? (3) Is there a difference regarding use between individual crucibles studied, i.e., metal-melting versus brass-making crucibles?

5.1.1 Historical background

The Romans established several military camps along the lower Rhine valley starting during the 1st century B.C. (Fig. 5-1) in order to enhance the fortification between Germania Inferior and the unallocated Germania Libera. Colonia Ulpia Traiana was founded 100 A.D. at a pre-existing probably Germanic settlement and persisted until the end of the 3rd century A.D. After Colonia Claudia Ara Agrippinensium (Cologne/Germany) and Augusta Treverorum (Trier/Germany), Colonia Ulpia Traiana (Xanten/Germany) has been the third biggest Roman settlement of Germania and Gallia Belgica. Colonia Claudia Ara Agrippinensium (Cologne/Germany) and Colonia Ulpia Traiana (Xanten/Germany) were the only two settlements with the status of Colonia, i.e., an outpost of the Roman Empire in conquered territory, but with Roman citizenship, in Germania Inferior. During the 2nd century A.D., Colonia Ulpia Traiana reached the heyday and all large buildings originate from this period. There is no post-Roman usage of the settlement known, except of quarrying for bricks to build up the medieval town of Xanten.

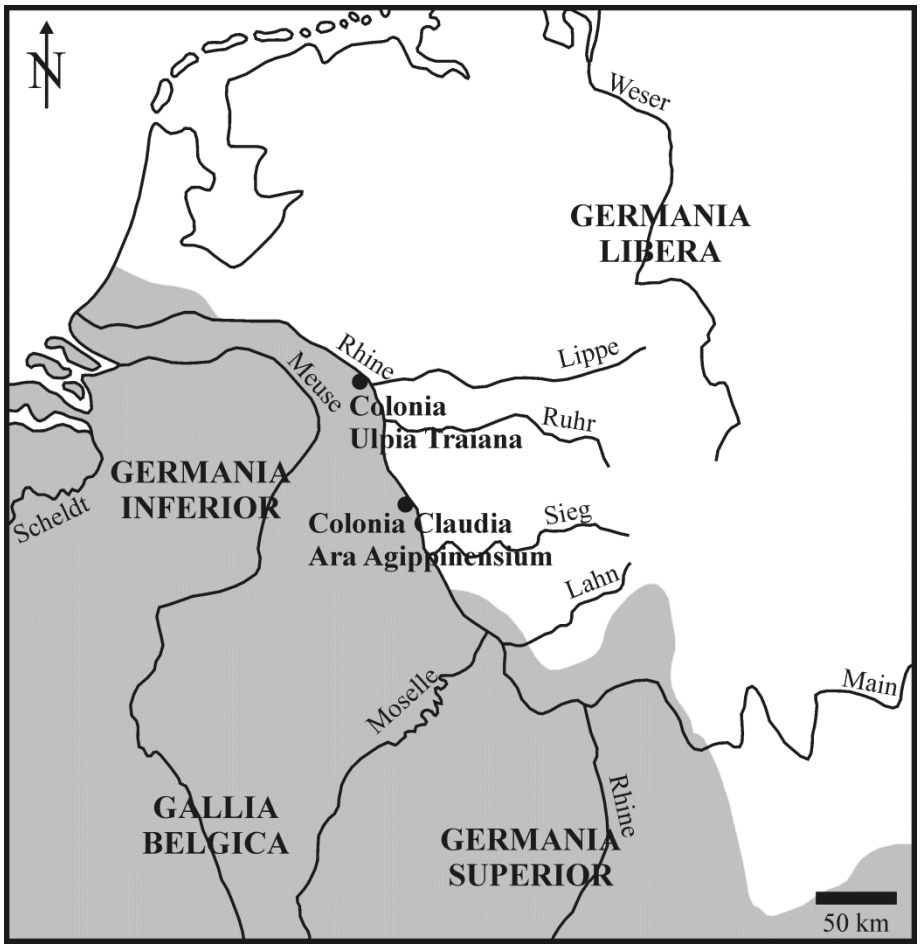

Figure 5-1. *The situation of Colonia Ulpia Traiana (Xanten/Germany) in Roman Inferior. The grey area show the extension of the Roman Empire (modified after Peron and Feiffer 1987) during the 3rd century A.D.*

5.1.2 Sample material

From the Roman crucible collection of Xanten/Germany, eight double-layered crucible fragments have been taken and studied in detail in order to obtain more information about the materials. The investigated samples originate from different excavation sites within the ancient Roman settlement Colonia Ulpia Traiana (Fig. 5-2) and were put by the "LVR-Archäologischer Park Xanten/Germany" at our disposal. All the mentioned excavation sites show only a small amount of copper-alloy related melting crucibles and additionally domestic pots reused as melting vessels. This gives a first hint for a small scale copper-alloy processing.

Most of these crucibles differ in shape, size and material composition due to the reuse of pottery formerly used for domestic purposes. All of the herein investigated crucibles were originally made for copper-alloy melting or brass-making purposes and are, thus, not recycled domestic pots. These copper-alloy crucibles are small in size, with a diameter of around fife centimetres, a height of eight to ten centimetres and a volumetric capacity between 0.1 and 0.2 L, i.e., 1.0 to 1.5 kg metallic charge (Fig. 5-3). All of them are characterised by a cylindrical shape with a pointed bottom and with charcoal imprints along the outside. In some cases slag residuals are preserved along the inside.

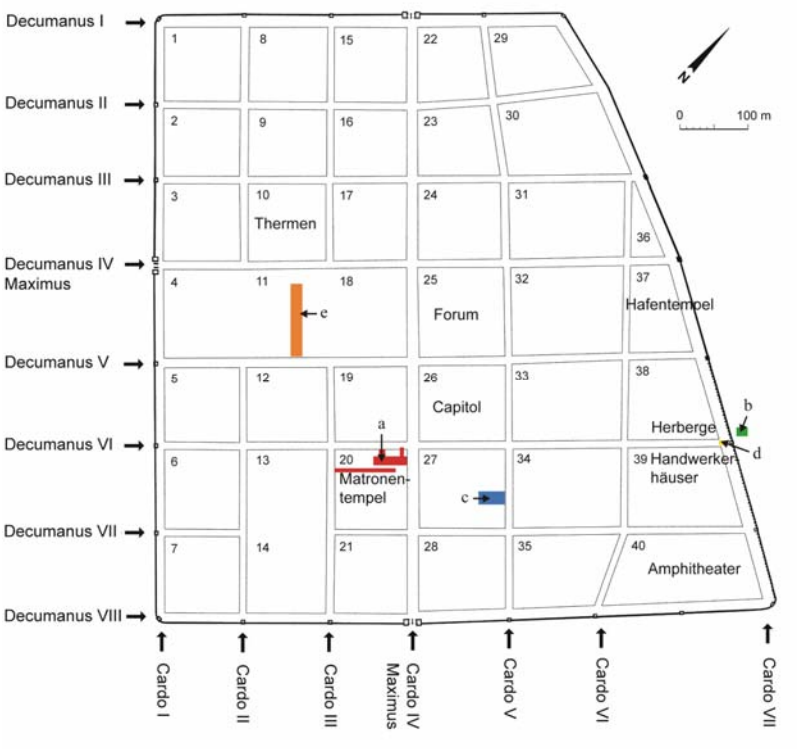

Figure 5-2. *City map of Colonia Ulpia Traiana; the finds 4628, 4002 and 4695are from the area a; the finds 9788a2 and 9831a1(1) were taken from the area b; the find 7177(3) originate from the area c; the find 9404 is from the area d; the find CUT 1959 00981 is taken from the area e (modified after LVR-Archäologischer Park Xanten/LVR RömerMuseum, S. Lauinger 2013).*

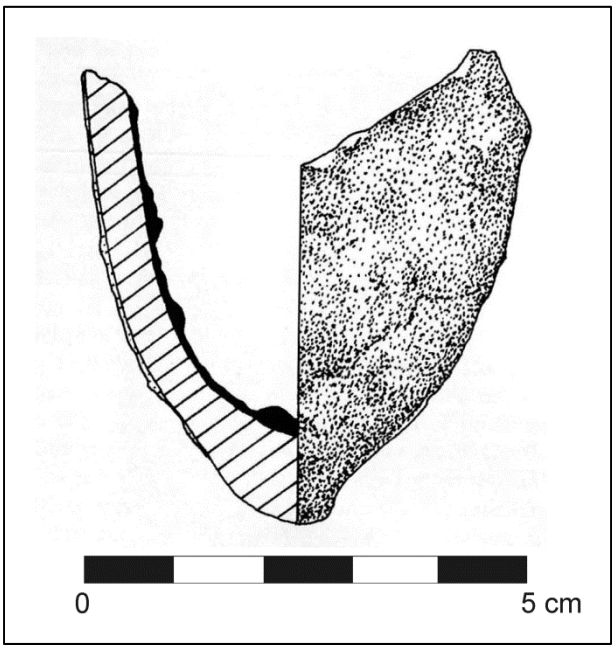

Figure 5-3. *Drawing of a Roman metal-melting crucible from Colonia Ulpia Traiana (modified after Rehren 1997).*

5.2 RESULTS AND DISCUSSION

To acquire a comprehensive petrographical database, macroscopic descriptions were complemented by data deriving from analytical techniques listed in the methodological section. Thus, optical and electron-optical microscopy studies done on thin-sections are used to verify macroscopic findings in detail. By using these methods, it is easily possible to distinguish three individual layers, i.e., two ceramic thick layers subdivided into an outer vitrified one and an inner non-vitrified one, plus a some micrometres thick vitrified but also tempered engobe (Fig. 5-4). The latter is an already macroscopically identifiable and demonstrable layer occurring on bottom shards as well as shards deriving from the upper part of the crucible. All macroscopically recognizable layers can also be identified and characterised in more detail by electron-optical techniques. Only one sample from Colonia Ulpia Traiana has no engobe (Table 5-1). As shown in Fig. 5-4, the two main layers are made of two different ceramics which are in some cases easily separable. This is obvious through the interstice between the two layers which has been formed during use as a consequence of different physico-chemical properties, e.g., expansion coefficient and refractory character.

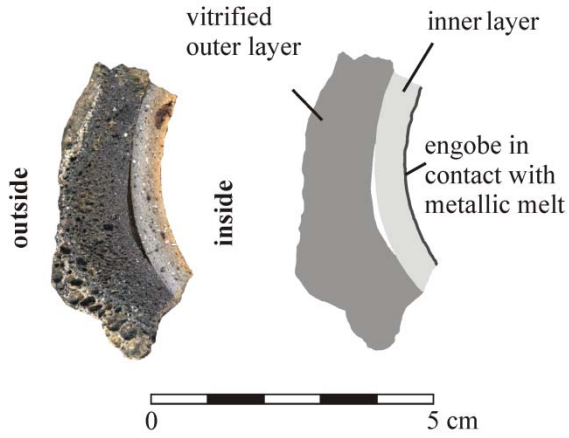

Figure 5-4. *The three different layers of the crucibles (sample 75/25 9831a1(1)).*

The inner ceramic layer bears a light to medium grey colour and an amount of 50 % to 55 % quartz and feldspar temper. Moreover, there is a semi-open porosity with elongated pores of 10 vol.%. The outer layer provides a higher and closed porosity of up to 35 volume %. Temper consists of quartz only and reaches an amount of about 25 %. The glassy matrix of this layer shows different colours varying between dark grey and black, whereas the outer surface of this layer is reddish to greenish as a direct consequence of the copper present and the atmospheric conditions. The outer surface is characterised by charcoal imprints which indicate a direct firing within a charcoal bed. Two of the crucible shards examined (3-4/B 04628 and 69/20 7177(3)) show a bright purple colour within

the inner non-vitrified ceramic layer. This property suggests either use as a brass-making crucible (König in prep. - Chapter 4) or a long dwell time within the fire. Both processes will cause evaporation and migration/diffusion of zinc into the ceramic material favoured by the porous character of the latter. All herein described crucibles are not comparable with the brass-making ones Rehren (1999) already described from Xanten/Germany as those crucibles are only single layered closed vessels and indicating an indirect firing in contrast to the herein investigated ones.

SEM micrographs of the engobe illustrate the occurrence of a closed porosity with spherical pores, a vitrified matrix and a high amount of temper grains mainly consisting of sharp edged quartz (Fig. 5-5). The engobe can be distinguished from the inner ceramic layer by aluminium, silicon and calcium element maps as aluminium is depleted whereas calcium is enriched within the engobe (Fig. 5-5). Silicon maps clearly show a much higher abundance of very fine grained silicon-rich grains within the ceramic matrix of the inner non-vitrified layer. The temper grains which are present in the inner layer are mainly composed of rounded quartz, rounded and partially melted feldspar grains (Fig. 5-6) as well as a few dehydroxylated mica flakes. The inner ceramic layer shows a semi-open porosity with elongated pores. However, the matrix of the outer ceramic layer is mainly vitrified with quartz temper only. This layer also shows a closed porosity similar to the structure of the engobe.

Sample	Investigated part	Thickness (mm)	Presence of an engobe	Mineral content
3-4/B 04628	mixed	10	-	Qtz+Crs+Mul
25/A 04002	mixed	9	x	Qtz+Crs+Mul+Pl
Helg. 6/A 04695	mixed	11	x	Qtz+Crs+Mul+Spl
75/25 9788a2	in	10	x	Qtz+Mul+Pl
75/25 9788a2	out	3		Qtz+Crs+Spl
75/25 9831a1(1)	in	5	x	Qtz+Pl+Spl
75/25 9831a1(1)	out	15		Qtz+Crs
69/20 7177(3)	in	11	x	Qtz+Mul+Pl+Spl
69/20 7177(3)	out	2		Qtz+Crs+Mul+Anl
74/41 09404	mixed	13-20	x	Qtz+Crs+Mul
CUT 1959 00981	mixed	11	x	Qtz+Mul+Pl

Mineral abbreviations: quartz (Qtz); cristobalite (Crs); mullite (Mul); plagioclase (Pl); spinel-like phase (Spl); analcime (Anl)

Table 5-1. *Crucible thickness, presence of an engobe and qualitative mineral content of both layers determined by XRPD; some specimens could not be separated (denoted as mixed).*

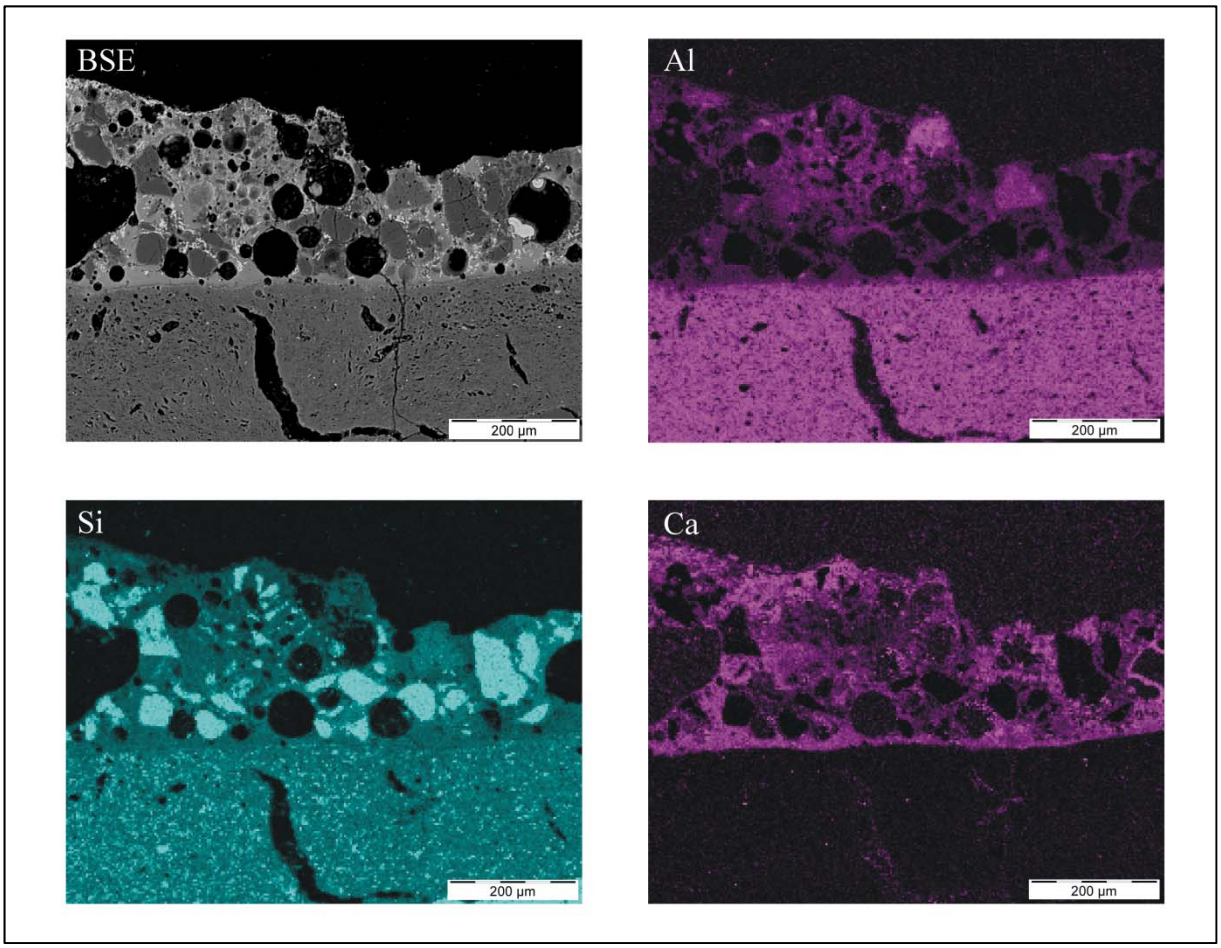

Figure 5-5. *SEM element maps of aluminium, silicon and calcium and the corresponding BSE picture of the engobe (sample 75/25 9788a2). The internal engobe (upper part) is made of sharp edged quartz grains in a calcium rich matrix. The inner layer (lower part) is made of a calcium poor matrix, containing micro-grains rich in silicon. The temper grains of the inner layer, much larger, are not visible in the measured area (see Fig. 5-6).*

XRD investigations (Table 5-1) confirm the presence of quartz and subordinate amounts of plagioclase as already seen in thin-sections. Minerals like mullite, a spinel-like phase and cristobalite, which have been formed during the firing process, were also identified within the crucible shards, although there crystal size is too small to see them via light optical and SEM techniques. Both, mullite and the spinel-like phase, which is probably a γ-Al_2O_3 spinel phase (Sonuparlak *et al.* 1987), are advanced dehydroxylation products of kaolinite (Lee *et al.* 2008).

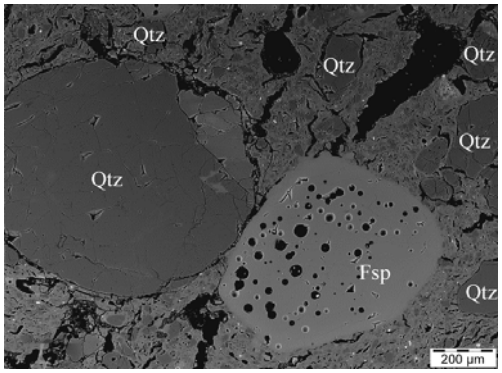

Figure 5-6. *SEM-BSE picture of sample 74/41 09404 which show two types of prevailing rounded temper grains, i.e., quartz (Qtz) and melted feldspar (Fsp) within the inner non-vitrified layer.*

The outer layer contains analcime as a secondary mineral crystallised within a calcium-enriched glassy matrix and formed as a devitrification product during the burial stage. The crystalline amount of both layers is predominantly built up of mullite as well as minor amounts of a spinel-like phase and cristobalite. However, three samples are lacking in mullite (Table 5-1). But, the occurrence of other high-temperature minerals like cristobalite and a spinel-like phase point to a presence of x-ray amorphous meta-kaolinite which is confirmed by SEM investigations. Crucibles containing mullite and a spinel-like phase must have reached firing temperatures of at least 700 °C to 950 °C, whereas those free of mullite but a spinel-like phase bearing are interpreted as crucibles which have experienced maximum temperatures of 500 °C up to 700 °C (Lee *et al.* 2008). The lack of the spinel-like phase, but presence of mullite is taken as an indication for firing temperature of at least 950 °C but below 1100 °C to 1200 °C. Otherwise elongated mullite needles in the surrounding of the melted feldspar grains must have been expected (Lee *et al.* 1999). Such mullite needles which are also labelled 'secondary mullite' in literature (Lee and Iqbal 2001) have not been found at all within the examined crucible shards.

In general, temperatures below 900 °C are too low for copper-alloy melting. That means samples without mullite could be interpreted as deriving from upper parts of the crucibles studied, and, therefore, have not been effected that much by a heat input as bottom parts in comparison. However, this can be excluded for the two samples investigated herein as they have been sampled from bottom parts. Another possible explanation is the duration of the heat impact, i.e., how long did the crucible stay inside the charcoal bed? As the transformation of kaolinite to mullite is a strongly time-dependent reaction (Bellotto *et al.* 1995. Gualtieri *et al.* 1995), a short period of firing at around 900 °C will not create detectable amounts of mullite. A third possibility for the lack of mullite is related to the primary clay composition, i.e., the ratio between kaolinite minerals and illite/smectite clays within the paste. Illite/smectite rich clays usually produce a high amount of melt during firing and inhibit, therefore, the formation of mullite (Ferrari and Gualteri 2006).

XRF bulk analyses (Table 5-2) point towards differences between the two main layers which, however, were separately investigated in only one sample due to the tiny sample amounts produced after separating both layers from each other. The semi-quantitative XRF analyses point towards a dominance of SiO_2 and Al_2O_3 in both layers. The outer layer compared with the inner one shows a higher amount of glass forming elements like calcium, potassium and iron. The amount of Fe_2O_{3tot}, in the investigated outer layers is doubled the amount of the inner ones. The same observation can be made for CaO and in minor amounts for K_2O. These elevated amounts are the result of an additive, which has not clearly been identified due to missing visible remnants within the vessel shards. Such heterogeneities between the two main layers of metal-melting crucibles are already known from other localities such as Autun/France (König and Serneels 2013 - Chapter 3).

Brass-making crucibles Rehren (1999) described from Xanten/Germany show distinct chemical differences especially for alkali and alkali-earth elements. Thus, the overall content of aluminium is up to 50 % higher within the herein examined crucibles, whereas the content of calcium within the outer glassy layer is twice as high as reported for crucibles studied by Rehren (1999). On the other hand, potassium and sodium are much lower than literature data for brass-melting crucibles from Xanten/Germany given by Rehren (1999). The refractory performance of the outer layer was drastically lowered by the calcium additive used and caused, thus, the glassy appearance of the layer. This is interpreted as caused by the functional purpose the layer was added for, i.e., good insulation to keep the melted alloy in a liquid state as long as possible.

	3-4/B 04628	25/A 04002	74/41 09404	75/25 9788a2 in	75/25 9788a2 out	75/25 9831a1(1) out	CUT 1959 00981	Helg. 6/A 04695
SiO_2 (wt.%)	79.2	80.4	81.7	73.5	69.9	75.8	81.0	69.2
TiO_2 (wt.%)	0.4	1.2	0.6	0.8	0.5	0.4	0.8	0.5
Al_2O_3 (wt.%)	12.3	25.1	15.4	23.8	16.4	13.2	17.2	14.9
Fe_2O_3 (wt.%)	3.4	3.7	3.3	2.7	6.6	6.8	2.3	4.0
MnO (wt.%)	0.09	0.04	0.10	0.02	0.70	0.18	0.05	0.21
MgO (wt.%)	1.1	0.7	1.2	1.1	2.3	1.3	0.6	1.4
CaO (wt.%)	3.5	1.0	4.0	0.7	2.9	1.7	0.6	2.1
Na_2O (wt.%)	0.9	0.8	0.8	0.4	1.0	1.0	0.4	0.9
K_2O (wt.%)	3.0	2.0	2.5	2.8	3.7	2.9	1.7	3.9
P_2O_5 (wt.%)	0.5	0.2	0.4	0.2	1.1	0.4	0.2	0.8
Sum before norm.(wt.%)	94,6	85,6	89,4	93,3	93,8	95,5	94,2	97,8
Sum norm. (wt.%)	100	100	100	100	100	100	100	100
Ba (ppm)	1360	790	760	1030	1510	1610	870	1340
Cr (ppm)	<100	130	<100	130	100	100	110	100
Cu (ppm)	980	<100	400	350	900	430	<100	17200
Nb (ppm)	<100	<100	<100	<100	<100	<100	<100	<100
Ni (ppm)	<100	<100	-	<100	<100	<100	<100	<100
Pb (ppm)	260	680	180	<100	120	760	<100	1130
Rb (ppm)	140	130	150	190	170	140	160	110
Sn (ppm)	270	<100	130	-	-	<100	-	2830
Sr (ppm)	200	170	220	170	180	130	120	190
V (ppm)	<100	100	120	200	120	<100	210	130
Y (ppm)	<100	<100	<100	<100	<100	<100	<100	<100
Zn (ppm)	2090	1040	7210	3280	390	140	3380	5390
Zr (ppm)	270	310	310	230	300	330	470	440

Table 5-2. *Semi-quantitative bulk chemical data of the crucibles separated by layer (XRF-WDS); shaded - main metallic charge material.*

The zinc content of the inner layer and bulk sample, respectively, is ten times higher in contrast to the outer layer. This fact is a direct result of use as solid zinc will be vaporized at temperatures higher than 900 °C and, thus, diffuse outwards. Similar signs for such an advanced zinc migration have also been shown in a study about metal-melting crucibles from Autun/France (König and Serneels 2013 - Chapter 3). This results support the hypothesis of the vessels use, i.e., they are rather metal-melting than brass-making crucibles. Typical brass-making crucibles described in literature reach a maximum of around one percent zinc in case of small vessels (Rehren 1999) and almost ten percent or even higher values in larger specimens found in Autun/France (König in prep. - Chapter 4), Augst/Switzerland and Avenches/ Switzerland (König *et al.* - Chapter 6). Exceptional high values of metal such as visible in case of sample Helg. 6/A 04695 are a result of alloy remnants within the powdered sample and are, thus, not representative. But this composition gives us a hint for metal alloys which were used within the crucibles itself. For this example, it is a leaded copper-tin-zinc alloy which could be expected.

5.3 Conclusion

As comprehensively discussed in the article all investigated crucibles are double-layered, with a non-vitrified ceramic inner layer and a strongly vitrified outer one. The inner layer is tempered with quartz and plagioclase. The matrix of the ceramic inner layer is built up of mullite and/or cristobalite and/or a spinel-like phase indicating firing temperatures between 950 °C and 1100 °C, but also of meta-kaolinite in some cases indicating firing temperatures below 700 °C. The outer layer is tempered with quartz only, it has higher calcium content, a higher degree of vitrification, a closed porosity and secondary analcime is formed during the burial stage. The matrix of this layer consists probably of the same clay like the inner layer plus an addition of calcium, potassium and iron rich material.

It is obvious by the shown petrographical and chemical data that the engobe is an additional layer not made by chance. Most evident features of the engobe are: a) high amount of quartz temper in contrast to the inner ceramic layer which in addition contains, feldspar grains ; b) vitrified and Ca-enriched appearance similar to the outer layer and, thus, indicating a common raw material. This layer was possibly produced by creating slurry of the outer layer material and put this suspension on the inner surface of the dried or low temperature fired ceramic inner layer. The engobe has clear functional properties, namely avoiding metal loss due to the semi-open porosity of the inner layer and to help to pour out the melted metal almost completely.

All results of this study favour the use as metal-melting crucibles instead of brass-making crucibles. The shape and structure of the investigated crucibles is not comparable with the investigated brass-making crucibles of Rehren (1999). But, these macroscopic properties correspond to metal-melting crucibles from Autun/France (König and Serneels 2013 - Chapter 3) and Augst/Switzerland as well as Avenches/ Switzerland (König *et al.* - Chapter 6). The purple colour in some of the investigated crucibles is rather the result of a long stay within the fire and, thus, a higher loss of zinc vapour phase than a use as brass-making crucible as such vessels usually reach even higher amounts of zinc.

Despite of the small-scaled copper-alloy processing workshops in Colonia Ulpia Traiana, the crucibles examined evince a remarkably uniform character which is compatible with other Roman settlements within Central Europe. It can, therefore, be assumed that there was a common transfer and exchange of technological knowledge between individual Roman settlements.

6 - *ROMAN CRUCIBLES FROM AUGUSTA RAURICA (AUGST/ SWITZERLAND) – AN INTERDISCIPLINARY APPROACH USING BOTH LABORATORY AND PORTABLE ANALYSES*

D. König, M. Helfert and A. R. Furger

First version of the paper which is under revision and will be splitted into at least three single papers for publication

ABSTRACT

The project involved analysing 893 Roman crucibles for non-ferrous alloys from Augusta Raurica (Switzerland) using laboratory and portable devices. This resulted in the identification of five clay groups, which were compared to 60 reference groups from the surrounding area. Most of the crucible clays came from two clay deposits, one of which was located nearby, while the other was situated 50 km away in the Jura region.

The crucibles were composed of three layers: a wheel made core of fired ceramic, a lutum layer made of local materials applied to the exterior and a thin engobe applied to the interior. In the casting process, the mechanically stabilising and insulating lutum swelled up and vitrified considerably; the sealing engobe bore a glassy texture due to sintering.

6.1 INTRODUCTION

6.1.1 The site of Augusta Raurica and the evidence of its bronze working

Augusta Raurica was a Roman town on the Upper Rhine near Basel in Switzerland (Fig. 6-1). Founded ca 15 BC, the colonia gradually evolved into the present-day village of Kaiseraugst from around AD 400 onwards (Furger 1995, Berger 2012). At the height of its boom around AD 200 the town had a population of some 16,000 inhabitants. Approximately one quarter of the ancient area of the town has to date been excavated. 1700 finds and a vast amount of excavation records are available to scientists for their active ongoing research into the town.

Augusta Raurica was an important trading hub and crafts centre located in the area where the River Rhine ceased to be navigable. Bronze foundries have been discovered and excavated in several places (Martin 1978, Furger 1998). The body of evidence pertaining to the casting of non-ferrous metals contains hundreds of artefacts which are currently being analysed as part of a project that will run over a period of several years (Furger in prep.). The crucibles alone account for 893 catalogue entries.

***Figure 6-1**. Map of Switzerland with the Roman sites of Augusta Raurica (Augst and Kaiseraugst) and Aventicum (Avenches).*

6.1.2 Material analysed and sample selection

Many amorphous finds, for the most part slag-like objects, cannot be interpreted by means of a visual examination and cannot be attributed to any particular craft. The same can be said for the crucible fragments, which often exhibit green discolouration pointing to the presence of copper alloys. Other remains and metalworking tools, including clay and stone moulds, miscast and semi-finished objects, possible touchstones, slag in various colours, as well as unidentifiable and even dubious objects, barely allow us to interpret them unless they are analysed with regard to their metal content.

Many of these objects connected to bronze working were analysed on site at the Museum Augusta Raurica, in a non-destructive manner, without sample preparation and in a timely fashion by using portable XRF analysis (chapter 2.4). In addition to the investigations dealt with here, this method will allow us to analyse casting moulds, soil samples, slag and utensils, and to identify hundreds of alloys (in uncorroded borings taken from bronze objects found in workshop contexts).

The Archaeometry Research Group at the University of Fribourg (Switzerland) was also able to analyse the mineralogy of a number of crucibles from Avenches (Aventicum, Fig. 6-1), a town similar in size to Augusta Raurica, situated 90 km to the southwest (Bögli 1996, crucible Fig. 71).

Our investigations are based on various earlier studies, particularly on crucibles from other Roman sites (Rehren 1997, Bayley *et al.* 2001, Bayley and Rehren 2007). The main emphasis was on the crucible clay and the identification of its origins, on the outer layers of clay, commonly known as lutum, on the engobe that can sometimes be found on the insides and on identifying any metals that are often only preserved in minute quantities. The study will differentiate between the type of crucible, its shape, size and former purpose (melting, cupellation etc.).

6.1.3 Shape, size and dating of the crucibles

The vast majority of the 893 crucibles (98 % of catalogue entries) used for processing non-ferrous alloys in Augusta Raurica are wheel made and egg-shaped (Fig. 6-2). Their rims are slightly inward-curving and thickened on the inside, the bases are usually rounded or even pointed. The crucibles measure approximately 4.5-18 cm in height and have a capacity to hold between 50 g and more than 4 kg of bronze.

Despite the sound archaeological basis consisting of numerous dated finds assemblages, it was not possible to identify a change in the crucible shapes, either for typological or technological reasons. The only detectable change over the course of the 300-year history of the town was in the size of the crucibles used by the different workshops and the use of five different types of clay (clays 1-5, see section 6.2.2) in their manufacture.

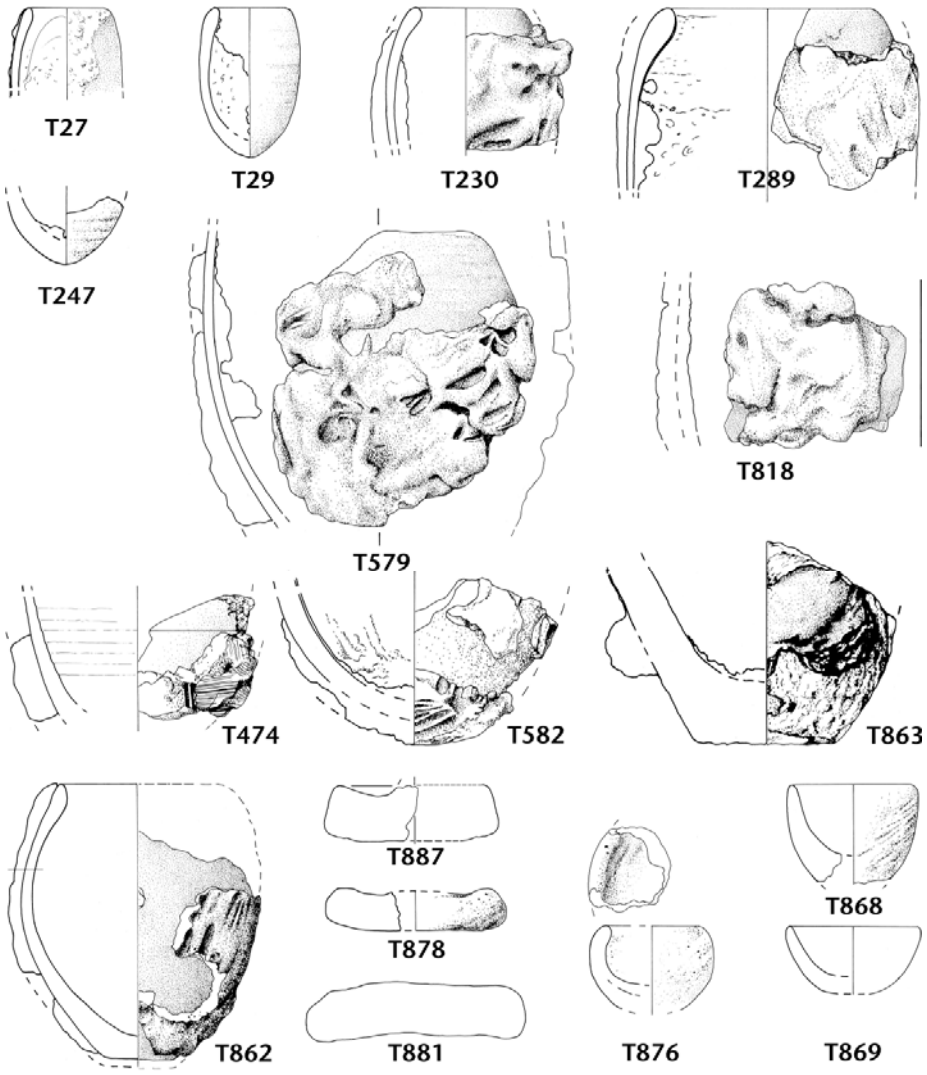

Figure 6-2. *Crucibles and lids from Augusta Raurica made of clays 1-5. All date from the 1st to the 3rd centuries AD; a more detailed typological or technological chronology could not be established. Shapes T27-T582, wheel made and usually encased in a layer of lutum, were the predominant shapes within the range (98 %); small bowl-shaped crucibles (T867-T869) were very rare, generally handmade using local clay 2. Scale 1:3.*

T27 *(Inv. 1961.6526): clay 1?, Cu++, Sn+, Zn, Pb+++, As++, Ag++;* ***T29*** *(Inv. 1967.29586): clay 1?, Cu+++, Sn+, Ag++, Au++;* ***T230*** *(Inv. 1978.24280): clay 1, Cu+, Sn+, Zn+++;* ***T289*** *(Inv. 1979.18596): clay 1, Zn+++;* ***T247*** *(Inv. 1969.13094): clay 1?, Cu+, Sn++, Zn+++, Pb, Au, Hg;* ***T579*** *(Inv. 1967.3543): clay 1, Cu++, Sn, Zn+++, Pb+;* ***T818*** *(Inv. 1978.10113): clay 1, Cu++, Zn+++, Ag;* ***T474*** *(Inv. 1978.24295): clay 2, Zn+++;* ***T582*** *(Inv. 1913.453): clay 2, Cu++, Zn+++, Hg;* ***T863*** *(Inv. 1913.452): clay 2, Cu++, Zn+++, Hg;* ***T862*** *(Inv. 1968.6215): clay 5 (inner lining clay 3?), Cu, Zn;* ***T887*** *(Inv. 1978.22766A): lid, clay ?, Cu++, Zn+++;* ***T878*** *(Inv. 1978.24302): lid, clay 2 (poss. 3?), Zn++;* ***T881*** *(Inv. 1969.13809): lid, clay 2?, Zn;* ***T867*** *(Inv. 1977.2214): clay ?, Ag, Au+, Hg;* ***T868*** *(Inv. 1978.783): clay 2?, Pb;* ***T869*** *(Inv. 1984.3005): clay ?, Pb+++, As++, Ag.*

Smaller crucibles were particularly common in the early 1st and – even more so – in the late 2nd and 3rd centuries, while large and very large examples appeared relatively late and only became more frequently used in the advanced 2nd century, possibly due to a rationalisation of the craft of casting.

Crucibles made of fine, light-grey clay 1 (section 6.2.2) were in use from the mid-1st to the third quarter of the 3rd centuries with an emphasis on the first half of the 3rd century. The crucibles made of clays 3-5 and particularly those made of the local clay 2, on the other hand, were in regular use from the second quarter of the 1st to the mid-3rd centuries, with an emphasis on the second half of the 2nd century. The overlap between the periods, both with regard to the crucible sizes and the clays used shows that all crucibles were used more or less at the same time.

6.1.4 Questions dealt with in this paper

In the most recent phase of the project the three authors of this paper dealt with the technological aspects of the crucibles and raised the following questions to be answered by the natural-scientific analyses:

1. Is it possible based on the thin sections and geochemical analyses to identify different clay types that correspond to different clay deposits and thus different origins of the crucible clays?

2. We took clay samples from approximately 60 deposits within a 50 km radius around Augusta Raurica and analysed them (in addition: Eramo 2006). Can any of the deposits be correlated with the crucible clay types defined?

3. Is it possible in the case of clays from outside the locality to ascertain whether they were brought to Augusta Raurica in order to be made into crucibles there or whether the crucibles themselves were sold to the consumers in Augusta Raurica as finished products?

4. How were the crucibles made, the clays prepared and the wheel thrown vessels fired? What was the difference between the temperature at which the crucibles were fired and the operational temperature with the addition of the melted copper alloys?

5. Many crucibles exhibit a second, outer layer of clay, which vitrified and became viscous when heated. Medieval and early modern sources call this substance lutum and several formulas for how it was made are known from that period. To what extent can the lutum on the Roman crucibles be reconstructed by means of analyses and experimentation?

6. Which methods are best suited to analysing the metal residue (green staining, coloured “glazing”, metal drops and spills) mainly visible in crucibles?

7. What other ways of improving the crucible characteristics can be observed and pinpointed by microstructural, mineralogical and chemical means (e.g., thin interior linings)?

8. What are the differences and similarities between the crucibles from the two Roman towns of Augusta Raurica and Aventicum? What was made on site using local materials? Were the crucibles from Aventicum, which are much less frequently found, the same as those from Augusta Raurica, and where did they originate from?

6.2 RESULTS AND DISCUSSION

6.2.1 Petrographic characteristics of the crucibles studied

Two different types of crucibles can be distinguished on the basis of macroscopic and microscopic features. Both types exhibit two main layers, an outer, mostly vitrified layer of lutum as well as an inner ceramic layer. Additionally, all crucibles contain an interior engobe which is a glassy layer of some tens of micrometres in thickness which came into direct contact with the metallic charge (Fig. 6-3). Differences between both types arise from their size and the amount of temper grains within the inner layer. Crucible type 1 shows micrometre-sized temper grains and a homogeneous matrix within the inner layer. This type corresponds with clay group 1 (section 6.2.2).

The second type of crucible is characterised by quartz and feldspar temper grains measuring several millimetres which are evenly distributed throughout the inner ceramic layer. These crucibles can be correlated with clay groups 2 to 5. Some samples show an additional outer layer (lutum) interpreted as resulting from repairs made necessary by the partial destruction of the outer layer during use. This implies that these crucibles were used more than once. Such repair marks were also observed in samples from other excavated Roman settlements (König and Serneels 2013 - Chapter 3).

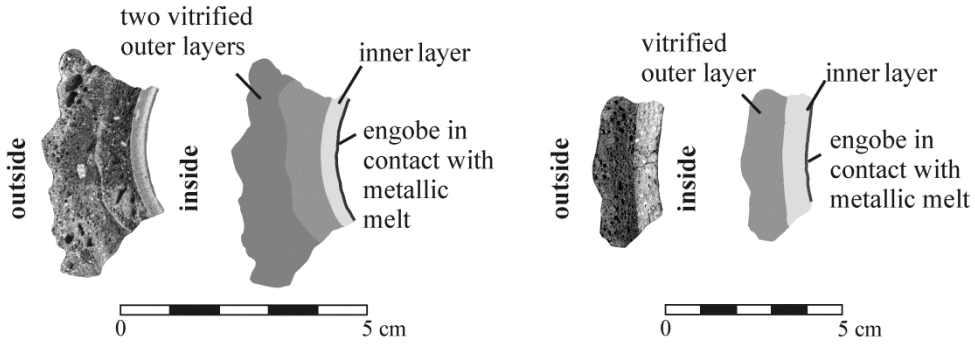

Figure 6-3. *Structure of the two different crucible types;* ***left*** *type 1 with small temper grains and sometimes a second outer layer (clay group 1);* ***right*** *type 2 with bigger temper grains within the inner ceramic body (clay groups 2 to 5).*

SEM investigations confirm the three layers mentioned above. The engobe (Fig. 6-4a) is a completely vitrified layer of around 200 micrometres (average) in thickness with a small amount of non plastic inclusions. The inner ceramic layer contains edged quartz and feldspar temper grains (Fig. 6-4b), while only a small amount of feldspar grains melted. The outer layer (lutum) shows quartz as the only visible temper and much like the engobe is almost always completely vitrified. The engobe and the outer layer both contain more calcium compared to the inner layer. Calcium acts as a glass former within these layers.

Table 6-1 summarises the acquired XRD results and points to a matrix mainly consisting of mullite and temper. On the other hand, the lack of mullite in few samples suggests the occurrence of X-ray amorphous meta-kaolinite due to the outer

high-temperature phases cristobalite and/or spinel. Some of the investigated crucibles from Augusta Raurica (T128; T168; T225) have never been used. Nevertheless, these three crucibles contain meta-kaolinite and/or mullite and thus clearly suggesting a pre-firing procedure. The X-ray detectable temper material confirms the microscopic observations, i.e. the presence of quartz, potassium feldspar and plagioclase in some samples. Spinel and cristobalite are minerals which are formed during the firing process. In contrast, willemite (Zn_2SiO_4) and gahnite ($ZnAl_2O_4$) are formed during use and are a direct consequence of brass production and melting. Samples containing at least one of both zinc minerals are always purple in colour.

Laboratory-based XRF-WDS results show close similarities between Roman crucibles from Augusta Raurica and Aventicum with regard to their geochemical composition (Table 6-2; Fig. 6-5). However, both datasets are not directly compatible with each other as can be seen by linear correlations between the main elements (Si, Fe) and strong deviations in chemical data in some of the crucibles studied (Tab. 6-3). Nevertheless, plotting both datasets into a SiO_2-Al_2O_3-Fe_2O_3+MgO+CaO+K_2O+Na_2O diagram (Fig. 6-5) gives two matching clusters. One group is characterised by a higher SiO_2 and Al_2O_3 content whereas the other is slightly depleted. The first chemical group corresponds to the crucibles of type 1, i.e., those that have a fine ceramic fabric with micrometre-sized temper grains. Therefore, they also correspond to clay group 1. The other, much bigger group in the series analysed in Fribourg corresponds to clay groups 2 to 5, i.e., the second type of crucibles found, which have temper grains several millimetres in size.

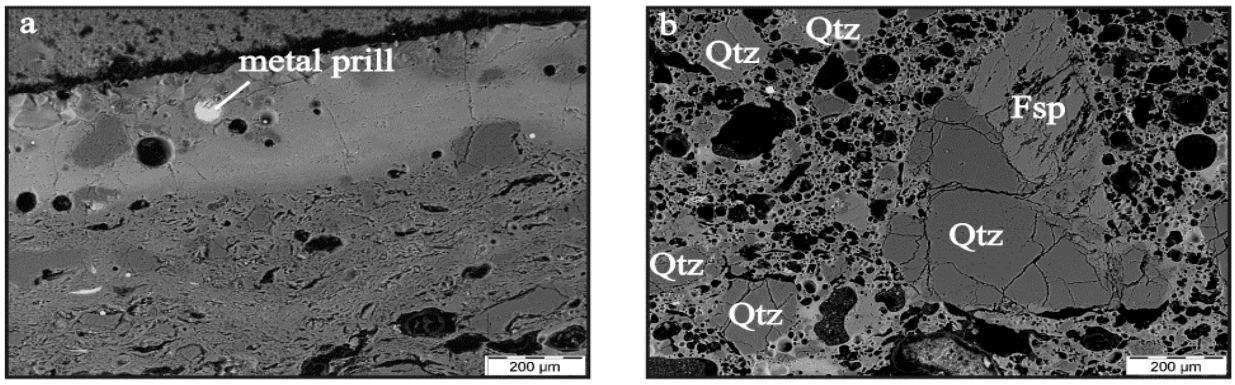

Figure 6-4. *SEM-EDX micrographs;* ***a*** *vitrified engobe (inside) with enclosed metal prill in contact with the inner ceramic layer;* ***b*** *quartz-feldspar intergrowth in a sharp edged temper grain within the inner ceramic layer; Qtz-quartz; Fsp-feldspar.*

Sample	*Thickness (mm)*	*Presence of an engobe*	*Mineral content*
Augusta Raurica			
T503	9	x	Qtz + Crs + Mul
T231	13	x	Qtz + Crs + Mul
T548	11	(x)	Qtz + Crs + Mul + Spl + Wil
T673	10	(x)	Qtz + Crs + Mul
T552i.l.	15	x	Qtz + Crs + Mul
T552o.l.			Qtz + Crs
T862i.l.	13	x	Qtz + k-Fsp + Mul + Spl
T862o.l.			Qtz + k-Fsp
T533	12	x	Qtz + Crs + Mul + Gah
T128	3	-	Qtz + Crs
T168	4	-	Qtz + k-Fsp
T688 i.l.	8	x	Qtz + k-Fsp + Mul + Spl
T688 o.l.			Qtz + Crs
T454	8	x	Qtz + Crs + Mul
T262i.l.	14	x	Qtz + Pl + Crs + Mul + Spl
T262o.l.			Qtz + Crs + Spl
T230i.l.	10	x	Qtz + k-Fsp + Crs + Mul + Gah
T230o.l.			Qtz + k-Fsp + Crs
T289	10	(x)	Qtz + k-Fsp + Crs + Mul + Wil
T225	5	-	Qtz + k-Fsp + Crs + Mul
Aventicum			
MRA 67/5437(1)i.l.	25	x	Qtz + Crs + Mul
MRA 67/5437(1)o.l.			Qtz + Crs + Mul
MRA 67/8442	22	x	Qtz + Pl + k-Fsp + Crs + Mul
MRA 67/8519	15	x	Qtz + Pl + k-Fsp
MRA 67/9918	7	x	Qtz + Pl + Mul + Wil
MRA 68/1215i.l.	18	x	Qtz + Crs + Mul
MRA 68/1215o.l.			Qtz + Crs
MRA 73/3409	22	x	Qtz + Pl + k-Fsp + Crs + Mul
MRA 79/13516	14	x	Qtz + Pl + k-Fsp + Crs + Mul
MRA 83/835	16	(x)	Qtz + Pl + k-Fsp + Crs + Mul
MRA 03/11712-21	9	-	Qtz + Pl + Mul
MRA X/3319i.l.	15	x	Qtz + Crs + Mul + Wil
MRA X/3319o.l.			Qtz + Crs

i.l.-inner layer ; o.l.-outer layer
Mineral abbreviations: cristobalite (Crs); gahnite (Gah); mullite (Mul); plagioklas (Pl); potassium feldspar (k-Fsp); quartz (Qtz); spinel (Spl); willemite (Wil)

Table 6-1. *Total thickness of crucibles from Augusta Raurica and Aventicum, presence of an engobe and qualitative mineral content determined by XRD partially separated by layers.*

	T503[1]	T231[1]	T548[3]	T673[1]	T552 i.l.[3]	T552 a.l.[1]	T862 i.l.[1]	T862 a.l.[1]	T128[1]*	T168[1]*	T688 i.l.[2]	T688 a.l.[1]	T533[2]	T454[2]	T262 i.l.[3]	T262 a.l.[2]	T230 i.l.[3]	T230 a.l.[1]	T289[1]	T225[1]*
SiO_2 (wt.%)	76.9	72.9	73.3	75.0	79.0	77.9	69.4	76.5	78.5	81.1	69.9	76.1	76.9	72.3	76.4	71.2	78.4	75.3	79.0	79.4
TiO_2 (wt.%)	0.7	0.8	0.7	1.0	0.7	0.6	0.8	0.7	0.9	0.9	0.5	0.5	0.5	0.6	0.7	0.4	0.9	0.7	0.9	1.3
Al_2O_3 (wt.%)	12.5	15.4	14.8	15.0	15.9	8.7	17.6	10.9	16.1	14.3	17.7	9.6	13.7	16.0	13.4	11.5	17.4	11.9	14.2	15.9
Fe_2O_3 (wt.%)	3.3	3.6	4.5	2.8	2.3	5.7	5.9	4.6	2.3	1.7	5.4	3.9	3.4	3.6	3.4	4.5	1.7	4.3	1.5	1.6
MnO (wt.%)	0.09	0.06	0.22	0.05	0.03	0.12	0.06	0.11	<0.01	<0.01	0.06	0.10	0.09	0.11	0.09	0.39	0.05	0.13	0.01	<0.01
MgO (wt.%)	1.0	0.9	1.1	0.8	0.4	0.9	1.0	1.2	0.6	0.5	1.0	1.3	0.9	1.1	1.1	1.9	0.4	1.3	0.3	0.4
CaO (wt.%)	2.1	2.7	2.1	3.0	1.0	2.1	0.7	2.0	1.0	0.8	0.7	3.7	1.7	3.2	2.8	4.3	0.5	2.0	0.7	0.9
Na_2O (wt.%)	1.1	1.3	0.7	0.6	0.2	1.2	0.5	1.3	0.1	0.2	0.6	1.3	0.8	0.8	0.7	1.4	0.1	1.3	2.6	0.3
K_2O (wt.%)	1.9	2.0	2.3	1.7	0.4	2.6	3.9	2.5	0.4	0.4	3.9	3.2	1.8	1.9	1.1	3.5	0.4	2.6	0.6	0.2
P_2O_5 (wt.%)	0.3	0.4	0.3	0.2	0.1	0.3	0.2	0.3	0.0	0.0	0.2	0.4	0.3	0.4	0.4	0.9	0.1	0.4	0.1	0.0
Sum before norm.(wt.%)	97.1	97.1	95.8	97.4	92.8	97.8	96.4	96.4	95.6	97.7	93.4	99.1	87.8	91.9	93.3	92.5	95.5	98.8	96.8	98.1
Sum norm.(wt.%)	100	100	100	100	100	100	100	100	100	100	100	100	100	100	100	100	100	100	100	100
Ba (ppm)	306	307	1400	215	2000	325	3498	365	91	112	3800	416	450	800	1400	1200	1900	440	88	87
Cr (ppm)	90	114	<100	114	100	76	98	88	115	105	<100	74	<100	100	100	<100	100	89	101	116
Cu (ppm)	550	1000	32000	200	7200	250	250	700	100	650	500	950	9600	4800	130800	21800	3200	500	600	46
Nb (ppm)	17	16	<100	20	<100	12	18	15	20	21	<100	13	<100	<100	<100	<100	<100	16	17	28
Ni (ppm)	34	44	100	35	-	45	42	45	27	27	<100	30	<100	<100	-	<100	-	44	37	19
Pb (ppm)	250	1200	9700	220	350	140	600	180	25	110	150	90	1100	550	14000	900	2900	610	140	190
Rb (ppm)	77	71	<100	64	<100	85	202	97	26	21	250	117	100	<100	<100	100	<100	101	21	7
Sn (ppm)	100[2]	-	4600	<100[2]	450	-	-	-	-	-	<100	-	250	1250	13200	3100	500	-	<100[2]	-
Sr (ppm)	115	296	<100	108	<100	98	157	131	52	45	150	117	100	150	<100	200	<100	124	38	41
V (ppm)	77	148	130	123	<100	59	108	79	102	90	100	71	100	100	150	<100	150	84	87	86
Y (ppm)	34	29	<100	27	<100	29	34	39	23	24	<100	31	<100	<100	<100	<100	<100	39	21	25
Zn (ppm)	4230	7060	94400	1445	38200	2615	2525	210	60	425	9300	190	15600	1400	9800	2000	36900	2640	73865	20
Zr (ppm)	307	306	300	283	300	341	255	355	242	278	300	276	400	400	300	450	450	365	248	277
Σ melt-%	0.53	0.95	14.69	0.20	4.98	0.31	0.35	0.11	0.02	0.12	1.07	0.12	3.02	0.87	17.98	3.00	4.55	0.38	7.71	0.03

[1] glass pill; [2] pressed pill; [3] glass-pressed pill; * unused

Table 6-2-1. *Semi-quantitative bulk chemical analyses (XRF-WDS) of crucibles from Augusta Raurica partly separated by layer (i.l.-inner layer; o.l.-outer layer).*

	MRA 67/5437[1] i.l. [3]	MRA 67/5437[1] a.l. [1]	MRA 67/8442[2]	MRA 67/8519[1]	MRA 67/9918[2]	MRA 68/1215 i.l. [3]	MRA 68/1215 a.l. [2]	MRA 73/3409[1]	MRA 79/13516[1]	MRA 83/835[1]	MRA 03/11712-21[1]	MRA X/3319 i.l. [3]	MRA X/3319 a.l. [2]
SiO_2 (wt.%)	77.4	73.4	73.4	66.0	72.3	71.2	75.5	76.8	78.5	77.8	81.1	77.9	71.8
TiO_2 (wt.%)	0.8	0.5	0.3	0.6	0.4	0.8	0.4	0.4	0.4	0.4	0.5	0.5	0.3
Al_2O_3 (wt.%)	17.1	12.1	11.8	14.7	13.0	22.4	10.7	11.2	11.2	10.6	11.2	14.0	11.0
Fe_2O_3 (wt.%)	2.0	3.8	4.3	5.2	3.4	2.1	3.6	3.8	2.5	3.0	2.6	3.6	3.5
MnO (wt.%)	0.02	0.13	0.13	0.13	2.56	0.04	0.18	0.11	0.11	0.09	0.05	0.03	0.24
MgO (wt.%)	0.7	1.5	1.3	2.9	1.3	0.7	1.3	1.2	1.2	1.1	0.7	0.8	1.5
CaO (wt.%)	1.2	2.9	2.8	4.7	3.2	0.6	3.8	1.5	1.1	2.3	1.3	1.4	5.7
Na_2O (wt.%)	0.3	2.0	1.9	1.9	0.4	0.4	1.1	2.0	2.2	2.0	0.9	0.6	1.8
K_2O (wt.%)	0.5	3.3	3.3	3.5	2.6	1.8	3.2	2.6	2.6	2.5	1.3	0.9	3.7
P_2O_5 (wt.%)	0.1	0.3	0.7	0.3	0.8	0.1	0.3	0.2	0.2	0.2	0.2	0.2	0.5
Sum before norm.(wt.%)	91.2	98.8	86.5	99.2	98.6	97.8	90.6	99.3	99.3	99.2	98.9	95.4	86.1
Sum norm.(wt.%)	100	100	100	100	100	100	100	100	100	100	100	100	100
Ba (ppm)	2100	441	680	412	1250	23700	1940	374	351	347	207	800	900
Cr (ppm)	150	82	<100	75	<100	<100	100	78	81	73	88	<100	<100
Cu (ppm)	4100	350	1500	900	5550	3000	3400	150	200	71	26	39100	1050
Nb (ppm)	<100	10	<100	14	<100	700	<100	10	8	10	14	<100	<100
Ni (ppm)	-	44	<100	37	<100	-	<100	33	24	29	33	-	<100
Pb (ppm)	800	350	450	1500	150	750	<100	140	500	143	28	26200	400
Rb (ppm)	<100	123	150	156	<100	400	150	103	102	99	59	<100	150
Sn (ppm)	<100	-	800	-	550	-	<100	<100[2]	<100[2]	-	-	28200	450
Sr (ppm)	<100	135	150	143	100	400	150	96	94	111	69	<100	200
V (ppm)	200	67	<100	89	100	-	<100	64	53	51	82	100	<100
Y (ppm)	<100	27	<100	36	<100	<100	<100	32	31	28	22	-	<100
Zn (ppm)	9300	129	4650	90	63500	2000	100	111	3738	92	54	8900	750
Zr (ppm)	350	157	250	153	200	1700	500	183	185	175	200	250	250
Σ melt-%	1.56	0.08	0.86	0.25	7.07	0.59	0.40	0.05	0.45	0.03	0.01	10.73	0.30

[1] glass pill; [2] pressed pill; [3] glass-pressed pill; * unused

Table 6-2-2. *Semi-quantitative bulk chemical analyses (XRF-WDS) of crucibles from Aventicum partly separated by layer (i.l.-inner layer; o.l.-outer layer).*

Sample	SiO_2 (wt.%)	TiO_2 (wt.%)	Al_2O_3 (wt.%)	Fe_2O_3 (wt.%)	MnO (wt.%)	MgO (wt.%)	CaO (wt.%)	K_2O (wt.%)	P_2O_5 (wt.%)	Sum norm. (wt.%)	Sum before norm. (wt.%)	Ba (ppm)	Cr (ppm)	Cu (ppm)	Pb (ppm)	Sn (ppm)	Sr (ppm)	Zn (ppm)
T226i.l.	77.8	0.8	17.0	1.9	-	0.6	1.2	0.5	0.1	100	100.1	160	60	40	790	10	40	50
T863i.l.	70.7	0.7	21.5	1.9	0.03	-	2.2	2.1	0.6	100	100.5	330	40	90	30	-	100	3960
T582i.l.	52.2	0.9	27.5	11.5	0.28	-	5.1	2.0	0.5	100	100.2	-	50	80	80	-	80	1430
T457i.l.	75.8	1.0	19.8	1.3	-	-	1.4	0.3	0.2	100	100.0	270	80	20	30	10	50	30
T503i.l.	75.0	1.1	18.2	1.3	-	1.0	1.0	0.4	-	100	102.0	50	80	90	170	30	40	18750
T503o.l.	74.5	0.5	8.6	4.8	0.18	1.5	6.9	2.3	0.6	100	100.2	380	80	280	210	70	130	620
T849i.l.	69.4	1.1	19.9	2.6	0.01	-	4.8	0.9	0.5	100	100.9	170	70	170	660	-	60	7360
T288i.l.	74.0	0.9	17.0	1.5	0.01	0.8	4.8	0.6	0.2	100	100.1	170	70	190	50	-	40	130
T181i.l.	75.1	0.9	18.4	3.2	0.01	-	1.3	0.9	0.2	100	100.0	200	110	20	30	-	60	30
T167i.l.	76.7	0.6	17.8	1.8	0.01	-	2.1	0.7	0.2	100	100.0	150	50	20	40	-	40	30
T128i.l.	75.6	0.7	18.4	3.1	0.01	-	1.2	0.8	0.2	100	100.0	170	70	20	30	-	60	40
T149i.l.	79.0	0.5	17.2	1.7	0.01	-	0.7	0.7	0.2	100	100.0	220	50	20	20	-	40	40
T412i.l.	72.9	0.6	16.9	4.5	0.04	-	0.8	3.5	0.4	100	100.4	480	60	140	1140	-	80	2050
T504i.l.	65.0	0.7	21.3	5.8	0.08	-	2.1	2.9	1.6	100	100.4	2290	60	360	170	-	420	540
T574i.l.	73.4	0.6	16.5	2.6	0.02	-	4.9	1.2	0.3	100	100.6	220	70	30	150	-	40	5400
T310i.l.	77.5	0.8	17.8	2.3	0.01	-	0.5	0.8	0.2	100	100.0	100	80	20	30	-	40	30
T688	70.6	0.9	17.8	5.4	0.06	-	0.5	3.9	0.2	100	100.7	1380	100	100	100	-	140	4730
T528o.l.	70.5	0.4	10.8	7.0	0.24	0.8	4.4	1.7	3.9	100	100.2	330	80	1000	70	60	100	680
T857i.l.	64.2	0.7	21.0	6.3	0.08	2.2	0.5	4.5	0.1	100	100.4	2090	120	60	200	10	340	1120
T258o.l.	63.0	0.6	9.3	4.4	0.23	2.7	13.2	3.4	2.7	100	100.5	450	90	2180	1360	280	160	260
T454i.l.	71.9	1.3	21.8	2.0	-	1.0	0.8	0.4	0.1	100	100.7	50	100	40	100	30	50	7070
T262i.l.	78.3	1.0	15.7	1.9	-	0.9	0.8	1.0	0.1	100	100.3	50	80	250	450	400	40	1710
T4i.l.	78.8	1.0	17.6	1.6	0.01	-	0.6	0.3	0.1	100	100.0	290	60	20	50	-	40	30
T76i.l.	75.9	0.8	14.4	1.8	0.10	1.7	3.9	0.8	0.5	100	100.1	240	80	70	170	120	60	120
T335o.l.	70.1	0.6	10.5	5.3	0.15	1.7	6.9	3.1	1.4	100	100.1	320	100	130	450	90	120	240
T225i.l.	67.5	1.0	18.4	2.3	0.02	-	9.5	1.0	0.3	100	100.0	160	70	20	40	-	50	30

Table 6-3. *Semi-quantitative portable XRF data from crucible samples from Augusta Raurica separated by layer (i.l.-inner layer; o.l.-outer layer) - Data performed by M. Helfert.*

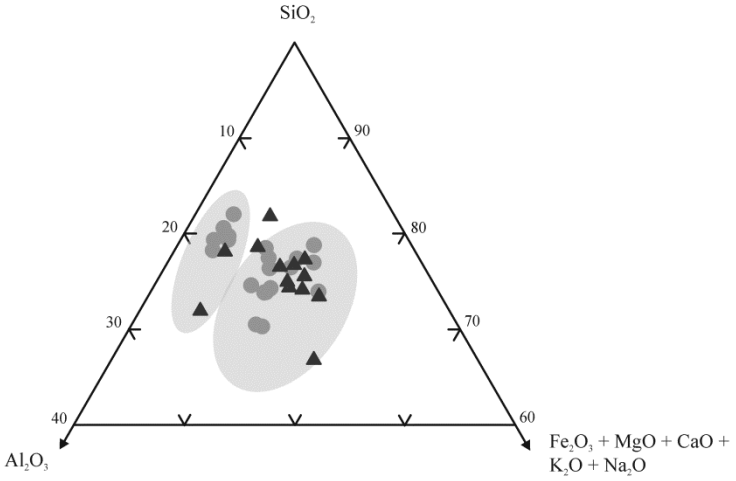

Figure 6-5. *Fe_2O_3+MgO+CaO+K_2O+Na_2O-SiO_2-Al_2O_3 diagram which shows laboratory XRF data from Augusta Raurica (●) and Aventicum (▲) as well as portable XRF results (greyish area). The grey area with a higher SiO_2 and Al_2O_3 content corresponds to clay group 1 and the bigger group corresponds to clay groups 2 to 5.*

6.2.2 Requirements and types of crucible clay

The clays used to make crucibles had to be easy to procure, yet at the same time meet serious challenges with regard to heat resistance, thermal shock resistance and insulating behaviour. The performance of the less heat-resistant clays could be somewhat improved by adding substantial amounts of quartz temper for high-temperature use (Bayley and Rehren 2007, Martinón-Torres *et al.* 2008). The lutum, which was added to the outside of the crucibles, on the other hand, had to adhere well to the crucible surfaces, blister and swell up in the heat and thus provide insulation; it was supposed to be viscous when fired to protect the crucible, which was being heated to its limit. The lutum was thus supposed to prevent breaks in the crucibles and keep them intact, and one of the casters' tasks was to apply the lutum and touch it up where necessary.

Interior crucible engobes, on the other hand, had to be thin and dense in order to prevent a loss of metal charge, e.g., through cracks in the crucibles or through absorption into the pores of the crucible ceramic.

Of the 893 crucibles investigated archaeologically, 102 were geochemically analysed with regard to their origins by portable XRF.

With the exception of 17 new, unused Roman crucibles from a deposit in Insula 19, the problem with the others was that they were contaminated to varying degrees by the components of the melted alloys, so that the elements Cu, Sn, Zn, Pb, Ni, and Cr could not be used for the characterisation of the crucibles or for the identification of their origins. 67 of the crucibles could be examined thanks to fresh breaks or saw cuts without interference due to crusts or slag on the interiors or exteriors. These samples formed the basis of the statistical analysis.

A total of five crucible clay groups could be identified among the finds analysed. They were clearly distinguishable, particularly due to the elements rubidium and strontium (Fig. 6-6).

Clay group 1 was the biggest group and contained 72 of the crucibles analysed. It was separated from the other four groups particularly by its very high silicon content of approximately 75 per cent by weight. The Rb concentration lay between 7 and 50 ppm, that of Sr between 31 and 66 ppm. The group is characterised by low Fe_2O_3 content with an average of 2.2 per cent by weight on one hand, and low CaO and K_2O concentrations of 1.7 and 0.7 wt.% on the other.

Groups 2 to 5 yielded Fe_2O_3 concentrations of approximately 5.2 wt.% and, based on the low CaO concentrations of between 2 and 3 wt.%, can be classed as calcium-poor (Maggetti and Galetti 1982).

Clay group 2 contained 12 crucibles with a Rb content of between 72 and 118 ppm and a Sr content of between 58 and 129 ppm. 25 lutum samples, some of which had been taken from group 1 crucibles, also belong to this group. The group also contained 4 lids that had been used for covering crucibles (Fig. 6-2, T878-T887).

Clay group 3, characterised by even higher concentrations of Rb (143 to 188 ppm) and a slightly higher Sr content (80 to 168 ppm), contained 12 crucibles, 6 lutum samples and 1 lid. Clay groups 4 and 5 contained three crucibles each. While group 4 was quite homogenous (Rb = 247 to 260 ppm, Sr = 121 to 140 ppm), the samples from group 5 with Rb values of between 138 and 259 ppm and a Sr content of between 285 and 426 ppm varied greatly. Since clay groups 2 to 5 are characterised by dense sand temper, we cannot exclude the possibility that groups 4 and 5 actually belonged to either group 2 or 3, and were just tempered to varying degrees using different types of sand.

A remarkable result obtained from the high-volume sampling of Roman crucibles from Augusta Raurica, which dated from three centuries, was that 71 % of the crucibles were made using the same type of clay, which probably even came from the same deposit. This allowed us to conclude that the clay, which was particularly well suited to producing fire-resistant pottery, was either already known at the beginning of the Roman occupation, or was discovered by systematically surveying the area and extracted over a long period of time because of its special properties.

6.2.3 Origins of the crucible clays

Reference data available for the discussion of the crucibles from Augusta Raurica included a series of analyses carried out by the Archaeometry Research Group at the University of Fribourg with regard to the pottery and tile production in Augst. They included 280 individual samples from reference groups and local clay deposits (Jornet 1982, Jornet and Maggetti 1986, Maggetti 1993, Schmid *et al.* 1999, Jornet and Maggetti 2003). Also used were analysis results on fire-resistant clays from the Swiss Jura region, so-called “hupper sand“, which were systematically studied by Eramo (2006). Moreover, in order to ascertain the origins of the crucible clays, raw clay samples were taken from 60 deposits within a 50 km radius around Augusta Raurica, analysed by p-XRF and used for comparison (Fig. 6-7). All the sites have been known at least since post-medieval times to yield fire-resistant clays. They have been used since then for various purposes and some are still in use today (e.g., in Lengnau/AG).

Because bronze working always requires crucibles, the hypothesis was formulated that all or at least the majority of them had been made in Augusta Raurica itself using local clay. However, no immediate connections could be identified between clay group 1 and the local clay deposits in Augst and Kaiseraugst.

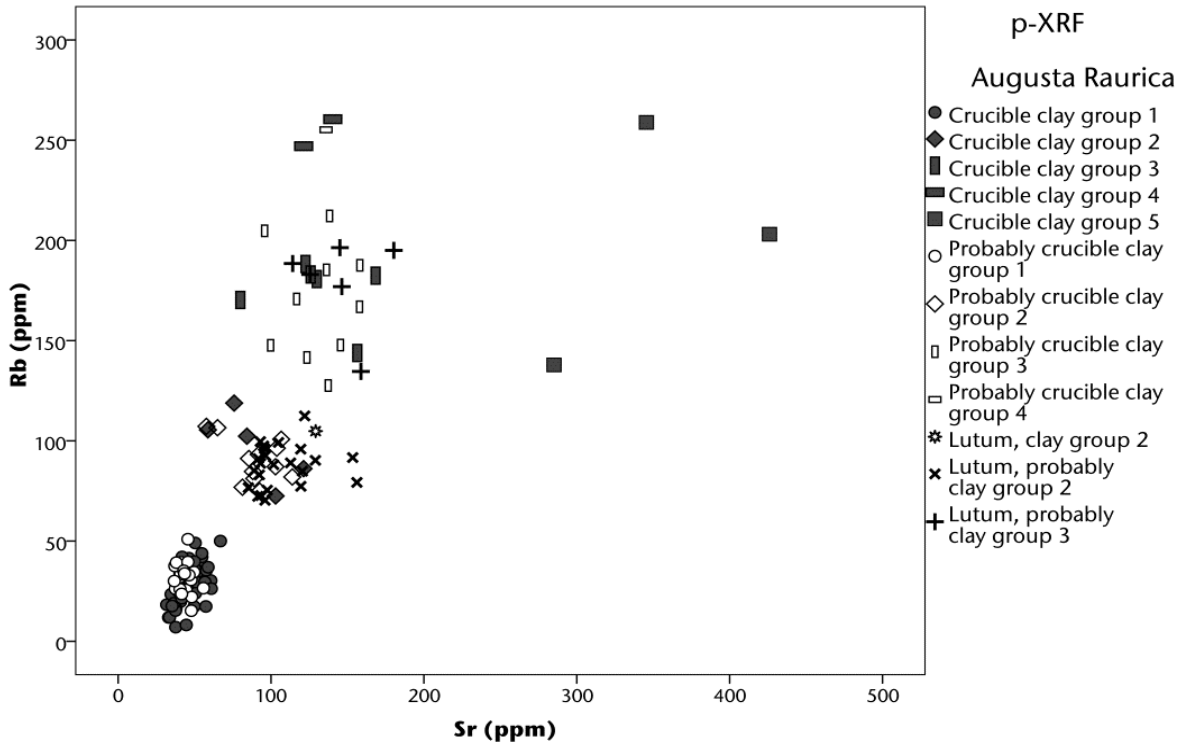

Figure 6-6. *Scatterplot Rb vs. Sr (ppm) of the geochemical groups of crucible and lutum samples from Augusta Raurica. The "probably crucible clay group ..." contains samples with the same Rb-Sr ratio like the samples of the special clay group but macroscopically and microscopically are this samples not out of the same group (only p-XRF data presented).*

On the contrary, by studying the geochemical element profiles of the 60 clay deposits, a process of elimination initially led to a selection of six potential deposits: Aedermannsdorf/SO, Châtelat/BE, Court/BE, Matzendorf/BE, Souboz/BE and Witterswil/SO. Strikingly, all potential clays were co-called "hupper sands" with high silicon content.

As the study progressed, Aedermannsdorf, Matzendorf, Souboz and Witterswil were excluded as potential places of origin due to the iron content being either too high or too low and due to varying trace element concentrations. The closest similarities with the crucibles in clay group 1 were identified in the Eocene siderolite clay samples from Châtelat, 50 km from Augusta Raurica as the crow flies, published by Eramo (2006, 191 Tab. 2 No. 249, 250). During fieldwork in the summer of 2013 various clays from different bands of clay in Châtelat were sampled and analysed using p-XRF. From a geochemical point of view, sample 364 and the clay variants extracted from it by means of wet and dry-sieving are identical to the crucibles of group 1 at Augusta Raurica (Fig. 6-8). We may therefore assume that the deposits associated with this type of clay in the Swiss Jura region (Eramo 2006, 188 Fig. 6-1, siderolite pockets, Eocene) were in all likelihood known in Roman times and deliberately targeted for the large-scale production of crucibles.

Analyses carried out on the crucibles from Aventicum revealed that the clays used there were very similar to the clay groups at Augst/Kaiseraugst.

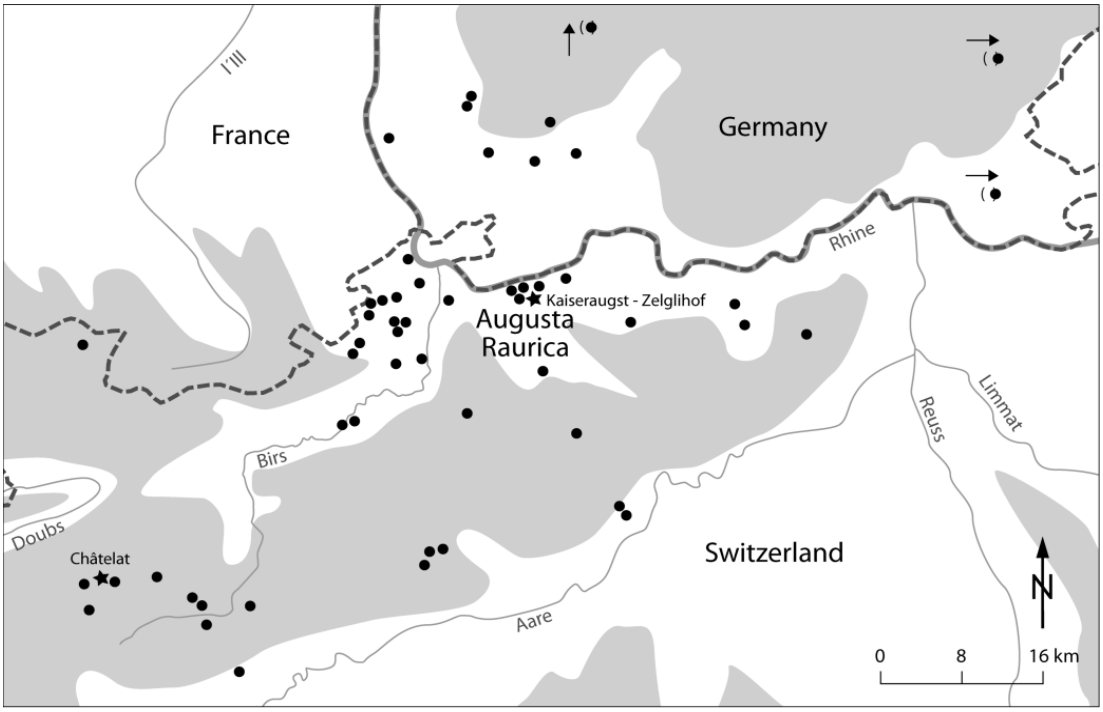

Figure 6-7. *Distribution of the deposits of the clays analysed for this paper in northwestern Switzerland and southern Germany. Most of the deposits (●) are located in ancient Colonia Raurica territory. ✶ indicate the deposits "47 Châtelat" and "3 Kaiseraugst-Zelglihof", clays from which were proved to have been used for groups 1 and 2.*

For example three unused crucibles from Augst (T128, T168, T225) fit together with the optical and geochemical properties from one investigated sample from Aventicum (MRA 03/11712-21).

We may therefore assume that the knowledge of the fire-resistant clays from the Jura region led to similar, if not even the same clay deposits, being used for the crucible production in Aventicum.

The determination of the origins of the crucible and lutum samples of clay group 2 was of particular interest. Once again it was assumed that this clay type was local because lutum suffered much from wear and tear and was often replaced several times, so that one would expect the raw material to have been available locally. From a geochemical point of view, however, clay group 2 does not match the ceramic products made in Augusta Raurica (Fig. 6-5). The attention therefore turned to the clay raw material analyses carried out by Maggetti and Galetti (1993) and the clay samples recently taken in and around Augusta Raurica. While, from a geochemical point of view, the deposits in the "Schwarzacker" area in Augst/BL and the "Im Liner" and "Im Sager" areas on the lower terrace of the River Rhine in Kaiseraugst/AG only partially match, the clays from the "Zelglihof" area (samples 60-63), classified as loess loams, correlate quite closely. An experiment was subsequently conducted where the loess loam from the "Zelglihof" area was mixed with the "Schwarzacker" lower terrace loam. The resulting clay bore the closest similarity to the lutum and crucible samples from clay group 2. We may therefore conclude that material was extracted in Roman times from the transition zone between loess loam and lower

terrace loam to produce crucibles and that the same material was also used to make lutum.

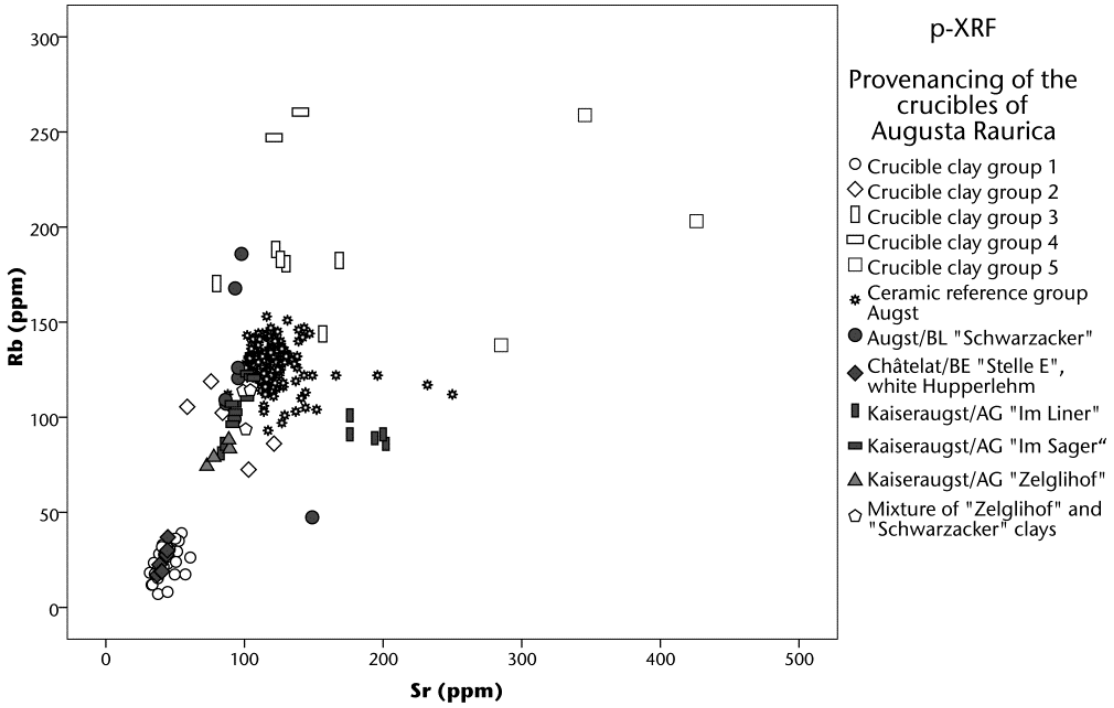

Figure 6-8. *Scatterplot Rb vs. Sr (ppm) of the geochemical groups of crucible and lutum samples from Augusta Raurica including different clay and ceramic reference groups (only p-XRF data presented).*

No correlations could be detected among the available data that would have matched the smaller crucible clay groups 3 to 5 at Augusta Raurica. It must remain an open question, therefore, whether these were local or imported clays. As mentioned earlier, it is possible that the geochemical variability was caused by varying temper components.

6.2.4 Firing temperatures

It is necessary to state that, based on the present mineral composition, only the highest firing temperatures of the crucibles used can be identified, because all parameters deriving from lower-temperature processes are lost once higher temperatures are attained. It is, therefore, impossible to ascertain the specific stage in the overall production cycle at which the highest temperature was reached. The different production stages and effects of multiple uses have already been outlined in section 6.2.1.

Samples containing mullite and/or spinel, which itself is a high-temperature breakdown product of kaolinite, within the matrix must have reached at least 700 °C and up to 950 °C. The spinel is a γ-Al_2O_3 spinel phase with ordered spinel structure with vacancies on octahedral sites (Onike *et al.* 1986, Sonuparlak *et al.* 1987). The samples that do not contain mullite but do contain meta-kaolinite can thus be interpreted as crucibles that were fired at temperatures of between 500 °C and 700 °C (Lee *et al.* 2008). The absence of

spinel and presence of mullite can be taken as an indication for firing temperatures of at least 950 °C but below 1100 °C to 1200 °C as this spinel-like phase is a transition phase between kaolinite and mullite. At even higher temperatures, a reaction occurs between feldspar rims and the mullite-rich matrix causing a growth of elongated (secondary) mullite needles around partially molten feldspar grains (Lee *et al.* 1999).

The Al_2O_3-SiO_2-K_2O diagram (Fig. 6-9) shows conformity between laboratory and portable XRF analyses. The results of both methods suggested possible (maximal) stability temperatures of up to 1600 °C. However, based on the metals that were melted in the crucibles and the technology available at the time, this temperature was never attained. It is also evident from Fig. 6-9 that samples showing a higher amount of glass-forming ingredients plot towards lower temperature ranges in contrast to samples that contained a low amount of the same elements. Geochemical data obtained from samples from Augusta Raurica and Aventicum plot together in almost identical regions of the diagram and, therefore, imply a strong similarity to each other. Almost all data obtained from portable XRF measurements coincide with the data from the laboratory-based XRF analysis.

6.2.5 Crucibles in metallurgical melting processes

The analysis of metal traces in the crucible ceramics and of metallic drops and reguli in the crucibles revealed the entire range of non-ferrous alloys commonly found at Roman sites: copper, tin bronze, brass, tin brass, tin lead-brass, speculum metal, silver-bearing lead bronze and lead-copper alloys. These melting processes, which were often a form of recycling old metals by using scrap metal usually took place in various-sized crucibles in the standard egg shape made of the light-coloured clay group 1 (Fig. 6-2, T27-T582). However, we realised that brass also tended to be made in crucibles made of dark-grey clay with dense quartz temper and fired in a reducing atmosphere. These crucibles often had flat bottoms and profiled rims and were usually made of the local clay group 2 (Fig. 6-2, T863).

It was possible for the first time to identify brass production using the cementation method in the Roman province of Germania superior. The calamine deposit in Wiesloch/Germany, which was mentioned by Pliny (*hist. nat.* 34, 2) and was only 208 km northeast of Augusta Raurica, was probably used to this end. The cementation was carried out using crucibles of medium size loosely covered with lids (Fig. 6-2, T878-T887). Both the crucible and lid ceramics yielded very high values of zinc; this had previously been seen in Autun/France and Lyon/France and also in Xanten/Germany (König and Serneels 2013 - Chapter 3, König in prep. (b) - Chapter 5).

The seven small bowl-shaped crucibles (0.8 % of the entire crucible assemblage) were all made from dark, probably local clays of clay groups 2 and 3 and usually contained quite dense temper (Fig. 6-2, T868-T876). They bore a variety of metal traces, which can be associated with various processes: silver and gold alloys on one hand and mixtures with a lot of lead as well as traces of mercury and arsenic on the other.

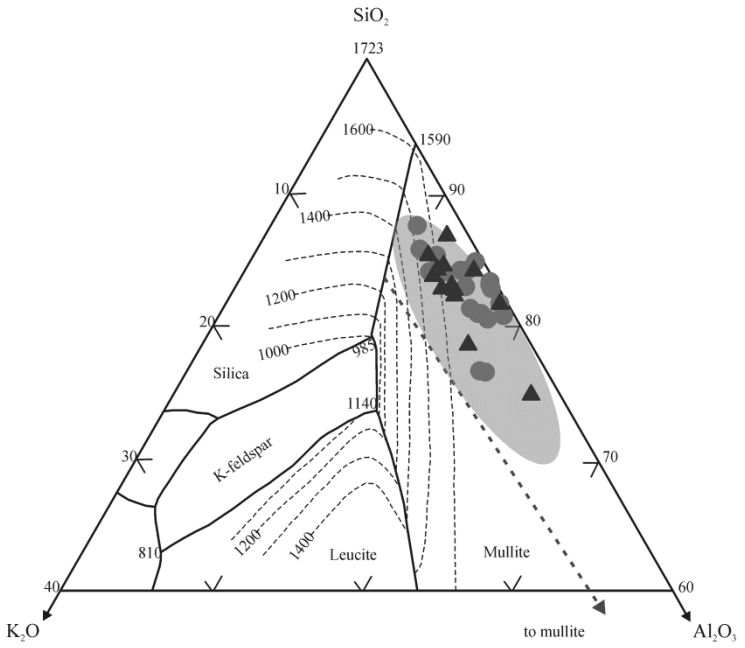

Figure 6-9. *High-silica part of the Al_2O_3-SiO_2-K_2O diagram (modified after Osborn 1977, Maggetti et al. 2010) showing stability temperatures of the crucible fragments from Augusta Raurica (●) and Aventicum (▲) as well as portable XRF results (greyish area). Isotherms are shown every hundred degrees (temperatures in °C). The fat dotted line projects towards the mullite-silica cotectic line.*

6.3 CONCLUSION

The interdisciplinary project on bronze working in the Roman town of Augusta Raurica/Switzerland revolved around 893 crucibles. With a few exceptions (seven in total) they were all of a uniform shape (Fig. 6-2), although their heights varied considerably (4.5-18 cm). 15 crucible fragments were analysed under laboratory conditions using SEM-EDX, XRPD and XRF-WDS, while 188 crucibles were analysed by means of 485 p-XRF measurements.

The large amount of data available allowed us to identify the crucible ceramics, the composition of the lutum on the crucible exteriors and the melting and cementation processes which took place in them.

By conducting a chemical trace analysis, the crucible ceramics could be divided into five clay groups. The two most frequently used groups could be correlated with some of the 60 clay deposits that we sampled and analysed: Châtelat in the Bernese Jura region (clay group 1) and Kaiseraugst-Zelglihof (clay group 2) in close proximity to Augusta Raurica (both in Switzerland). Clay groups 3 to 5 were only used in a small number of cases and their origins have not yet been pinpointed.

While the crucibles of clay group 1 were brought to Augusta Raurica as finished products ("traders hoard" with unused clay group 1 crucibles in Insula 19), those of clay group 2 were produced by local potters on site. The lutum, also often made of clay group 2, was probably applied to the crucibles by the casters themselves (in some cases repairs were carried out repeatedly). The metalworkers evidently used the same local clay to make their moulds.

Traces of the entire range of "bronzes" commonly used during the Roman period were identified on the ceramics and also in metal stains and drips. They included tin bronzes, brass, lead bronzes and mixtures of all three. A few small crucibles also yielded marked traces of silver. Based on crucible lids and crucibles with very high zinc concentrations, it was possible to identify cementation of brass with copper and zinc ore (calamine) for the first time in the Roman province of Germania superior.

The highest temperatures reached when using the crucibles lay between approximately 950 and 1200 °C. The high SiO_2 and Al_2O_3 contents (Fig. 6-9) suggest that the crucibles had stability temperatures of up to 1600 °C which, however, were never attained during their use.

The lutum layers that were archaeometrically examined differed from the crucible ceramics in that they yielded higher Ca, K, P and S values (Tables 6-2 and 6-3). Numerous experiments have since been conducted which have allowed us to reconstruct these properties and understand how lutum was made (Furger in prep.). The analysis results can be explained by the addition of certain substances such as animal hair, dung, urine, potash and others.

With the exception of the new and unused crucibles, they all bore traces of metals. Both the crucible ceramic and the lutum always contained the volatile element zinc and often also higher concentrations of lead. Copper and tin were always underrepresented and present only in slightly higher traces. More representative results with regard to the alloys created by the craftsmen were obtained by taking surface measurements on green bronze stains and the often colourless remnants of glaze on the crucible fragments. However, as in corrosion and patina layers on bronze objects, the metallic elements in these stains often significantly changed so that we may only speak of qualitative surface data. The most secure method of achieving quantitative results is to carry out p-XRF measurements on borings from large bronze drops in the crucibles.

An engobe at the inside of the crucibles was identified more often than previously expected. It was a thin layer of finely sieved clay, 200 to 300 µm thick and with small amounts of extremely fine temper; it adhered to the inside of the crucible and was completely vitrified. Minute metal drips on the engobe showed that it came into direct contact with the charge and probably formed a protective layer on the crucible.

Crucibles used in Roman-period non-ferrous crafts were found much less often in Aventicum than in Augusta Raurica. Both visual examinations on one hand and mineralogical and geochemical analyses on the other revealed that the crucibles from both urban centres were made from more or less the same raw materials and that some of them were probably created at a central location. The majority of the crucibles would then have been brought to the individual metal-processing workshops via the usual trade routes.

In summary we can state that the two methods – using sample specimens in the laboratory on one hand and entire objects in the museum storage rooms on the other – complement each other very well. While the two methods of analysing crucible ceramics differ with regard to certain elements (e.g., Si, Al), they are well suited to determining the origins by comparing artefacts with reference deposits. Of course, in order to answer petrographic and mineralogical questions (e.g., firing temperatures) and carry out structural examinations (Fig. 6-3) laboratory analyses are indispensable. With regard to achieving efficiency in dealing with large amounts of finds, however, and obtaining representative series of measurements as well as identifying metallic remnants, portable XRF is ideal.

7 - COMPARISON OF ROMAN METAL-MELTING CRUCIBLES FROM AUTUN/FRANCE, AUGST/SWITZERLAND, AVENCHES/ SWITZERLAND AND XANTEN/GERMANY

D. König

ABSTRACT

This article compares Roman metal-melting crucibles from different excavation sites all over Western and Central Europe (Xanten/Germany, Autun/France, Augst/Switzerland and Avenches/Switzerland) regarding their overall structure, geochemical composition and use. The investigated crucibles show slightly different shapes and in some cases clear differences in their size. A commonality of all crucibles studied is their two layer structure with an additionally occurring engobe. Assessed firing temperatures are slightly different as a function of size, metal load of individual crucibles and thus their dwell time within the fire. We suggest a common Roman recipe to produce metal-melting crucibles, at least applied within the four investigated sites.

7.1 INTRODUCTION

The herein discussed metal-melting crucibles are reaction vessels in which copper-alloys, e.g., brass, bronze or gun metal was melted. Such crucibles are well known from different excavations of Roman age in Western and Central Europe, e.g., Nida-Heddernheim/Germany (Bachmann 1976), Augst/Switzerland (Martin 1978, König *et al.* - Chapter 6), Britain (Bayley 1987) etc. Bachmann (1976) described metal-melting crucibles from Nida-Heddernheim/Germany which date to the 2nd century A.D. This vessels show a typically double-layered structure with a notable hole in the upper third of their height. The function of this hole is still a matter of debate but it has been suggested that it was used to pour out the liquid metal and hold back the slag within the crucible itself (Bachmann 1976). Another type of metal-melting crucible from Augst/Switzerland was described by Martin (1978). The latter characterise these crucibles as single layered with an outer slag layer. In a recent publication of König *et al.* (Chapter 6) disprove the supposed slag nature of the outer layer described by Martin (1978) and document in addition the widespread occurrence of an engobe.

Bayley (1987) published a typical double-layered melting-crucible from the Roman period in Britain. This type of crucible is remarkably different compared to the aforementioned vessels with respect to their shape. This crucible shows a pear shape with a flat bottom. All other metal-melting crucibles (Bachmann 1976, Martin 1978, Rehren 1995, Rehren 1997, König and Serneels 2013 - Chapter 3, König *et al.* - Chapter 6, König in prep.(b) - Chapter 5) are more or less egg shaped or cylindrical in shape with a rounded or pointed bottom. But, a common and important feature of all these vessels is their double-layered ceramic body. Such metal-melting crucibles are also preserved in Xanten/Germany and have been analysed by Rehren (1995, 1997). Two different types of crucibles can be distinguished after Rehren (1995, 1997). One type has a two layered structure and shows a hole of almost one centimetre in diameter. It has been suggested that it

was used to grab the crucible with the forge tong in order to pull out the metal in a more suitable way (Rehren 1995). The second type comprises egg shaped vessels without any visible holes (Rehren 1997). This metal-melting crucibles are also double-layered but showing an additional internal layer which the author interpreted as slag layer. The interpretation of the latter was disproved by recent investigations (König in prep. (b) - Chapter 5). The authors stress that the tiny innermost and vitrified layer is an intendedly added engobe with a clear functional purpose.

Nielen (2006) described Roman double-layered metal-melting crucibles with an occurring engobe from Neuss/Germany. These differ to the aforementioned crucibles with respect to the engobe layer. The documented engobe therein is present on both sides of the inner ceramic layer which might point to a differing production process.

Detailed geochemical-mineralogical studies of Roman metal-melting crucibles from Autun/France were recently published by König and Serneels (2013 - Chapter 3). Similar analytical approaches of Roman age metal-melting crucibles were undertaken by König *et al.* (Chapter 6) dealing with vessels deriving from Avenches/Switzerland and Augst/ Switzerland. Their macroscopic and microscopic appearance is almost similar and gives rise to speculations on trade relations between the Roman settlements Aventicum/Switzerland and Augusta Raurica/Switzerland (König *et al.* - Chapter 6).

This article aims to compare and summarize the current state of knowledge about double-layered Roman metal-melting crucibles from Autun/France, Augst/Switzerland, Avenches/ Switzerland and Xanten/Germany regarding their macroscopic (e.g., shape, overall structure etc.) and microscopic-geochemical properties (mineral content, clay compositions, source rocks, temperature stability, alloy composition etc.) in order to provide a common data base for comparisons with other investigations in future. The acquired and compiled data can help to understand the Roman technology in the production of metal-melting crucibles in the area of Western and Central Europe in more detail.

7.1.1 HISTORICAL BACKGROUND

All herein studied Roman settlements are situated in Western and Central Europe (Fig. 7-1). The samples originating from Autun/France (Augustodunum) constitute of remnants of 50 metal-working workshops which were producing between the 1st and the 3rd century A.D. (Chardron-Picault and Pernot 1999). In total, 650 kg of crucible fragments and appropriate lids were found in the excavated area of the Lycée militaire. The design of individual vessels is almost identical to each other, although three different groups differing in size can be distinguished (Chardron-Picault and Pernot 1999, König and Serneels 2013 - Chapter 3). The remnants and all excavated artefacts belonging to this former Roman settlement point to a large scaled copper-alloy manufacturing at Autun/France (König and Serneels 2013 - Chapter 3).

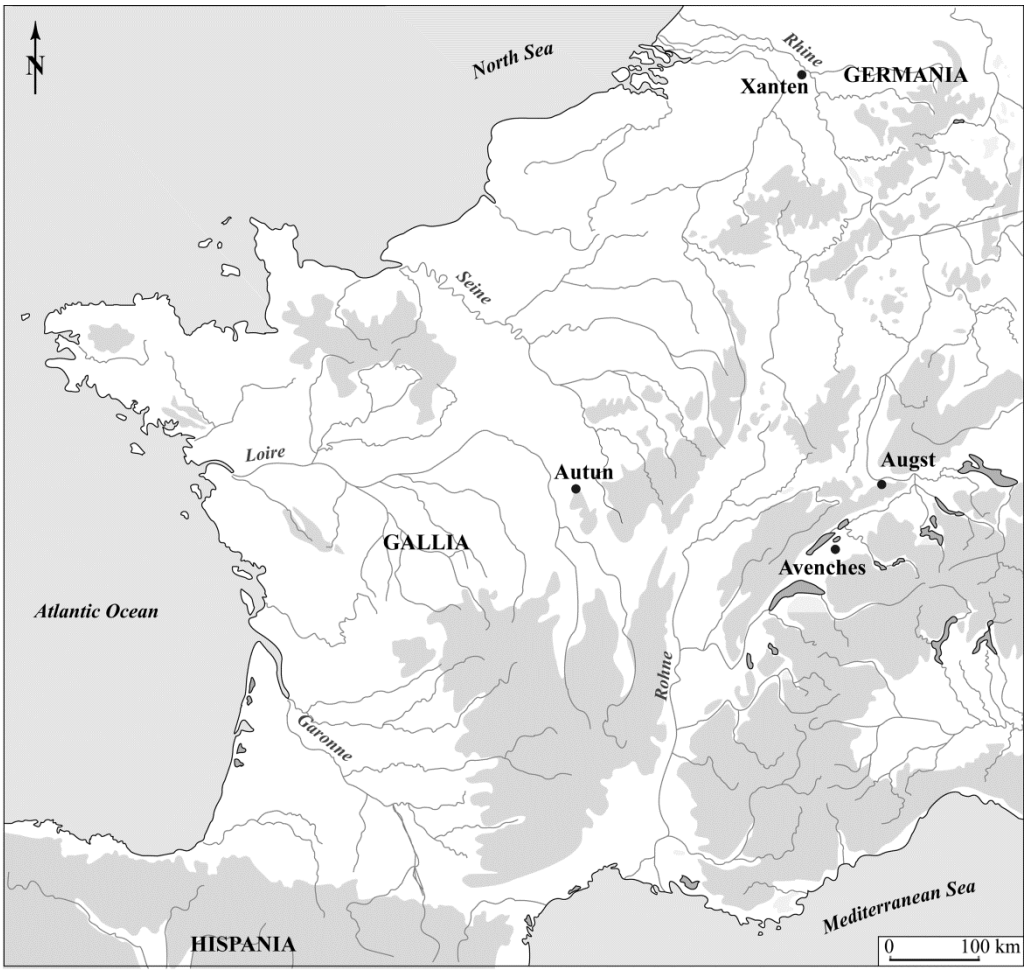

Figure 7-1. *Map providing the localities studied of former Roman settlements and the nowadays cities located at or nearby these historical settlements (Augustodunum - Autun/France, Augusta Raurica - Augst/Switzerland, Aventicum - Avenches/Switzerland and Colonia Ulpia Traiana - Xanten/Germany.*

Metal-melting crucibles from Augst/ Switzerland (Augusta Raurica and Kaiseraugst) and Avenches/Switzerland (Aventicum) are much smaller than the ones from Autun/France. They initially appear in the early 1st century A.D. but become more frequent in the advanced 2nd to 3rd century A.D. Around 900 crucibles and crucible fragments were found in Augst/ Switzerland but only a few tens of pieces in the storage in Avenches/ Switzerland. In general, samples coming from both excavation sites are similar with respect to their overall appearance (size and shape), but also their mineralogical and geochemical properties. Therefore, a trading of crucibles either between both towns or between both towns and a third place has been suggested by König *et al.* (Chapter 6). Archaeological work documents and favours the hypothesis that Augusta Raurica/Switzerland was an important Roman settlement with a large scaled manufacturing site for copper-alloys. Aventicum instead is interpreted as of less importance in this matter, a hypothesis also resting on the fact that only small amounts of copper-alloy crucibles were excavated. It is, therefore, assumed that it was easier to trade crucibles for these purposes than to produce them in the right way on-site.

Crucibles from Xanten/Germany (Colonia Ulpia Traiana) descend from a small scale production site as deduced from the small amount of sample material which was found in scattered places throughout the former Roman settlement. Although reused domestic pots for metal-melting purposes were also found, they were not of particular interest for this study. The Roman town were founded as an outpost along the border to Germania Libera at around 100 A.D. and persisted until the 3rd century A.D. The heyday of Colonia Ulpia Traiana was in the 2nd century A.D. (König in prep. (b) - Chapter 5).

7.2 Results and Discussion

An overview about petrographic and chemical characteristics of Roman metal-melting crucibles from Xanten/Germany, Autun/France, Augst/ Switzerland and Avenches/Switzerland is summarized within Table 7-1. The properties of the different ceramic vessels are, therefore, easily recognizable and comparable with each other. It is evident from Table 7-1 that the total numbers of layers, the individual petrographic character as well as the used materials are pretty much similar to each other. The investigated metal-melting crucibles show large differences in their appearance but no differences in terms of use and just a few in terms of material characteristics.

7.2.1 Shape

Metal-melting crucibles from Autun/France are the largest vessels studied and also the largest Roman metal-melting crucibles documented in literature. At least three sizes with a volumetric capacity between 0.3 and 2.2 L, i.e., 2.5 - 19 kg metallic charge, have been distinguished so far (König and Serneels 2013 - Chapter 3). Crucibles from Augst/Switzerland and Avenches/Switzerland are much smaller than the ones from Autun/France but slightly larger than the ones from Xanten/Germany (see Table 7-1). The majority of these vessels were wheel-thrown, as recognizable from distinct handling traces, and egg-shaped with a rounded or even pointed bottom (König *et al.* - Chapter 6). These crucibles show a diameter of at least eight centimetres, a height of 4.5 up to 18 centimetres and, therefore, a volumetric capacity between 50 g and 4 kg metallic charge (König *et al.* - Chapter 6). The shape is almost identical with those of Xanten/Germany. All excavated metal-melting crucibles from Xanten/Germany are small in size, with a diameter of around five centimetres, a height of eight up to ten centimetres and a volumetric capacity between 0.1 and 0.2 L, i.e., 1.0 to 1.5 kg metallic charge (König in prep. (b) - Chapter 5).

7.2.2 Structure

One major finding in all investigated metal-melting crucibles is the three-parted nature of the wall (i.e. vitrified engobe, inner ceramic layer, outer vitrified layer) and their very similar mineralogical structure (vitrification state, porosity and kind of temper used). It is important to note that the thickness and chemical composition of the engobe is similar between the individual localities. The engobes' thickness range from 200 µm to 400 µm and is significantly enriched in calcium and, thus, completely vitrified. A common characteristic of the crucibles engobe from Xanten/Germany, Augst/Switzerland and Avenches/Switzerland is the appearance of temper grains therein which are mainly made of quartz only. Studied crucibles from Autun/France show an engobe free of temper which might give a first hint for slight variations in the production routine. It was suggested that the engobe was made by slurry produced from the same clay the outer layer was built up (König and Serneels 2013 - Chapter 3). That means the amount and size of temper grains is dependent on deposition time, i.e., time the bigger temper material needs to deposite. This layer is interpreted as protecting layer as the

presence of an engobe avoids the unwanted loss of the liquid metal charge into the pore space of the ceramic. It also helps to pour out the liquid metal almost completely (König and Serneels 2013 - Chapter 3).

The inner ceramic layer is always a non-vitrified body including temper of quartz, feldspar and in a few samples mica also. Feldspar crystals are completely vitrified in the majority of the studied ceramic fragments and in samples from Autun/France additionally characterised by an occurrence of secondary mullite along the feldspar-matrix interface (Lee and Iqbal 2001, König and Serneels 2013 - Chapter 3). However, feldspar temper in crucibles from Augst/Switzerland (plagioclase and potassium feldspar)and Avenches/Switzerland (plagioclase and potassium feldspar) is less vitrified or even free of vitrification. They are, thus, less fired ceramics than vessels from Xanten/Germany (plagioclase) and Autun/France (plagioclase and potassium feldspar). But that above mentioned fact is not independent of the type of feldspar, i.e., potassium feldspar shows a much lower melting temperatures than plagioclase. The matrix of all examined metal-melting crucibles predominantly consists of primary mullite, except of those crucibles from Autun/France which are additionally characterised by large secondary mullite needles (König and Serneels 2013 - Chapter 3). A few of the investigated samples have a matrix composed of x-ray amorphous meta-kaolinite.

The outer layer is entirely vitrified and enriched in calcium. Remnants of temper are composed of quartz and minor amounts of feldspar. The calcium additive or source is not identifiable within the investigated crucibles as a direct consequence of the combustion temperature. The latter either cause a total decarbonisation in case of carbonate additives (chalk, limestone, marl etc.) or a complete oxidation of calcium-rich organic compounds such as ash additives. The vitrification of the layer matrix, which is a direct result of an added calcium-rich compound, will not help identifying such an additive due to a certain degree of homogenisation process stimulated by the vitrification process itself. Overall, this calcium-additive induces a reduction of the refractory performance and, thus, increasing the insulation function of the whole crucible. Regarding their use, all investigated metal-melting crucibles were fired from the outside and have, therefore, typical charcoal imprints along the outside and the outer ceramic layer, respectively. The latter shows reddish and greenish redox colours as resulting from copper alloy handling.

A doubled outer layer appears in some of the investigated fragments (Fig. 7-2) and was interpreted as a kind of repairing mark above cracks formed during firing (König and Serneels 2013 - Chapter 3). This clearly indicates a multiple use of such vessels. The border between primary and secondary outer layer shows typical multiplication of redox colours created during individual uses as well as the charcoal imprints. This also implies that the clay which was used for the outer layer was available within the workshops to perform the repairing directly before the next use. The hypothesis of a multiple use is supported by investigations focussing of the chemical composition of metal droplets within single crucibles from Autun/France (Appendix 2). Single metal droplets therein deliver a broad compositional range, namely brass, bronze and gun-metal within one individual metal-melting crucible. A main problem arising from such investigations is the comparability due to the low amount of residual metal droplets present which are large enough to analyse them and “fresh” enough to exclude a preferential metal loss due to reheating processes. As already mentioned, the minor amount of metal left in the crucibles is a result of the engobes’ properties. All remnants situated along the surface of the engobe are strongly altered and thus insufficiently suited for determining elemental characteristics. Thus, it would be much better to use metal prills coming from rarely occurring cracks within the inner surface.

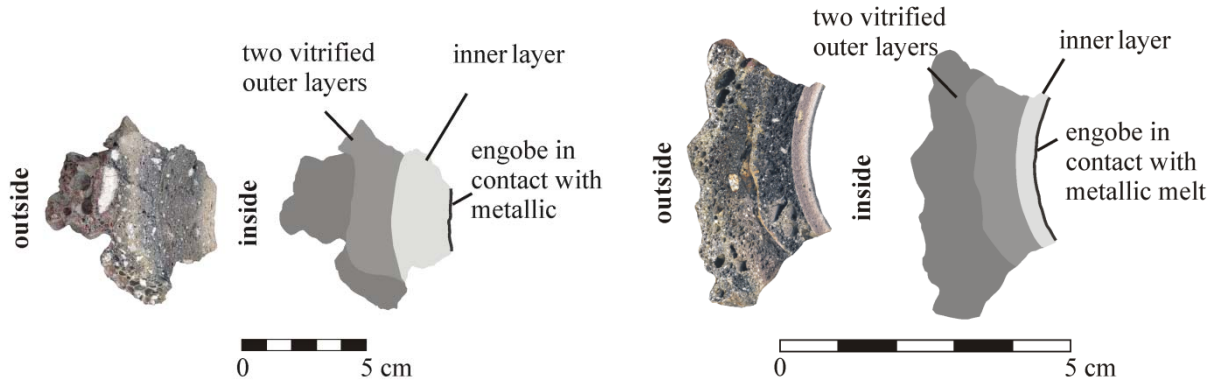

Figure 7-2. *Doubled vitrified outer layers in the metal-melting crucibles; left: sample from Autun/France; right: sample from Avenches/Switzerland.*

7.2.3 PETROGRAPHICAL AND MINERALOGICAL PROPERTIES

The inner ceramic layer of the crucibles studied is characterised by quartz, feldspar (k-feldspar and/or plagioclase) and in some samples mica as temper material. The ceramic temper of samples from Autun/France and Avenches and Augst (both Switzerland) is angular in shape and lithic fragments besides the mentioned minerals are also common. The Xanten/Germany crucibles are characterised by (very) well rounded quartz and feldspar as temper within the inner ceramic layer. Mineralogically, primary mullite, cristobalite and/or a spinel-like phase are the main constituents of the crucible matrix in samples coming from Switzerland and Germany, while samples from Autun/France are rich in primary and secondary mullite as well as cristobalite, but with less frequent amounts of a spinel-like phase. Only a small amount of samples is characterised by x-ray amorphous meta-kaolinite, an interpretation taken from the absence of mullite peaks within XRD data, but the presence of a mullite-like chemical composition of the matrix as identifiable by SEM-EDS.

Temper of the entirely vitrified outer layer is usually composed of quartz and feldspar remnants, although samples from Xanten/Germany show quartz temper only. Shape properties of the temper are identical with those of the inner layer. The vitrified matrix hosts primary mullite, cristobalite and/or analcime. The latter is a secondary mineral often formed during the burial stage in highly fired ceramics with an elevated amount of calcium (Buxeda *et al.* 2002, Schwedt *et al.* 2006, Pradell *et al.* 2010). It is therefore possible to estimate firing temperatures from such ceramics (see section 7.2.4).

The geochemical composition of all metal-melting crucibles studied is shown in Fig. 7-3. The ternary diagram SiO_2-Al_2O_3-Fe_2O_3+MgO+CaO+K_2O+Na_2O illustrates a common chemical area of the three investigated groups of samples with a tendency towards a higher Al_2O_3 content in samples from Autun/France. Except of a few samples, there is a complete overlap of the chemical composition of the studied crucible fragments. This fact suggests a similarity of raw materials used, i.e., clay plus temper. These materials mainly derive from local sources as already been demonstrated in case of Autun/France (König and Serneels 2013 - Chapter 3), Augst/Switzerland and Avenches/Switzerland (König *et al.* - Chapter 6).

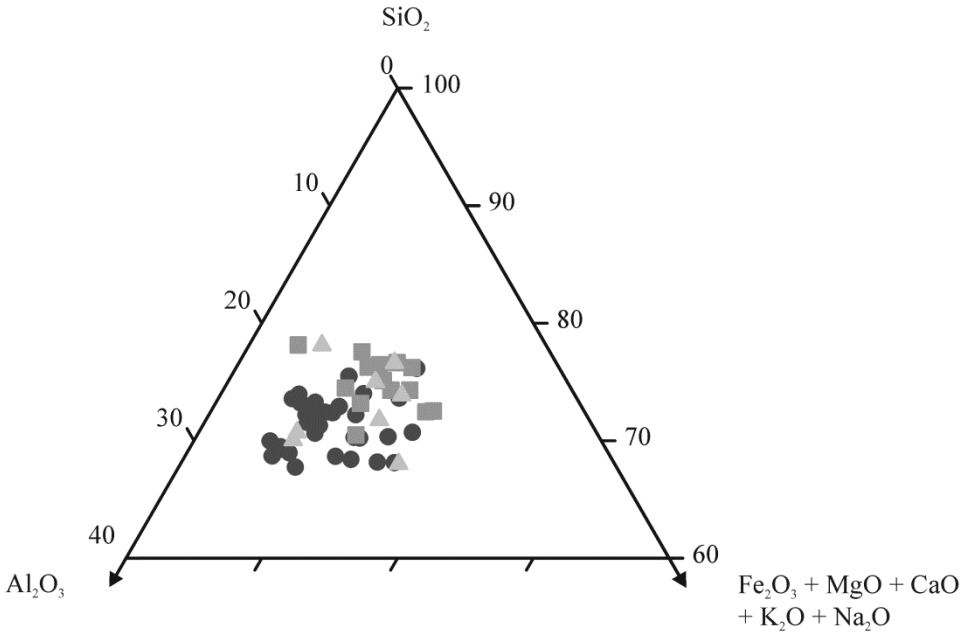

Figure 7-3. *Ternary diagram of SiO_2-Al_2O_3-Fe_2O_3+MgO+CaO+K_2O+Na_2O which show the sample composition of the metal-melting crucibles from Autun/France (dark grey dots), Augst/Switzerland and Avenches/Switzerland (medium grey squares), Xanten/Germany (light grey triangles).*

Due to the high amount of SiO_2, Al_2O_3 and K_2O, which yield together between 90 and 97 wt.%, it is possible to estimate maximum stability temperatures from the ternary diagram SiO_2-Al_2O_3-K_2O (Fig. 7-4) as published by Maggetti *et al.* (2010). The residual 3 to 10 wt.% are shared between CaO and Fe_2O_{3tot}, which are attributed to plagioclase, the clay material used and an unknown calcium enriched additive. This diagram shows chemical differences within the set of investigated metal-melting crucibles concerning K_2O which is mainly caused by the presence of potassium feldspar as temper, different initial clay compositions and additives within the outer layers.

A comparison of the acquired chemical data with literature data of typical groups of clay (Newman 1987), i.e., kaolinite, illite, smectite etc., allows to determine possible clays used as raw materials for the analysed Roman ceramics. Thus, the inner layer of metal-melting crucibles is always characterised by a raw material bearing a certain amount of kaolinite group minerals as interpreted from the abundant occurrence of mullite, meta-kaolinite and a kaolinite breakdown related spinel-like phase. The significantly enriched content of Al_2O_3 in crucibles coming from Autun/France points to a much higher amount of kaolinite clay than used for ceramics from the other localities studied. There, the geochemical composition shown in Fig. 7-3 is much closer to a raw clay rich in kaolinite, but also containing illite/smectite or montmorillonite rich clay minerals. Probably, similar clays like for the inner layer have been taken for the outer one. This can clearly be stated due to the close chemical similarity between both layers. But, there must be an extra additive causing the calcium and potassium enrichments within the outer layer of all ceramics studied. This is most probably coming from a marly limestone, a marl or even an ash additive. However, there are no optical determinable remnants visible for such an additive within any of the investigated fragments which is

presumably caused by the high firing temperatures (experiments by Alex R. Furger).

As the vast majority of temper grains is angular to sub-angular in shape, mainly composed of quartz, potassic and plagioclase feldspar, minor amounts of phyllosilicates and some lithic fragments, an artificial source for temper such as a crushed granitic rock or any related material have to be expected in case of Autun/France, Augst/Switzerland and Avenches/Switzerland. However, rounded temper dominated by quartz in case of ceramics deriving from Xanten/Germany suggest a much simpler scenario, namely the use of an unconsolidated sedimentary rock either taken from a fluviatile or eolian deposit within the vicinity of the former Roman settlement. This is most likely due to the proximity of the Rhine River and his tributaries.

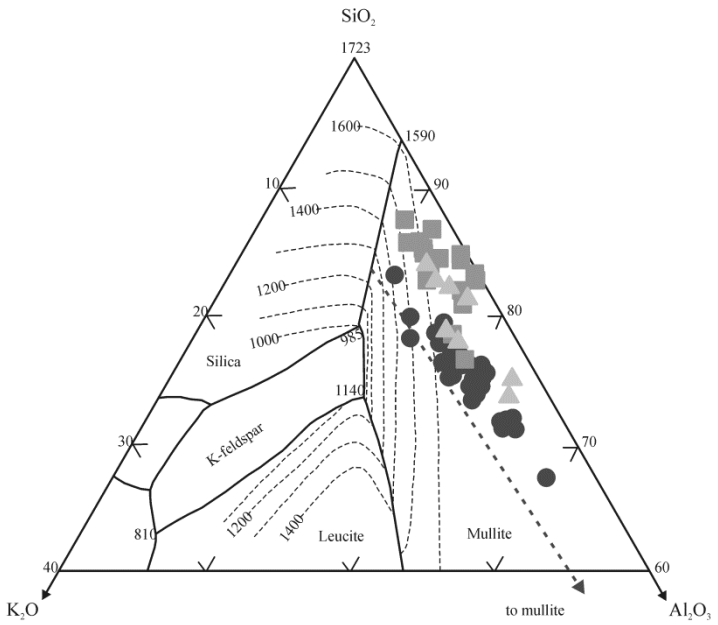

Figure 7-4. *High-silica part of the SiO_2-Al_2O_3-K_2O phase diagram (modified after Osborn 1977, Maggetti et al. 2010). Isotherms are shown every hundred degrees; temperatures in °C. The fat dotted line is the projection toward the mullite-silica cotectic line. Samples from Autun/France are marked by dark grey dots, samples from Augst/Switzerland and Avenches/Switzerland are characterised by medium grey squares, samples from Xanten/Germany are indicated by light grey triangles.*

7.2.4 FIRING TEMPERATURES

For the estimation of firing temperatures different minerals present within the crucibles were used. The temperature-induced kaolinite breakdown reaction is a comprehensively studied phase transformation reaction (Bellotto *et al.* 1995, Gualteri *et al.* 1995, Lee *et al.* 2008, Sperinck *et al.* 2011) and therefore well suited to estimate firing temperatures. A general and simplified (non-stoichiometric) reaction sequence can be given as follows (Lee *et al.* 2008, Sperinck *et al.* 2011):

$$\text{kaolinite } Al_2Si_2O_5(OH)_4 \xrightarrow{500\text{-}700\ ^\circ C} \text{metakaolinite } Al_2Si_2O_7 + H_2O$$

$$\text{metakaolinite } Al_2Si_2O_7 \xrightarrow{700\text{-}950\ ^\circ C} \text{spinel-like phase } \gamma\text{-}Al_2O_3 + \text{amorphous } SiO_2$$

$$\text{spinel-like phase } \gamma\text{-}Al_2O_3 + \text{amorphous } SiO_2 \xrightarrow{\geq 1100\text{-}1200\ ^\circ C} \text{mullite } Al_6Si_2O_{13} + \text{cristobalite } SiO_2$$

The spinel-like phase has an ordered γ-Al_2O_3 spinel structure with vacancies on octahedral sites (Onike *et al.* 1986, Sonuparlak *et al.* 1987). With the help of this generalised reaction sequence it is now possible to estimate ancient firing temperatures. Thus, ceramic samples containing mullite and cristobalite must have reached at least 1100 °C. Samples showing a mixture between mullite and the spinel-like phase must have experienced temperatures lower than this critical temperature. However, as the mineral formation or transformation of γ-Al_2O_3 and amorphous silica to mullite is a function of the elapsed time also, there is a second way to interpret this data, namely a dwell time too short for a complete transformation of γ-Al_2O_3 and amorphous silica to mullite. Samples characterised by the spinel-like phase only have presumably reached temperatures in the range of 700 °C to 950 °C. Crucible fragments free of mullite but kaolinite also, have a meta-kaolinite rich matrix as recognisable from SEM-EDS investigations. There maximum heat impact is thus limited to a temperature range of 500 °C to 700 °C (Lee *et al.* 2008).

The temperature range higher than 1200 °C is additionally characterised by the growth of secondary mullite (Lee *et al.* 1999). The formation of the latter is caused by a reaction between potassic feldspar and a mullite-rich matrix evoking a growth of elongated and much larger sized acicular mullite needles around partially molten feldspar grains (Lee *et al.* 1999). Such mullite needles were only observed in SEM micrographs of thin-sections of samples from Autun/France (König and Serneels 2013 - Chapter 3), i.e., the largest vessels studied. They must have experienced the highest temperature from a technological point of view as only a major heat impact can cause a complete melting of such a large metal charge in a sufficient time frame. Samples from the other three excavations show only primary mullite and thus slightly lower firing temperatures (König *et al.* - Chapter 6, König in prep. (b) - Chapter 5).

In general, temperatures lower than 900 °C are too low for melting copper-alloys. Thus, there must be an alternative explanation for crucibles indicating such a temperature range, which is caused by a lack of mullite and the spinel-like phase. As the transformation of kaolinite to mullite is a strongly time-dependent reaction (Bellotto *et al.* 1995, Gualtieri *et al.* 1995), it is possible that the total time duration at temperature supporting a formation of the spinel-like phase and mullite was simply too short to produce a detectable amount of this phases. In other words, the crucibles have not stayed long enough within the charcoal bed at temperatures necessary for the melting of the used copper-alloys to initiate a detectable amount of kaolinite dehydroxylation products.

An alternative interpretation for the lack of mullite is related to the primary clay composition (see section about petrographical and mineralogical properties). Illite/smectite rich clays usually produce a high amount of melt fraction within the ceramic matrix during firing as a consequence of their high amount of alkaline and alkaline earth elements. They can inhibit, therefore, the formation of mullite (Ferrari and Gualteri 2006).

Analcime $NaAlSi_2O_6 \cdot H_2O$, a zeolite mineral which is usually formed as a devitrification product during the burial stage, is another mineral which can also be used for temperature estimations. It was often been used in literature to indicate ceramic firing temperatures above 1200 °C, while the total amount of analcime itself seems to be a function of time and temperature (e.g., Buxeda *et al.* 2002, Schwedt *et al.* 2006, Pradell *et al.* 2010).

Cristobalite bearing samples from Autun/France were additionally checked for the $d_{(101)}$ cristobalite peak positions (König and Serneels 2013 - Chapter 3), which also allows temperature estimations as shown by Verduch (1958), Sosman (1965) and Eramo (2005). They state that the crystalline order of cristobalite is increasing with increasing temperature and, thus, extractable from the $d_{(101)}$ cristobalite peak position. The latter shifts to lower d-values as the formation temperatures increase (Verduch 1958, Eramo 2005). The temperature range thereby obtained reaches 1200 - 1400 °C (König and Serneels 2013 - Chapter 3).

7.3 CONCLUSION

The aforementioned results point to a well known and widely used production routine ("chaîne operatoire") for metal-melting crucibles within the Roman Empire. All investigated samples show three diagnostic layers, i.e., an engobe, an inner non-vitrified, ceramic layer and an outer entirely vitrified layer except of some temper remnants. In all cases it was easily possible to separate the inner and the outer layer, which can be explained by adding the outer layer after firing or at least dry the inner layer first. Although both main layers are chemically similar and attributed to a kaolinite bearing clay source, the outer layer is always enriched in calcium and also slightly enriched in other alkali elements (e.g., potassium and sodium). This has been interpreted as coming from an impure calcium-additive, i.e., something similar to marl, marly limestone or even a calcium-rich ash. Chemically, the engobe is composed of equivalent clay. But, this clay was elutriated first and afterwards dispersed along the inner wall/layer of the metal-melting crucibles. This procedure is causal for the micrometre thin layer covering the whole inside. It is impossible to reconstruct if the engobe and the outer vitrified layer have been pre-fired or not before the first use with a metallic charge.

Estimated firing temperatures of the various samples studied differ from excavation to excavation. Crucibles from Autun/France might have reached the highest firing temperature estimated for all analysed samples, i.e., in the range of 1200 °C to 1400 °C as demonstrated by König and Serneels (2013 - Chapter 3). Samples from Xanten/Germany point towards firing temperatures slightly lower than those of Autun/France, i.e., around 1100 °C at highest. Samples from Augst/Switzerland and Avenches/Switzerland indicate similar firing temperatures based on the mineralogical similarities between them and those from Xanten/Germany (König *et al.* - Chapter 6). The range of firing temperatures proposed for the samples from Autun/France is slightly higher than described for metal-melting crucibles in literature (e.g., Tylecote 1982, Freestone 1989, Rehren 2003, Hein *et al.* 2007). This deviation is seen as a direct consequence of the crucibles sizes, i.e., a high metal load causes higher firing temperatures than those reached for small sized crucibles. It is necessary to achieve a higher amount of overheating (= temperature difference between the melting point and the effective temperature) in case of largely sized crucibles than it is the case for small (standard sized) crucibles. Estimated firing temperatures of Xanten/Germany, Augst/Switzerland and Avenches/Switzerland are compatible with the aforementioned references (Tylecote 1982, Freestone 1989, Rehren 2003, Hein *et al.* 2007) as the crucible size therein is much smaller than in Autun/France.

Finally, all mentioned results of this study imply a high state of knowledge in producing metal-melting crucibles and the carefully selection of raw materials, i.e., Roman craftsmen must have had a detailed knowledge of different groups of clays and their refractory character. For sure, the craftsmen had no mineralogical evidences for the differences of their used clays, but it seems probable that they carefully observed the behaviour of these clays and ceramics made out of it during firing and the features caused by a chosen procedure .It has been shown that at four different excavations of Roman settlements in Europe (France, Germany and Switzerland) a pure (in case of Autun/France) respectively an impure (in case of Augst/Switzerland, Avenches/Switzerland and Xanten/Germany) white firing clay (= kaolinitic clay) has been used for the production of metal-melting crucibles and that their interior (= petrographic characteristics) are related to each other, i.e., almost identical temper composed of quartz and feldspar grains and minor amounts of mica, three-parted nature of all crucibles. Therefore, a common Roman recipe for the production of suchlike crucibles seems rather likely, at least within the four settlements studied herein.

	Autun/France [a]	Augst/Switzerland & Avenches/Switzerland [b]	Xanten/Germany [c]
surface and shape properties			
shape and size	• mainly cylindrical with a hemi-spherical base and some of them show a tapering shape to the top • three sizes with a volumetric capacity between 0.3 and 2.2 L, i.e., 2.5 - 19 kg metallic charge	• egg-shaped with a rounded or pointed bottom, the edges are mainly thickened and a little bit retracted • mainly one size 4.5 - 18 cm high and with a volumetric capacity between 50 g and 4 kg metallic charge	• cylindrical shape with a pointed bottom and some of them are retracted on the upper rim • mainly one size 8 to 10 cm high and with a volumetric capacity of 1 to 1.5 kg metallic charge

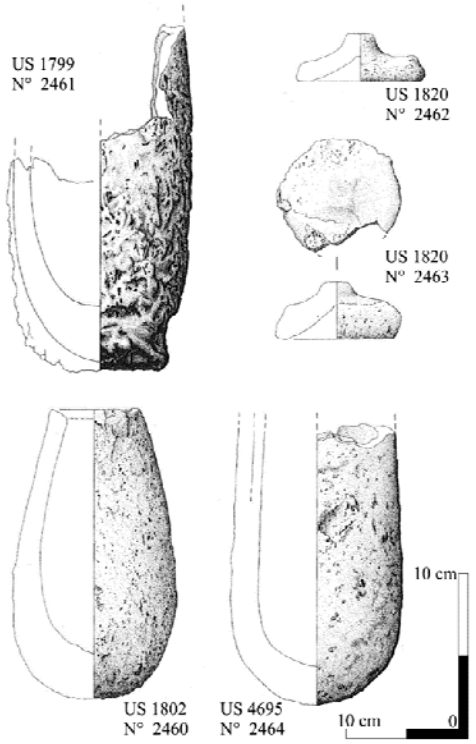

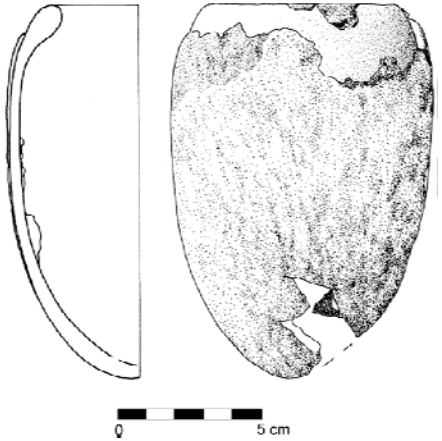

	Autun/France [a]	Augst/Switzerland & Avenches/Switzerland [b]	Xanten/Germany [c]
lids	x	(x)	-
number of layers scale1:1	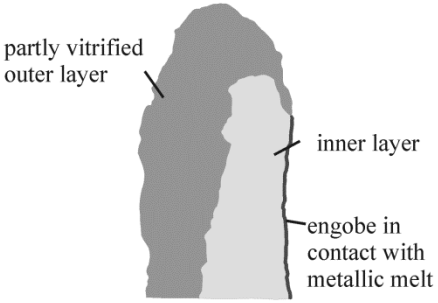	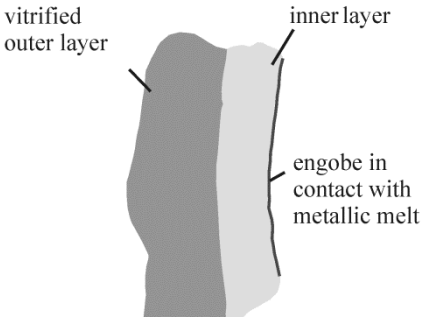	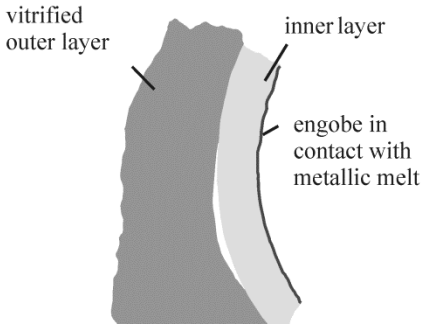
existence of an engobe	x	x	x
repairing traces	x	x	-

petrographical and mineralogical properties

vitrification	engobe and partly the outer layer		engobe and outer layer		engobe and outer layer	
porosity	**i.l.** semi-open porosity	**o.l.** mainly closed porosity with rounded shaped pores	**i.l.** semi-open porosity	**o.l.** closed porosity with rounded shaped pores	**i.l.** semi-open porosity	**o.l.** closed porosity with rounded shaped pores
temper composition	**i.l.** quartz + feldspar + mica	**o.l.** quartz + feldspar	**i.l.** quartz + feldspar + (mica)	**o.l.** quartz + feldspar	**i.l.** quartz + feldspar + (mica)	**o.l.** quartz
shape	**i.l.** angular; feldspar totally molten; micas completely dehydrated	**o.l.** angular; feldspar totally molten	**i.l.** angular; feldspar totally molten; micas completely dehydrated	**o.l.** angular; feldspar totally molten	**i.l.** rounded; feldspar partially molten; micas partially dehydrated	**o.l.** rounded

	Autun/France [a]		Augst/Switzerland & Avenches/Switzerland [b]		Xanten/Germany [c]	
matrix composition	**i.l.** primary mullite and secondary mullite needles + cristoballite + (spinel)	**o.l.** primary mullite + cristobalite + analcime	**i.l.** primary mullite + cristobalite + spinel	**o.l.** primary mullite + cristobalite	**i.l.** primary mullite + cristobalite; in some cases meta-kaolinite instead of mullite	**o.l.** primary mullite + cristobalite + analcime; in some cases meta-kaolinite instead of mullite
interpretation						
used clay material	**i.l.** kaolinitic clay	**o.l.** kaolinitic clay + marly limestone, marl or ash additive	**i.l.** mixture between kaolinitic and illite/smectite clay	**o.l.** mixture between kaolinitic and illite/smectite clay + calcium containing organic material or ash additive	**i.l.** mixture between kaolinitic and illite/smectite clay	**o.l.** mixture between kaolinitic and illite/smectite clay + marly limestone, marl or ash additive
used temper	**i.l. + o.l.** granitic material or something related to that		**i.l. + o.l.** granitic material or something related to that		**i.l. + o.l.** fluviatile or aeolian sediments	
firing temperature	1200 °C up to 1400 °C		around 1100 °C		around 1100 °C	

i.l. - inner layer; **o.l.** - outer layer
[a] König and Serneels 2013; [b] König *et al.* in prep.; [c] König in prep. (b)

Table 7-1 *Comparison between different metal-melting crucibles from France, Germany and Switzerland.*

8 - KERAMISCHE PROBEN AUS DER AUSGRABUNG MARSENS EN BARRAS 1981/86

D. König

part of a research report about Marsens En Barras (Archaeological Service of Fribourg/Switzerland)

ZUSAMMENFASSUNG

Bei den aus der Ausgrabung in Marsens En Barras/Schweiz untersuchten Proben handelt es sich um fünf Schmelztiegelfragmente, drei Fragmente von Brennofenwandungen, einem „Bouchon“ zur Herstellung von Plastiken und neun weiteren keramischen Proben, die nicht genau zugeordnet werden konnten. Die Schmelztiegel können auf Grund der geringen Anzahl der Fragmente und ihrer Größe nicht rekonstruiert werden. Aus diesem Grund ist auch keine Zuordnung der Fragmente zu einem bestimmten Teil der Tiegel möglich. Gleiches gilt für die Bruchstücke der Ofenwandungen, auch bei diesen kann keine Aussage über die Position im eigentlichen Ofen getroffen werden. Alle Bruchstücke wurden mittels Lichtmikroskopie, Rasterelektronenmikroskopie, Röntgenpulverdiffraktometrie und Röntgenfluoreszenzanalyse untersucht.

ABSTRACT

The studied samples from Marsens En Barras/Switzerland are consisting of five metal-melting crucibles, three fragments of oven-walls, one “bouchon” used for making sculptures and nine ceramic samples with unclear relation to its origin. The metal-melting crucibles could not be reconstructed due to the limited amount and size of preserved fragments. Thus, it was not possible to assign them to a specific part of the crucible. For a similar reason, it was not possible to reconstruct the ancient oven with the help of the oven-wall remnants. All fragments were investigated by petrographic microscopy, scanning electron microscopy, X-ray fluorescence and X-ray powder diffraction analyses.

8.1 MARSENS EN BARRAS

Die archäologische Grabung um Marsens En Barras fand zwischen 1981 und 1986 im Rahmen des Autobahnbaues A12 statt. Es handelt sich um eine kleine Handwerkersiedlung die an dem römischen Hauptwegenetz durch das Greyerzer Land lag. Die Siedlung bestand aus rund 10 Gebäuden, die sich von Nord nach Süd an der Straße aufreihten (Meylan Krause und Rossier 2009). Eine Vielzahl der Gebäude wurde von Handwerkern bewohnt, die vorwiegend Eisen verarbeiteten, was mit Hilfe von fast drei Tonnen Schlacke eindrücklich nachgewiesen werden konnte. Darüber hinaus wurden Feuerstellen, Metallabfälle und Werkzeuge aus Stein gefunden. Außerdem konnte mittels

Schmelzresten und Bruchstücken von Gussformen Bronzehandwerk nachgewiesen werden (Meylan Krause und Rossier 2009). Das folgende Kapitel beschäftigt sich mit den keramischen Überresten dieses lokalen Bronzehandwerks.

8.2 MAKROSKOPISCHE BESCHREIBUNG

Die Fragmente der Schmelztiegel weisen makroskopisch eine scheinbare Doppellagigkeit auf. Hierbei erscheint die äußere Lage glasig, die innere Lage ist aus keramischem Material aufgebaut. Die Schmelztiegel wurden, wie es zu römischer Zeit üblich war und anhand der Holzkohleabdrücke eindeutig nachgewiesen werden kann, von außen befeuert. Die innere Oberfläche ist nur in einem der Fragmente in Resten erhalten, sodass deren Aufbau makroskopisch nicht näher beschrieben werden kann. Die Magerung dieser Keramikscherben ist nicht organisch, im Gegensatz zu einer Vielzahl von gefundenen Scherben in dieser Ausgrabung.

Bei den Ofenwandungen handelt es sich um Bruchstücke, welche an der einen Seite eine Schwarzfärbung aufweisen (Innenseite) und auf der anderen Seite (Außenseite) rötlich gefärbt sind. Dies deutet auf ein reduzierendes Milieu im Inneren des Ofens hin, wobei die Außenseite unter oxidierendem Milieu verwendet wurde. Die Bruchstücke der Ofenwandungen zeigen zu einem geringen Teil organische Magerungsreste, die sich wie bei den anderen untersuchten nicht eindeutig zuzuordnenden keramischen Proben zusammensetzt.

Der „Bouchon“, welcher vermutlich zur Herstellung von Teilen einer Plastik verwendet wurde, zeigt einen keramischen Kern. Dieser unterscheidet sich in seiner Zusammensetzung nicht von den anderen untersuchten Proben der Ausgrabung. Die Magerung der Keramik ist wie bei den Schmelztiegeln anorganisch. Das Bruchstück weist am Rand einen schwarzen Überzug auf, welcher magnetisch ist. Dies deutet auf die Herstellung von Überzügen auf Glocken hin.

Die anderen neun untersuchten keramischen Bruchstücke können makroskopisch nochmals unterteilt werden. Eines der Fragmente (N° 96/3074) sticht durch einen violetten Überzug an einer der beiden Seiten hervor. Dieser Überzug befindet sich auf der Seite, die eine stufenförmige Absetzung aufweist. Dieses Stück besitzt nur einen geringen Anteil organischer Magerung. Die anderen acht Fragmente unterscheiden sich makroskopisch nur wenig und weisen allesamt einen Anteil von 30 % organischer Magerung auf.

8.3 ERGEBNISSE DER MATERIALANALYSE

8.3.1 Lichtmikroskopie

Die Tiegelfragmente zeigen unter dem Polarisationsmikroskop einen zweischichtigen Aufbau, welcher durch die bereits beschriebenen Unterschiede in dem Aufbau der Grundmatrix (glasig vs. kristallin/keramisch) bedingt ist. Die Innenseite der Tiegel kann auf Grund der schlechten Erhaltung auch unter dem Lichtmikroskop nicht eindeutig beschrieben werden. Die Magerung besteht vorwiegend aus Quarz und Feldspat, sowie zu geringeren Teilen aus Glimmern. Eine organische Magerung kann in den Tiegelfragmenten nicht nachgewiesen werden. Die Porosität der Keramik ist im Außenbereich, welcher im direkten Kontakt mit der Holzkohle stand, vollständig geschlossen. Hingegen zeigt der innere Bereich eine halb offene Porosität. Dies kann bei allen untersuchten Tiegelfragmenten festgestellt werden. Die Mächtigkeit der beiden optisch und materiell differenzierbaren Bereiche variiert in den Fragmenten zwischen ein Drittel bis zwei Drittel der Gesamtmächtigkeit.

Dünnschliffe der Ofenwandungsfragmente zeigen den gleichen zweifarbigen Aufbau, der bereits makroskopisch beschrieben wurde. Dabei nimmt der unter reduktiven Bedingungen gebrannte Teil der Keramik (schwarz) circa ein Drittel und der oxidativ gebrannte Teil (rot) zwei Drittel der Gesamtdicke ein. Die farblich unterscheidbaren Lagen sind nicht vollständig keramisch, sondern in einigen Bereichen auch glasig aufgebaut, wobei der Anteil an Glas im reduzierten, dem Feuer zugewandten Teil, deutlich höher ist als im Feuer abgewandten Bereich. Die Magerung der Keramik ist nur zu geringen Teilen organisch. Vielmehr findet man, ähnlich wie in den Schmelztiegeln, Quarz und Feldspat als Hauptbestandteil der Magerung. Die Porenräume können als offen bis halb offen beschrieben werden.

Der Rand des im Dünnschliff untersuchten „Bouchon“ zeigt einen ein Millimeter mächtigen schwarzen Überzug. Die keramische Grundmatix besitzt eine Magerung, die sich hauptsächlich aus Quarz zusammensetzt. Organische Partikel sind nicht erkennbar. Die Grundfarbe der Keramik ist grau, was auf einen Brand unter reduktiven Bedingungen hindeutet. Die vorhandenen Poren sind, soweit erkennbar, geschlossen und variieren in ihrer Größe zwischen Submikrometer und mehreren Millimetern.

Die restlichen untersuchten keramischen Fragmente besitzen einen geringen Anteil mineralischer Magerung aus Quarz und Feldspat, allerdings zusätzlichen einen organischen Anteil von bis zu 30 %. Komponenten der organischen Magerung die größer als 0,5 Zentimeter sind, zeigen eine bevorzugte Orientierung die möglicherweise einen Nutzen für die mechanische Stabilisierung hatte (Abb. 8-1). Diese organischen Komponenten weisen in vielen Fällen eine ringartige Internstruktur auf, die an Wachstumsringe von Holz erinnert. Die Porosität ist in allen untersuchen Fragmenten sehr gering (<10 %) und überwiegend halb offen. Nur vereinzelt können größere Poren (2 - 5 Millimeter) beobachtet werden, welche optisch ausgebrannten Pflanzenhäckseln entsprechen. Die Matrix ist vorwiegend gelblich-orange.

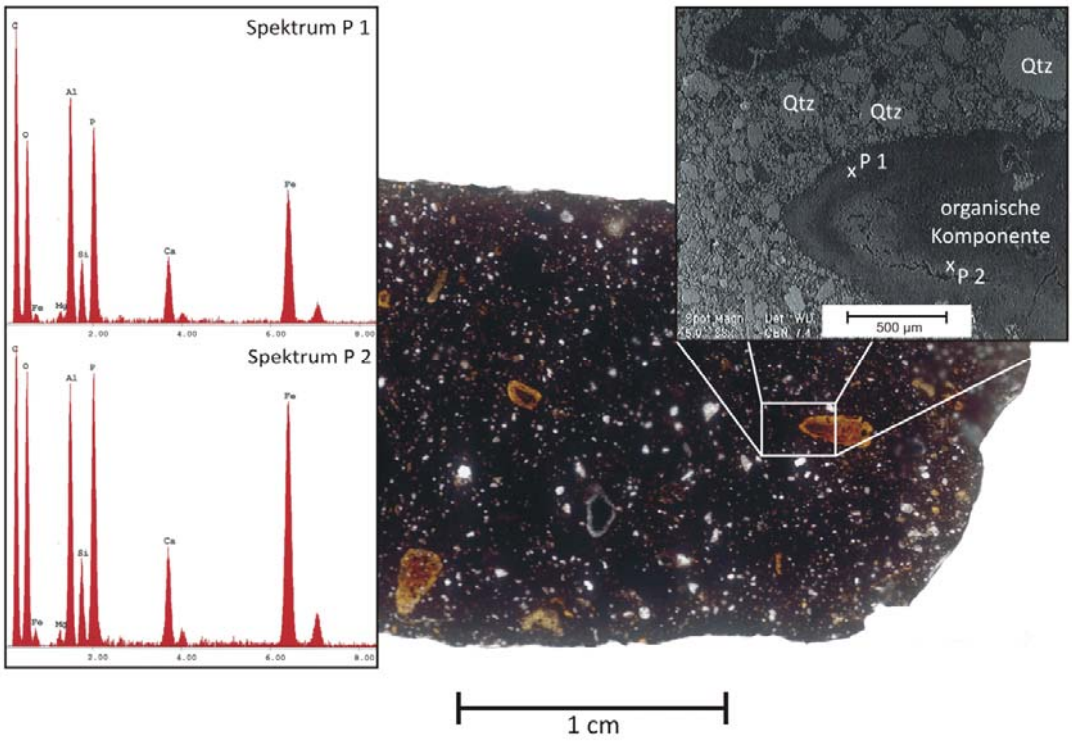

Abbildung 8-1. *Dünnschlifffoto (Ma-Ba N° 678) mit unterschiedlichen organischen Komponenten, welche eine ringartigen Internstruktur zeigen. Eine der Komponenten wurde genauer mittels REM-EDS untersucht.* ***rechts oben:*** *Rückstreuelektronenbild mit organischer Komponente und Quarz (Qtz) als Magerung;* ***links:*** *zwei SEM-EDS Spektren, die die Variabilität in der Zusammensetzung der organischen Komponente, in Abhängigkeit von der Lage, zeigen.*

8.3.2 Rasterelektronenmikroskopie (REM)

Alle Dünnschliffe wurden mit Hilfe des REMs analysiert. Bei den Schmelztiegeln wurde das Hauptaugenmerk auf die Charakterisierung der inneren Oberfläche und damit verbundene Verwendungsspuren gelegt. Die fünf untersuchten Tiegelbruchstücke besitzen einen vergleichbaren Aufbau der Grundmatrix und einen Anteil von circa 50 bis 60 % Magerung, welche sich überwiegend aus Quarz und Feldspat und in geringeren Teilen aus Pyroxen (Augit), Spinell und Glimmern zusammensetzt. Des Weiteren ist erkennbar, dass die Magerung nicht nur aus Einzelmineralen besteht, sondern vielmehr aus Gesteinsbruchstücken, die sich aus Quarz, Feldspat und Glimmern zusammensetzen (Abb. 8-2a). Da die Minerale der Magerung keine hitzebedingten Veränderungen zeigen (z.B. Aufblähen der Zwischenschichten der Glimmer oder Vorhandensein von entwässerungsbedingten Poren) kann man Rückschlüsse auf die maximalen Brenntemperaturen ziehen. In einem der Tiegel ist eine innere Engobe erhalten (Abb. 8-2b), welche vorwiegend mit organischem Material gemagert ist und einige µm mächtig ist. Allerdings konnten in keinem der Tiegel Metallreste nachgewiesen werden, die Rückschlüsse auf die Verwendung zulassen.

Die Fragmente der Ofenwandungen sind in ihrer Zusammensetzung sehr ähnlich den Tiegelfragmenten, sie besitzen eine inhomogene

Matrix, welche in einigen Bereichen glasig ist (Abb. 8-2c). Außerdem besteht die Magerung zu größeren Teilen aus Quarz, Feldspat, Glimmern, sowie aus in geringen Mengen vorhandene Pyroxene (Augit) und Granate (Andradit). Allerdings können auch geringe Anteile einer organischen Magerung nachgewiesen werden.

Der „Bouchon“ zeigt im REM einen eisenreichen Überzug auf der Außenseite und zusätzlich treten erhöhte Eisengehalte an verfüllten Rissstrukturen innerhalb der Keramik auf. Dies deutet auf eine Verwendung im direkten Kontakt mit Eisen hin. Eine Verwendung im direkten Kontakt mit Kupferlegierungen kann somit ausgeschlossen werden. Die Magerung des „Bouchon“ besteht, im Gegensatz zu den anderen für technische Zwecke verwendeten Keramiken, vorwiegend aus Quarz und zu geringen Teilen aus Granat (Andradit). Mit Hilfe des REMs konnten keine Feldspäte und Glimmer nachgewiesen werden. Einerseits kann dies am primären Fehlen dieser Minerale liegen, andererseits kann es als Resultat des Brennvorganges gewertet werden. Organische Magerung konnte für diese Keramik nicht nachgewiesen werden. Die Matrix des „Bouchons“ ist homogen und vollständig verglast, sie zeigt eine geschlossene Porosität. Dies kann als Resultat erhöhter Brenn- bzw. Verwendungstemperaturen gewertet werden.

Die nicht näher klassifizierten keramischen Fragmente weisen eine homogene keramische Grundmatrix auf, welche durch eine organische Magerung (Abb. 8-2d), sowie eine Magerung aus Mineralen und Gesteinsbruchstücken gekennzeichnet ist. Bei den Mineralen bilden Quarz und Feldspat die Hauptbestandteile, es können aber auch Pyroxen (Augit), Glimmer und Granat (Andradit) nachgewiesen werden. Es ist innerhalb der Keramik eine Gleichverteilung der Magerung erkennbar, so dass von einer homogenen Keramik gesprochen werden kann.

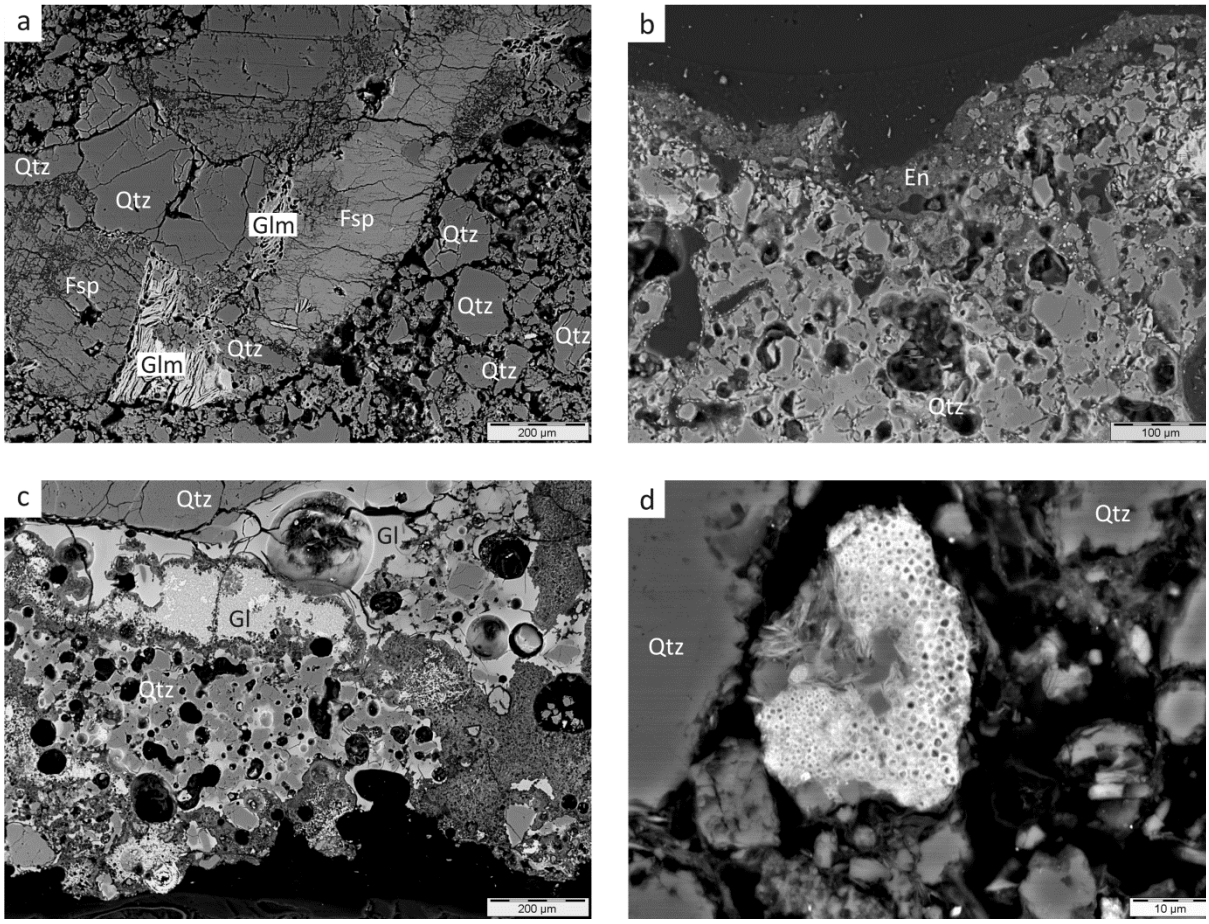

Abbildung 8-2. a) *Gesteinsfragment (Ma-Ba N° 801) in der Magerung, bestehend aus Quarz (Qtz), Feldspat (Fsp) und Glimmer (Glm);* ***b)*** *innere Engobe (En) in dem Schmelztiegel Ma-Ba 359-126;* ***c)*** *glasige Matrix (Ma-Ba 361-120) an der Innenseite der Ofenwandungskeramik - Glas (Gl);* ***d)*** *Pflanzenhäcksel als Magerung zwischen Quarzkörnern (Ma-Ba N° 708).*

8.3.3 Röntgenpulverdiffraktion (RPD)

Die RPD Daten wurden erhoben um die mineralogische Zusammensetzung der Keramiken genauer zu charakterisieren. Dabei wurden von jedem Fragment einige Gramm Probe aufgemahlen und untersucht. Die Resultate sind in Tabelle 8-1 zusammenfassend dargestellt. Diese Ergebnisse decken sich mit den Untersuchungen am REM. Die mit Hilfe von optischen Methoden nachgewiesenen Magerungskomponenten zeigen sich auch in den Diffraktogrammen. Allerdings geben die RPD Daten in den meisten Fällen keinen Hinweis auf die Matrixzusammensetzung. Nur eine Probe (Ma-Ba 361-120/2) besitzt Mullit-Reflexe, welche einen Rückschluss auf Brenntemperaturen und Matrix-zusammensetzungen gestattet. Die Matrix der anderen Fragmente kann mittels dieser Methode nicht genauer beschrieben werden, da diese vermutlich röntgenamorph ist.

Probenbezeichnung	Mineralbestand	Maximale Probendicke (mm)
Schmelztiegel		
359-126	Qtz + Crs + Spl + Ab	17
360-80	Qtz + Crs + Ab + Sa	22
460-27	Qtz + Crs + Spl	16
460-27/2	Qtz + Crs + Spl	10
460-30	Qtz + Crs + Spl	16
Ofenwandungen		
361-119	Qtz + Crs + Aug + Adr + Eisen-Silizium-Oxid	16
361-120	Qtz + Crs + Aug + Adr + Mul	16
361-120/2	Qtz + Crs + Aug + Adr	11
„Bouchon“		
361-114	Qtz + Crs + Adr + Mag	30
Keramische Proben		
N° 96/2646	Qtz + Ab + Aug + Adr + Di	10
N° 96/3074	Qtz + Spl + Aug	12
N° 678	Qtz + Ab + Aug	23
N° 708	Qtz + Ab + Aug	11
N° 715	Qtz + Ab + Aug + Adr	9
N° 718	Qtz + Ab + Spl + Adr	27
N° 722	Qtz + Ab + Aug + Adr	14
N° 750	Qtz + Ab + Sa	31
N° 801	Qtz + Ab + Spl + Adr	30

Mineralabkürzungen: Quarz (Qtz), Cristobalit (Crs), Spinell (Spl), Albit (Ab), Sanidin (Sa), Augit (Aug), Andradit (Adr), Mullit (Mul), Diopsid (Di), Magnetit (Mag)

Tabelle 8-1. *Maximale Probendicke und mineralogische Probenzusammensetzung (Daten mittels RPD erhoben); Gesamtprobendaten, es wurde keine Separation der Lagen durchgeführt.*

8.3.4 Röntgenfluoreszenzanalyse (RFA)

Die RFA Daten wurden von den meisten der keramischen Fragmente erhoben, um eine Vergleichbarkeit der einzelnen verwendeten Materialien für die unterschiedlichen Keramiken zu erhalten. Dabei wird deutlich, dass sich die unterschiedlichen Keramiken in den Anteilen der Hauptbestandteile, sowie der Spurenelemente sehr ähnlich sind (Tabelle 8-2). Allerdings kann man je nach Verwendung der einzelnen Fragmente eine Unterteilung vornehmen.

Die Schmelztiegelfragmente unterscheiden sich in den Hauptbestandteilen (SiO_2, Al_2O_3, Fe_2O_{3tot}, Na_2O, MgO) nicht von den anderen Proben, nur der CaO Gehalt ist im Vergleich zu

den anderen keramischen Proben etwas erhöht. Jedoch ist dieser Gehalt wiederum ähnlich dem der Ofenwandungen. Unter den Spurenelementen fallen Kupfer und Zink in erhöhten Mengen innerhalb der Proben auf. Eine Probe enthält zusätzlich einen erhöhten Zinngehalt. Diese Metallanreicherungen sind als Resultat der Nutzung dieser Schmelztiegel anzusehen.

Die Ofenwandungen besitzen eine sehr ähnliche Zusammensetzung wie die Schmelztiegel, nur die Spurenelemente (Kupfer, Zinn, Zink, Blei) weichen ab. Dies ist allerdings zu einem großen Teil der Verwendung zuzuschreiben.

Der „Bouchon“ besitzt einen leicht erhöhten Fe_2O_{3tot} Gehalt, wie er nur in einer weiteren Probe der normalen Keramiken auftritt. Die Spurenelementgehalte weichen hingegen nicht von denen der normalen Keramiken ab. Somit kann eine Verwendung in direktem Kontakt mit Kupferlegierungen ausgeschlossen werden.

Die restlichen keramischen Proben sind bis auf Probe N° 722 homogen zusammengesetzt. Die Probe N° 722 weist einen deutlich erhöhten Fe_2O_{3tot} Gehalt und einen niedrigeren SiO_2 Gehalt auf. Auch ist dies die einzige Probe mit einem verhältnismäßig hohen Wassergehalt von 8,44 Gew.%.

Das SiO_2-Al_2O_3-CaO+MgO+Fe_2O_3+K_2O +Na_2O Diagramm in Abb. 9-3 zeigt die geringen Unterschiede in der Zusammensetzung der Hauptbestandteile innerhalb der untersuchten Keramikbruchstücke. Das Diagramm bestätigt auf Grund der sehr geringen Variabilität in der Zusammensetzung die Ähnlichkeit der Schmelztiegel- und Ofenwandungsfragmente, sowie dem „Bouchon“. Die Werte der nicht näher charakterisierten keramischen Bruchstücke zeigen infolge ihrer ursprünglichen Verwendung und der damit einhergehenden Materialunterschiede die am stärksten streuende Gruppe innerhalb der Abb. 8-3.

8.4 INTERPRETATION

Ein Ziel dieser Analysen war es, die scheinbare Doppellagigkeit der Schmelztiegelfragmente zu untersuchen und zu beweisen, ob es sich wirklich um komplexe zweilagige Exemplare handelt. Die Untersuchungen haben ergeben, dass sämtliche Tiegel aus nur einer keramischen Lage bestehen, die durch den direkten Kontakt mit der Holzkohle im äußeren Bereich thermisch stärker überprägt wurde, als dies im inneren Bereich der Fall war. Des Weiteren konnte in einem der Tiegel eine innere Engobe identifiziert werden. Die Engobe ermöglicht eine restlose Entleerung des Tiegels ohne den Verlust von Schmelztröpfchen in der offenen bis halb-offenen Porosität der Keramik. Dadurch können nahezu 100 % der geschmolzenen Legierung verlustfrei genutzt werden. Derartige Engoben wurden auch in anderen Schmelztiegeln für die Verarbeitung von Kupferlegierungen nachgewiesen (König und Serneels 2013, Modarressi-Teherani 2004).

Alle im Vorfeld gezeigten Daten weisen auf eine einheitliche Tonquelle hin, die allerdings nicht genauer identifiziert werden kann. Auf Grund des markanten Anteils an Schwermineralen, wie Granat (Andradite) und Pyroxen (Augit), kann auf eine Tonquelle aus der Molasse (tertiäre Sedimente) geschlossen werden, da in dieser der Anteil von derartigen Mineralen höher ist, als in quartären Ablagerungen. Dieser Ton besitzt spezielle Eigenschaften, wie sie für antike „feuerfest Keramiken“ normalerweise notwendig sind. Dazu zählen unter anderem der Al_2O_3-Gehalt, der zwischen 10 und 20 Prozent liegt, und eine Magerung, welche vorwiegend aus Quarz oder anderen Temperatur beständigen Mineralien besteht. Die Magerung der einzelnen Scherben ist bei den untersuchten Stücken eindeutig verwendungsspezifisch, da die Schmelztiegelfragmente, der „Bouchon“ und anteilig die Ofenwandungsfragmente keine

Spuren einer organischen Magerung zeigen. Dies deutet auf ein abgewandeltes Herstellungsverfahren für „Hochtemperatur-keramiken“ im Gegensatz zu den normalen Keramiken in Marsens En Barras hin. Die keramischen Bruchstücke, bei denen kein spezifischer Verwendungszweck nachgewiesen werden konnte, weisen eine organische Magerung von bis zu 30 % auf.

Die organischen Bestandteile, die größer als 0,5 Zentimeter sind und eine orientierte Ausrichtung in einiger der Bruchstücke besitzen, könnten zur Stabilisierung der Keramiken verwendet wurden sein.

Für die Brenntemperaturen der einzelnen Keramiken kann keine einheitliche Aussage getroffen werden. Allgemein ist festzuhalten, dass alle untersuchten Bruchstücke einem thermischen Ereignis ausgesetzt waren (Brennvorgang), da in keiner der untersuchten Probe Tonminerale nachgewiesen werden konnten. Nur eine der Proben zeigte einen geringen Anteil von Mullit, welcher sich aus Kaolinit-reichem Ton beim Brennen über 800 °C bilden kann. Kaolinit wandelt sich bei Temperaturen über 450 °C in Meta-Kaolinit um, welcher röntgenamorph ist und daher mittels RPD nicht nachgewiesen werden kann (Chen und Tuan 2002). Die in einigen Proben nachgewiesene Spinellphase deutet ebenfalls auf eine Kaolinit führende Tonzusammensetzung hin, da bei der Umwandlung von Kaolinit zu Meta-Kaolinit oftmals Spinell als Zwischenphase gebildet wird (Eitel 1966).

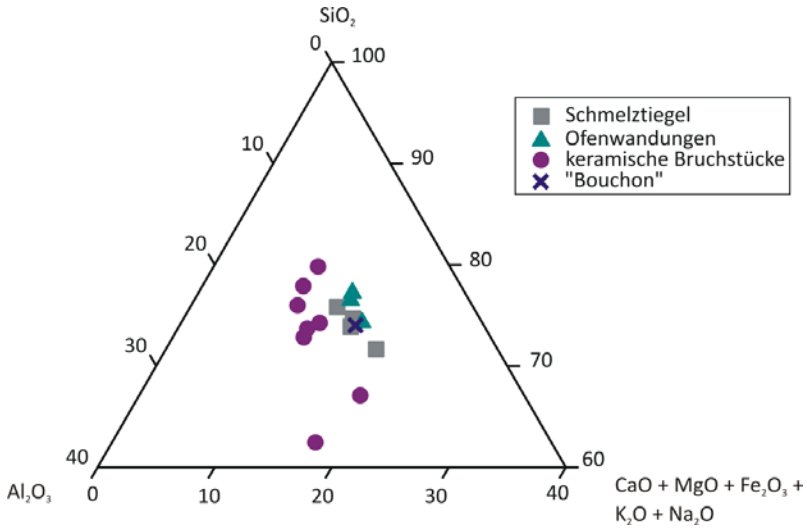

Abbildung 8-3. *Das Dreiecksdiagramm zeigt die Unterschiede in den Hauptbestandteilen der untersuchten keramischen Fragmente.*

Sample	SiO_2 (Gew.%)	TiO_2 (Gew.%)	Al_2O_3 (Gew.%)	Fe_2O_{3tot} (Gew.%)	MnO (Gew.%)	MgO (Gew.%)	CaO (Gew.%)	Na_2O (Gew.%)	K_2O (Gew.%)	P_2O_5 (Gew.%)	Sum norm. (Gew.%)	LOI (Gew.%)	Ba (ppm)	Cu (ppm)	Pb (ppm)	Sn (ppm)	Sr (ppm)	Zn (ppm)
Schmelztiegel																		
359-126	73,7	0,6	10,7	8,2	0,14	1,3	5,2	1,0	2,9	1,9	100	2,1	960	150	<100	<100	170	<100
360-80	78,7	0,7	12,2	7,2	0,18	1,6	3,2	1,1	2,6	1,0	100	1,2	960	120	<100		140	770
460-27	78,0	0,6	11,9	6,2	0,18	1,5	2,1	1,0	2,1	1,7	100	1,9	970	<100	<100		110	140
460-30	77,4	0,6	11,2	6,5	0,15	1,5	3,4	1,0	2,7	0,9	100	0,9	1320	110	<100		140	530
Ofenwandungen																		
361-119	79,9	0,6	10,0	6,4	0,21	1,2	2,7	0,8	2,6	0,8	100	1,5	910	<100	<100		120	<100
361-120	74,5	0,6	10,3	9,1	0,18	1,2	1,7	0,8	2,7	1,2	100	1,9	790	<100	<100		100	<100
361-120/2	77,7	0,6	10,3	5,9	0,19	1,3	2,5	0,9	3,1	0,8	100	1,5	1130	<100	<100		110	<100
„Bouchon"																		
361-114	83,4	0,7	12,4	11,7	0,25	1,4	1,0	1,1	1,8	0,5	100	1,8	450	<100	<100		<100	100
Keramische Proben																		
N° 96/3074	63,4	0,9	20,5	8,1	0,08	3,7	0,9	1,3	3,8	1,1	100	2,1	1440	<100	<100		<100	140
N° 678	69,6	0,6	15,3	4,4	0,15	2,0	2,0	0,8	1,7	2,9	100	4,7	940	<100	<100		110	<100
N° 708	70,1	0,6	13,7	4,0	0,13	1,1	1,2	07	1,6	4,1	100	5,8	1400	<100	<100		130	<100
N° 715	71,9	0,6	13,5	4,4	0,15	1,8	2,6	0,9	1,9	2,6	100	3,7	1420	<100	<100		130	<100
N° 718	83,9	0,6	11,8	4,6	0,20	1,6	1,0	0,9	1,6	0,8	100	2,0	1270	<100	<100		<100	110
N° 722	64,0	0,6	13,4	13,7	0,15	1,5	1,0	0,6	1,4	3,1	100	8,4	1020	<100	<100		<100	<100
N° 750	73,8	0,7	15,3	5,2	0,14	2,3	0,8	0,8	2,1	0,5	100	1,5	900	<100	<100		<100	<100
N° 801	76,7	0,6	13,3	4,3	0,17	1,7	0,5	0,8	1,4	1,0	100	2,6	820	<100	<100		<100	110

Tabelle 8-2. *Semi-quantitative RFA-Analyse der einzelnen Fragmente; grau schattiert - Hauptbestandteile von Kupferlegierungen.*

8.5 SCHLUSSFOLGERUNG

Die aus der Ausgrabung Marsens En Barras untersuchten keramischen Fragmente unterschiedlicher Zuordnung, lassen auf eine lokale Produktion schließen. Diese Annahme wird durch die einheitliche chemische Zusammensetzung der unterschiedlichen technischen Keramiken und Alltagskeramiken gestützt. Die Rezepturen wurden gezielt auf bestimmte Erfordernisse abgestimmt, wodurch anwendungsspezifische Keramiken gefertigt werden konnten. Es wird jedoch deutlich, dass die Schmelztiegel in ihrer Feuerfestigkeit, nicht mit denen größerer römischer Siedlungen oder Legionslager wie in Autun/Frankreich zu vergleichen sind (König and Serneels 2013).

Die Engobe und der glasige äußere Rand der Schmelztiegel lassen darauf schließen, dass die Technologie der Herstellung derartiger Tiegel nicht regional neu entwickelt wurde, sondern als Technologie bereits bekannt war. Durch die geringen Fundmengen keramischen Materials, welches der direkten Verarbeitung von Kupferlegierungen zugeordnet werden konnte, ist eine umfangreiche Verarbeitung von Kupferlegierungen in Marsens En Barras unwahrscheinlich. Vielmehr scheint das Hauptaugenmerk dieser Siedlung auf der Verarbeitung von Eisen zu liegen.

CONCLUSIONS AND PERSPECTIVES

The Ph.D. thesis deals with different types of Roman age technical ceramics, i.e., metal-melting crucibles, brass-making crucibles and lost-wax moulds from different excavation sites in Western and Central Europe. All analysed metal-melting crucibles are characterised by a ceramic structure made of three individual layers, i.e., a vitrified engobe covering the inner part of the crucibles, an inner ceramic layer and an outer vitrified layer. Brass-making crucibles are built up of an engobe and one main ceramic layer with an added second layer in the upper part of the vessel in order to fix the lid on top of the crucible. Moulds, in contrast, possess one single ceramic body only with a very fine clay cover in direct contact with the metal artefact.

It was possible to acquire a detailed knowledge about the clay material used as inferred from the present day mineral composition within the matrix. Thus, the clay used to build up the technical ceramics is refractory in nature, i.e., kaolinite-rich or at least kaolinite containing. Samples from Autun/France are extraordinary rich in primary and secondary mullite as due to a clay material very rich in kaolinite minerals. Such a clay source is linked to the geological setting of Autun/France which is rich in granitic and rhyolitic rocks as well as their weathering products, i.e., kaolinitic clay. All other investigated technical ceramics are less rich in mullite. Chemical data point to a clay mixture of kaolinite plus an illitic/smectitic component. The only exception is Marsens En Barras/Switzerland which clearly point to local Molasse sediments which are lacking in kaolinite.

The comparison of the chemical and mineralogical characteristics of individual layers of the metal-melting crucibles studied revealed relevant differences. The outer layer as well as the engobe is always enriched in calcium compared to the inner one. Such a chemical commonality is not formed by chance, but the deliberately change of the raw materials properties. This chemical difference causes the high degree of vitrification and the closed porosity of the outer layer, respectively. A calcium-rich additive, e.g., marly limestone, marl or ash additive, added to the inner layer clay seems to be causal for this glassy texture.

The added temper material always consists of quartz, feldspar and a provably lower amount of mica. There sharp edged nature is evident in all studied fragments except of those coming from Xanten/Germany which are rounded. This feature has been interpreted as coming from an actively selected and added raw material, either produced by crushing a granitic rock or collecting disintegration products of the latter. Samples from of Marsens En Barras/Switzerland additionally have organic temper within the ceramic matrix.

Summing up, it is possible to deduce advanced technological skills and a high state of knowledge regarding a carefully selection of raw materials in order to guarantee a high-temperature stability, the effect of adding fluxes to produce requested material properties and to avoid metal loss due to the porous structure of the main ceramic layer.

On base of the aforementioned findings it is possible to suggest a main recipe for the

production of Roman metal-melting crucibles and, therefore, an exchange or transfer of knowledge between larger settlements within a part of the Roman Empire.

This study also shows for the first time that the Romans were able to construct refractory ceramics in an “industrial way”. In this context it is necessary to state that the estimated firing temperatures of ceramics from Autun/France (up to 1400 °C) are slightly higher than usual for this period considering the literature present. All other investigated crucibles point to firing temperatures of around 1100 °C and, thus, situated in a range often mentioned in former studies.

Some of the probed excavation sites (Autun/France and Avenches/Switzerland) show clear evidences for a multiple use of crucibles as deduced from doubled outer layers and a largely varying metal droplet composition within single crucibles.

Further studies will be necessary to compare other Roman metal-melting crucibles with the herein comprehensively studied ones in order to confirm a common Roman recipe for making similar technical ceramic herein discussed. Future studies should also incorporate analytical work on the large brass-making crucibles from Lyon/France as they are macroscopically similar to those of Autun/France. Especially the idea of trading crucibles between individual settlements should be examined in more detail as a common recipe requires technological skills and raw materials which are not present everywhere. Additionally, it would also be useful to compare Roman vessel finds and their interior with those of modern replica made by experimental archaeologists. Moreover, it can help to get a feeling how difficult it is to produce such crucibles with the required ceramic properties by using only simple firing techniques.

APPENDIX 1 - PETROGRAPHISCHE UND GEOCHEMISCHE BESCHREIBUNG RÖMISCHER SCHMELZTIEGEL IN BEZUG AUF VERGLEICHBARKEIT UND TONHERKUNFT

BEISPIELE AUS AUGUSTA RAURICA (AUGST/BL UND KAISERAUGST/AG) UND AVENTICUM (AVENCHES/VD)

König, D. (mit einem Beitrag von Alex R. Furger)

planned for „Jahresberichte aus Augst und Kaiseraugst 2015“

ZUSAMMENFASSUNG

Ein Teil der ausgegrabenen Schmelztiegel aus Augusta Raurica (Augst/BL und Kaiseraugst/AG) welche für das Einschmelzen von Kupferlegierungen Verwendung fanden, wurden im Vergleich zu augenscheinlich ähnlichen Schmelztiegeln aus Aventicum (Avenches/VD) untersucht. Dabei galt ein besonderes Interesse der Anzahl der keramischen Lagen und deren chemischer Zusammensetzung. Auch sollte mithilfe der durchgeführten Untersuchungen geklärt werden, welche Brenntemperaturen, entweder als Erstbrand oder als Verwendungstemperaturen, für die Schmelztiegel angenommen werden können. Außerdem ging es in den Untersuchungen darum eine Handelsbeziehung zwischen beiden römischen Städten zu diskutieren und mögliche Quellen für die Tiegelproduktion zu identifizieren oder zumindest einzugrenzen. Des Weiteren war es wichtig, eventuelle Unterschiede in den fein gemagerten und in den grob gemagerten Schmelztiegeln zu untersuchen und verschiedenen Quellen respektive Tiegelmanufakturen zuzuordnen. Diese Zuordnung der Tongruppen respektive Quellen basiert auf früherer Untersuchungen im Umkreis von Augst und auf portablen XRF Daten von Markus Helfert.

ABSTRACT

This article deals with a part of excavated metal-melting crucibles from Augusta Raurica (Augst/BL und Kaiseraugst/AG) in comparison to optically similar metal-melting crucibles from Aventicum (Avenches/VD). The main focus was set on the identification of ceramic layers and their chemical composition. This study also aims to estimate firing temperature, either in terms of pre-firing temperature or final using temperature. Geochemical analyses were made in order to examine probable trading connections between both Roman settlements. There is a special focus on the identification or at least a better description of raw materials used in order to define the kind or group of clay(s) used. Here, it was also important to clarify and illustrate differences between crucibles showing fine and coarse grained temper, respectively, to distinguish between individual sources and different crucible manufacturers. The comparison of clay groups and sources, respectively, is the result of earlier investigations in the vicinity of Augst and the portable XRF analyses done by Markus Helfert.

1.1 EINLEITUNG

Die in diesem Artikel untersuchten Tiegelfragmente entstammen zwei unterschiedlichen Ausgrabungen römischer Städte in der Schweiz (Abb. A1-1), zum Einen Augusta Raurica (Augst/BL und Kaiseraugst/AG) und zum Anderen Aventicum (Avenches/VD).

In Augusta Raurica konnte belegt werden, dass die kleineren Schmelztiegel vorrangig im frühen 1. Jahrhundert sowie im 2. bis 3. Jahrhundert n.Chr. auftraten. Größere Schmelztiegel traten erst ab dem späten 2. Jahrhundert n.Chr. in größerer Stückzahl in Erscheinung. Ein Import von Tiegeln kann ebenfalls belegt werden, wobei dessen Höhepunkt in der ersten Hälfte des 3. Jahrhunderts n.Chr. erreicht wurde.

Abbildung A1-1. *Geographische Lage von Augusta Raurica (Augst/BL und Kaiseraugst/AG) und Aventicum (Avenches/VD).*

1.2 DAS UNTERSUCHTE TIEGELMATERIAL

ALEX R. FURGER

1.2.1 Auswahlkriterien

Die 893 Tiegelfragmente von Augusta Raurica (Abb. A1-2) sind grösstenteils formal sehr einheitlich. In der Grundform sind sie eiförmig mit spitzem bis verrundetem Boden und haben einen leicht eingezogenen, oftmals innen verdickten Rand. Diese als «Augster Normaltypus» bezeichnem Stücke sind ausnahmslos auf der Scheibe getöpfert und machen 95,2 % des Gesamtbestandes aus (Katalognummern **T1** bis **T850**). Einige ebenfalls scheibengedrehte Tiegel (Katalognummern **T851**–**T864**) haben abweichende Ränder respektive Böden.

Eine Sondergruppe bilden kleine, handgemachte «Schälchentiegel» (**T865**–**T871**). Sie machen nur 0,8 % des Gesamtbestandes aus. Hinzu kommen noch einige wenige Tiegeldeckel (**T875**–**T883**), die speziellen Prozessen, etwa der Messing-Zementation, vorbehalten waren. Die Katalognummern **T872**–**T874** und **T884–T893** sind Varia und Unbestimmbares.

Für die hier vorgelegten naturwissenschaftlichen Untersuchungen wurden der Autorin 15 Individuen aus Augusta Raurica im Juni 2012 zur Verfügung gestellt. Bewusst konzentrierten wir uns dabei auf Tiegel des Normaltypus, versuchten aber, verschiedene Tongruppen und Tiegelgrössen zu berücksichtigen. Wegen musealer Kriterien kamen nur fragmentierte Stücke in Frage, von denen problemlos und nach fotografischer Dokumentation (Abb. A1-3) ein Teilstück für zerstörende Analysen abgesägt werden durfte. Alle diese Tiegel wurden parallel auch von Markus Helfert mit der p-RFA bezüglich Tonen, Lutum und Metallresten untersucht (Furger in prep. 1).

Die Augster Stücke kamen als letzte Serie in das Tiegelprojekt der Autorin. Aus der römischen Stadt Aventicum (Avenches/VD) standen schon vorher zehn Tiegelfragmente zur Verfügung (Abb. 8-4). Sie wurden nach ähnlichen Kriterien wie die Augster Probengruppe vom Team des Musée Romain in Avenches herausgesucht und durch Vermittlung von Vincent Serneels für das Archäometrieprojekt von D. König ausgeliehen.

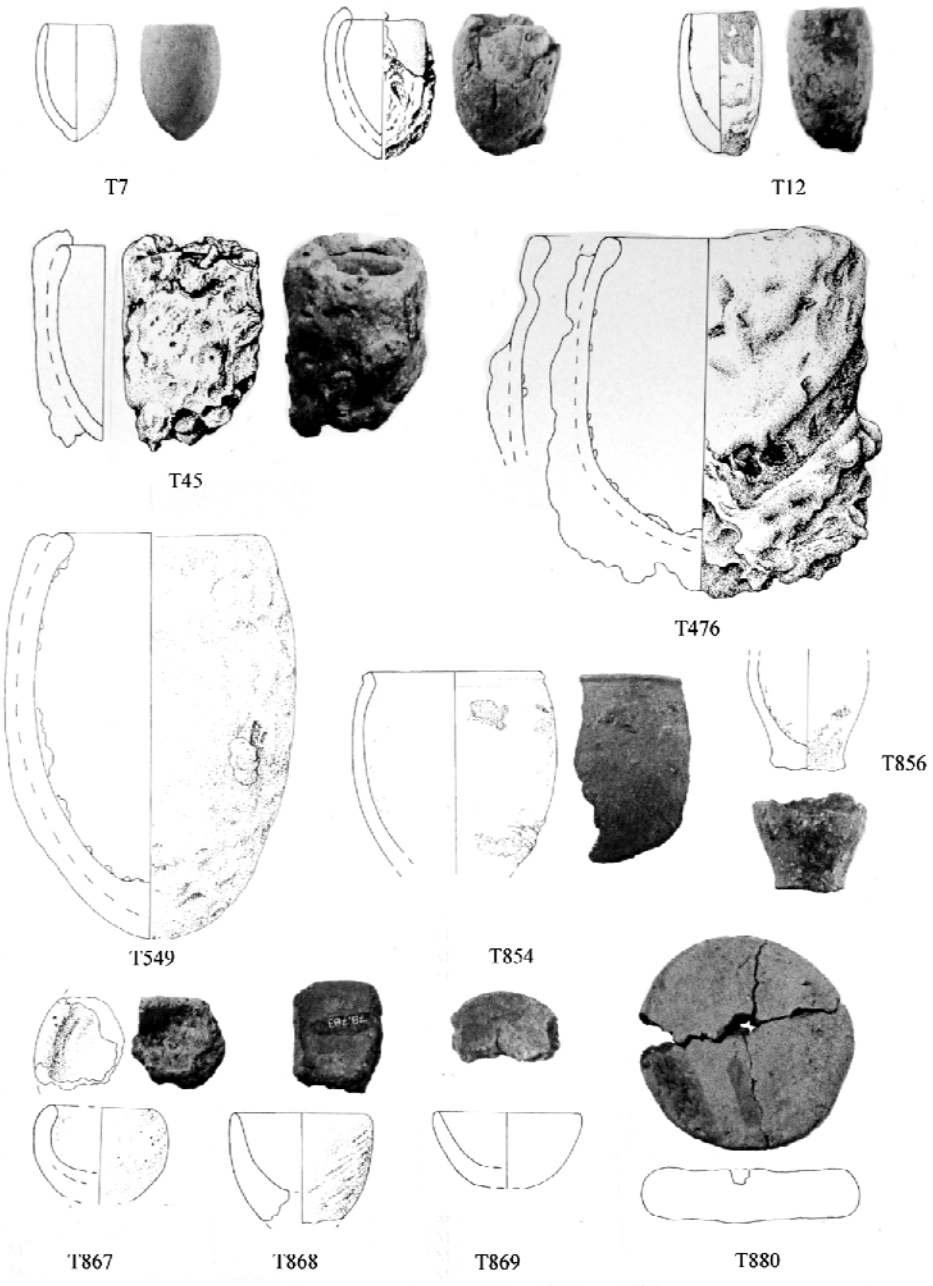

Abbildung A1-2. *Kleine Auswahl römischer Schmelztiegel aus Augusta Raurica. Die Katalognummern* ***T1*** *bis* ***T850*** *sind formal sehr einheitlich und werden als «Augster Normaltyp» bezeichnet;* ***T851***–***T864*** *haben abweichende Ränder resp. Böden,* ***T865***–***T871*** *werden als Schälchentiegel bezeichent und* ***T875***–***T883*** *sind Deckel. M. 1:2.*

1.2.2 Katalog der analysierten Schmelztiegelfragmente aus Augusta Raurica

Von den 893 Augster Tiegeln (Auswahl Abb. A1-2) standen der Autorin nur 15 Exemplare für ihre archäometrischen Untersuchungen zur Verfügung (Abb. A1-3). Die beiden Tiegel **T128** und **T168** sind ungebraucht und stammen aus einem grösseren Händlerdepot in Insula 19 mit einem engem Formen- und Grössenspektrum (Furger in prep. 1, Furger in prep. 3). Alle hier in Analysen vorgestellten Tiegel aus Augusta Raurica sind scheibengedreht und gehören zum «Augster Normaltypus» (Abb. A1-2, **T7**–**T549**):

1960_02066L_a: RS eines grossen Schmelztiegels, Ton hellgrau, sandig; Rand innen verdickt; Oberfläche innen am Rand Lehmflecken, innen anthrazitfarben, innen an der Wandung Spritzer (grün), aussen Lutum, oben am Rand horizontal abgestrichen. Die Lutumoberfläche ist sauber abgearbeitet und zeigt keine Bruchstruktur eines «angeklebten» Deckels oder dergleichen.

(Katalognummer Furger **T503**) Fundkomplex V03648; Grabung 1960.051, Insula 30 («Schicht 1 Profil C-D Kiste 1»). – FK-Datierung: um 240–260. – p-RFA-Analysen (Furger in prep. 1) Tiegelkeramik: wahrscheinlich Tongruppe 1; Lutum: Tongruppe 2 (3 Messungen). - Metallspuren: Zn.

1963_01576_c:WS eines mittelgrossen Schmelztiegels, Ton hellgrau, fein; Oberfläche innen mit Spritzern und Metalltröpfchen, oben gelbliche Verglasung, aussen Lutum.

(Katalognummer Furger **T231**) Fundkomplex X02519; Grabung 1963.053, Insula 18 («Verschmutzter grauer Lehm: S21/29»). – FK-Datierung: um 30–50. – p-RFA-Analysen M. Helfert: Tiegelkeramik: wahrscheinlich Tongruppe 1. – Metallspuren: Cu+++ (3 Messungen), Sn+, Pb (2 Messungen), Zn+++ (3 Messungen), Au, Hg (2 Messungen).

1963_04791E_b: WS eines grossen Schmelztiegels, Ton hellgrau, sandig; Oberfläche innen mit hart verschlackter Kruste (schwarz), darunter grösserer Bronze(?)-Tropfen, aussen Lutum.

(Katalognummer Furger **T548**) Fundkomplex Y00835; Grabung 1963.054, Insula 31 («S 34/35, S 46/37»). – FK-Datierung: offen. – p-RFA-Analysen M. Helfert: Tiegelkeramik: Tongruppe 1; Lutum: wahrscheinlich Tongruppe 3 (2 Messungen). – Metallspuren: Cu++, Zn+++, Hg+, MnO+ (Tabelle £27£). – Metalltropfen (Modus «alloy»): Zinn-Bleimessing.

1963_04726_a: 2 WS eines grossen Schmelztiegels, Ton hellgrau, sandig; Oberfläche innen naturbelassen (bläulichgrau), aussen Lutum.

(Katalognummer Furger **T673**) Fundkomplex Y00720; Grabung 1963.054, Insula 31 («S 30/31/30a/31a, S42/43 Sondierschnitt»). – FK-Datierung: um 150–230. – p-RFA-Analysen M. Helfert: Tiegelkeramik: Tongruppe 1; Lutum: wahrscheinlich Tongruppe 3 (2 Messungen).

1963_04791D_a: 2 WS eines grossen Schmelztiegels, Ton hellgrau, sandig, stark aber fein gemagert; Oberfläche innen bläulichgrau, Spritzer (Bronze), aussen Lutum.

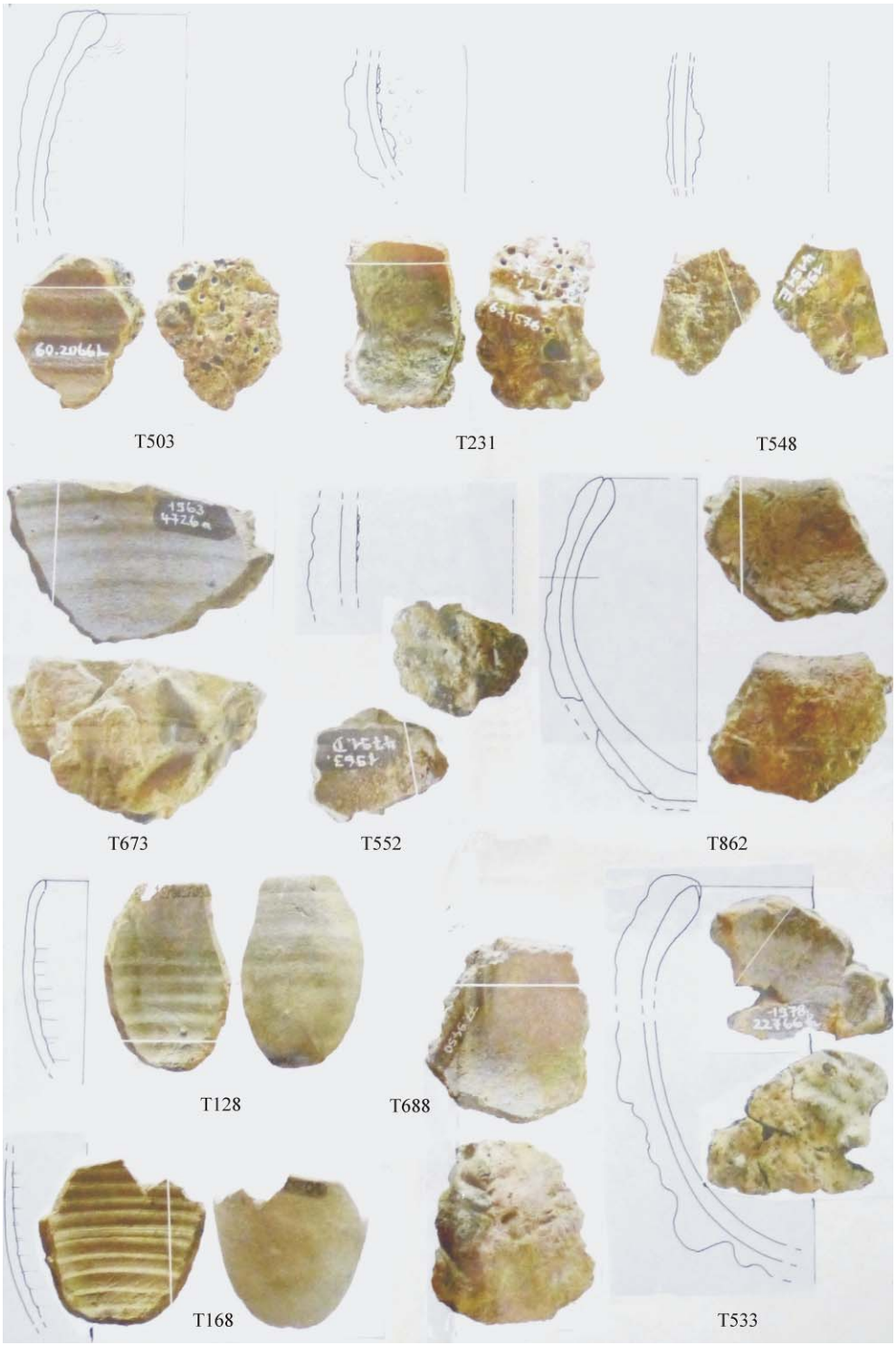

Abbildung A1-3. *Analysierte Tiegelfragmente aus Augusta Raurica (Augst/BL und Kaiseraugst/AG), sortiert nach Inventarnummern (Museums Augusta Raurica; Suffixe wie «_a» geben die Probennummer an). Fette Zahlen in Klammern = Katalognummern (Furger* in prep. *1). Die weissen Linien zeigen die Sägeschnitte zur Probenentnahme; das jeweils kleinere Teilstück stand für die Analysen zur Verfügung. M. 1:2.*

*1960_02066L_a (**T503**)*
*1963_01576_c (**T231**)*
*1963_04791E_b (**T548**)*
*1963_04726_a (**T673**)*
*1963_04791D_a (**T552**)*
*1968_06215_c (**T862**)*
*1970_05202_c (**T128**)*
*1970_05206_c (**T168**)*
*1977_09450_b (**T688**)*
*1978_22766_b (**T533**)*
*1978_22766B_d (**T454**)*
*1978_24279_a (**T262**)*
*1978_24280_a (**T230**)*
*1979_18596_c (**T289**)*
*1984_10803_c (**T225**)*

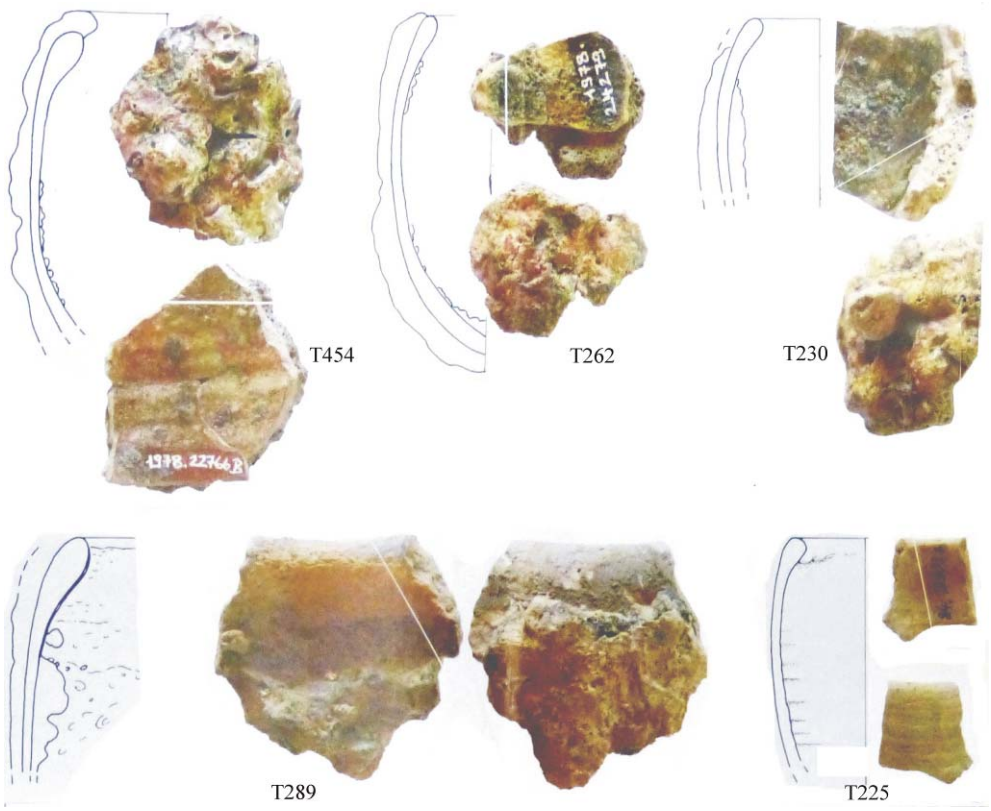

Abbildung A1-3. *Fortgesetzt.*

(Katalognummer Furger **T552**) Fundkomplex Y00835; Grabung 1963.054, Insula 31 («S 34/35, S 46/37»). – FK-Datierung: offen. – p-RFA-Analysen M. Helfert: Tiegelkeramik: Tongruppe 1; Lutum: wahrscheinlich Tongruppe 2 (2 Messungen).

1968_06215_c: RS und 8 WS (nicht anpassend) eines mittelgrossen Schmelztiegels, Höhe ca. 130 mm, Randdurchmesser 85 mm; Ton dunkelgrau, viele grössere Quarzkörner; Oberfläche innen dunkelgrau, stellenweise mit brauner Lehm-Auflage, aussen Lutum. Der Gefässkörper ist stark verzogen, der Rand innen verdickt, Boden aussen abgeflacht (Durchmesser 27 mm; innen rund; sehr kleine Standfläche).

(Katalognummer Furger **T862**) Fundkomplex A00094; Grabung 1968.053, Insula 43 («sandig, grau, ocker, Mörtel, Kies: S27/T27»). – FK-Datierung: um 80–120 (wenig Material). – p-RFA-Analysen M. Helfert: Tiegelkeramik: Tongruppe 5; Lehmkruste innen: wahrscheinlich Tongruppe 3 (3 Messungen).

1970_05202_c: RS und WS eines kleinen Schmelztiegels, Boden eiförmig-spitz, Ton beige-grau, fein; Oberfläche innen und aussen naturbelassen, deutliche Drehrillen.

(Katalognummer Furger **T128**) Fundkomplex A01959; Grabung 1970.053, Insula 19 («R6/R7/R8/R9»). – FK-Datierung: offen . – p-RFA-Analysen M. Helfert: Tiegelkeramik: Tongruppe 1.

1970_05206_c: WS eines kleinen Schmelztiegels, Boden eiförmig-spitz; Ton beige-grau, fein; Oberfläche innen und aussen naturbelassen.

(Katalognummer Furger **T168**) Fundkomplex A01959; Grabung 1970.053, Insula 19 («R6/R7/R8/R9»). –

FK-Datierung: offen. – p-RFA-Analysen M. Helfert: Tiegelkeramik: Tongruppe 1.

1977_09450_b: WS eines grossen Schmelztiegels, Ton dunkelgrau, mit vielen groben Quarzkörnern; Oberfläche innen fleckig (grau bis rötlichbraun), aussen Lutum.

(Katalognummer Furger **T688**) Fundkomplex B00246; Grabung 1977.052, Insula 31 («N11/N12/O12/O13»). – FK-Datierung: um 30–130. – p-RFA-Analysen M. Helfert: Tiegelkeramik und Lutum: wahrscheinlich Tongruppe 3; innere Engobe: wahrscheinlich Tongruppe 4 (3 Messungen). – Metallspuren: Cu++.

1978_22766_b: 2 RS und 15 WS eines grossen Schmelztiegels, Rand innen verdickt; Ton hellgrau, (im Bruch hellbraun), fein; Oberfläche innen an der Wand bläulichgrau, im Bodenbereich dunkelgrauer dünner Überzug: unten glatt und seitlich mit vertikalken Striemen eines Werkzeugs, aussen Lutum, über den Rand nach innen verstrichen. (Die Striemen sind offenbar Spuren vom Wegkratzen der Messingschlacken nach einem Zementationsprozess. Die Striemen reichen unten nur bis auf eine gewissen Höhe und lassen den Boden frei; ein Regulus-Abruck im Tiegelboden ist allerdings nicht erkennbar.)

(Katalognummer Furger **T533**) Fundkomplex B01781; Grabung 1963.054, Insula 31 (R17/S16–S18/T15–T18/U15–U18/V17»). – FK-Datierung: um 125–175. – p-RFA-Analysen M. Helfert: Metallspuren (am markanten dunkelgrauen Überzug innen): Cu++, Zn+++ (3 Messungen), Hg.

1978_22766B_d: 2 RS und 8 WS eines grossen Schmelztiegels, Rand innen verdickt, Durchmesseer 76 mm; Ton hellgrau, fein; Oberfläche innen: Glasur (rotbraun), innen an der Wand Spritzer, aussen Lutum (bis 6 mm hoch über den Rand verlaufend).

(Katalognummer Furger **T454**) Fundkomplex B01781; Grabung 1978.052, Insula 31 («R17/S16–S18/T15–T18/U15–U18/V17»). – FK-Datierung: um 125–175. – p-RFA-Analysen M. Helfert: Tiegelkeramik: Tongruppe 1 – Metallspuren: Cu++ (4 Messungen), Zn++, Au, Hg.

1978_24279_a: 5 RS, 5 WS und 1 BS eines grossen Schmelztiegels, Höhe ca. 118 mm, Randdurchmessser 53 mm, Rand innen verdickt, Boden eiförmig-spitz; Ton hellgrau, weich verbrannt; Oberfläche: innen grünlicher Belag, Bronzespritzer, aussen Lutum. In der äusseren Lutumschicht 40 mm lange und 4 mm breite, geradlinige Kerbe (Eindruck).

(Katalognummer Furger **T262**) Fundkomplex B01611; Grabung 1978.052, Insula 31 («U18/V18/V19/W18/W19»). – FK-Datierung: um 190–250. – p-RFA-Analysen M. Helfert: Tiegelkeramik: Tongruppe 1. – Metallspuren: Cu++ (2 Messungen), Sn+ (2 Messungen), Zn+ (2 Messungen).

1978_24280_a: 2 RS eines mittelgrossen Schmelztiegels, Ton hellgrau, fein, Rand einfach verrundet; Oberfläche innen am Rand anthrazit, innen in der Wandung mit dickem Belag (sandiges Gemisch, mit viel Bronzetropfen), aussen Lutum.

(Katalognummer Furger **T230**) Fundkomplex B01611; Grabung 1978.052, Insula 31 («U18/V18/V19/W18/W19»). – FK-Datierung: um 190–250. – p-RFA-Analysen M. Helfert: Tiegelkeramik: Tongruppe 1. – Metallspuren: Cu+, Sn+, Zn+++.

1979_18596_c: RS und WS eines mittelgrossen Schmelztiegels, Randdurchmesser ca. 100 mm, Rand innen verdickt; Ton hellgrau, sandig; Oberfläche innen am Rand lehmiger Belag (braun), innen in der Wandung dicker Bronzebelag (Füllung ca. 2/3 des Tiegels), aussen Lutum.

(Katalognummer Furger **T289**) Fundkomplex B03172; Grabung 1979.054, Insula 29 («J13/J14/H13/H14»). – FK-Datierung: um 150–210. – p-RFA-Analysen M. Helfert: Tiegelkeramik: Tongruppe 1. – Metallspuren: Zn+++ (2 Messungen). – Zwei Bronzetropfen (Bohrproben): Zinnmessinge (Modus «alloy»).

1984_10803_c: 3 RS eines mittelgrossen Schmelztiegels, Randdurchmesser 52 mm, Rand innen verdickt, sehr schlank (Wanddurchmesser 58 mm), Ton hellgrau, sandig; Oberfläche innen am Rand naturbelassen, inen in der Wandung dünne Glasurflecken (gelb-grünlich), aussen naturbelassen. Innen deutliche feine Drehrillen.

(Katalognummer Furger **T225**) Fundkomplex C00825; Grabung 1984.051, Insula 36 («H'8/H'9/J'8/J'9»). – FK-Datierung: offen. – p-RFA-Analysen M. Helfert: Tiegelkeramik: Tongruppe 1. – Metallspuren: Pb, Ag, As.

1.2.3 Katalog der analysierten Schmelztiegelfragmente aus Aventicum

Mit Ausnahme der bekannt gewordenen Giesserei für Grossbronzen (Morel und Chevalley 2001) sind aus Avenches/VD bisher erst relativ wenige Spuren und Funde aus Bronze verarbeitenden Werkstätten bekannt geworden (Bögli 1996). Der Fundbestand von Avenches bezüglich Schmelztiegel scheint weit geringerer als jener von Augst/Kaiseraugst zu sein. Dennoch springt die extrem grosse Ähnlichkeit der Tiegel beider Fundorte ins Auge: Die Stücke sind optisch austauschbar und würden am jeweils anderen Fundort nicht auffallen. Im Gegensatz zu den anderen Tiegelserien im Untersuchungsmaterial der Autorin – jenen aus Autun/Frankreich und Xanten/Deutschland – lassen sie keine orts- respektive regionsspezifischen Eigenheiten in Form, Keramik oder Lutum erkennen. Die Bronzegiesser in Augusta Raurica und ihre Kollegen in Aventicum benutzten Schmelztiegel derselben Machart.

Aus dem Avencher Tiegelbestand wurden der Bearbeiterin folgende zehn Exemplare zur Analyse zur Verfügung gestellt (Abb. A1-4). Alle Stücke sind scheibengedreht:

Inv. MRA 67/5437: WS/BS eines mittelgrossen Schmelztiegels; Ton im Bruch innen hellgrau und aussen grau, fein; Oberfläche innen wenig verkrustet, aussen sehr dickes Lutum, aufgetragen in zwei deutlichen separaten Schichten von 6 mm respektive ca. 11 mm.

(Probennummer D. König: 67/5437[1]) Fundkomplex K3434; Grabung 1967.06, Insula 8 («carrés N 10-14 ; terre végétale, surface»). – FK-Datierung: 1.–3. Jh.

Inv. MRA 67/8442: Vertikales Teilstück eines kleinen Schmelztiegels, Rand spitz-verrundet, unten spitz zulaufend, Höhe ca.

65 mm (ohne Lutum), Randdurchmesser ca. 45 mm; Ton grau und stark blasig verbrannt (mit feiner Rissbildung im Innern), sandig; Oberfläche innen völlig verbrannt, aussen Lutum.

(Probennummer D. König: 67/8442) Fundkomplex K3270; Grabung 1967.01, Insula 20 («couche d'occupation»). – FK-Datierung: um 50–80/100 n. Chr.

Inv. MRA 67/8519: Vertikales Teilstück eines kleinen Schmelztiegels, Rand verrundet, unten spitz zulaufend, Höhe ca. 70 mm (ohne Lutum), Randdurchmesser ca. 40 mm; Ton dunkelgrau, porös und weich verbrannt, sandig; Oberfläche innen ausgeglüht, aussen Lutum, das fast 20 mm über den Rand hinaus reicht (Abdrücke eines Deckels nicht sichtbar; Funktion des Lutum-Überstads unklar).

(Probennummer D. König [Inv. abweichend, aber im selben Fundkomplex]: 67/8515) Fundkomplex K3273; Grabung 1967.01, Insula 20 («carrés R-U 14-15; terre végétale, surface»). – FK-Datierung: um 50–250.

Inv. MRA 67/9918: Boden eines mittelgrossen Schmelztiegels; Ton hellgrau (im Bruch gelblich), fein; Oberfläche innen mit einer 1–4 mm dicken anthrazitfarbenen Schicht überzogen, darin Bronzespritzer und -tröpfchen, aussen dünnes glattes Lutum.

(Probennummer D. König: 67/9918) Fundkomplex K3294; Grabung 1967.01, Insula 20 («carrés R-U 15-16 ; surface, terre végétale»). – FK-Datierung: um 70–250 (1 Fragment 40–80).

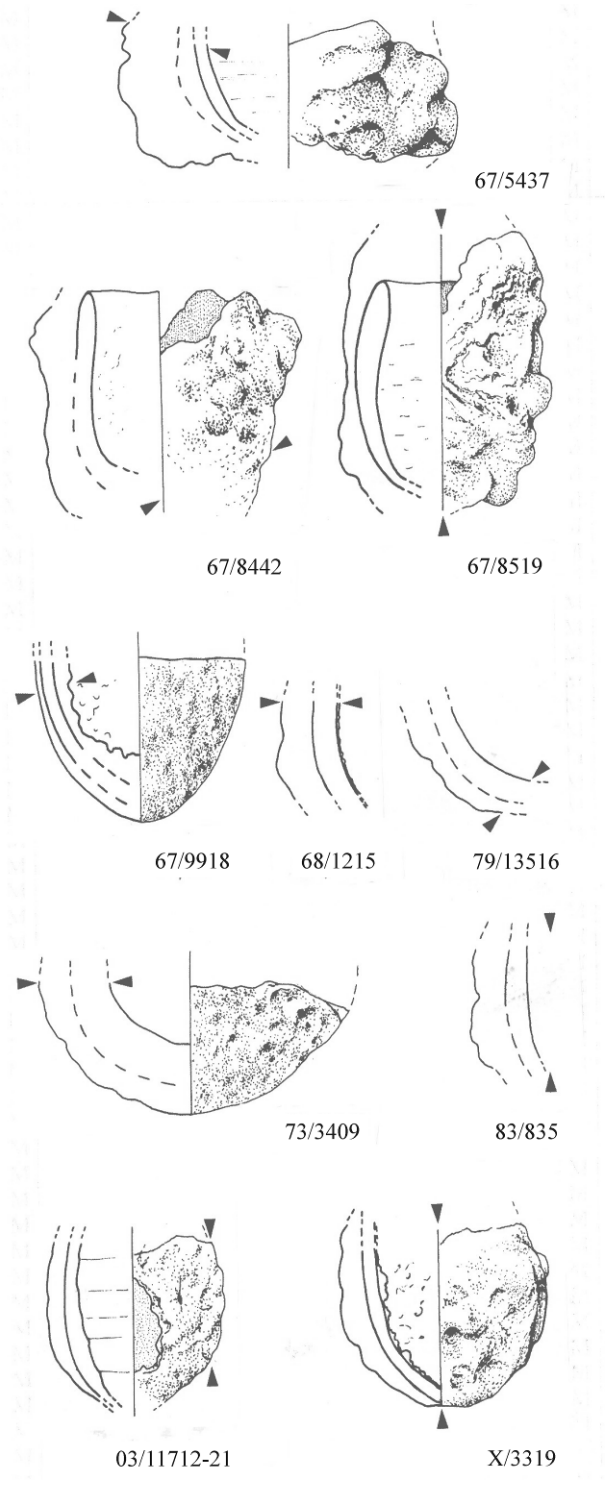

Abbildung A1-4. *Analysierte Tiegelfragmente aus Aventicum (Avenches/VD), sortiert nach Inventarnummern (Musée Romain Avenches). Die Doppelpfeile zeigen die Sägeschnitte zur Probenentnahme; das in der Abbildung fehlende, in der Regel kleinere Teilstück stand für die Analysen zur Verfügung. M. 1:2.*

Inv. MRA 68/1215: WS eines grossen Schmelztiegels; Ton grau mit vielen weissen Magerungskörnern, sandig; Oberfläche innen anthrazit, aussen dick aufgequollenes Lutum.

(Probennummer D. König: 68/1215) Fundkomplex K3489; Grabung 1968.03, Insula 8 («carrés S-U 28 ; démolition générale [couches supérieures]»). – FK-Datierung: um 50–250.

Inv. MRA 73/3409: Boden eines grossen Schmelztiegels; Ton dunkelgrau, mit wenigen erkennbaren hellen Magerungskörnern, sandig; Oberfläche innen naturbelassen (grau), mit feinen Haarrissen, aussen Lutum.

(Probennummer D. König: 73/3409) Fundkomplex K4172; Grabung 1973.01, Insula 23 ouest («carrés O-P 36-37; couche grise»). – FK-Datierung: um 50–200.

Inv. MRA 79/13516: WS eines grossen Schmelztiegels; Ton dunkelgrau, porös verbrannt, sandig, mit wenigen erkennbaren hellen Magerungskörnern; Oberfläche innen ausgebrannt, aussen dünnes Lutum.

(Probennummer D. König: 79/13516) Fundkomplex K5060; Grabung 1979.04, Insula 14 (Tuor 1981) («sondage NE-SO sous la route entre insula 14 et insula 15; trouvaille isolée de dégagement»). – Bemerkung zur Datierung: Mitfunde eines Kruges des 1. Jh.

Inv. MRA 83/835: WS eines mittelgrossen Schmelztiegels; Ton grau, porös, mit feinen hellen Magerungskörnern, sandig; Oberfläche innen naturbelassen mit braunen Flecken, aussen dickes Lutum.

(Probennummer D. König: 83/835) Fundkomplex K5552; Grabung 1983.05, Insula 23 («Section G; couche non stratifiée, nettoyage superficiel de la surface»). Ohne FK-Datierung.

Inv. MRA 03/11712-21: WS/BS eines kleinen Schmelztiegels, unten spitz zulaufend; Ton hellgrau, fein; Oberfläche innen grau-weisslich verbrannt (und ein vertikaler Hitzeriss im Innern), aussen Lutum.

(Probennummer D. König: 03/11712-21) Fundkomplex K11712; Grabung 2003.02, Aux Conches Dessus, voirie en bordure du forum («carré: L 16-17 ; démolition générale [couches supérieures]»). – FK-Datierung: 1.–3. Jh. (mehrheitlich 2./3. Jh.).

«X/3319»: Boden eines kleinen Schmelztiegels, unten spitz zulaufend; Ton hellgrau, fein; Oberfläche innen grünlichschwarz verkrustet, schwarze dünne Schicht auf dem Tiegelton, aussen dickes Lutum.

(Probennummer D. König: X/3319): Grabung, Lokalisierung und Datierung unbekannt.

1.3 ZIELSETZUNG

Ziele der vorliegenden Arbeit bestehen darin, die unterschiedlichen Gruppen von Schmelztiegeln beider Ausgrabungsstätten (Augusta Raurica und Aventicum) zu charakterisieren. Hierbei sollen folgende Fragen respektive Punkte geklärt werden:

- Anzahl der keramischen Lagen
- geochemische und mineralogische Zusammensetzung einzelner Lagen
- Brenntemperaturen (Erstbrand oder Verwendungstemperaturen) der unterschiedlichen Tiegel
- mögliche Ausgangsmaterialien für die unterschiedlichen Lagen zu identifizieren

- Nachweis von Handelsbeziehungen zwischen den benutzten Lehmlagerstätten und den beiden römischen Städten beziehungsweise Handel der Schmelztiegel von einem dritten Ort in die beiden Städte herzustellen und/oder kritisch zu betrachten.

1.4 Petrographische und geochemische Beschreibung der untersuchten Schmelztiegel

1.4.1 Makroskopische, mikroskopische und Rasterelektronenmikroskopische Charakterisierung der Tiegelfragmente

Die untersuchten Tiegel wurden nach makroskopischer Ansprache grob in drei Gruppen unterteilt. Eine Gruppe bilden die Schmelztiegel aus Augusta Raurica (insbesondere das vermutete Händlerdepot in Insula 19), die ungebraucht waren und keine äussere Lage *(Lutum)* aufwiesen (**T128**, **T168**, **T225**). Dieser Gruppe von Tiegeln konnte auch ein Exemplar aus Aventicum (**MRA 03/11712-21**) zugeordnet werden, welches jedoch mindestens einmal verwendet wurde und partiell eine äußere Lage *(Lutum)* aufweist. Ansonsten zeigt die innere Lage des Tiegels makroskopisch und mikroskopisch gleiche Eigenschaften und lässt somit auf eine gemeinsamen Ursprung/ Produzenten schließen. Was diesen Schmelztiegeln gemein ist, ist ihre relativ geringe Größe und die markanten Rillen die durch die Herstellung auf der Töpferscheibe entstanden sind.

Als eine weitere Gruppe können die grob gemagerten Schmelztiegel genannt werden, welche sowohl in Augusta Raurica (**T862**, **T688**) als auch in Aventicum (**MRA 67/8519**, **MRA 68/1215**, **MRA 73/3409**, **MRA 83/835**) gefunden wurden. Diese Tiegel zeichnen sich durch eine mit bloßem Auge deutlich erkennbare Magerung aus, die überwiegend aus weißen bis farblosen Mineralen (Feldspat und Quarz) besteht. Alle Tiegel dieser Gruppe zeigen eine zweite äußere Lage *(Lutum)*, welche in allen Fällen verglast ist. In dieser Lage findet man nur in seltenen Fällen mineralische Magerungskomponenten.

Die dritte und größte Gruppe der von mir untersuchten Tiegel bilden jene, die keine makroskopisch erkennbare Magerung aufweisen, jedoch Verwendungsspuren zeigen. Zu diesen Tiegeln zählen **T503**, **T231**, **T548**, **T673**, **T552**, **T533**, **T454**, **T262**, **T230** und **T289** aus Augusta Raurica und **MRA X/3319**, **MRA 67/5437[1]**, **MRA 67/8442**, **MRA 67/9918** und **MRA 79/13516** aus Aventicum. Diese Gruppe ist charakterisiert durch eine meist hellgraue feinkörnige Matrix, mit geringer halb-offener Porosität in der inneren keramischen Lage. Mikroskopisch sind aber auch in diesen Tiegeln mineralische Magerungskomponenten erkennbar, sie setzen sich vorwiegend aus Quarz und Feldspat zusammen, wie sie auch bei den grob gemagerten Tiegeln vorkommen. Die äußere Lage *(Lutum)* hingegen ist auch bei diesen Schmelztiegeln überwiegend verglast, wie schon bei den grobgemagerten Tiegeln beschrieben.

Sowohl die grob, als auch die fein gemagerten Tiegel zeichnen sich durch eine dünne (200 - 400 µm) verglaste Lage *(Engobe)* an der Innenseite aus. Der Nutzen dieser Lage ist noch nicht ganz eindeutig geklärt, jedoch kann man davon ausgehen, dass diese Lage eine Art Schutzfunktion inne hatte. Das bedeutet sie schützte vor Metallverlust durch die halb-offene Porosität der inneren keramischen Lage. Außerdem konnte an dieser sehr glatten Oberfläche das Metall deutlich leichter ausgegossen werden und nahezu 100 % des geschmolzenen Metalls zurückgewonnen werden.

Im Querschnitt betrachtet sind die beiden verwendeten Typen von Schmelztiegeln gleich aufgebaut (Abb. A1-5). Wobei die innere Lage der grob gemagerten Tiegel oftmals etwas dicker ist als es bei den fein gemagerten Tiegeln der Fall ist.

Die Schmelztiegel bestehen alle aus einer keramischen, nicht verglasten, inneren Lage, welche je nach Typ grob oder fein gemagert sein kann. Des Weiteren besitzen sie eine mehr oder minder stark verglaste äußere Lage, welche als *Lutum* bezeichnet wird. Mit den unterschiedlichen Möglichkeiten der Herstellung und Zusammensetzung dieses *Lutums* beschäftigt sich Alex R. Furger in seiner Monographie über die Schmelztiegel von Augusta Raurica (Furger in prep. 1). Diese äußere Lage kann doppelt vorkommen (Abb. A1-5, links) und ist deshalb ein erstes Indiz für Mehrfachnutzung der Schmelztiegel. Oftmals konnte beobachtet werden, dass die innere Lage vollkommen intakt blieb, wohingegen die äußere Lage bei zu großer Hitze zu fließen begann und sich am Boden des Gefäßes verdickte. Um den Tiegel dann erneut verwenden zu können, wurde einfach eine neuerliche Lage aufgebracht, um den vollständigen Isolationseffekt dieser Lage wieder herzustellen. Außerdem stellt die äußere Lage eine Art Schutzschicht dar, welche durch die hohe plastische Verformbarkeit beim Kaputtgehen der inneren keramischen Lage, beispielsweise durch zu hohen mechanischen Druck durch die Tiegelzange, den Tiegel dennoch zusammen hält.

Abbildung A1-5. *Aventicum. Querschnitt durch einen fein gemagerten Schmelztiegel (links) mit doppelter äußerer Lage (**MRA 67/5437[1]**) und einen grob gemagerten Schmelztiegel (rechts) mit einfacher äußerer Lage (**MRA 68/1215**). Maßstab ca. 1:2.*

Eine weitere charakteristische Eigenschaft, die in einigen der analysierten Tiegelfragmente beobachtet werden konnte, ist eine violette Färbung der inneren Tiegelkeramik, welche im direkten Zusammenhang mit der Migration von Zink steht und vorwiegend bei Zementationstiegeln beobachtet werden kann. Der Farbgradient geht dabei von dunkelviolett am inneren Rand zu hellviolett am Übergang zwischen innerer Keramik und äußerer verglaster Lage *(Lutum)*. Dabei ist bei der chemischen Untersuchung mittels des REMs eine Abnahme des Zinkgehaltes von innen nach außen zu beobachten.

Bei den Untersuchungen, welche mithilfe des REMs durchgeführt wurden, können die drei makroskopisch beziehungsweise mikroskopisch unterscheidbaren Lagen der Schmelztiegel deutlich voneinander abgegrenzt werden. Durch die Aufnahme unterschiedlicher Elemente (Elementverteilungskarten) getrennt nach Einzelelementen, kann besonders bei den Elementen Kalzium, Aluminium und Silizium eine Trennung

der einzelnen Lagen durchgeführt werden (Abb. A1-6). Dabei ist Kalzium in der dünnen verglasten Innenlage im Gegensatz zur inneren keramischen Lage angereichert und Aluminium und Silizium sind abgereichert. Ein ähnliches Bild zeichnet sich beim Übergang von innerer keramischer Lage *(Tiegelkeramik)* hin zur äußeren verglasten Lage *(Lutum)* ab, in der auch Kalzium angereichert und Aluminium und Silizium in Verhältnis abgereichert sind.

Des Weiteren können mithilfe der REM-Analysen die makroskopischen und mikroskopischen Beobachtungen bestätigt werden, dass die Magerungskomponenten aus zwei unterschiedlichen Mineralen zusammengesetzt sind, nämlich Quarz und Feldspat (Abb. A1-7). Dabei wird sehr deutlich, dass die Feldspäte nicht angeschmolzen sind, wie dies in anderen römischen Schmelztiegeln bereits beobachtet werden konnte (König und Serneels 2013 - Chapter 3). Das deutet auf Verwendungstemperaturen von circa 1000 °C hin (Schairer und Bowen 1955, Osborn 1977).

Die äußere vollständig verglaste Lage *(Lutum)* zeigt zumeist nur noch Quarz als Magerung und runde Porenräume, die als geschlossene Porosität bezeichnet werden können (Abb. A1-8; schwarze Kreise). Die Feldspäte, welche möglicherweise auch einen Teil der Magerung dieser Lage darstellen, können nicht mehr nachgewiesen werden, da sie vollständig verglast sind und damit ein Teil der verglasten Grundmatrix geworden sind. Es ist jedoch nicht ausgeschlossen, dass es in der äußeren Lage *(Lutum)* keine Feldspäte gegeben hat.

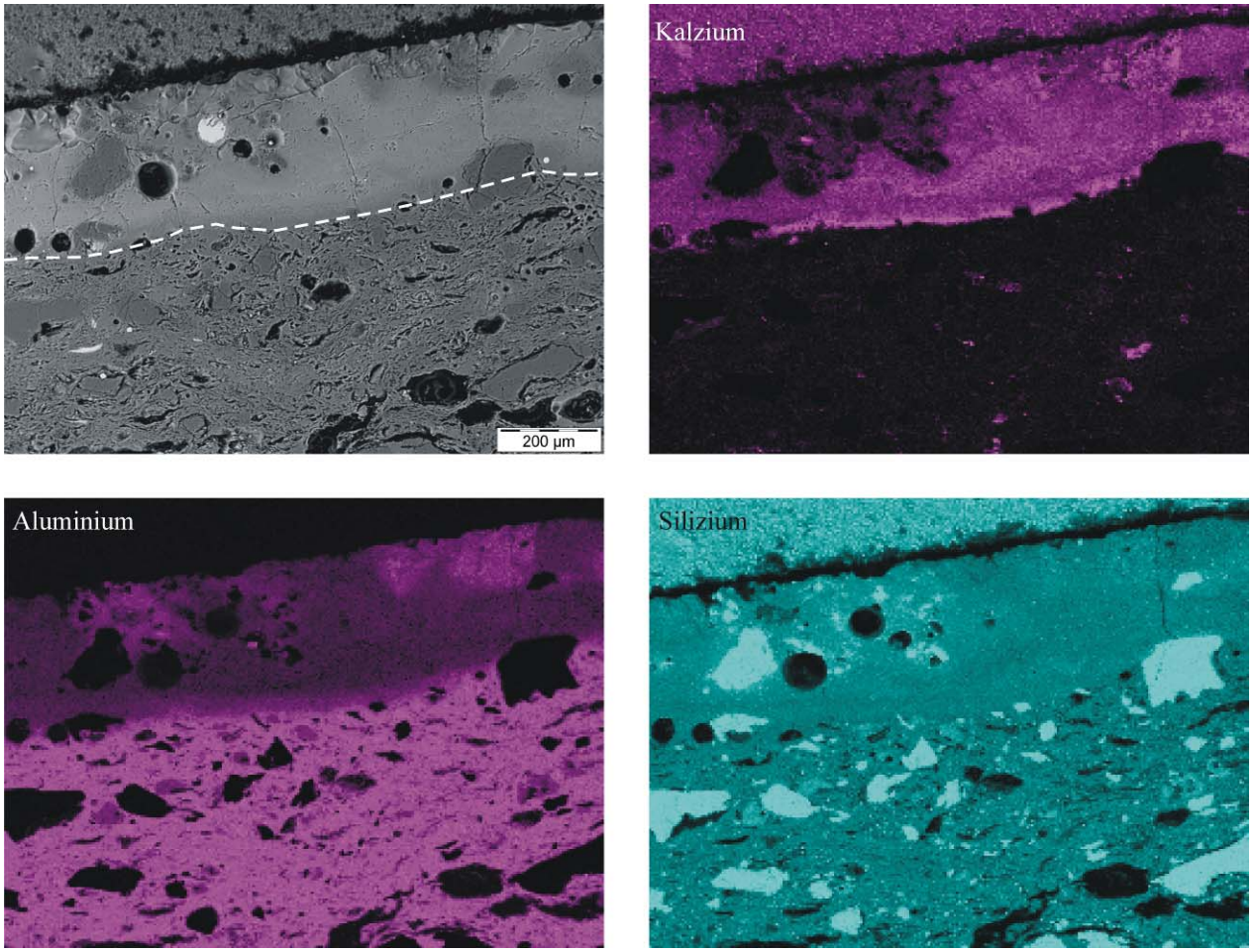

Abbildung A1-6. *Aventicum. Elementverteilungskarten von den Elementen Kalzium, Aluminium und Silizium aus der inneren keramischen Lage (Tiegelkeramik - unten) mit der verglasten innersten Schicht (Engobe - oben); die Grenze zwischen Engobe und innerer keramischer Lage ist als gestrichelte Linie eingetragen (**MRA 68/1215**).*

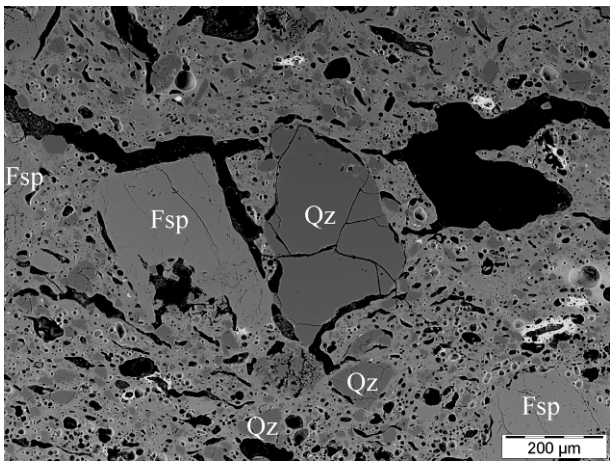

Abbildung A1-7. *Augusta Raurica. REM-Aufnahme der inneren keramischen Lage des Schmelztiegels (Tiegelkeramik) **T862** mit Quarz (Qz) und Feldspat (Fsp) als Magerungskomponenten, wobei der Feldspat bereits vollständig aufgeschmolzen ist. Das Bild stammt aus dem äußeren Bereich der inneren keramischen Lage.*

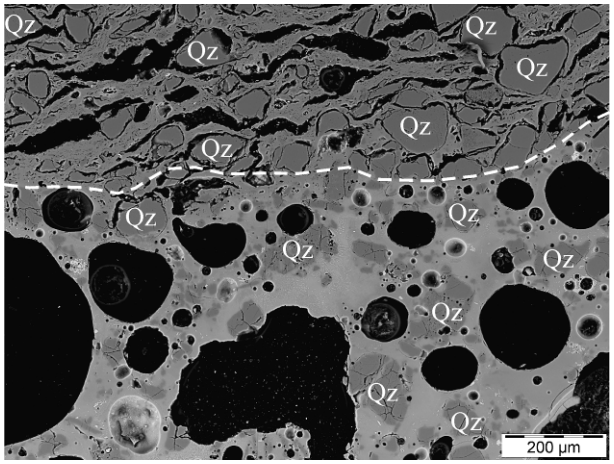

Abbildung A1-8. *Aventicum. REM-Aufnahme von der Grenze (gestrichelte Linie) zwischen innerer keramischer Lage (oben) und der äußeren verglasten Lage (Lutum*; unten*) mit Quarz (Qz) als Hauptmagerungskomponente und einer halb offenen Porosität (längliche Porenräume) in der inneren Lage und einer vollständig geschlossenen Porosität (runde Porenräume) in der äußeren Lage. Bild stammt aus Schmelztiegel* ***MRA 67/5437[1]****.*

Weiterhin konnten mittels des REMs feinste Metalltröpfchen, die sich innen auf der Engobe fanden, analysiert werden. Bei diesen Tröpfchen handelt es sich vorwiegend um Kupfer-Zinn-Legierungen (Abb. A1-9), aber auch Kupfer-Zink-Legierungen können nachgewiesen werden. Da die Anzahl der Tröpfchen jedoch auf Grund der Engobe und deren Oberflächeneigenschaften sehr gering ist, kann mithilfe dieser Methode keine allgemeingültige Aussage über die Zusammensetzung der eingeschmolzenen Metalle getroffen werden (Furger in prep. 1).

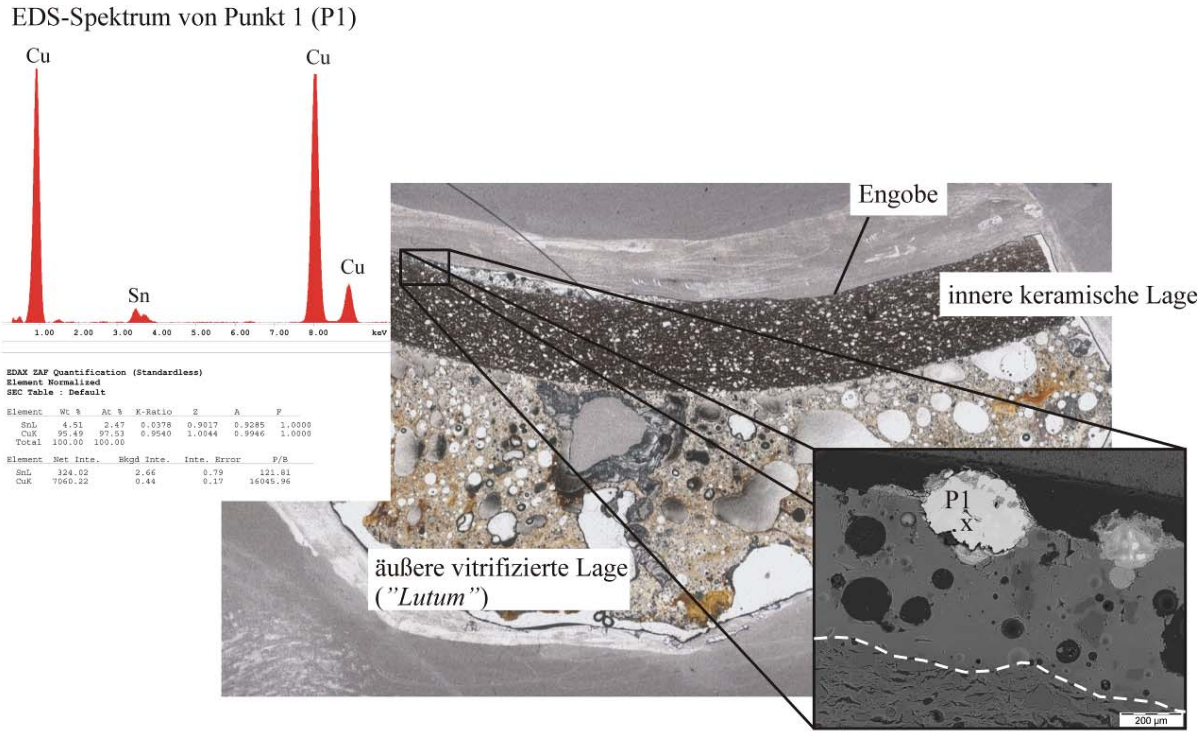

Abbildung A1-9. *Augusta Raurica. Dünnschliff von Probe* ***T454*** *mit einer REM-Aufnahme aus der inneren keramischen Lage mit Engobe und darin eingebettetem Metalltröpfchen. Das Metalltröpfchen besteht aus einer Kupfer-Zinn-Legierung und wurde mittels energiedispersiver Röntgenspektroskopie (EDS) gemessen.*

1.4.2 Chemische Zusammensetzung

Die chemische Gesamtzusammensetzung der Schmelztiegel wurde mittels Röntgen-fluoreszensspekrometrie an aufgemahlenen Gesamtproben bestimmt (Tabelle A1-1), d.h. keramische Grundmatrix und Magerung wurden nicht voneinander getrennt gemessen. Die Resultate entsprechen daher nicht der Ausgangstonzusammensetzung, sondern gelten als chemisch durch die Magerung "verunreinigte" Tondatensätze. Jedoch erfolgte eine Trennung der inneren keramischen Lage *(Tiegelkeramik)* und der äußeren verglasten Lage *(Lutum)* durch mechanische Separation. Da die daraus resultierenden Probenmengen für eine chemische Analyse teilweise zu gering waren, wurde bei kleinen Probemengen auf eine Separation der Lagen verzichten. Daher konnten die Lagen nur bei acht von 26 getrennt untersucht werden (Augusta Raurica: **T552**, **T862**, **T688**, **T262**, **T230**; Aventicum: **MRA X/3319**, **MRA 67/5437[1]**, **MRA 68/1215**). Bei allen weiteren untersuchten Schmelztiegeln wurde die chemische Zusammensetzung für beide Lagen gemeinsam bestimmt. Abbildung A1-10 zeigt die geochemischen Ergebnisse der in Tabelle A1-1 aufgelisteten Analysen. Aus den erhobenen Daten lassen sich zwei Gruppen von Keramiken unterscheiden, die jedoch nicht auf unterschiedliche Fundorte zurückzuführen sind, sondern eine chemische Differentiation als Folge der genutzten Art der Magerung (grob/fein) und der Grundtone darstellen. Auf Grund der unterschiedlichen Magerungszusammensetzungen und deren Auswirkung auf die chemische Gesamtzusammensetzung, kann leider kein differenziertes Bild über die Art der verwendeten Tone getroffen werden. Nichtsdestoweniger liefert die chemischen Zusammensetzungen ein erstes Indiz für die Temperaturstabilitäten der verwendeten Schmelztiegel und deren Erweichungspunkt (Abb. A1-11). Der Abbildung A1-11 ist zu entnehmen, dass die Keramiken bis zu Temperaturen von 1600 °C stabil sind. Diese Temperaturen sollten nicht als Betriebstemperaturen verstanden werden, sondern ausschließlich als maximale Stabilitätstemperaturen, d. h. Temperaturen denen die Keramik maximal Stand halten würde, welche aber während der Nutzung nicht erreicht wurden. Die erreichten Betriebstemperaturen lassen sich mittels der geochemischen Analysen nicht ermitteln, dafür sind optische und röntgenographische Analysen notwendig.

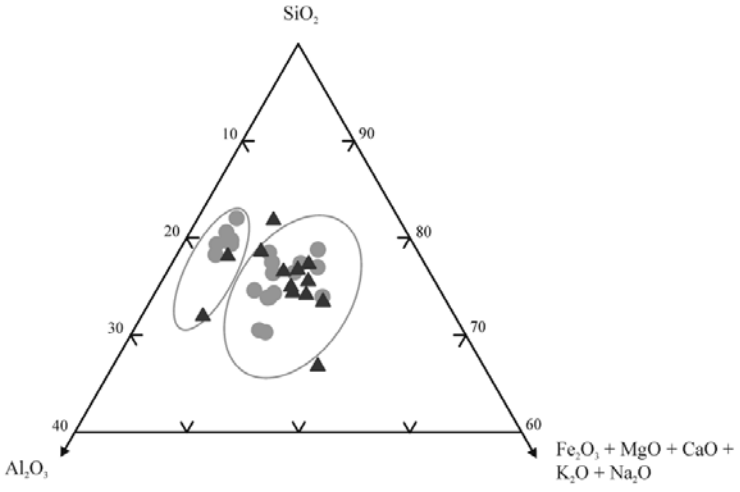

Abbildung A1-10. *Ternäres Diagramm, welches die chemische Verteilung der Proben aus Augusta Raurica (●) und Aventicum (▲) zeigt. Dabei sind deutlich zwei Gruppen voneinander zu unterscheiden.*

	T503[1]	T231[1]	T548[3]	T673[1]	T552 i.l.[3]	T552 a.l.[1]	T862 i.l.[1]	T862 a.l.[1]	T128[1]*	T168[1]*	T688 i.l.[2]	T688 a.l.[1]	T533[2]	T454[2]	T262 i.l.[3]	T262 a.l.[2]	T230 i.l.[3]	T230 a.l.[1]	T289[1]	T225[1]*
SiO_2 (gew.%)	76,9	72,9	73,3	75,0	79,0	77,9	69,4	76,5	78,5	81,1	69,9	76,1	76,9	72,3	76,4	71,2	78,4	75,3	79,0	79,4
TiO_2 (gew.%)	0,7	0,8	0,7	1,0	0,7	0,6	0,8	0,7	0,9	0,9	0,5	0,5	0,5	0,6	0,7	0,4	0,9	0,7	0,9	1,3
Al_2O_3 (gew.%)	12,5	15,4	14,8	15,0	15,9	8,7	17,6	10,9	16,1	14,3	17,7	9,6	13,7	16,0	13,4	11,5	17,4	11,9	14,2	15,9
Fe_2O_3 (gew.%)	3,3	3,6	4,5	2,8	2,3	5,7	5,9	4,6	2,3	1,7	5,4	3,9	3,4	3,6	3,4	4,5	1,7	4,3	1,5	1,6
MnO (gew.%)	0,09	0,06	0,22	0,05	0,03	0,12	0,06	0,11	<0,01	<0,01	0,06	0,10	0,09	0,11	0,09	0,39	0,05	0,13	0,01	<0,01
MgO (gew.%)	1,0	0,9	1,1	0,8	0,4	0,9	1,0	1,2	0,6	0,5	1,0	1,3	0,9	1,1	1,1	1,9	0,4	1,3	0,3	0,4
CaO (gew.%)	2,1	2,7	2,1	3,0	1,0	2,1	0,7	2,0	1,0	0,8	0,7	3,7	1,7	3,2	2,8	4,3	0,5	2,0	0,7	0,9
Na_2O (gew.%)	1,1	1,3	0,7	0,6	0,2	1,2	0,5	1,3	0,1	0,2	0,6	1,3	0,8	0,8	0,7	1,4	0,1	1,3	2,6	0,3
K_2O (gew.%)	1,9	2,0	2,3	1,7	0,4	2,6	3,9	2,5	0,4	0,4	3,9	3,2	1,8	1,9	1,1	3,5	0,4	2,6	0,6	0,2
P_2O_5 (gew.%)	0,3	0,4	0,3	0,2	0,1	0,3	0,2	0,3	0,0	0,0	0,2	0,4	0,3	0,4	0,4	0,9	0,1	0,4	0,1	0,0
Summe bevor Norm.(gew.%)	97,1	97,1	95,8	97,4	92,8	97,8	96,4	96,4	95,6	97,7	93,4	99,1	87,8	91,9	93,3	92,5	95,5	98,8	96,8	98,1
Summe Norm.(gew.%)	100	100	100	100	100	100	100	100	100	100	100	100	100	100	100	100	100	100	100	100
Ba (ppm)	306	307	1400	215	2000	325	3498	365	91	112	3800	416	450	800	1400	1200	1900	440	88	87
Cr (ppm)	90	114	<100	114	100	76	98	88	115	105	<100	74	<100	100	100	<100	100	89	101	116
Cu (ppm)	550	1000	32000	200	7200	250	250	700	100	650	500	950	9600	4800	130800	21800	3200	500	600	46
Nb (ppm)	17	16	<100	20	<100	12	18	15	20	21	<100	13	<100	<100	<100	<100	<100	16	17	28
Ni (ppm)	34	44	100	35	n.g.	45	42	45	27	27	<100	30	<100	<100	n.g.	<100	n.g.	44	37	19
Pb (ppm)	250	1200	9700	220	350	140	600	180	25	110	150	90	1100	550	14000	900	2900	610	140	190
Rb (ppm)	77	71	<100	64	<100	85	202	97	26	21	250	117	100	<100	<100	100	<100	101	21	7
Sn (ppm)	100[2]	n.g.	4600	<100[2]	450	n.g.	n.g.	n.g.	n.g.	n.g.	<100	n.g.	250	1250	13200	3100	500	n.g.	<100[2]	n.g.
Sr (ppm)	115	296	<100	108	<100	98	157	131	52	45	150	117	100	150	<100	200	<100	124	38	41
V (ppm)	77	148	130	123	<100	59	108	79	102	90	100	71	100	100	150	<100	150	84	87	86
Y (ppm)	34	29	<100	27	<100	29	34	39	23	24	<100	31	<100	<100	<100	<100	<100	39	21	25
Zn (ppm)	4230	7060	94400	1445	38200	2615	2525	210	60	425	9300	190	15600	1400	9800	2000	36900	2640	73865	20
Zr (ppm)	307	306	300	283	300	341	255	355	242	278	300	276	400	400	300	450	450	365	248	277
Σ Schmelz-%	0,53	0,95	14,69	0,20	4,98	0,31	0,35	0,11	0,02	0,12	1,07	0,12	3,02	0,87	17,98	3,00	4,55	0,38	7,71	0,03

[1] Glastabletten; [2] Presstabletten; [3] Glas-Presstabletten; * unbenutzt; n.g. - nicht gemessen

Tabelle A1-1.1. *Gesamtchemische Analysen der Proben aus* ***Augusta Raurica,*** *teilweise nach Lagen getrennt (i.l. - innere Lage; a.l. - äussere Lage). Grau unterlegt sind die Hauptlegierungsbestandteile, die in den Tiegeln eingeschmolzen wurden.*

	MRA 67/5437[1] i.l. [3]	MRA 67/5437[1] a.l. [1]	MRA 67/8442[2]	MRA 67/8519[1]	MRA 67/9918[2]	MRA 68/1215 i.l. [3]	MRA 68/1215 a.l. [2]	MRA 73/3409[1]	MRA 79/13516[1]	MRA 83/835[1]	MRA 03/11712-21[1]	MRA X/3319 i.l. [3]	MRA X/3319 a.l. [2]
SiO_2 (gew.%)	77,4	73,4	73,4	66,0	72,3	71,2	75,5	76,8	78,5	77,8	81,1	77,9	71,8
TiO_2 (gew.%)	0,8	0,5	0,3	0,6	0,4	0,8	0,4	0,4	0,4	0,4	0,5	0,5	0,3
Al_2O_3 (gew.%)	17,1	12,1	11,8	14,7	13,0	22,4	10,7	11,2	11,2	10,6	11,2	14,0	11,0
Fe_2O_3 (gew.%)	2,0	3,8	4,3	5,2	3,4	2,1	3,6	3,8	2,5	3,0	2,6	3,6	3,5
MnO (gew.%)	0,02	0,13	0,13	0,13	2,56	0,04	0,18	0,11	0,11	0,09	0,05	0,03	0,24
MgO (gew.%)	0,7	1,5	1,3	2,9	1,3	0,7	1,3	1,2	1,2	1,1	0,7	0,8	1,5
CaO (gew.%)	1,2	2,9	2,8	4,7	3,2	0,6	3,8	1,5	1,1	2,3	1,3	1,4	5,7
Na_2O (gew.%)	0,3	2,0	1,9	1,9	0,4	0,4	1,1	2,0	2,2	2,0	0,9	0,6	1,8
K_2O (gew.%)	0,5	3,3	3,3	3,5	2,6	1,8	3,2	2,6	2,6	2,5	1,3	0,9	3,7
P_2O_5 (gew.%)	0,1	0,3	0,7	0,3	0,8	0,1	0,3	0,2	0,2	0,2	0,2	0,2	0,5
Summe bevor Norm.(gew.%)	91,2	98,8	86,5	99,2	98,6	97,8	90,6	99,3	99,3	99,2	98,9	95,4	86,1
Summe Norm.(gew.%)	100	100	100	100	100	100	100	100	100	100	100	100	100
Ba (ppm)	2100	441	680	412	1250	23700	1940	374	351	347	207	800	900
Cr (ppm)	150	82	<100	75	<100	<100	100	78	81	73	88	<100	<100
Cu (ppm)	4100	350	1500	900	5550	3000	3400	150	200	71	26	39100	1050
Nb (ppm)	<100	10	<100	14	<100	700	<100	10	8	10	14	<100	<100
Ni (ppm)	n.g.	44	<100	37	<100	n.g.	<100	33	24	29	33	n.g.	<100
Pb (ppm)	800	350	450	1500	150	750	<100	140	500	143	28	26200	400
Rb (ppm)	<100	123	150	156	<100	400	150	103	102	99	59	<100	150
Sn (ppm)	<100	n.g.	800	n.g.	550	n.g.	<100	<100[2]	<100[2]	n.g.	n.g.	28200	450
Sr (ppm)	<100	135	150	143	100	400	150	96	94	111	69	<100	200
V (ppm)	200	67	<100	89	100	n.g.	<100	64	53	51	82	100	<100
Y (ppm)	<100	27	<100	36	<100	<100	<100	32	31	28	22	n.g.	<100
Zn (ppm)	9300	129	4650	90	63500	2000	100	111	3738	92	54	8900	750
Zr (ppm)	350	157	250	153	200	1700	500	183	185	175	200	250	250
Σ Schmelz-%	1,56	0,08	0,86	0,25	7,07	0,59	0,40	0,05	0,45	0,03	0,01	10,73	0,30

Tabelle A1-1.2. *Gesamtchemische Analysen der Proben aus* ***Aventicum,*** *teilweise nach Lagen getrennt (i.l. - innere Lage; a.l. - äussere Lage). Grau unterlegt sind die Hauptlegierungsbestandteile, die in den Tiegeln eingeschmolzen wurden.*

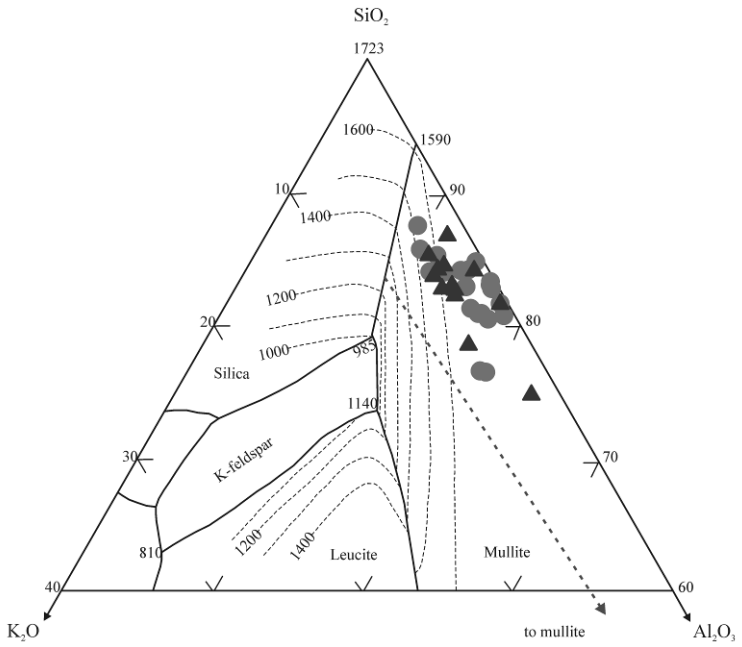

Abbildung A1-11. *Ternäres Diagramm, welches die Temperaturstabilität der untersuchten Keramiken verdeutlicht. Graue Kreise (●) entsprechen den Proben aus Augusta Raurica und dunkelgraue Dreiecke (▲) denen aus Aventicum (verändert nach Osborn 1977, Maggetti et al. 2010).*

1.4.3 Röntgendiffraktometrie

Pulverförmige Proben der keramischen Schmelztiegel wurden mittels Röntgendiffraktometrie untersucht, um den heutigen Mineralbestand zu ermitteln (Tabelle A1-2). Die hierbei ermittelten Mineralphasen repräsentieren die durch die Schmelzprozesse überprägte primäre Zusammensetzung und gestatten daher keine eindeutigen oder direkten Rückschlüsse auf die exakten Ausgangston- und Magerungszusammensetzungen. Tonminerale, Glimmer oder Feldspäte sind während des Brennprozesses zumeist soweit umgewandelt wurden, z.B. durch Entwässerungsreaktionen, dass diese nicht mehr röntgenographisch nachgewiesen werden konnten. Eine Entwässerung des Kristallwassers der Tonmineralen setzt bei vielen Vertretern bereits bei relativ niedrigen Temperaturen, im Vergleich zum Temperaturbereich metallurgischer Prozesse, ein, z.B. Kaolinit zu Meta-Kaolinite bei 500 - 600 °C, Illitische Tone bei ca. 900 °C (Velde und Druc 1999). Eine Bodenlagerung verursacht oftmals eine zusätzliche Veränderung des Mineralbestandes, infolge der Devitrifizierung glasiger (amorpher) Bestandteile und verursacht durch chemische Austauschprozesse mit dem Bodenwasser. Diese Veränderungen müssen bei der Interpretation der mineralogischen Zusammensetzung der Schmelztiegel berücksichtigt werden,.

Probe	**Mineralzusammensetzung**
Augusta Raurica	
T503	Qz + Crs + Mul
T231	Qz + Crs + Mul
T548	Qz + Crs + Mul + Spl + Wil
T673	Qz + Crs + Mul
T552 i.L.	Qz + Crs + Mul
T552 a.L.	Qz + Crs

Probe	Mineralzusammensetzung
T862 i.L.	Qz + k-Fsp + Mul + Spl
T862 a.L.	Qz + k-Fsp
T128	Qz + Crs
T168	Qz + k-Fsp
T688 i.L.	Qz + k-Fsp + Mul + Spl
T688 a.L.	Qz + Crs
T533	Qz + Crs + Mul + Gah
T454	Qz + Crs + Mul
T262 i.L.	Qz + Pl + Crs + Mul + Spl
T262 a.L.	Qz + Crs + Spl
T230 i.L.	Qz + k-Fsp + Crs + Mul + Gah
T230 a.L.	Qz + k-Fsp + Crs
T289	Qz + k-Fsp + Crs + Mul + Wil
T225	Qz + k-Fsp + Crs + Mul
Aventicum	
MRA 67/5437[1] i.L.	Qz + Crs + Mul
MRA 67/5437[1] a.L.	Qz + Crs + Mul
MRA 67/8442	Qz + Pl + k-Fsp + Crs + Mul
MRA 67/8519	Qz + Pl + k-Fsp
MRA 67/9918	Qz + Pl + Mul + Wil
MRA 68/1215 i.L.	Qz + Crs + Mul
MRA 68/1215 a.L.	Qz + Crs
MRA 73/3409	Qz + Pl + k-Fsp + Crs + Mul
MRA 79/13516	Qz + Pl + k-Fsp + Crs + Mul
MRA 83/835	Qz + Pl + k-Fsp + Crs + Mul
MRA 03/11712-21	Qz + Pl + Mul
MRA X/3319 i.L.	Qz + Crs + Mul + Wil
MRA X/3319 a.L.	Qz + Crs

Tabelle A1-2. *Mineralogische Zusammensetzung der untersuchten Schmelztiegel, teilweise nach Lagen getrennt (i.L.- innere Lage; a.L. - äußere Lage). Die aufgeführten Mineralabkürzungen stehen für folgende Minerale: Cristobalit (Crs); Gahnit (Gah); Mullit (Mul); Plagioklas (Pl); Kalium-Feldspat (k-Fsp); Quarz (Qz); Spinell (Spl); Willemit (Wil).*

Die ermittelten Mineralphasen zeigen deutlich, dass die Zusammensetzungen der inneren *(Tiegelkeramik)* und der äußeren Lage *(Lutum)* voneinander abweichen. Die Migration von Zink ist hierfür ursächlich und ermöglichte die Bildung von Gahnit ($ZnAl_2O_4$) und Willemit ($Zn_2(SiO_4)$) innerhalb der inneren Lage *(Tiegelkeramik)*. Diese Minerale sind im *Lutum* nicht vorhanden. Die heterogene Hitzeeinwirkung innerhalb und zwischen einzelnen Tiegeln und die Temperaturbeständigkeit einiger Minerale (z.B. Quarz) verursacht überdies einen Mix aus teilweise primären und durch den Brennprozess entstandenen Mineralbestand. Alle Proben zeigen ausnahmslos Quarz, welcher auch makroskopisch und mikroskopisch überall als Magerung identifiziert werden konnte. Die Feldspäte, welche nicht in allen Diffraktogrammen identifiziert werden konnten, setzen sich vorwiegend aus Kalium-Feldspat und Plagioklasen zusammen. Eine genauere Differenzierung der einzelnen Plagioklase wurde im Rahmen dieser Arbeit nicht vorgenommen. Mullit als Hauptmatrixmineral ist nicht in allen Proben vorhanden. Dies kann, wie oben bereits erwähnt, seine Ursache in unterschiedlich starken Hitzeeinwirkungen auf die Keramik haben. Die Proben, die keinen Mullit zeigen, besitzen vermutlich Meta-Kaolinit, welcher röntgenamorph ist und mittels dieses Analyseverfahrens nicht dargestellt werden kann. Cristobalit tritt nur in einigen Proben auf und kann als primärer Magerungsbestandteil ausgeschlossen werden. Das bedeutet, dass auch dieses Mineral als Indikator für Temperatureinwirkungen verwendet werden kann.

1.5 VERWENDETE TONE FÜR DIE TIEGELHERSTELLUNG UND DEREN BRENNTEMPERATUREN

1.5.1 Ausgangsmaterialien für die unterschiedlichen keramischen Lagen

Es kann theoretisch davon ausgegangen werden, dass die innere und äußere keramische Lage aus dem gleichen Grundton hergestellt worden ist. Für die äußere Lage, das *Lutum*, sind die Zuschlagsstoffe entscheidend, die zu einem unterschiedlichen Verhalten bei bei hohen Temperaturen führen. Die keramische innere Lage, die eigentliche Tiegelkeramik, besteht aus einem Ton, der in seiner Grundzusammensetzung aus einer Mischung zwischen kaolinitischem und illitischem Ton besteht. Die zugegebene Magerung besteht aus Quarz, Kalium-Feldspat und Plagioklas. Da diese Komponenten teilweise als Gesteinsbruchstücke auftreten, kann davon ausgegangen werden, dass es sich entweder um zerkleinerte Gesteinsbruchstücke oder um Verwitterungsmaterial von Gesteinen handelt.

Bei der äußeren verglasten Lage, dem *Lutum*, kann von einer ähnlichen Grundton-zusammensetzung ausgegangen werden. Allerdings müssen weitere Zuschlagsstoffe außer der Magerung, welche vorwiegend aus Quarz besteht, zugegeben worden sein. Die dafür in Frage kommenden historischen Rezepte werden von Alex R. Furger in einem ausführlichen Exkurs über das *Lutum* zusammengestellt. In archäologischen Experimenten mit verschiedenen Tonmischungen wird versucht, den römischen Originalen möglichst nahe zu kommen (Furger in prep. 1). Die hier durchgeführten Analysen zeigen lediglich, dass die äußere Lage *(Lutum)* einen erhöhten Anteil an Kalzium als Glasbildner aufweist. Mögliche Rückstände die eine weitergehende Charakterisierung des verwendeten Materials gestatten würden (ein bestimmtes Gestein, ein spezieller Ton oder organischen Komponenten wie Haare) konnten im Rahmen dieser Studie und vermutlich als Folge der erhöhten Temperatureinwirkungen nicht nachgewiesen werden.

Die auf der Innenseite der Tiegel aufgebrachte Engobe wurde vermutlich aus derselben Tonmischung hergestellt, wie diejenige für die äußere Lage *(Lutum)*. Dafür war ein Aufschlämmen erforderlich, um eine möglichst *dünne* Lage zu erzeugen. Der Mangel an Magerungskomponenten in dieser dünnen Schicht unterstützt diese Hypothese, da ein Aufschlämmen eines natürlichen Tones auch zu einer Separation grober und feiner Bestandteile führt. Die Lage wurde vermutlich auf die bereits vorgetrocknete oder bei niedrigen Temperaturen vorgebrannte innere Keramik durch Ausschwenken mit der Emulsion aufgebracht, denn sie hat sich im anschließenden Brand mit der Tiegelkeramik fest verbunden.

1.5.2 Brenntemperaturen

Eine Bestimmung der Brenntemperaturen kann immer nur die höchste im metallurgischen Prozess erreichte Temperatur erfassen, jedoch nicht die allenfalls niedrigere Brenntemperatur des Tiegels bei seiner Herstellung. Dabei stützt sich die hier angewendete Methode ausschließlich auf die mittels XRD ermittelten Mineralparagenesen. Für die Bestimmung können vor allem Mullit und Cristobalit sowie Spinell verwendet werden. Die Abwesenheit von Mullit in einigen Proben kann als Vorhandensein einer röntgenamorphen Phase, nämlich Meta-Kaolinit, gewertet werden. Für diese Proben kann eine Brenntemperatur zwischen 500 °C und 700 °C angenommen werden (Lee *et al.* 2008). Proben, in denen nur Spinell vorhanden ist, zeichnen einen Übergangsbereich von Meta-Kaolinit zu Mullit nach und sprechen für eine Brenntemperatur von etwa 700 °C (Lee

et al. 2008). Proben, in denen Mullit nachgewiesen werden konnte, sprechen für Brenntemperaturen über 950 °C (Lee *et al.* 2008). Da mittels REM Analysen nur primärer und kein sekundärer Mullit nachgewiesen werden konnte, kann eine Betriebstemperatur zwischen 1100 °C bis 1200 °C angenommen werden (Lee and Iqbal 2001).

Für die Nutzung als Schmelztiegel für Kupferlegierungen kann, je nach Metallkapazität und Legierungszusammensetzung, eine Verwendungstemperatur von 900 °C bis 1000 °C postuliert werden. Diese Temperatur deckt sich sehr gut von den mittels Mineralparagenesen bestimmbaren Temperaturen.

1.5.3 Vergleichbarkeit der Tone zwischen Augusta Raurica und Aventicum

Die relativ wenigen untersuchten Schmelztiegel aus Augusta Raurica und Aventicum können mittels der vorgenommenen Analysemethoden nicht voneinander unterschieden werden. Dieses Resultat kann sowohl makroskopisch, als auch mikroskopisch und mittels der geochemischen Analysen belegt werden. Der einzige Unterschied in den analysierten Tiegeln, ergibt sich aus der Größe der Magerungskomponenten, die eine Unterscheidung in grob und fein gemagerte Tiegel zulässt. Auch die Gruppe der deutlich kleineren und im Fall von Augusta Raurica ungebrauchten Tiegel (Abb. A1-3, **T128**, **T168**, **T225**), kann mit dem einen zwar benutzen, aber optisch und geochemisch identischen Tiegel aus Aventicum (Abb. A1-4, **MRA 03/11712-21**) korreliert werden. Die fein gemagerten Schmelztiegel beider Ausgrabungsorte zeigen eine Magerung, bestehend aus Quarz und Feldspat in der *Tiegelkeramik* und ausschließlich Quarz im *Lutum.* Die keramische Grundmatrix der *Tiegelkeramik* besteht aus Mullit. Dies wird als Hinweis auf die Verwendung eines Kaolinit reichen Tons gedeutet. In einigen Proben ließ sich Cristobalit nachweisen. Dieses Mineral bildet sich zumeist während des Brennvorgangs durch die Umwandlung unterschiedlicher Tone oder aus Quarz. Außerdem zeigen einige Tiegel Gahnit und Willemit, d.h. Zinkminerale, die bei der Verwendung der Schmelztiegel und durch die Reaktion gasförmigen Zinks mit der keramischen Masse gebildet wurden.

Die grob gemagerten Tiegel kommen ebenfalls in beiden Römerstädten vor und können weder optisch, noch chemisch oder mineralogisch unterschieden werden. Vielmehr scheinen sie, genau wie die fein gemagerten, aus einer Tiegelmanufaktur zu stammen und aus dem geochemisch gleichen Grundton und Zuschlagsstoffen hergestellt worden zu sein.

1.6 Handel von Tiegeln oder Tiegeltonen zwischen Lagerstätten und Verbraucherzentren (Augusta Raurica und Aventicum)

Die in dieser Studie erhobenen Daten lassen vermuten, dass die helltonigen, feinkeramischen Schmelztiegel aus Augusta Raurica und Aventicum eine einheitliche Gruppe bilden. Für die dunklen, stark gemagerten Tiegel, die ebenfalls an beiden Fundstätten vorkommen, ist dies nicht ganz eindeutig belegbar, da die in Augusta Raurica gefundenen Stücken nachweislich aus lokalen Tonen hergestellt sind (Furger in prep. 1). Das würde einen Handel dieser Tiegel zwischen Augusta Raurica und Aventicum voraussetzen. Eine Besonderheit in Augusta Raurica ist eine größere Serie von ungebrauchten Tiegeln aus Insula 19, die vermutlich direkt von einer Lieferung eines Händlers stammen.

Die unbenutzten Tiegel wurden in einem Händlerdepot in Augusta Raurica gefunden und gelten als nicht in Augusta Raurica hergestellt, weil ihr Ton aufgrund seiner Spurenelementzusammensetzung aus der Gegend von Châtelat/BE im Jura stammt (Furger in prep. 1). Da ein identischer Tiegel, jedoch mit Verwendungsspuren, in Aventicum gefunden wurde, scheinen diese Tiegelrohlinge auch dort hin gehandelt worden zu sein. Die äußere verglaste Lage *(Lutum*) wurde bei diesen Schmelztiegeln erst vor Ort auf den Tiegeln angebracht.

Die fein gemagerten und verwendeten Schmelztiegel stammen vermutlich auch aus einer zentralen Manufaktur, wobei die hier durchgeführten Analysen keinen Aufschluss darüber geben, ob die Schmelztiegel an einem Ort in Augusta Raurica, Aventicum oder gar in der Nähe der eigentlichen Tonlagerstätte gefertigt wurden (Furger in prep. 1). Ersichtlich jedoch ist, dass sowohl die innere keramische Lage *(Tiegelkeramik)* als auch die äußere keramische Lage *(Lutum)* geochemisch identisch sind. Das deutet eher darauf hin, dass die Tiegel bereits zweilagig mit Engobe gefertigt und erst im Anschluss gehandelt wurden (Furger in prep. 1). Die Verdopplung der äußeren verglasten Lage in einem Fall von Augusta Raurica (Abb. A1-5, links) lässt schließen, dass der Ton für diese Lage in Augusta Raurica selbst vorhanden gewesen sein muss.

Eine ähnliche Interpretation kann für die grob gemagerten Schmelztiegel gemacht werden. Auch diese Tiegel sind untereinander geochemisch sehr ähnlich und deuten vermutlich darauf hin, dass diese aus den gleichen Tonen und Magerungskomponenten (einer einzigen Quelle) gefertigt wurden. Diese Aussage bezieht sich auch hier auf beide Lagen und die Engobe (Furger in prep. 1).

Ein weiteres Indiz ist die Form der Schmelztiegel (Abb. A1-2, **T7**–**T549**), die unabhängig der Tonqualitäten identisch zu sein scheint. Das deutet auf einen zentralen Herstellungsort für jede Tongruppe hin.

Nach den erworbenen Erkenntnissen kann davon ausgegangen werden, dass die Tiegel nur eingeschränkt gebrauchsfertig (d.h. teilweise noch ohne *Lutum*) gehandelt wurden. Das «Lutieren» der Tiegel erfolgte erst vor Ort – vermutlich durch die Gießer selbst – mit einem Gemisch von lokalen Lehmen und verschlackenden Zuschlägen

APPENDIX 2 - TABLE ABOUT METHODS PERFORMED PER SAMPLE

sample name		metal-melting crucible	brass-making crucible	mould	thin-section	SEM	Microprobe	XRD	XRF	TGA	Raman-Spectroscopy
Autun											
ATM 001	in	x			x	x		x	x	x	
	out							x	x	x	
ATM 002	in	x			x	x	x	x	x	x	x
	out							x	x	x	
ATM 003	in	x			x	x	x	x	x	x	
	out							x	x	x	
ATM 004	in	x			x	x	x	x	x	x	x
	out							x	x	x	
ATM 005	in	x			x	x		x	x	x	
	out							x	x	x	
ATM 006	in	x			x	x	x	x	x	x	x
	out							x	x	x	
ATM 007		x			x	x		x	x	x	
ATM 008	in	x			x	x	x	x	x	x	
	out							x	x	x	
ATM 009	in	x			x	x		x	x	x	
	out							x	x	x	
ATM 010	in	x			x	x	x	x	x	x	
	out							x	x	x	
ATM 011	in	x			x	x		x	x	x	x
	out							x	x	x	
ATM 012		x			x	x	x	x	x	x	x
ATM 013	in	x			x	x	x	x	x	x	x
	out							x	x	x	
ATM 014	in	x			x	x	x	x	x	x	x
	out							x	x	x	
ATM 015		x			x	x		x	x	x	
ATM 016		x			x	x	x	x	x	x	
ATM 017	in	x			x	x		x	x	x	
	out							x	x	x	
ATM 018	in	x			x	x		x	x	x	x
	out							x	x	x	

sample name	metal-melting crucible	brass-making crucible	mould	thin-section	SEM	Microprobe	XRD	XRF	TGA	Raman-Spectroscopy
ATM 019			x				x	x	x	
ATM 020			x				x	x	x	
ATM 021			x				x	x	x	
ATM 022			x				x	x	x	
ATM 023			x				x	x	x	
ATM 024			x	x	x		x	x	x	
ATM 025			x				x	x	x	
ATM 026			x				x	x	x	
ATM 027			x	x	x		x	x	x	
ATM 028			x				x	x	x	
ATM 029			x	x	x		x	x	x	
ATM 030			x	x	x		x	x	x	
ATM 031			x				x	x	x	
ATM 032			x	x	x		x	x	x	
ATM 033			x				x	x	x	
ATM 034			x	x	x		x	x	x	
ATM 035		x		x	x		x	x	x	
ATM 036		x		x	x		x	x	x	
ATM 037 in		x		x	x		x	x	x	
out							x	x	x	
ATM 038		x					x	x	x	
ATM 039		x					x	x	x	
ATM 040		x					x	x	x	
ATM 041 in		x					x	x	x	
out							x	x	x	
ATM 042		x					x	x	x	
Xanten										
3-4/B 04628	x			x	x		x	x	x	
25/A 04002	x			x	x		x	x	x	
69/20 7177(3) in	x			x	x		x			
out							x			
74/41 09404	x			x	x		x	x	x	
75/25 9788a2 in	x			x	x		x	x	x	

sample name	metal-melting crucible	brass-making crucible	mould	thin-section	SEM	Microprobe	XRD	XRF	TGA	Raman-Spectroscopy
75/25 9788a2 out							x	x	x	
75/25 9831a1(1) in	x			x	x		x			
out							x	x	x	
CUT 1959 00981	x			x	x		x	x	x	
Helg. 6/A 04695	x			x	x		x	x	x	
Augst (Augusta Raurica)										
T503	x						x	x	x	
T231	x			x	x		x	x	x	
T548	x						x	x	x	
T673	x			x	x		x	x	x	
T552 in	x						x	x	x	
out							x	x	x	
T862 in	x			x	x		x	x	x	
out							x	x	x	
T533	x						x	x	x	
T128	x						x	x	x	
T688 in	x			x	x		x	x	x	
out							x	x	x	
T168	x						x	x	x	
T454	x			x	x		x	x	x	
T262 in	x						x	x	x	
out							x	x	x	
T230 in	x			x	x		x	x	x	
out							x	x	x	
T289	x						x	x	x	
T225	x						x	x	x	
Avenches (Aventicum)										
MRA 67/5437(1)in	x			x	x		x	x	x	
out							x	x	x	
MRA 67/8442	x						x	x	x	
MRA 67/8519	x			x	x		x	x	x	
MRA 67/9918	x			x	x		x	x	x	

sample name	metal-melting crucible	brass-making crucible	mould	thin-section	SEM	Microprobe	XRD	XRF	TGA	Raman-Spectroscopy
MRA 68/1215 in	x			x	x		x	x	x	
out							x	x	x	
MRA 73/3409	x						x	x	x	
MRA 79/13516	x						x	x	x	
MRA 83/835	x						x	x	x	
MRA 03/11712-21	x						x	x	x	
MRA X/3319 in	x			x	x		x	x	x	
out							x	x	x	
Marsens En Barras										
359-126	x			x	x		x	x	x	
360-80	x			x	x		x	x	x	
460-27	x			x	x		x	x	x	
460-27/2	x			x	x		x			
460-30	x			x	x		x	x	x	
361-119	furnace walls						x	x	x	
361-120				x	x		x	x	x	
361-120/2							x	x	x	
361-114	“bouchon”			x	x		x	x	x	
N° 96/2646	ceramic samples			x	x		x			
N° 96/3074				x	x		x	x	x	
N° 678				x	x		x	x	x	
N° 708				x	x		x	x	x	
N° 715				x	x		x	x	x	
N° 718				x	x		x	x	x	
N° 722				x	x		x	x	x	
N° 750	ceramic samples			x	x		x	x	x	
N° 801				x	x		x	x	x	

APPENDIX 3 - METAL PRILL INVESTIGATIONS

Electron microprobe analyses on preserved metal particles are reported in Table A3-1. In general, there are two kinds of alloys present, Cu-Zn and Cu-Sn, with minor traces of iron and lead. These results confirm the primary assumption of a brass working-related origin of the analysed crucibles. Only two analyses (ATM 004) indicate a bronze composition. Chardon-Picault and Pernot (1999) published data for brass and bronze artefacts from Autun/France which fit the composition of the bronze droplets quite well. With respect to the reported brass artefacts from Autun/France, the brass droplets in this study show a significant Zn deviation of 6 to 10 wt.%. The lead content in our droplets is much smaller than the metal artefacts investigated by Chardon-Picault and Pernot (1999). Moreover, the occurrence of such differing alloy compositions in one and the same crucible fragment (ATM 004) is an evidence for a multiple usage. The different brass, gunmetal and bronze compositions in the two investigated samples and the disparity of these alloys related to their zinc and tin contents are illustrated in Fig. A3-1. The zinc content of the droplets decreases with the degree of reuse, because of the high diffusion rate during firing (Smigelskas and Kirkendall 1946). Overall, these differences in metal composition are only obtainable during several metal-melting processes within the same crucible and not explainable by an immiscibility of different alloys during one melting process.

Sample	Fe (wt.%)	Cu (wt.%)	Ni (wt.%)	Pb (wt.%)	Sn (wt.%)	Zn (wt.%)	Total
ATM 004	0.092	84.43	-	0.032	17.090	-	101.64
	0.156	93.23	-	0.056	1.770	2.390	97.60
	0.151	83.65	-	0.085	13.410	0.550	97.84
ATM 010	0.122	95.65	0.048	0.565	0.333	2.260	98.98
	0.613	89.84	-	0.065	0.596	8.850	99.96
	0.602	89.46	0.126	0.107	0.831	8.970	100.10
	0.568	88.94	-	0.034	0.968	9.330	99.84
	0.667	89.91	-	0.047	0.886	9.130	100.64
	0.486	89.51	-	0.105	0.772	9.080	99.95
	0.508	90.37	0.133	0.022	0.665	8.930	100.63
	0.616	89.80	0.099	0.038	0.607	8.810	99.97
	0.504	88.80	0.086	0.026	0.732	9.280	99.43
	0.638	89.58	0.026	0.143	0.583	8.420	99.39
	0.436	89.41	0.091	0.035	0.742	8.810	99.52

Sample	Fe (wt.%)	Cu (wt.%)	Ni (wt.%)	Pb (wt.%)	Sn (wt.%)	Zn (wt.%)	Total
ATM 010	0.651	89.74	0.221	0.107	0.726	8.890	100.33
	0.600	90.03	0.178	0.047	0.856	9.110	100.82
	0.506	89.66	-	0.019	0.994	9.110	100.29
	0.610	90.77	-	0.055	0.753	8.690	100.88
	0.488	89.98	0.176	0.087	0.912	8.860	100.50
	0.464	90.11	-	0.044	0.808	8.240	99.67
	0.456	90.00	-	0.051	0.800	8.330	99.64
	0.742	90.79	-	0.079	0.463	8.190	100.26
	0.632	90.45	-	0.030	0.378	7.560	99.05
	0.562	89.61	0.117	0.014	0.574	8.350	99.23
	0.490	89.37	-	0.049	0.886	8.390	99.19
	0.699	90.96	0.472	0.112	0.459	8.000	100.70

Table A3-1. *Microprobe analyses of the metal particles found in two of the investigated crucibles.*

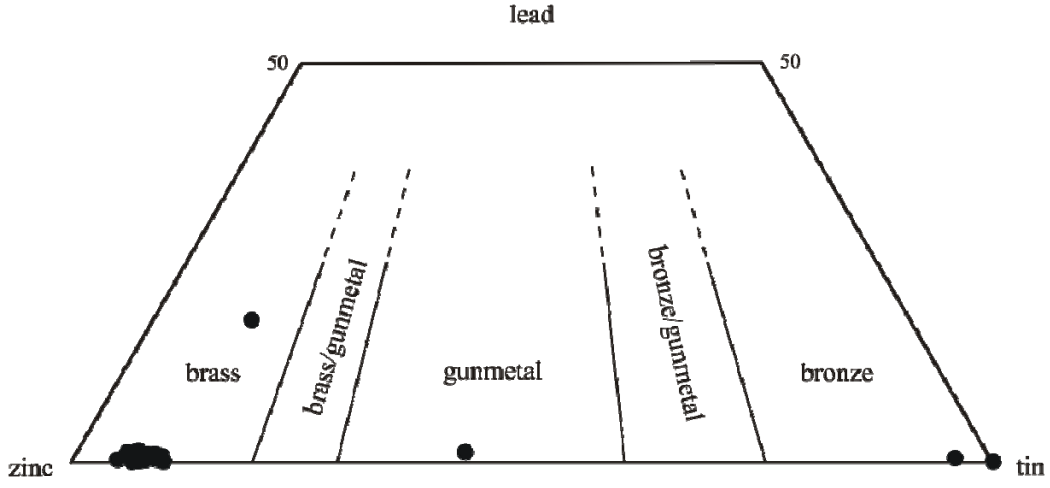

Figure A3-1. *Ternary diagram discriminating common copper-alloys (after Bayley and Butcher 2004) and demonstrating the variability of molten copper-alloys within single crucibles.*

APPENDIX 4 - LIST OF XRF-INVESTIGATIONS

	ATM 001_2 in	ATM 001_2 out	ATM 002_1	ATM 002_3 in	ATM 002_3 out	ATM 003_2 in	ATM 003_2 out	ATM 004_2 in	ATM 004_2 out	ATM 005_1 in	ATM 005_1 out	ATM 006_2 in	ATM 006_2 out	ATM 007_1	ATM 008_2 in	ATM 008_2 out
SiO_2 (wt.%)	68.5	69.2	70.7	72.8	67.5	72.2	74.6	68.6	73.2	73.2	72.1	69.9	67.2	71.5	69.2	67.9
TiO_2 (wt.%)	0.6	0.7	0.6	0.6	0.6	0.8	0.6	0.7	0.6	0.6	0.6	0.6	0.3	0.4	0.7	0.6
Al_2O_3 (wt.%)	23.9	15.3	20.6	20.8	19.0	20.3	15.7	23.6	15.3	20.1	17.7	20.5	17.2	18.4	24.1	20.0
Fe_2O_3 (wt.%)	1.8	3.1	1.4	1.3	1.7	2.0	2.4	1.6	3.2	1.5	3.4	1.9	1.9	1.3	1.6	2.9
MnO (wt.%)	0.02	0.07	0.05	0.02	0.13	0.04	0.07	0.02	0.05	0.02	0.03	0.05	0.16	0.03	0.01	0.06
MgO (wt.%)	0.6	0.8	0.5	0.4	0.9	0.4	0.7	0.5	0.9	0.5	0.6	0.6	0.8	0.5	0.4	0.9
CaO (wt.%)	0.5	4.3	1.4	0.3	4.8	0.3	0.9	0.4	0.6	0.3	0.6	1.1	5.7	2.2	0.2	1.7
Na_2O (wt.%)	0.4	1.1	0.4	0.3	0.4	0.4	0.8	0.4	1.0	0.4	0.5	0.5	0.6	0.6	0.2	0.7
K_2O (wt.%)	3.5	4.8	4.0	3.2	4.5	3.2	4.0	3.8	4.9	3.2	4.2	4.6	5.4	4.4	3.2	5.0
P_2O_5 (wt.%)	0.2	0.7	0.3	0.2	0.3	0.3	0.3	0.3	0.3	0.2	0.3	0.3	0.7	0.6	0.2	0.3
Sum before norm. (wt.%)	99.1	94.1	92.1	93.5	94.7	94.3	96.3	91.2	96.0	91.4	89.5	90.2	92.7	91.4	93.1	90.2
Sum norm. (wt.%)	100	100	100	100	100	100	100	100	100	100	100	100	100	100	100	100
Ba (ppm)	1000	1390	2120	1410	3140	1110	1400	1340	1930	1300	960	2080	1790	1300	1470	1670
Cr (ppm)	<100	<100	<100	<100	<100	<100	<100	<100	<100	<100	<100	<100	<100	<100	<100	<100
Cu (ppm)	1320	770	600	260	810	450	970	520	200	400	1060	410	2330	9210	240	200
Nb (ppm)	<100	<100	<100	<100	<100	<100	<100	<100	<100	<100	<100	<100	<100	<100	<100	<100
Ni (ppm)	<100	<100			<100		<100		<100	<100	<100	<100	<100		<100	<100
Pb (ppm)	<100	<100	<100	<100	<100	<100	<100	<100	<100	<100	100	<100	<100	120	<100	<100
Rb (ppm)	210	370	190	160	200	190	250	220	260	170	320	220	420	360	160	340
Sn (ppm)	230	<100	<100	<100	<100	<100	<100	<100		<100	<100	<100	<100	393	<100	
Sr (ppm)	<100	120	120	<100	210	100	110	110	120	<100	<100	110	170	100	<100	120
V (ppm)	<100	<100	<100	<100	<100	<100	<100	<100	<100	<100	<100	<100	<100	<100	<100	<100
Y (ppm)	<100	<100	<100	<100	<100	<100	<100	<100	<100	<100	<100	<100	<100	<100	<100	<100
Zn (ppm)	3960	1010	8880	3580	1540	25500	2650	28700	1760	15200	11600	12900	4400	8510	340	460
Zr (ppm)	240	340	230	240	220	260	300	280	350	240	300	230	160	160	220	220

	ATM 009_1 in	ATM 009_1 out	ATM 010_1 in	ATM 010_1 out	ATM 011_1 in	ATM 011_1 out	ATM 012_2	ATM 013_2 in	ATM 013_2 out	ATM 014_1 in	ATM 014_1 out	ATM 015_2	ATM 016_1	ATM 017_1 in	ATM 017_1 out	ATM 018_1 in	ATM 018_1 out
SiO_2 (wt.%)	64.5	71.4	67.8	65.7	68.6	74.7	71.6	70.4	69.6	68.1	69.5	72.5	66.9	71.3	69.4	71.1	72.6
TiO_2 (wt.%)	0.7	0.7	0.7	0.6	0.7	0.6	0.6	0.6	0.3	0.8	0.6	0.6	0.8	0.8	0.4	0.6	0.8
Al_2O_3 (wt.%)	28.5	16.8	24.6	15.6	23.6	10.3	18.9	19.9	17.9	23.2	13.3	19.2	23.4	20.4	17.5	19.8	12.9
Fe_2O_3 (wt.%)	1.7	3.0	2.0	4.1	1.8	2.7	1.7	2.0	1.8	2.0	3.9	1.8	2.1	2.1	1.8	1.8	2.5
MnO (wt.%)	0.01	0.05	0.03	0.46	0.03	0.39	0.06	0.06	0.11	0.02	0.45	0.03	0.02	0.04	0.25	0.05	0.15
MgO (wt.%)	0.6	0.8	0.5	0.5	0.6	0.7	0.5	0.7	0.7	0.6	0.7	0.7	0.6	0.5	0.8	0.6	0.8
CaO (wt.%)	0.2	1.7	0.3	3.0	0.3	4.0	1.6	1.1	3.1	0.4	3.8	0.5	1.4	0.5	4.4	1.0	3.5
Na_2O (wt.%)	0.3	0.9	0.3	2.7	0.4	0.8	0.7	0.5	0.8	0.5	0.9	0.5	0.4	0.5	0.6	0.4	0.7
K_2O (wt.%)	3.2	4.4	3.4	5.1	3.7	5.1	3.9	4.5	5.3	4.1	6.3	3.9	4.1	3.6	4.6	4.2	5.7
P_2O_5 (wt.%)	0.2	0.2	0.3	2.3	0.3	0.8	0.3	0.3	0.3	0.2	0.5	0.3	0.3	0.3	0.4	0.3	0.3
Sum before norm. (wt.%)	99.4	93.5	92.4	91.6	97.9	91.4	89.5	91.8	96.0	90.4	94.6	88.8	89.6	91.4	93.5	92.8	91.0
Sum norm. (wt.%)	100	100	100	100	100	100	100	100	100	100	100	100	100	100	100	100	100
Ba (ppm)	1070	1020	930	2810	1070	3800	1800	2040	1640	1160	1870	1350	1190	1130	1710	2190	1520
Cr (ppm)	<100	<100	<100	<100	<100	<100	<100	<100	<100	<100	<100	<100	<100	<100	<100	<100	<100
Cu (ppm)	150	390	4150	1520	1000	1830	880	450	5040	680	1810	140	770	200	330	300	710
Nb (ppm)	<100	<100	<100	<100	<100	<100	<100	<100	<100	<100	<100	<100	<100	<100	<100	<100	<100
Ni (ppm)	<100	<100	-	<100	<100	-	<100	-	-	-	-	-	-	<100	-	-	<100
Pb (ppm)	<100	<100	<100	<100	100	<100	<100	<100	<100	<100	<100	<100	<100	<100	<100	<100	<100
Rb (ppm)	210	270	220	630	240	320	310	230	450	260	410	240	270	230	400	200	440
Sn (ppm)	<100	<100	<100	<100	204	<100	<100	<100	165	<100	<100	<100	100	<100	<100	-	-
Sr (ppm)	100	120	<100	250	110	110	120	110	130	120	150	<100	130	100	210	100	170
V (ppm)	<100	<100	<100	<100	<100	<100	<100	<100	<100	<100	<100	<100	<100	<100	<100	<100	<100
Y (ppm)	<100	<100	<100	<100	<100	<100	<100	<100	<100	<100	<100	<100	<100	<100	<100	<100	<100
Zn (ppm)	6900	1060	7370	930	1000	450	8170	7670	4620	10900	470	7980	18300	12400	3180	7350	570
Zr (ppm)	240	330	250	280	250	400	240	230	140	280	370	230	300	280	170	220	510

	ATM 019	ATM 020 in	ATM 020 out	ATM 021	ATM 022	ATM 023	ATM 024	ATM 025	ATM 026	ATM 027	ATM 028	ATM 029	ATM 030	ATM 031	ATM 032	ATM 033	ATM 034
SiO_2 (wt.%)	67.1	72.1	68.3	67.2	66.5	71.1	70.4	68.3	70.9	68.5	70.5	70.4	70.7	70.1	66.9	69.9	70.2
TiO_2 (wt.%)	0.7	0.3	0.7	0.7	0.5	0.4	0.5	0.5	0.5	0.6	0.5	0.4	0.6	0.6	0.5	0.6	0.5
Al_2O_3 (wt.%)	19.8	19.1	19.6	20.3	21.3	20.5	19.1	20.3	19.1	19.6	19.6	19.7	17.8	18.5	21.3	19.4	20.2
Fe_2O_3 (wt.%)	4.8	2.0	4.6	4.8	4.2	2.4	3.3	3.7	3.6	4.4	3.6	2.9	3.5	3.3	3.5	3.7	3.0
MnO (wt.%)	0.04	0.03	0.04	0.04	0.04	0.02	0.05	0.03	0.04	0.03	0.04	0.02	0.04	0.04	0.04	0.03	0.02
MgO (wt.%)	1.6	0.7	1.5	1.6	1.4	0.9	1.0	1.1	0.8	1.3	0.8	1.1	1.0	1.0	1.3	1.1	1.0
CaO (wt.%)	0.8	0.9	0.4	0.6	0.5	0.4	0.3	0.4	0.4	0.6	0.4	0.5	0.6	1.0	0.8	0.6	0.4
Na_2O (wt.%)	1.0	0.2	0.9	0.8	1.0	0.4	0.9	0.9	0.4	0.8	0.4	0.8	1.1	0.7	0.7	0.6	0.6
K_2O (wt.%)	3.6	3.6	3.6	3.6	4.3	3.6	4.2	4.6	3.8	3.8	4.0	4.0	4.2	3.9	4.2	3.7	3.9
P_2O_5 (wt.%)	0.6	1.1	0.3	0.4	0.4	0.4	0.1	0.2	0.3	0.4	0.3	0.2	0.3	0.9	0.8	0.4	0.2
Sum before norm.(wt.%)	97.0	100.0	98.7	98.2	96.3	99.7	97.4	96.8	98.1	97.4	96.0	98.1	96.2	94.9	99.2	97.0	98.7
Sum norm. (wt.%)	100	100	100	100	100	100	100	100	100	100	100	100	100	100	100	100	100
Ba (ppm)	2150	2210	2430	1870	1260	1220	1500	1650	1190	1740	1130	1900	1900	1250	1700	1630	1190
Cr (ppm)	<100	<100	<100	<100	<100	<100	<100	<100	<100	<100	<100	<100	<100	<100	<100	<100	<100
Cu (ppm)	180	370	100	270	350	270	<100	280	120	500	140	140	370	1300	280	230	<100
Nb (ppm)	<100	<100	<100	<100	<100	<100	<100	<100	<100	<100	<100	<100	<100	<100	<100	<100	<100
Ni (ppm)	-	-	-	-	-	-	-	-	-	-	-	-	-	-	-	-	-
Pb (ppm)	120	110	120	130	110	110	110	110	110	120	120	130	210	120	150	140	110
Rb (ppm)	340	380	350	330	390	370	370	400	320	340	350	390	320	310	380	360	390
Sn (ppm)	-	-	-	-	<100	-	-	-	<100	-	-	-	<100	<100	-	<100	-
Sr (ppm)	120	110	110	110	110	100	100	100	<100	100	85	100	120	120	120	100	<100
V (ppm)	<100	<100	<100	<100	<100	<100	<100	<100	<100	<100	<100	<100	<100	<100	<100	<100	<100
Y (ppm)	<100	<100	<100	<100	<100	<100	<100	<100	<100	<100	<100	<100	<100	<100	<100	<100	<100
Zn (ppm)	460	400	250	340	900	1030	290	540	760	910	660	1370	900	1270	1690	1030	1750
Zr (ppm)	320	150	330	310	260	190	300	270	310	290	330	220	390	360	240	290	230

	ATM 035	ATM 036	ATM 037 in	ATM 037 out	ATM 038	ATM 039	ATM 040	ATM 041 in	ATM 041 out
SiO_2 (wt.%)	69.8	69.3	68.0	66.4	72.5	72.5	65.5	71.2	70.1
TiO_2 (wt.%)	0.7	0.8	0.9	0.6	0.5	0.4	0.5	0.4	0.4
Al_2O_3 (wt.%)	22.1	22.8	23.0	23.4	19.3	20.5	23.1	21.5	21.5
Fe_2O_3 (wt.%)	2.6	2.5	3.1	3.7	2.2	2.3	4.8	2.9	2.6
MnO (wt.%)	0.02	0.03	0.02	0.05	0.01	0.03	0.12	0.05	0.02
MgO (wt.%)	0.6	0.6	0.7	0.6	0.6	0.5	1.0	0.5	0.4
CaO (wt.%)	0.3	0.3	0.5	0.6	0.3	0.3	1.1	0.4	0.2
Na_2O (wt.%)	0.5	0.1	0.5	0.3	0.7	0.3	0.6	0.0	0.4
K_2O (wt.%)	3.2	3.5	3.2	3.5	3.7	3.0	2.7	2.9	4.3
P_2O_5 (wt.%)	0.2	0.1	0.2	0.7	0.1	0.1	0.6	0.1	0.1
Sum before norm.(wt.%)	95.9	104.2	94.5	96.7	91.1	97.5	94.5	96.4	88.1
Sum norm. (wt.%)	100	100	100	100	100	100	100	100	100
Ba (ppm)	960	830	900	1770	1330	890	1090	580	1020
Cr (ppm)	<100	<100	<100	<100	<100	<100	<100	<100	<100
Cu (ppm)	<100	150	1040	360	<100	<100	490	100	<100
Nb (ppm)	<100	<100	<100	<100	<100	<100	<100	<100	<100
Ni (ppm)	-	-	-	-	-	-	-	-	-
Pb (ppm)	160	<100	320	180	350	<100	190	<100	<100
Rb (ppm)	290	250	320	270	260	190	210	150	310
Sn (ppm)	<100	-	-	-	-	-	-	<100	-
Sr (ppm)	<100	<100	110	130	100	<100	100	<100	110
V (ppm)	<100	<100	<100	<100	<100	<100	<100	<100	<100
Y (ppm)	<100	<100	<100	<100	<100	<100	<100	<100	<100
Zn (ppm)	102500	208200	60700	19000	99600	133900	87100	213800	39900
Zr (ppm)	320	150	330	310	260	190	300	270	310

	T503[1]	T231[1]	T548[3]	T673[1]	T552 i.l.[3]	T552 a.l.[1]	T862 i.l.[1]	T862 a.l.[1]	T128[1]*	T168[1]*	T688 i.l.[2]	T688 a.l.[1]	T533[2]	T454[2]	T262 i.l.[3]	T262 a.l.[2]	T230 i.l.[3]	T230 a.l.[1]	T289[1]	T225[1]*
SiO_2 (wt.%)	76.9	72.9	73.3	75.0	79.0	77.9	69.4	76.5	78.5	81.1	69.9	76.1	76.9	72.3	76.4	71.2	78.4	75.3	79.0	79.4
TiO_2 (wt.%)	0.7	0.8	0.7	1.0	0.7	0.6	0.8	0.7	0.9	0.9	0.5	0.5	0.5	0.6	0.7	0.4	0.9	0.7	0.9	1.3
Al_2O_3 (wt.%)	12.5	15.4	14.8	15.0	15.9	8.7	17.6	10.9	16.1	14.3	17.7	9.6	13.7	16.0	13.4	11.5	17.4	11.9	14.2	15.9
Fe_2O_3 (wt.%)	3.3	3.6	4.5	2.8	2.3	5.7	5.9	4.6	2.3	1.7	5.4	3.9	3.4	3.6	3.4	4.5	1.7	4.3	1.5	1.6
MnO (wt.%)	0.09	0.06	0.22	0.05	0.03	0.12	0.06	0.11	<0.01	<0.01	0.06	0.10	0.09	0.11	0.09	0.39	0.05	0.13	0.01	<0.01
MgO (wt.%)	1.0	0.9	1.1	0.8	0.4	0.9	1.0	1.2	0.6	0.5	1.0	1.3	0.9	1.1	1.1	1.9	0.4	1.3	0.3	0.4
CaO (wt.%)	2.1	2.7	2.1	3.0	1.0	2.1	0.7	2.0	1.0	0.8	0.7	3.7	1.7	3.2	2.8	4.3	0.5	2.0	0.7	0.9
Na_2O (wt.%)	1.1	1.3	0.7	0.6	0.2	1.2	0.5	1.3	0.1	0.2	0.6	1.3	0.8	0.8	0.7	1.4	0.1	1.3	2.6	0.3
K_2O (wt.%)	1.9	2.0	2.3	1.7	0.4	2.6	3.9	2.5	0.4	0.4	3.9	3.2	1.8	1.9	1.1	3.5	0.4	2.6	0.6	0.2
P_2O_5 (wt.%)	0.3	0.4	0.3	0.2	0.1	0.3	0.2	0.3	0.0	0.0	0.2	0.4	0.3	0.4	0.4	0.9	0.1	0.4	0.1	0.0
Sum before norm. (wt.%)	97.1	97.1	95.8	97.4	92.8	97.8	96.4	96.4	95.6	97.7	93.4	99.1	87.8	91.9	93.3	92.5	95.5	98.8	96.8	98.1
Sum norm. (wt.%)	100	100	100	100	100	100	100	100	100	100	100	100	100	100	100	100	100	100	100	100
Ba (ppm)	306	307	1400	215	2000	325	3498	365	91	112	3800	416	450	800	1400	1200	1900	440	88	87
Cr (ppm)	90	114	<100	114	100	76	98	88	115	105	<100	74	<100	100	100	<100	100	89	101	116
Cu (ppm)	550	1000	32000	200	7200	250	250	700	100	650	500	950	9600	4800	130800	21800	3200	500	600	46
Nb (ppm)	17	16	<100	20	<100	12	18	15	20	21	<100	13	<100	<100	<100	<100	<100	16	17	28
Ni (ppm)	34	44	100	35	-	45	42	45	27	27	<100	30	<100	<100	-	<100	-	44	37	19
Pb (ppm)	250	1200	9700	220	350	140	600	180	25	110	150	90	1100	550	14000	900	2900	610	140	190
Rb (ppm)	77	71	<100	64	<100	85	202	97	26	21	250	117	100	<100	<100	100	<100	101	21	7
Sn (ppm)	100[2]	-	4600	<100[2]	450	-	-	-	-	-	<100	-	250	1250	13200	3100	500	-	<100[2]	-
Sr (ppm)	115	296	<100	108	<100	98	157	131	52	45	150	117	100	150	<100	200	<100	124	38	41
V (ppm)	77	148	130	123	<100	59	108	79	102	90	100	71	100	100	150	<100	150	84	87	86
Y (ppm)	34	29	<100	27	<100	29	34	39	23	24	<100	31	<100	<100	<100	<100	<100	39	21	25
Zn (ppm)	4230	7060	94400	1445	38200	2615	2525	210	60	425	9300	190	15600	1400	9800	2000	36900	2640	73865	20
Zr (ppm)	307	306	300	283	300	341	255	355	242	278	300	276	400	400	300	450	450	365	248	277
Σ melt-%	0.53	0.95	14.69	0.20	4.98	0.31	0.35	0.11	0.02	0.12	1.07	0.12	3.02	0.87	17.98	3.00	4.55	0.38	7.71	0.03

[1] glass pills; [2] press pills; [3]glass-press pills; * unused

	MRA 67/5437[1] i.l. [3]	MRA 67/5437[1] a.l. [1]	MRA 67/8442[2]	MRA 67/8519[1]	MRA 67/9918[2]	MRA 68/1215 i.l. [3]	MRA 68/1215 a.l. [2]	MRA 73/3409[1]	MRA 79/13516[1]	MRA 83/835[1]	MRA 03/11712-21[1]	MRA X/3319 i.l. [3]	MRA X/3319 a.l. [2]
SiO_2 (wt.%)	77.4	73.4	73.4	66.0	72.3	71.2	75.5	76.8	78.5	77.8	81.1	77.9	71.8
TiO_2 (wt.%)	0.8	0.5	0.3	0.6	0.4	0.8	0.4	0.4	0.4	0.4	0.5	0.5	0.3
Al_2O_3 (wt.%)	17.1	12.1	11.8	14.7	13.0	22.4	10.7	11.2	11.2	10.6	11.2	14.0	11.0
Fe_2O_3 (wt.%)	2.0	3.8	4.3	5.2	3.4	2.1	3.6	3.8	2.5	3.0	2.6	3.6	3.5
MnO (wt.%)	0.02	0.13	0.13	0.13	2.56	0.04	0.18	0.11	0.11	0.09	0.05	0.03	0.24
MgO (wt.%)	0.7	1.5	1.3	2.9	1.3	0.7	1.3	1.2	1.2	1.1	0.7	0.8	1.5
CaO (wt.%)	1.2	2.9	2.8	4.7	3.2	0.6	3.8	1.5	1.1	2.3	1.3	1.4	5.7
Na_2O (wt.%)	0.3	2.0	1.9	1.9	0.4	0.4	1.1	2.0	2.2	2.0	0.9	0.6	1.8
K_2O (wt.%)	0.5	3.3	3.3	3.5	2.6	1.8	3.2	2.6	2.6	2.5	1.3	0.9	3.7
P_2O_5 (wt.%)	0.1	0.3	0.7	0.3	0.8	0.1	0.3	0.2	0.2	0.2	0.2	0.2	0.5
Sum before norm.(wt.%)	91.2	98.8	86.5	99.2	98.6	97.8	90.6	99.3	99.3	99.2	98.9	95.4	86.1
Sum norm. (wt.%)	100	100	100	100	100	100	100	100	100	100	100	100	100
Ba (ppm)	2100	441	680	412	1250	23700	1940	374	351	347	207	800	900
Cr (ppm)	150	82	<100	75	<100	<100	100	78	81	73	88	<100	<100
Cu (ppm)	4100	350	1500	900	5550	3000	3400	150	200	71	26	39100	1050
Nb (ppm)	<100	10	<100	14	<100	700	<100	10	8	10	14	<100	<100
Ni (ppm)	-	44	<100	37	<100	-	<100	33	24	29	33	-	<100
Pb (ppm)	800	350	450	1500	150	750	<100	140	500	143	28	26200	400
Rb (ppm)	<100	123	150	156	<100	400	150	103	102	99	59	<100	150
Sn (ppm)	<100	-	800	-	550	-	<100	<100[2]	<100[2]	-	-	28200	450
Sr (ppm)	<100	135	150	143	100	400	150	96	94	111	69	<100	200
V (ppm)	200	67	<100	89	100	-	<100	64	53	51	82	100	<100
Y (ppm)	<100	27	<100	36	<100	<100	<100	32	31	28	22	-	<100
Zn (ppm)	9300	129	4650	90	63500	2000	100	111	3738	92	54	8900	750
Zr (ppm)	350	157	250	153	200	1700	500	183	185	175	200	250	250
Σ melt-%	1.56	0.08	0.86	0.25	7.07	0.59	0.40	0.05	0.45	0.03	0.01	10.73	0.30

	3-4/B 04628	25/A 04002	74/41 09404	75/25 9788a2 in	75/25 9788a2 out	75/25 9831a1(1) out	CUT 1959 00981	Helg. 6/A 04695
SiO_2 (wt.%)	79.2	80.4	81.7	73.5	69.9	75.8	81.0	69.2
TiO_2 (wt.%)	0.4	1.2	0.6	0.8	0.5	0.4	0.8	0.5
Al_2O_3 (wt.%)	12.3	25.1	15.4	23.8	16.4	13.2	17.2	14.9
Fe_2O_3 (wt.%)	3.4	3.7	3.3	2.7	6.6	6.8	2.3	4.0
MnO (wt.%)	0.09	0.04	0.10	0.02	0.70	0.18	0.05	0.21
MgO (wt.%)	1.1	0.7	1.2	1.1	2.3	1.3	0.6	1.4
CaO (wt.%)	3.5	1.0	4.0	0.7	2.9	1.7	0.6	2.1
Na_2O (wt.%)	0.9	0.8	0.8	0.4	1.0	1.0	0.4	0.9
K_2O (wt.%)	3.0	2.0	2.5	2.8	3.7	2.9	1.7	3.9
P_2O_5 (wt.%)	0.5	0.2	0.4	0.2	1.1	0.4	0.2	0.8
Sum before norm.(wt.%)	94,6	85,6	89,4	93,3	93,8	95,5	94,2	97,8
Sum norm. (wt.%)	100	100	100	100	100	100	100	100
Ba (ppm)	1360	790	760	1030	1510	1610	870	1340
Cr (ppm)	<100	130	<100	130	100	100	110	100
Cu (ppm)	980	<100	400	350	900	430	<100	17200
Nb (ppm)	<100	<100	<100	<100	<100	<100	<100	<100
Ni (ppm)	<100	<100	-	<100	<100	<100	<100	<100
Pb (ppm)	260	680	180	<100	120	760	<100	1130
Rb (ppm)	140	130	150	190	170	140	160	110
Sn (ppm)	270	<100	130	-	-	<100	-	2830
Sr (ppm)	200	170	220	170	180	130	120	190
V (ppm)	<100	100	120	200	120	<100	210	130
Y (ppm)	<100	<100	<100	<100	<100	<100	<100	<100
Zn (ppm)	2090	1040	7210	3280	390	140	3380	5390
Zr (ppm)	270	310	310	230	300	330	470	440

REFERENCES

Artioli, G., Angelini, I., and Polla, A., 2008, Crystals and phase transitions in protohistoric glass materials, *Phase Transit,* **81**, 233-52.

Bachmann, H.-G., 1976, Crucibles from Roman settlement in Germany, *Journal of the Historical Metallurgy Society*, **10**, 139-44.

Bayley, J., 1984, Roman brass-making in Britain, *Historical Metallurgy*, **18(1)**, 42-43.

Bayley, J., 1987, Non-ferrous metalworking: continuity and change, in Science and Archaeology, BAR, *International Series,* **169**, 193-208.

Bayley, J., 1990, The production of brass in antiquity with particular reference to Roman Britain, 2000 years of Zinc and Brass, *British Museum*, 7-28.

Bayley, J., 1992, Metalworking ceramics. *Medieval Ceramics,* **16**, 3-10.

Bayley, J., and Butcher, S., 2004, Roman Brooches in Britain: A Thechnological and Typological Study based on the Richborough Collection, The Society of Antiquaries of London (No. 68), London.

Bayley, J., Dungworth, D., and Paynter, S., 2001, *Archaeometallurgy*, Swindon.

Bayley, J., and Rehren, Th., 2007, Towards a functional and typological classification of crucibles, in Metals and Mines - Studies in Archaeometallurgy (eds. S. La Niece, D. Hook, and P. T. Craddock), 46-55, Archetype, London.

Beck, F., Monthel, G., and Rabeisen, E., 1982/3, Note sur un moule à fibules de Bibracte. *Antiquités Nationales,* **14/15**, 78-85.

Bellotto, M., Gualtieri, A. F., Artioli, G., and Clark, S. M., 1995, Kinetic Study of the Kaolinite- Mullite Reaction Sequence. Part I: Kaolinite Dehydroxylation, *Physics and Chemistry of Minerals,* **22**, 207-14.

Berger, L., 2012, Führer durch Augusta Raurica, Basel (7th ed.).

Bögli, H., 1996, Aventicum. La ville romaine et le musée, *Guides archéologiques de la Suisse*, **19**, Avenches (3rd ed.).

Buxeda, J., Mommsen, H., and Tsolakidou, A., 2002, Alterations of Na, K and Rb concentrations in Mycenaean pottery and a proposed explanation using X-ray diffraction. *Archaeometry,* **44**, 187-98.

Chardron-Picault, P., and Picon, M., 1997, La fabrication du laiton, à Autun, durant la période romaine: premières recherches, *Mémoires de la Société éduenne,* LVI, **2**, 171-81.

Chardron-Picault, P., and Pernot, M., 1999, Un quartier antique d'artisanat métallurgique à Autun- Le site du Lycée militaire. Editions de la Maison des sciences de l'homme. *Documents d'Archéologie Française*, **76**, Paris.

Chardron-Picault, P., Guillaumet, J.-P., and Labaune, Y., 2010, De Bibracte à Augustodunum: Permanences et évolutions de activités manufacturières de L'epoque

Gauloise à la fin du Haut-Empire, in Aspects de l'artisanat en milieu urbain: Gaule et Occident romain (eds. P. Chardron-Picault), 109-22, Revue Archéologique de L'Est, Dijon.

Chen, C.-Y., and Tuan, W.-H., 2002, Evolution of Mullite Texture on Firing Tape-Cast Kaolin Bodies. *Journal of the American Ceramic Society*, **85**, 1121-26.

Craddock, P., and Eckstein, K., 2003, Production of brass in Antiquity by direct reduction, in Mining and Metal Production Through the Ages (eds. P. Craddock and J. Lang), 216-230, The British Museum Press, London.

Daszkiewicz, M., and Schneider, G., 2011, Archäokeramologische Klassifizierung am Beispiel kaiserzeitlicher Drehscheibenkeramik aus Brandenburg, in *Drehscheibentöpferei im Barbaricum. Technologietransfer und Professionalisierung eines Handwerks am Rande des Römischen Imperiums* (eds. J. Bemmann, M. Hegewisch, M. Meyer and M. Schmauder), 17-33, Bonner Beiträge zur Vor- und Frühgeschichtlichen Archäologie, **13**, Bonn.

Davey, C. J., 2009, The early history of lost-wax casting, in Metallurgy and Civilization: Eurasia and Beyond Archetype (eds. J. Mei, and Th. Rehren), 147-54, London.

Dungworth, D. B., 1995, Iron Age and Roman copper alloys from northern Britain, Doctoral thesis, Durham University.

Eitel, W., 1966, Silicate Science. Volume 5. Ceramics and Hydraulic Binders. Academic Press, New York, London.

Eramo, G., 2005, The melting furnace of the Derrière Sairoche glassworks (Court, Swiss Jura): heat-induced mineralogical transformations and their technological signification, *Archaeometry,* **47**, 571-92.

Eramo, G., 2006 (a), The glass-melting crucibles of Derrière Sairoche (1699-1714 AD, Ct. Bern, Switzerland): a petrological approach, *Journal of Archaeological Science,* **33**, 440-52.

Eramo, G., 2006 (b), Pre-industrial glassmaking in the Swiss Jura: the refractory earth for the glassworks of Derrière Sairoche (ct. Bern, 1699–1714), in *Geomaterials in Cultural Heritage* (eds. M. Maggetti and B. Messiga), 187-99, Geological Society London, Special Publications, **257**, London.

Ferrari, S., and Gualteri, A. F., 2006, The use of illitic clays in the production of stoneware tile ceramics, *Applied Clay Science,* **32**, 73-81.

Freestone, I. C., 1989, Refractory Materials and Their Procurement, in, Old World Archaeometallurgy (eds. A. Hauptmann, E. Pernicka, and G. Wagner), 155-62, *Der Anschnitt*, Beiheft **7**, Deutsches Bergbau-Museum, Bochum.

Furger, A. R., 1995, Augusta Raurica. English Guide. *Archaeological guide to Augst and Kaiseraugst*, **2**, Augst.

Furger, A. R., 1998, Die Bronzewerkstätten in der Augster Insula 30. *Jahresberichte aus Augst und Kaiseraugst*, **19**, 121-40.

Furger, A. R., forthcoming (a), Das Bronzehandwerk in Augusta Raurica 1: Die Schmelztiegel und die darin nachgewiesenen Legierungen; ibid. 2: Die Gussformen, Halbfabrikate, Werkzeuge und Werkstattabfälle; ibid. 3: Die Werkstätten, ihre Technologie und Produkte (= *Forschungen in Augst*, 3 vol.).

Furger, A. R., forthcoming (b), Das Bronzehandwerk in Augusta Raurica 1 (mit einem Beitrag von M. Helfert), Die Schmelztiegel und die darin nachgewiesenen Legierungen, *Forschungen in Augst*, 2014/2015.

Furger, A. R., forthcoming (c), Das Bronzehandwerk in Augusta Raurica 2 (mit einem Beitrag von M. Helfert), Die Gussformen, Halbfabrikate, Werkzeuge und Werkstattabfälle, *Forschungen in Augst*.

Furger, A. R., forthcoming (d), Das Bronzehandwerk in Augusta Raurica 3 (mit einem Beitrag von M. Helfert), Die Werkstätten, ihre Technologie und Produkte, *Forschungen in Augst*.

Goren, Y., Mommsen, H., and Klinger, J., 2011, Non-destructive provenance study of cuneiform tablets using portable X-ray fluorescence (pXRF), *Journal of Archaeological Science,* **38**, 684-96.

Gualtieri, A., Bellotto, M., Artioli, G., and Clark, S. M., 1995, Kinetic study of the kaolinite-mullite reaction sequence. Part II: mullite formation. *Physics and Chemistry of Minerals,* **22**, 215-22.

Guggenheim, S., Chang, Y.-H., and Koster van Groos, A. F., 1987, Muscovite dehydroxylation: High-temperature studies, *American Mineralogist*, **72**, 537-50.

Helfert, M., 2013, Die portable energiedispersive Röntgenfluoreszenzanalyse (P-ED-RFA) – Studie zu methodischen und analytischen Grundlagen ihrer Anwendung in der archäologischen Keramikforschung, in *Naturwissenschaftliche Analysen vor- und frühgeschichtlicher Keramik III: Methoden, Anwendungsbereiche, Auswertungsmöglichkeiten* (eds. B. Ramminger, O. Stilborg and M. Helfert), 11-43, Universitätsforschungen zur Prähistorischen Archäologie, **238**, Habelt, Bonn.

Helfert, M., and Böhme, D., 2010, Herkunftsbestimmung von römischer Keramik mittels portabler energiedispersiver Röntgenfluoreszenzanalyse (p-ED-RFA) - erste Ergebnisse einer Anwendungsbezogenen Teststudie, in *Naturwissenschaftliche Analysen vor- und frühgeschichtlicher Keramik I: Methoden, Anwendungsbereiche, Auswertungsmöglichkeiten* (eds. B. Ramminger and O. Stilborg,), 11-30, Universitätsforschungen zur Prähistorischen Archäologie, **176**, Habelt, Bonn.

Helfert, M., and Ramminger, B., 2012, Neue Perspektiven für geochemische Untersuchungen von neolithischen Steingeräten – Ein Methodenvergleich zwischen portabler energiedispersiver Röntgenfluoreszenzanalyse (P-ED-RFA) und wellenlängendispersiver Röntgenfluoreszenzanalyse (WD-RFA) am Beispiel von bandkeramischenschen Dechselklingen aus Diemarden (Südniedersachsen), *Hamburg University Press*, Hamburg.

Helfert, M., Mecking, O., Lang, F., and von Kaenel, H.-M., 2011, Neue Perspektiven für die Keramikanalytik. Zur Evaluation der portablen energiedispersiven Röntgenfluoreszenzanalyse (P-ED-RFA) als neues Verfahren für die geochemische Analyse von Keramik in der Archäologie. *Frankfurter elektronische Rundschau zur Altertumskunde,* **14**, 1-30.

Hein, A., Kilikoglou, V., Kassianidou, V., 2007, Chemical and mineralogical examination

of metallurgical ceramics from a Late Bronze Age copper smelting site in Cyprus, *Journal of Archaeological Science,* **34**, 141-54.

Hill, V. G., and Roy, R., 1958, Silica structure studies, VI, on tridymite, *Transactions of the British Ceramic Society*, **57**, 496-510.

Holmquist, S. B., 1961, Conversion of quartz to tridymite, *Journal of the American Ceramic Society,* **44**, 82-6.

Jackson, R. P. J., and Craddock, P. T., 1995, The Ribchester Hoard: a descriptive and technical study, in Sites and Sights of the Iron Age (eds. B. Raftery, V. Megaw and V. Rigby), Oxbow Monograph, **56**, Oxford, 75-102.

Jornet, A., 1982, Analyse minéralogique et chimique de la céramique romaine suisse à enduit brillant. PhD Thesis n°846, Institut de Minéralogie et de Pétrographie, Université de Fribourg.

Jornet, A., and Maggetti, M., 1986, Chemische Analyse von 40 Scherben der Grabungen beim Augster Osttor im Jahre 1966, *Jahresberichte aus Augst und Kaiseraugst*, **5**, 107-22.

Jornet, A., and Maggetti, M., 2003, Analyse chimique, minéralogique et technique de la céramique de vaisselle de Liebrüti, in *AUGUSTA RAURICA. Probleme, Anregungen und Neufunde* (eds. T. T. Buck), 55-79, Schriften des Vorarlberger Landesmuseums. Reihe A, Landschaftsgeschichte und Archäologie, **7**.

Kearns, T., Martinón-Torres, M., and Rehren, Th., 2010, Metal to mould: alloy identification in experimental casting moulds using XRF, *Historical Metallurgy,* **44(1)**, 48–58.

König, D., and Serneels, V., 2013, Roman double-layered crucibles from Autun/France: a petrological and geochemical approach, *Journal of Archaeological Siences,* **40**(1), 156-65.

König, D., in prep. (a), A petrographical and geochemical characterisation of Roman moulds and brass-making crucibles from Autun/France, *Journal of Archaeological and Anthropological Sciences.*

König, D., in prep. (b), An analytical study of Roman crucibles from Xanten/Germany.

König, D., Helfert, M., and Furger, A. R., in prep., Roman crucibles from Augusta Raurica (Augst, Switzerland) – an interdisciplinary approach with laboratory and portable analysis, *Archaeometry.*

Lee, W. E., and Iqbal, Y., 2001, Influence of mixing on mullite formation in porcelain, *Journal of the European Ceramic Society*, **21**, 2583-86.

Lee, S., Kim, Y. J., and Moon, H., 1999, Phase transformation sequence from kaolinite to mullite investigated by energy-filtering transmission electron microscope, *Journal of the American Ceramic Society,* **43**, 2841-48.

Lee, W. E., Souza, G. P., McConville, C. J., Tarvornpanich, T., and Iqbal, Y., 2008, Mullite formation in clays and clay-derived vitreous ceramics, *Journal of the European ceramic society,* **28**, 465-71.

Maggetti, M., and Kahr, G., 1980, Homogenität archäologischer keramischer Objekte: Teil I. Porosität und Porenradienverteilung, *Archäologie und Naturwissenschaften,* **2**, 1-20.

Maggetti, M., and Galetti, G., 1993, Die Baukeramik von Augusta Raurica- eine mineralogisch-chemisch-technische Untersuchung, *Jahresberichte aus Augst und Kaiseraugst,* **14**, 199-225.

Maggetti, M., Rosen, J., Neururer, C., and Serneels, V., 2010, Paul-Louis Cyfflé's (1724-1806) Terre de Lorraine: a technological study, *Archaeometry,* **52**, 707-32.

Marquart, M., 1935, Note sur les moules à fibules découverts à Nandin (Château-Porcien, Ardennes), *B Societe de Archéologie Champenoise,* **1.4**, 18-25.

Martin, M., 1978, Römische Bronzegiesser in Augst BL*, Archäologie der Schweiz,* **1**, 112-20.

Martinón-Torres, M., Freestone, I. C., Hunt, A., and Rehren, Th., 2008, Mass-Produced Mullite Crucibles in Medieval Europe: Manufacture and Material Properties, *Journal of the American Ceramic Society,* **91**(6), 2071-74.

Martinon-Torres, M., and Rehren, Th., 2002, Agricola and Zwickau: theory and practice of Renaissance brass production in SE Germany, *Historical Metallurgy,* **36**(2), 95-111.

May, J. O., and Butterworth, B., 1962, Studies of pore size distribution III. The effect of firing temperatures. *Science of Ceramics*, **1**, 201-21.

Meylan Krause, M.-F., and Rossier, E., 2009, Marsens-Riaz, une agglomeration romaine au coeur de la Gruyere, Cahiers d'Archeologie Fribourgeoise, **11**, 110-129.

Moesta, H., 1986, Erze und Metalle - ihre Kulturgeschichte im Experiment, Springer Verlag, Berlin.

Morel, J., and Chevalley, Ch., 2001, (avec la coll. de D. Castella), La fabrication de grands bronzes à Aventicum: une fosse de coulée dans l'insula 12. *Bulletin de l'Association Pro Aventico*, **43**, 141-62.

Modarressi-Tehrani, D., 2004, Ein Ensemble frühlatènezeitlicher Metallverarbeitung aus der Siedlung von Eberdingen-Hochdorf (Lkr. Ludwigsburg). *Metalla*, **11.1**, Bochum.

Newman, A. C. D., 1987, Chemistry of clay minerals, *Mineralogical society monograph*, **No.6**, Wiley, New York.

Nielen, H.-D., 2006, Zink oder Messing? Ein Beitrag zu den metallurgischen Tätigkeiten im Legionslager Neuss, *Metalla,* **13.1**, Bochum.

Onike, F., Martin, G. D., and Dunham, A. C., 1986, Time-temperature transformation curves for kaolinite, *Material Science Forum,* **7**, 73-82.

Osborn, E. F., 1977, Phase-Diagrams and Refractories, *American Ceramic Society Bulletin*, **56**, 654-59.

Peron, P., and Feiffer, L.-C., 1987, Les Francs. Tome 1 : A la conquête de la Gaule, Armand Colin (Coll. Civilisations), Paris.

Picon, M., le Nezet-Celestin, M., and Desbat, A., 1995, Un type particulier de grands recipients en terre refractaire utilises pour la fabrication du laiton par cementation, *Société Française d'Étude de la Céramique Antique en Gaule*, Actes du Congrès de Rouen, 207-15.

Potts, Ph. J., and West, M., 2008, Portable X-ray fluorescence spectrometry, Capabilities for in situ analysis, Cambridge.

Pradell, T., Molera, J., Salvado, N., and Labrador, A., 2010, Synchrotron radiation micro-XRD in the study of glaze technology, *Applied Physics a-Materials Science & Processing,* **99**, 407-17.

Rehren, Th., 1995, Bericht über die Untersuchungen zweier römischer

Gußtiegel aus Vetera Castra (Xanten), in Vetera I. Die Funde aus den römischen Lagern auf dem Fürstenberg bei Xanten (ed. Hassel, N.), *Rheinische Ausgrabungen*, **35**, Köln.

Rehren, Th., 1997, Tiegelmetallurgie - Tiegelprozesse und ihre Stellung in der Archäometallurgie, Habilitation Thesis TU Bergakademie Freiberg, 115 p.

Rehren, Th., 1999, Small size, large scale: Roman brass production in Germania Inferior, *Journal of Archaeological Sciences,* **26**(8), 1083-87.

Rehren, Th., 2003, Crucibles as reaction vessels in ancient metallurgy, in *Mining and Metal Production Through the Ages* (ed. Craddock, P.T., and Lang, J.), 207-215, British Museum Press, London, UK.

Rehren, Th., and Martinón-Torres, M., 2008, Archaeology, History and Science: Integrating approaches to Ancient Materials. Walnut Creek: Left Coast Press.

Schmid, D., Thierrin-Michael, G., and Galetti, G., 1999, L'atelier Venusstrasse-Ost, partie sud, à Augusta Raurica (Augst) et la distribution de sa production: résultats des analyses, *SFECAG, Actes du Congrès de Fribourg*, 63-70.

Schwedt, A., Mommsen, H., Zacharias, N., and Buxeda, J., 2006, Analcime crystallization and compositional profiles - comparing approaches to detect post-depositional alterations in archaeological pottery. *Archaeometry,* **48**, 237-51.

Serneels, V., and Wolf, S., 1999, Les témoignages du travail der fer et au bronze provenant des fouilles En Selley à Avenches en 1997. *Bulletin de l'Association Pro Aventico*, **41**, 111-23.

Shackley, M. S., 2012, An introduction to X-Ray fluorescence (XRF) analysis in archaeology, in X-Ray fluorescence spectrometry (XRF), in *Geoarchaeology* (eds. M. S. Shackley), 7-44, Berlin/New York.

Shugar, A. N., and Mass, J. L., 2012, Handheld XRF for art and archaeology, *Studies in Archaeological Sciences*, **3**, Leuven.

Smigelskas, A. D., and Kirkendall**,** E. O., 1946, Zinc Diffusion in Alpha Brass, *American institute of mining and metallurgical engineers, Technical Publication* **No. 2071**.

Somiya, S., 1989, Part I: Introduction to Ceramics, In: Advanced Technical Ceramics, London: Academic Press, 14-16.

Sonuparlak, B., Sarikaya, M. and Aksay, I. A., 1987, Spinel phase formation during the 980 ◦C exothermic reaction in the kaolinite-to-mullite reaction series. *Journal of the American Ceramic Society*, **70**(11), 837-42.

Sosman, R. B., 1965, The Phases of Silica. Rutgers University Press, New Brunswick, New Jersey.

Sperinck, S., Raiteri, P., Marks, N., and Wright, K., 2011, Dehydroxylation of Kaolinite to Metakaolin - A Molecular Dynamics Study, *Journal of Materials Chemistry,* **21(7)**, 2118-25.

Stevens, S. J., Hand, R. J., and Sharp, J. H., 1997, Polymorphism of silica. *Journal of Material Science,* **32**, 2929-35.

Thornton, C. P., and Rehren, Th., 2009, A truly refractory crucible from fourth millennium Tepe Hissar, Northeast Iran. *Journal of Archaeological Science*, **36**, 2700-12.

Tite, M. S., Freestone, I. C., Meeks, N. D., and Craddock, P. T., 1985, The examination of refractory ceramics from metal-production and metalworking sites, in: The archaeologist and the laboratory. *Council for British Archaeology Research Report*, **58**, 50-5.

Tylecote, R. F., 1982, Metallurgical crucibles and crucible slags, in Archaeological Ceramics (ed. Olin, J. S., and Franklin, A. D.), 231-43, Smithsonian Institution Press, Washington.

Velde, B., and Druc, I. C., 1999, Archaeological Ceramic Materials, Origin and Utilisation, Springer-Verlag, Berlin, Heidelberg.

Verduch, A. G., 1958, Kinetics of cristobalite formation from silicic acid. *Journal of the American Ceramic Society*, **41**, 427-32.